Technical Report Documentation Page

1. REPORT No.
TE-74-2

2. GOVERNMENT ACCESSION No.

3. RECIPIENT'S CATALOG No.

4. TITLE AND SUBTITLE
Nondestructive Pavement Evaluation By The Wave Propagation Method

5. REPORT DATE
July 1974

6. PERFORMING ORGANIZATION

7. AUTHOR(S)
Watkins, D.J.; Lysmer, J.; and Monismith, C.L.

8. PERFORMING ORGANIZATION REPORT No.

9. PERFORMING ORGANIZATION NAME AND ADDRESS

10. WORK UNIT No.

11. CONTRACT OR GRANT No.

13. TYPE OF REPORT & PERIOD COVERED

12. SPONSORING AGENCY NAME AND ADDRESS
Office of Research Services of the College of Engineering
University of California at Berkeley
Berkeley, CA

14. SPONSORING AGENCY CODE

15. SUPPLEMENTARY NOTES

16. ABSTRACT

The wave propagation method for the nondestructive testing of layered structures offers a potentially powerful tool to air in the design of new pavements and overlays. While early forms of the technique were reported in 1933, the method has remained, essentially, in the form of a research aid. Widespread use has been restricted by the complexity and expense of the equipment and predominantly by difficulties in interpreting the raw data obtained in the field. There is a close relationship between equipment design and the method used to interpret the results.

The historical development of the technique is traced and the advantages and limitations of the modern procedures are considered. Basic phenomena of wave propagation in layered elastic systems are studied. Characteristics of the modes of propagation and the form of the solutions to the secular equation are important elements in interpretation. Properties of singularities and other features occurring in these functions are studied. Two methods for the analysis of wave propagation in multi-layered structures are developed. One method is based on the solution to the general equations of motion as constrained by the boundary conditions imposed by the structure. The other involves the discretization of a model of the structure into finite sub-layers and the analysis of this system by the direct stiffness method. Computer programs have been written employing both of these techniques. The numerical methods required in these programs are developed and their limitations discussed.

17. KEYWORDS

18. No. OF PAGES:
268

19. DRI WEBSITE LINK
http://www.dot.ca.gov/hq/research/researchreports/1974-1975/74-40.pdf

20. FILE NAME
74-40.pdf

74-40

SOIL MECHANICS AND BITUMINOUS MATERIALS
RESEARCH LABORATORY

NONDESTRUCTIVE PAVEMENT EVALUATION BY THE WAVE PROPAGATION METHOD

by
D. J. WATKINS
J. LYSMER
C. L. MONISMITH

REPORT NO. TE-74-2
to
STATE OF CALIFORNIA
DEPARTMENT OF TRANSPORTATION
DIVISION OF HIGHWAYS
TRANSPORTATION LABORATORY

DEPARTMENT OF CIVIL ENGINEERING
INSTITUTE OF TRANSPORTATION AND TRAFFIC ENGINEERING

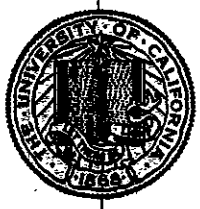

University of California · Berkeley

Soil Mechanics and Bituminous Materials
Research Laboratory

NONDESTRUCTIVE PAVEMENT EVALUATION BY THE WAVE PROPAGATION METHOD

A report on an investigation

by

D. J. Watkins
J. Lysmer
C. L. Monismith

to

Transportation Laboratory
Division of Highways
State of California Department of Transportation

under research technical agreement
13945-192234

Report No. TE-74-2
Office of Research Services
University of California, Berkeley

July 1974

FOREWORD

An important aspect of a successful program of highway maintenance involves the effective evaluation of pavements in their existing state. The wave propagation method of nondestructive testing offers a potentially valuable method for the determination of the properties of the various structural units within a pavement.

To ascertain the feasibility of this method for pavement evaluation a research group of the Department of Civil Engineering and the Institute of Transportation and Traffic Engineering at the University of California, Berkeley undertook a study of the wave propagation method of testing in which special emphasis was placed on problems of interpretation of test results. The work was commenced in January 1972 and supported by the Transportation Laboratory of the Division of Highways, State of California Department of Transportation under research technical agreement 13945-192234. This report presents the results of this study.

At an early stage in the research, it was realized that there is an important interaction between problems involving data interpretation and equipment design and test procedures. Consequently, in addition to analytic studies, an effort was made to evaluate the various versions of the test equipment in use at present. Discussions were held with the staff of the Transport and Road Research Laboratory, Department of the Environment, U.K. and a visit was made to a site at Grangemouth, Scotland where the wave propagation method was in use.

The general principles of the wave propagation method are discussed in Chapter 1. Some of the basic phenomena of wave propagation are described in Chapter 2 and the analytic methods developed for the study of waves in layered media are presented in Chapter 3. A critical review of methods

of interpretation of raw data from testing is undertaken in Chapter 4. Chapter 5 summarizes findings from the survey of equipment design and test procedures. There are eight appendices each dealing with special aspects of the analytic treatment or the properties of materials. These include descriptions of two computer programs developed during the course of the project.

An improvement in the understanding of the theoretical principles underlying the wave propagation method of nondestructive testing has been achieved but further advances will be required to take advantage of its full potential. Recommendations are made for further research.

This report was prepared by Mr. D. J. Watkins with the guidance of the faculty investigators, Professor John Lysmer and Professor Carl L. Monismith. The project was administered by the Office of Research Services of the College of Engineering, University of California at Berkeley.

ABSTRACT

The wave propagation method for the nondestructive testing of layered structures offers a potentially powerful tool to aid in the design of new pavements and overlays. While early forms of the technique were reported in 1933, the method has remained, essentially, in the form of a research aid. Widespread use has been restricted by the complexity and expense of the equipment and predominantly by difficulties in interpreting the raw data obtained in the field. There is a close relationship between equipment design and the method used to interpret the results.

The historical development of the technique is traced and the advantages and limitations of the modern procedures are considered. Basic phenomena of wave propagation in layered elastic systems are studied. Characteristics of the modes of propagation and the form of the solutions to the secular equation are important elements in interpretation. Properties of singularities and other features occurring in these functions are studied. Two methods for the analysis of wave propagation in multi-layered structures are developed. One method is based on the solution to the general equations of motion as constrained by the boundary conditions imposed by the structure. The other involves the discretization of a model of the structure into finite sub-layers and the analysis of this system by the direct stiffness method. Computer programs have been written employing both of these techniques. The numerical methods required in these programs are developed and their limitations discussed.

A critical review of interpretation techniques used to reduce field data is presented and proposals for improvement offered. The

range of test equipment and operating procedures developed to date is surveyed.

It is recommended that further analytic studies of layered structures subject to vibratory loading should be coordinated with field work and well documented case histories.

CONTENTS

LIST OF TABLES

LIST OF FIGURES

LIST OF SYMBOLS

A	arbitrary constant, arbitrary parameter
A'	arbitrary constant
a	arbitrary parameter
B	arbitrary constant, arbitrary parameter
B'	arbitrary constant
$\hat{B}$	arbitrary parameter
b	arbitrary parameter
C	arbitrary constant, arbitrary parameter
C'	arbitrary constant
C_k	arbitrary constant
c	phase velocity
D	arbitrary constant, arbitrary parameter
D'	arbitrary constant
d	layer thickness
E	Young's modulus, arbitrary parameter
E_1	real part of Young's modulus
E_2	imaginary part of Young's modulus
E*	Young's modulus of viscous layer
e	base of natural logarithm
exp(x)	e^x
F	function, force, arbitrary parameter
f	circular frequency, function, angle
f'	angle
G	shear modulus, function, arbitrary parameter
G_1	real part of shear modulus
G_2	imaginary part of shear modulus

G^*	shear modulus of viscous layer
g	function, arbitrary parameter
h	element width, step size
I	number of iterations
i	$\sqrt{-1}$
j	layer number
k	wave number of wave mode
k_1	real part of wave number
k_2	imaginary part of wave number
L	wave length of surface motion
ℓ	direction cosine
$\ell n(x)$	natural logarithm of x
M	arbitrary parameter
m	layer number
n	direction cosine, interface number, arbitrary parameter
P	force, arbitrary parameter
p_1	angle, order of predictor, arbitrary parameter
p	angle
p_c	critical angle
Q	arbitrary parameter
q	angle
R	pavement reaction, arbitrary parameter
r	arbitrary parameter
S	stiffness of road construction
s	arbitrary parameter
t	time
U	group velocity

u	displacement in x direction, arbitrary parameter
$\dot{u}$	velocity in x direction
v	displacement in y direction, arbitrary parameter
w	displacement in z direction, arbitrary parameter
$\dot{w}$	velocity in z direction
X	arbitrary parameter
x	horizontal distance, arbitrary parameter
y	horizontal distance, arbitrary parameter
Z	amplitude of motion
z	vertical distance
α	velocity of P-wave, phase lag, arbitrary parameter
α_1	real part of velocity of P-wave
α_2	imaginary part of velocity of P-wave
β	velocity of S-wave, phase lag
β_1	real part of velocity of S-wave
β_2	imaginary part of velocity of S-wave
β_{fc}	fraction of critical damping in compression
β_{fs}	fraction of critical damping in shear
γ	velocity of Rayleigh wave
Δ	characteristic determinant of secular equation
Δ_{cd}	specific damping capacity
δ	logarithmic decrement, vibratory displacement, arbitrary parameter
ε	strain, arbitrary parameter
θ	dilation
λ	Lamé's constant
λ_1	real part of Lamé's constant
λ_2	imaginary part of Lamé's constant

λ_d	damping ratio
λ^*	Lamé's constant of viscous layer
ν	Poisson's Ratio
ν_1	real part of Poisson's Ratio
ν_2	imaginary part of Poisson's Ratio
ρ	mass density
ρ^*	mass density of viscous layer
σ	stress
σ_1	real component of stress
σ_2	imaginary component of stress
τ	shear stress
ϕ	displacement potential
ϕ_L	loss angle
ψ	displacement potential
ω	angular frequency
∇^2	the operator $\frac{\partial^2}{\partial x^2} + \frac{\partial^2}{\partial y^2} + \frac{\partial^2}{\partial z^2}$
∞	infinity

CONVERSION FACTORS

Units of measurement used herein may be converted to Standard International (SI) units as follows:

Multiply	By	To obtain
inches	2.540	centimeters
feet	0.305	meters
miles	1.61	kilometers
square inches	6.45	square centimeters
square feet	0.093	square meters
acres	4047	square meters
cubic inches	16.4	cubic centimeters
cubic feet	0.028	cubic meters
gallons	3.8	liters
acre-feet	1233	cubic meters
pounds	0.454	kilograms
tons	907.2	kilograms
pounds force	4.45	newtons
kilograms force	9.81	newtons
pounds per square foot	47.9	newtons per square meter
pounds per square inch	6.9	kilonewtons per square meter

ACKNOWLEDGMENTS

The authors wish to express their gratitude to Dr. Günter Waas, without whose contributions to the dynamic analysis of discretized systems a major portion of the work reported here could not have been undertaken.

Mr. E. N. Thrower of the Transport and Road Research Laboratory, Department of the Environment, U. K., gave freely of his advice and arranged for the senior author to be present at Grangemouth, Scotland, during the testing of an experimental pavement. Mr. Frank Fawcett of TRRL ably demonstrated the use of the wave propagation technique at this site and offered valuable insights into problems of equipment design.

Mrs. Gloria Pelatowski skillfully prepared the figures and Mrs. Phyllis De Fabio typed the text.

CHAPTER 1

INTRODUCTION

An effective pavement maintenance management program requires a procedure by which the in-situ condition of existing pavements may be evaluated. Such a procedure should have the capability to yield data from which estimates can be made of the remaining life of the structure. In addition, the procedure should provide data which is useful for estimating the capability of the pavement to carry increased traffic loads and for the design of overlays.

Unfortunately, no single test or observation can produce all of the required information; accordingly evaluations must be based on several types of data. Fig. 1.1 illustrates how such methods can be combined to examine the problem of cracking associated with repetitive loading. One part of the procedure involves a determination of the in-situ elastic properties of the materials in the existing pavement. Traditional methods of pavement design did not call for a detailed knowledge of these properties. Advances in the ability to analyze multi-layered structures subject to arbitrary loading by methods based on elastic theory (Peutz, van Kempen and Jones, 1968) and the introduction of the finite element method (Duncan, Monismith and Wilson, 1968) have required the development of methods for the determination of the properties of each sub-unit of a pavement structure. Increasing loads, particularly on airfield pavements due to the introduction of wide bodied, large capacity aircraft, have accented the importance of these improved methods of analysis. Recent developments, such as thick-lift asphalt pavements, for which limited in-service performance

records are available, also require a technique which may be applied without heavy reliance upon experience, since sufficient time may not be available to develop the necessary performance data. Analytic methods capable of dealing with the generalized loadings imposed by multiple wheels have recently been developed. See, for example, Pichumani (1973) and Crawford (1972) who have studied pavement structures subjected to heavy aircraft loading. These methods require the fundamental properties of the structural materials as inputs.

A method which offers considerable potential to provide the type of data required to determine the material and geometric characteristics of in-situ pavements is the wave propagation technique. It is a nondestructive method of testing which involves the excitation of the pavement by means of a suitable vibratory source and the measurement of the response of the structure to this loading.

Vibratory methods of testing layered civil engineering structures have their origin in the field of pavement design. Their development has been motivated by two classic testing principles; a) in-situ testing is generally to be preferred over laboratory testing and b) test loading conditions should, as far as possible, simulate working loads. Two principal but separate methods have evolved over the years, both of which test for the in-situ properties of a structure but with only one involving a technique which attempts to simulate in-service loading conditions. The history of the two methods are, however, very much interrelated.

Historical Development of Vibratory Testing Methods

Vibratory testing of highway subgrades was pioneered by the German Society for Soil Mechanics (Deutsche Forchungsgesellschaft für

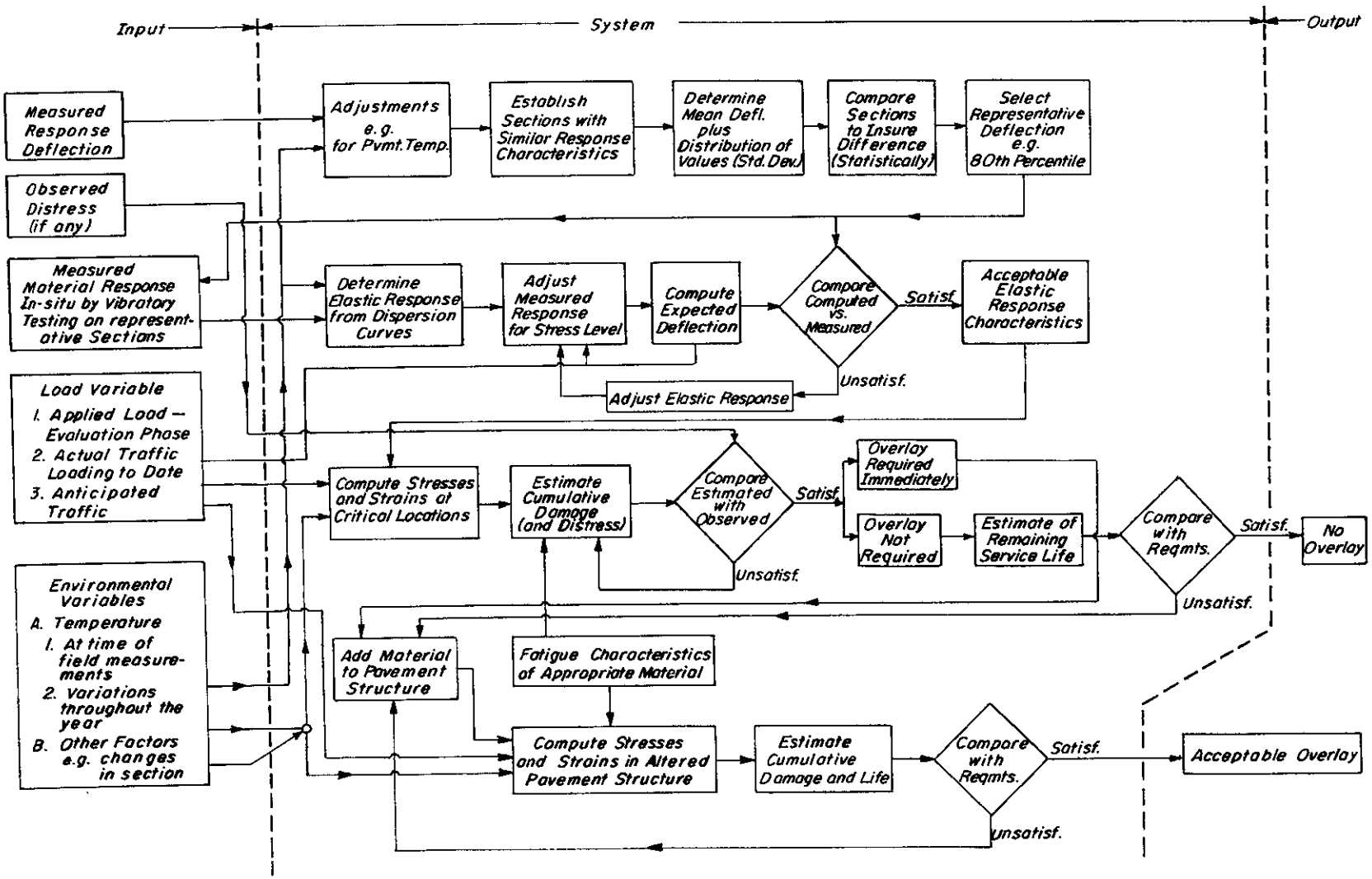

Fig. I.1 EXAMPLE OF AN OVERLAY DESIGN SUBSYSTEM OF THE PAVEMENT DESIGN AND MANAGEMENT SYSTEM

Bodenmechanik, 1933, 1936, and 1938). With the exception of some experimentation in the United States by Bernhard (1939) and in Sweden by Bergstrom and Linderholm (1946), the method was next subjected to study at the Royal Dutch Shell Laboratory in Holland by Van der Poel (1948, 1951, and 1953), and Nijboer (1955). Their work has been extensively reported in the literature. See, for example, Nijboer and Van der Poel (1953) and Nijboer and Jones (1944).

The basis of the Dutch method is to measure the response of a highway structure to a dynamic loading designed to approximate the loading induced by vehicular traffic. This is achieved by a machine consisting, essentially, of rotating, eccentric masses and a ballasting mass. The eccentric masses are driven at a steady frequency, designed to simulate vehicles passing over the pavement, i.e.: between 10 and 100 cycles per second. The loading generated by the machine is transferred to the pavement through a plate, e.g., 30 cm diameter.

The machine developed at the Royal Dutch Shell Laboratory produces forces varying between zero and 40 kn. Figs. 1.2 and 1.3 illustrate the loading system. Due to the inertia of the system the pavement reaction and deflection are not in phase with the force generated by the rotating masses and, if the masses rotate sinusoidally with time, the following relationships hold:

$$P = P_{max} e^{i\omega t} \tag{1.1}$$

$$R = R_{max} e^{i(\omega t - \alpha)} \tag{1.2}$$

$$z = z_{max} e^{i(\omega t - \beta)} \tag{1.3}$$

where

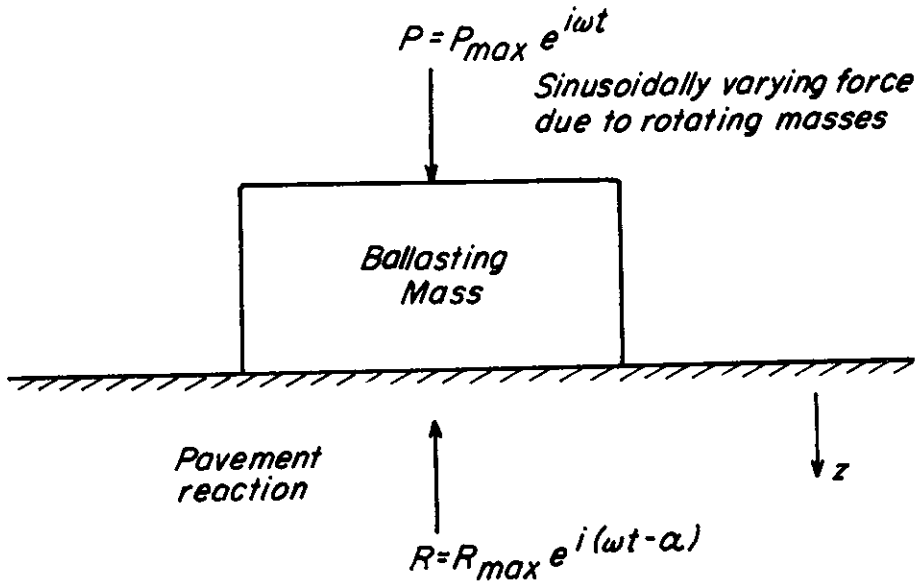

Fig. 1.2 SCHEMATIC OF FORCE SYSTEM FOR ROYAL DUTCH SHELL MACHINE

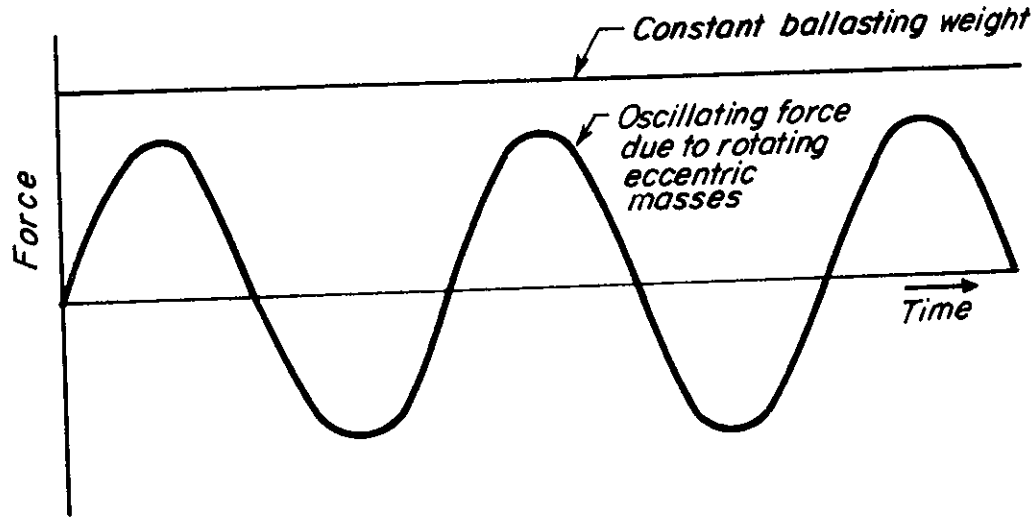

Fig. 1.3 PAVEMENT LOADING PRODUCED BY ROYAL DUTCH SHELL VIBRATORY TESTING MACHINE

where

P = force due to rotating masses

R = pavement reaction

z = deflection of pavement under center of loading

ω = angular frequency of rotating masses

α = phase lag of R behind P

β = phase lag of z behind P

$i = \sqrt{-1}$

t = time

Nijboer and Van der Poel (1953) defined the ratio,

$$S = \frac{R_{max}}{z_{max}} \tag{1.4}$$

as the stiffness of a road construction. By testing a variety of pavements, it was possible to use this factor as a guide to the ability of a structure to sustain traffic loading without distress. For example, Nijboer and Van der Poel (1953), from empirical studies, proposed that the stiffness required to prevent cracking of an asphalt surface is 200,000 kN/m.

In addition to stiffness measurements, it is possible to investigate the characteristics of the surface disturbance produced in the pavement, which propagates away from the vibratory machine. Dutch workers achieved this by moving a detector progressively away from the loading center and noting the distances at which the signal from the detector was in phase with the sinusoidal motion of the vibrator. From this data it was possible to compute the wave length of the propagating wave.

The experiment was repeated at a number of different frequencies. Assuming the waves to be shear waves and that those observed at high frequencies propagate primarily in the near surface layers of the pavement while low frequency waves are influenced by properties of deep layers, it was possible to make estimates of the shear moduli of a pavement structure.

The combination of stiffness and elastic moduli obtained from the Dutch tests was employed by Nijboer (1955) as input parameters to analyses of pavement models which yielded predicted pavement strains which agreed well with strains measured under traffic loads. Improved theoretical modelling of the vibrator/pavement system (Heukelom, 1961, Heukelom and Foster, 1960) combined with extended experimental data (Nijboer and Metcalf 1962) and refinement of the equipment (Klomp and Niesman, 1967) has progressed these methods to such a stage that they are in widespread use throughout the world. See, for example, Mucci (1968).

In surveying the state of the art of dynamic testing of roads and runways, Jones and Whiffin (1960) pointed out important differences between the loading generated by the Dutch vibratory machine and that imposed by traffic. The vibratory machine loads both the surface and lower layers at the same rate of loading. A moving wheel loads the surface with a stress pulse which rises from zero, reaches a peak, and returnsto zero again in the time taken for the tire contact area to travel over a point on the road surface. However, the load spreading action of the pavement results in a stress pulse of longer duration and lower intensity at deeper points. The experimental work of Nijboer and Metcalf (1962) support these criticisms. Pavement deformation were found to be greatest for static loads and to decrease with increasing

vehicle speed up to a constant value at about 25 km/hr. and different relationships were found for different pavement sections; pointing out the influence of the rates of loading.

These limitations in the ability of the system to simulate traffic loading led a group of engineers at the Transport and Road Research Laboratory in England to develop a testing technique which relies upon the observation of the surface waves propagating away form a simple vibrator placed on the surface of a layered structure (Jones, 1968, and Nair, 1971). Their approach assumes that the surface disturbance produced by a source of excitation is some function of the geometry and material properties of the layered system involved in the excitation. If this is the case, it should be possible, theoretically, to infer from measurements of the characteristics of the surface disturbance details of the underlying structure.

The development of the experimental and analytic methods required for the exploitation of this technique have been described by Jones (1968) and Jones, Thrower and Gatfield (1967). Only the principal elements will be outlined here. More detailed discussion will be found in Chapters 3, 4 and 5.

Experimentally, the wave propagation method involves the measurement of the phase velocity and wave length of the surface waves propagating away from a vibratory source placed on the surface. A vibrator is placed in position on the surface and set in operation at a constant frequency. The phase angle of the sinusoidal vibration of this source is then electronically compared with the phase angle of the excitation produced in a detector placed at some known distance from the source. Details of the electronic equipment used to obtain this comparison

vary considerably but Fig. 1.4 is a schematic of a typical arrangement. Variations in the experimental procedure, which depend upon the equipment type and purpose of the test, are also encountered. Commonly, however, the pick-up is moved successively further away from the source in constant increments of distance and the phase difference recorded at each point. From the data thus obtained a plot of the type shown in Fig. 1.5 is made. Similar plots are generated for waves produced by the vibrator when operating over a wide range of individual frequencies. The slope of the mean drawn through the points on these plots allows the wave lengths and phase-velocity of the surface disturbance to be computed from:

$$L = 360 \frac{a}{b} \tag{1.5}$$

and

$$c = Lf \tag{1.6}$$

where L = the wave length of the surface wave

a/b = the slope of the phase difference/distance curve

c = the phase velocity of the surface wave

f = the circular frequency

A graphical representation of the relationship between phase velocity and wave length, known as a dispersion curve, may be prepared from this information. An example obtained from tests on the surface of an experimental pavement constructed at Conington Lodge, England, is presented in Fig. 1.6.

The interpretation of test results, presented in the form of dispersion curves, requires a thorough understanding of the behavior of wave propagation phenomena and considerable practical experience.

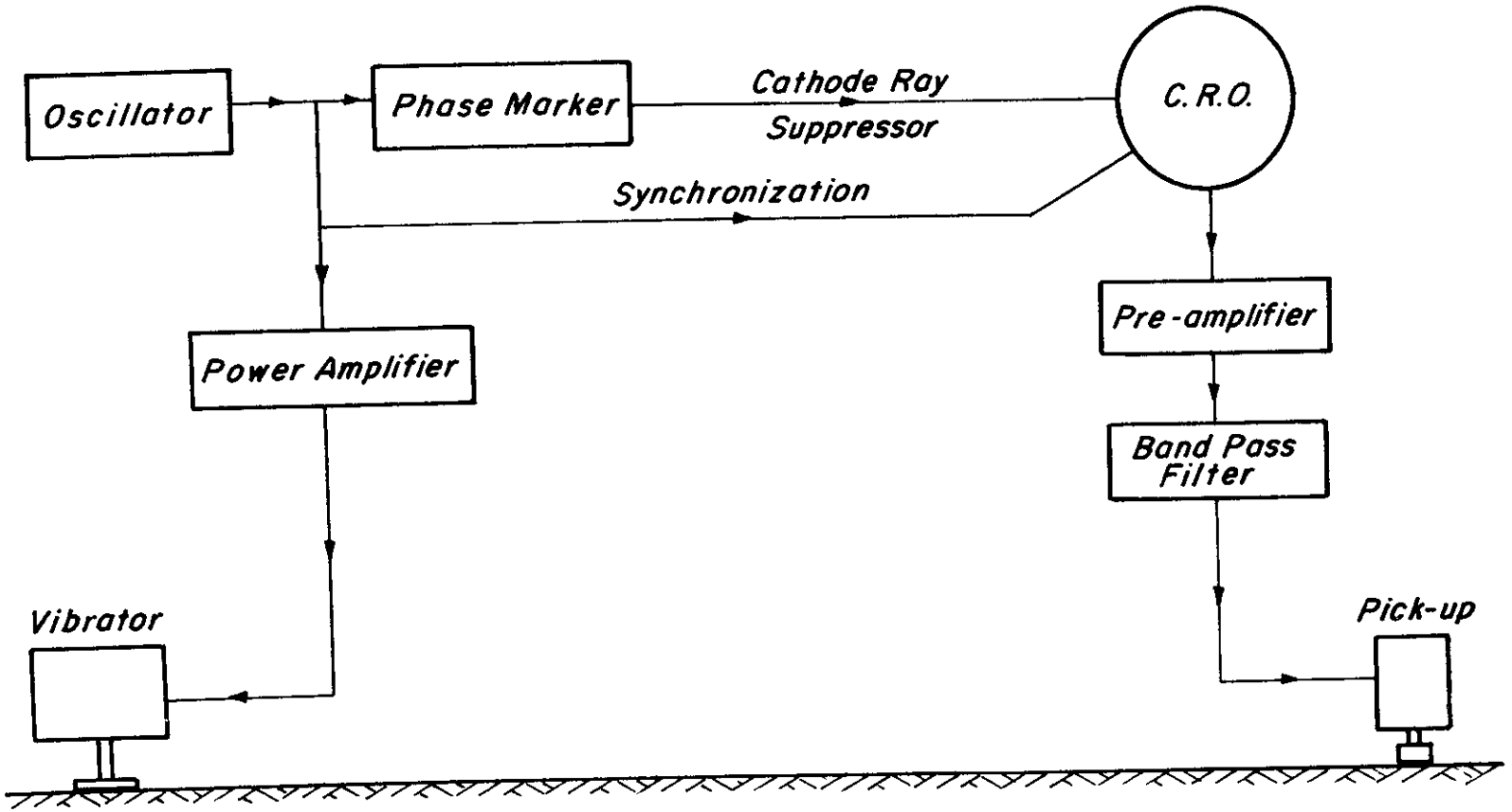

Fig. I.4 SCHEMATIC DIAGRAM OF TYPICAL EQUIPMENT FOR WAVE PROPAGATION TEST

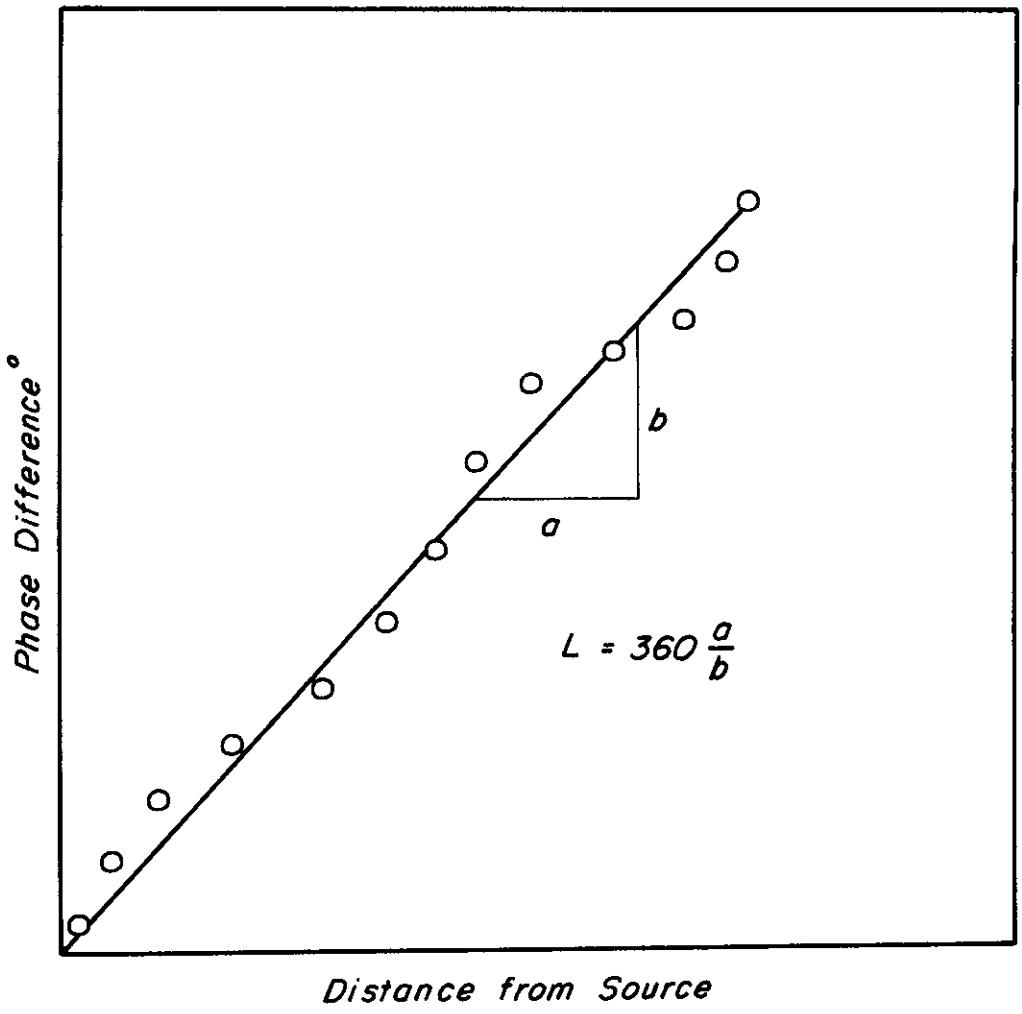

Fig. 1.5 HYPOTHETICAL FIELD DATA FROM A WAVE PROPAGATION TEST

This problem, sometimes known as the "inversion problem", has various levels of difficulty, depending upon the type of information sought and the complexity of the structure being tested. For example, the curves presented in Fig. 1.6 may be interpreted, at the simplest level, as follows. Assuming that the surface waves observed are of the Rayleigh type (see Chapter 2 for a discussion of wave types) and that at high frequencies (short wave lengths) the disturbance is confined to a region close to the surface, then, as the frequency is raised, the phase velocities will asymptotically approach the speed of a Rayleigh wave in the hot rolled asphalt surfacing. The points on Fig. 1.6 obtained from the high frequency portion of the test are used to construct Branch A of the dispersion curve and extrapolation to the zero wave length ordinate yields the Raleigh wave velocity for the surfacing. The Raleigh wave velocity is defined as:

$$\gamma = n\sqrt{\frac{G}{\rho}} \qquad (1.7)$$

where

γ = Rayleigh wave velocity

G = shear modulus

ρ = mass density

n = a factor depending upon Poisson's ratio ν

If ρ and ν for the surfacing are known, then the shear modulus G may be computed. In the above example γ is estimated to be approximately 1370 m/sec. For tests at very low frequencies (long wave lengths) it may be assumed that the surface motion is dominantly affected by the subgrade so that Branch B on Fig. 1.6 is asymptotic, at long wave

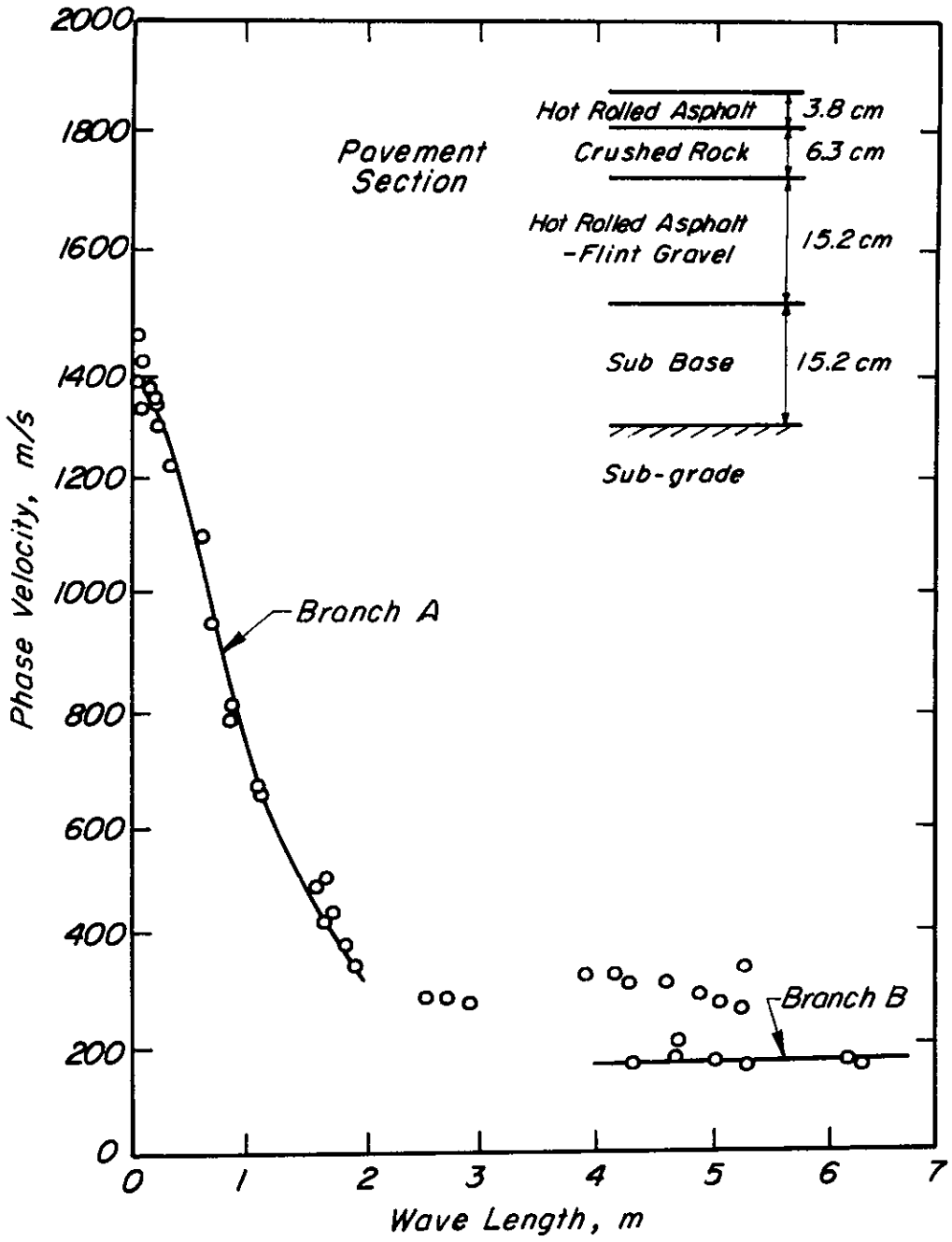

Fig. 1.6 TYPICAL DISPERSION CURVES PREPARED FROM FIELD DATA.

(after Page, 1969)

lengths, to the Rayleigh wave velocity of the material at great depth. In this case about 170 m/sec. The numerous points on Fig. 1.6 which are not assigned to either Branch A or Branch B require the application of more sophisticated theoretical analysis if they are to yield additional information about the properties of the pavement structure.

In recent years there has been considerable interest expressed in the extension of the wave propagation method to applications in fields other than pavement evaluation and design, in the improvement of equipment and experimental techniques and, especially, in improved method of interpretation of experimental data. French workers are active in the extension of the work begun at the Transport and Road Research Laboratory in England and have made significant contributions by formalizing much of the existing knowledge, improving equipment design and investigating some of the theoretical problems. See, for example, Gramsammer (1968) and Dosso and Keryell (1968). In the United States the U. S. Army Engineer Waterways Experiment Station (WES), Vicksburg, have studied the use of the method in the evaluation of the properties of soil and rock at depth (Ballard, 1964) and for site investigation for the foundations of such structures as radar towers.

The Eric H. Wang, Civil Engineering Research Facility (CERF) at the University of New Mexico has been actively engaged in the design of sophisticated equipment with a high degree of automation for the testing of airfield pavements by this technique (Rao and Harnage, 1972, and Rao, 1971). In Australia Kurzeme (1970b) has investigated the use of vibratory testing using a source generating shear waves and in Sweden the method has been used as a high speed technique to assess the effects of changing traffic patterns on road foundations (Statens

Väginstitut, 1969)

This widespread interest may be attributed to a number of advantages which nondestructive vibratory testing methods offer.

Advantages of the Wave Propagation Method

1. The method is nondestructive.
2. The materials are tested in-situ. This eliminates the need to account for a number of variables which are difficult to reproduce with precision in the laboratory. For example, the confining pressure resulting from a complex stress field.
3. Properties of the materials are determined over a wide area rather than from a localized test sample.
4. Material properties are determined in the form of their various moduli. This allows their use in rational analyses of the response of the structure to loading.
5. There is a minimum of disruption to site activity. This is of major importance in testing highway pavements and airport runways.

The limitations of the method must also be considered, however.

Limitations of the Wave Propagation Method

1. The stress levels induced in the layered structure are generally much lower than those produced by the working loads. As many natural materials have non-linear stress/strain characteristics, moduli determined by the test cannot be used directly in the analyses of structure under traffic loading. Modifications incorporating the effects of stress level must be applied. (See Appendix 6).

2. The equipment is relatively expensive.
3. The complexity of the equipment and the need for a rather sophisticated interpretation of the data requires an operator with some knowledge of electronics, an understanding of the nature of wave propagation in layered media and a considerable period of experience with the technique. This may reduce the number of routine applications for which the method is viable.
4. The interpretation of the data is founded upon the ability of theoretical analyses to correctly predict the nature of wave propagating in layered media. At present these methods are insufficiently advanced to allow full advantage to be taken of data available from testing programs. Reliable information is available for only the simplest of structures, such as a single stiff layer over a soft half-space, and in many cases simplifications and idealizations are used whose practical implication are not fully understood.

This latter limitation is probably the greatest single problem hindering the widespread use of the wave propagation method (Kurzeme, 1971). Its solution requires advances in the quality of the theoretical models used to represent practical structures and the full exploitation of existing analytic tools. The foundations of these analytic methods are all based upon a mathematical representation of the basic phenomena of wave propagation. These phenomena will be discussed in Chapter 2.

CHAPTER 2

WAVES IN LAYERED MEDIA

Elastic Waves in Layered Media

There are two basic wave types which can exist in elastic media. Such waves are propagated as dilational (P-waves) and rotational waves (S-waves, frequently referred to as shear waves). Under certain unique conditions these two basic wave types combine to form other waves which have been assigned special names, such as, Rayleigh waves, Love waves and Stonely waves. For example, Lamb (1904) demonstrated that Rayleigh waves arise from the diffraction of curved fronts of P- and S-waves at the free boundary of a homogeneous elastic body.

General Equations of Motion

The general equations of motion in terms of the rectangular coordinate system (x, y, z) are, neglecting body forces, (Ewing, Jardetsky, and Press, 1957):

$$\begin{aligned} \rho \frac{\partial^2 u}{\partial t^2} &= (\lambda + G)\frac{\partial \theta}{\partial x} + G\nabla^2 u \\ \rho \frac{\partial^2 v}{\partial t^2} &= (\lambda + G)\frac{\partial \theta}{\partial y} + G\nabla^2 v \\ \rho \frac{\partial^2 w}{\partial t^2} &= (\lambda + G)\frac{\partial \theta}{\partial z} + G\nabla^2 w \end{aligned} \qquad (2.1)$$

where

u, v and w are the displacements with respect to the x, y and z axes respectively

ρ = density

t = time

G = the shear modulus

λ = Lame's constant

$\theta = \frac{\partial u}{\partial x} + \frac{\partial v}{\partial y} + \frac{\partial w}{\partial z}$ (the dilation)

∇^2 = the operator $\frac{\partial^2}{\partial x^2} + \frac{\partial^2}{\partial y^2} + \frac{\partial^2}{\partial z^2}$

The corresponding stress-strain relationships are:

$$\begin{aligned}
\sigma_{xx} &= \lambda\theta + 2G\frac{\partial u}{\partial x} \\
\sigma_{xy} &= G\left(\frac{\partial u}{\partial y} + \frac{\partial v}{\partial x}\right) \\
\sigma_{yy} &= \lambda\theta + 2G\frac{\partial v}{\partial y} \\
\sigma_{yz} &= G\left(\frac{\partial v}{\partial z} + \frac{\partial w}{\partial y}\right) \\
\sigma_{zz} &= \lambda\theta + 2G\frac{\partial w}{\partial z} \\
\sigma_{zx} &= G\left(\frac{\partial w}{\partial x} + \frac{\partial u}{\partial z}\right)
\end{aligned} \tag{2.2}$$

The velocity of P-waves (α) and of S-waves (β) in a linear elastic material (Fung, 1965) are given by:

$$\alpha = \sqrt{\frac{\lambda + 2G}{\rho}} \tag{2.3}$$

$$\beta = \sqrt{\frac{G}{\rho}} \tag{2.4}$$

Plane Waves

There are many instances in which wave propagation in a system of elastic layers reduces to an essentially plane problem, so that the P- and S-waves do not depend upon y, the axis normal to the plane of the paper in Fig. 2.2. To simplify the discussion it will now be assumed that there are no body forces and only plane waves are generated. Thus the equations of motion (Eq. 2.1) reduce to:

$$\rho \frac{\partial^2 u}{\partial t^2} = (\lambda + 2G) \frac{\partial \theta}{\partial x} + G\nabla^2 u$$
$$\rho \frac{\partial^2 w}{\partial t^2} = (\lambda + 2G) \frac{\partial \theta}{\partial z} + G\nabla^2 w \qquad (2.5)$$

where ∇^2 = the operator $\frac{\partial^2}{\partial x^2} + \frac{\partial^2}{\partial z^2}$.

Eqs. (2.5) can be simplified if they are expressed in the form:

$$\frac{\partial^2 \phi}{\partial t^2} = \alpha^2 \nabla^2 \phi$$
and
$$\frac{\partial^2 \phi}{\partial t^2} = \beta^2 \nabla^2 \psi \qquad (2.6)$$

where,

$$u = \frac{\partial \phi}{\partial x} - \frac{\partial \psi}{\partial z}$$
and
$$w = \frac{\partial \phi}{\partial z} - \frac{\partial \psi}{\partial x} \qquad (2.7)$$

ϕ and ψ are known as displacement potentials and an examination of Eqs. (2.5) and (2.6) will show that ϕ is associated only with the P-wave and ψ only with the S-wave.

Eqs. (2.6) are solved by making the trial substitutions

$$\begin{aligned} \phi &= f(z) \exp\left(ik_\phi(\ell_\phi x + n_\phi z)\right) \\ \psi &= g(z) \exp\left(ik_\psi(\ell_\psi x + n_\psi z)\right) \end{aligned} \tag{2.8}$$

where

$k_\phi = \omega/\alpha$

$k_\psi = \omega/\beta$

ω = the frequency of the excitation

ℓ and n = the direction cosines of the normal to the advancing wave with respect to the x and z axes respectively

c = the apparent velocity of the advancing wave

$i = \sqrt{-1}$

The general solutions for $f(z)$ and $g(z)$ in Eqs. (2.8) are:

$$f(z) = A'\exp(ik_\phi(\ell_\phi x + n_\phi z)) + B'\exp(ik_\phi(\ell_\phi x - n_\phi z))$$

and

$$g(z) = C'\exp(ik_\psi(\ell_\psi x + n_\psi z)) + D'\exp(ik_\psi(\ell_\psi x - n_\psi z)) \tag{2.9}$$

so that the potentials take the form:

$$\phi = \{A'\exp(ik_\phi(\ell_\phi x + n_\phi z)) + B'\exp(ik_\phi(\ell_\phi x - n_\phi z))\}\exp(i\omega t)$$
$$\psi = \{C'\exp(ik_\psi(\ell_\psi x + n_\psi z)) + D'\exp(ik_\psi(\ell_\psi x - n_\psi z))\}\exp(i\omega t) \qquad (2.10)$$

where A' , B' , C' and D' are constants which can only be determined by the application of the boundary conditions for the system to be analyzed.

The Boundary Between Two Elastic Media

The principal boundary conditions to be considered in the analysis of waves propagating in layered media are those imposed at the interface between two layers. Consider a P-wave travelling in layer 2 of Fig. 2.1 incident at some angle q to the interface. This wave will, in general, produce compressional and distortional (P and S) waves in both media. Four boundary conditions must be satisfied, requiring continuity of the two components of displacements, u and w, and of the two stresses, σ_{zz} and σ_{zx}, across the interface, i.e.

$$u_1 = u_2 \qquad w_1 = w_2$$
$$[\sigma_{zz}]_1 = [\sigma_{zz}]_2 \qquad [\sigma_{zx}]_1 = [\sigma_{zx}]_2 \qquad (2.11)$$

The direction cosines required for the solution of Eqs. (2.10) can be obtained from Snell's Law:

$$\frac{c}{\text{Cos } q} = \frac{\alpha_2}{\text{Cos } p} = \frac{\beta_2}{\text{Cos } f} = \frac{\alpha_1}{\text{Cos } p'} = \frac{\beta_1}{\text{Cos } f'} \qquad (2.12)$$

where

c = apparent velocity of wave propagation in both media (since the boundary conditions Eqs. (2.11) are independent of x and t)

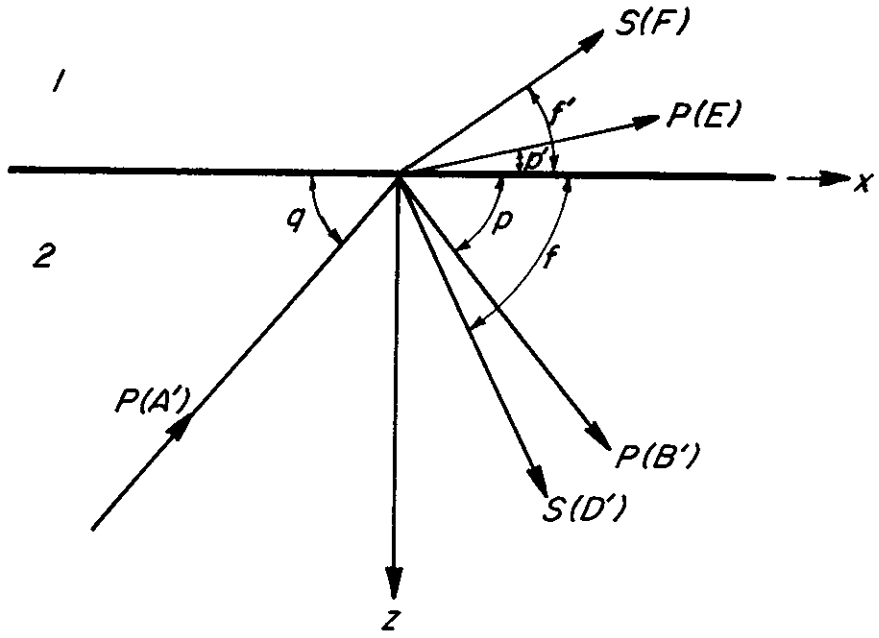

Fig. 2.1 REFLECTION OF P WAVES AT AN INTERFACE

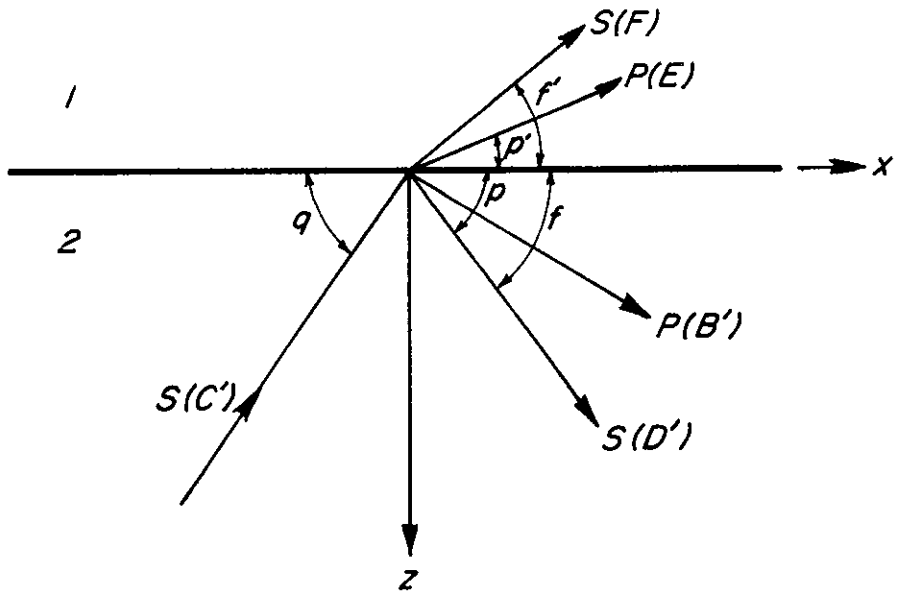

Fig. 2.2 REFLECTION OF S WAVES AT AN INTERFACE

There is a certain critical value of the angle q beyond which no energy is reflected from the boundary to penetrate back into the lower medium (1). Thus, designating the critical angle for the reflection of P-waves p_c, two conditions are possible.

1. $0 \leq q \leq p_c$ angle p will be real and angle p' imaginary

and

2. $q \geq p_c$ angle p will be imaginary and angle p' real

At this stage it will be convenient to simplify the wave equations (Eqs. 2.10) for each of the waves in Fig. 2.1 to:

$$\begin{aligned}
\phi_1 &= \{A'\exp(ikr_1 z) + B'\exp(-ikr_1 z)\}\exp[ik(ct - x)] \\
\psi_1 &= \{C'\exp(iks_1 z) + D'\exp(-iks_1 z)\}\exp[ik(ct - x) \\
\phi_2 &= E\exp(ikr_2 z) \cdot \exp[ik(ct - x)] \\
\psi_2 &= F\exp(-iks_2 z) \circ \exp[ik(ct - x]
\end{aligned} \tag{2.13}$$

and

$$\begin{aligned}
r &= \sqrt{c^2/\alpha^2 - 1} \quad \text{for} \quad C > \alpha \\
r &= -i\sqrt{1 - c^2/\alpha^2} \quad \text{for} \quad C > \alpha \\
s &= \sqrt{c^2/\beta^2 - 1} \quad \text{for} \quad C > \beta \\
s &= -i\sqrt{1 - c^2/\beta^2} \quad \text{for} \quad C < \beta
\end{aligned} \tag{2.14}$$

By the application of trigonometric identities it can be shown that

$$r = \text{Cot } p$$

$$\text{and} \qquad (2.15)$$

$$s = \text{Cot } f$$

For $c < \alpha_2$ no disturbance is transmitted into the interior of the upper layer because by Eq. (2.12) p' is imaginary. However, this does not mean that there is no disturbance in the upper medium. There is, in fact, a disturbance which propagates along the interface, decreasing exponentially with the distance away from it in both the $+z$ and $-z$ directions. The effect on the wave reflected back into the interior of the lower medium (P(B') in Fig. 2.1) under these circumstances is to produce a phase shift such that the first equation of Eqs. (2.13) may be expressed as

$$\phi_1 = A'\exp(ikr_1 z) \cdot \exp[ik(ct - x)] + A'\exp(-ikr_1 z) \cdot \exp[ik(ct - x)] \cdot \exp\frac{2\varepsilon}{\omega}$$

where ε is a function of the incident angle q for $0 \leq q \leq p_c$ (Ewing, Jardetsky and Press, 1957).

Similar arguments can be made for the case of an incident S-wave of the type shown in Fig. 2.2. When both an S-wave and a P-wave travel simultaneously, and confining attention to conditions within a single layer the motion can be described by the equations:

$$\begin{aligned} \phi &= \{A \text{ Sinh}(ikrz) + B \text{ Cosh}(ikrz)\}\exp[ik(ct - x)] \\ \psi &= \{C \text{ Cosh}(iksz) + D \text{ Sinh}(iksz)\}\exp[ik(ct - x)] \end{aligned} \qquad (2.16)$$

where by reference to Eqs. (2.10) and Eqs. (2.13)

$$A' = \frac{A + B}{2} \qquad B' = \frac{B - A}{2}$$
$$C' = \frac{C + D}{2} \qquad D' = \frac{C - D}{2} \tag{2.17}$$

and

$k = \omega/c$

c = apparent phase velocity

which is a convenient form for use in analysis.

For a multi-layered system of elastic media composed of n layers there are $4n - 2$ boundary conditions to be satisfied: continuity of two displacement components and two stress components at each interface, and the vanishing of two stress components at the free surface. Using Eqs. (2.5), Eqs. (2.7) and Eqs. (2.16) to obtain the mathematical expression of these conditions leads to $4n - 2$ homogeneous simultaneous equations to determine an equal number of constants of the type A, B, C and D in Eqs. (2.16). The solutions to these sets of equations are usually extremely complex and pose many numerical problems. However, there are two special cases which are somewhat simpler and which can give valuable insights into the basic phenomena associated with the propagation of waves in layered elastic media. These are the homogeneous, isotropic half-space and the single elastic layer over a rigid solid.

The Homogeneous and Isotropic Half-space

The boundary conditions for a half-space are zero stresses at the free surface and zero displacement or velocity at infinite depth. Using

Eq. (2.3), Eq. (2.4), Eq. (2.7) and Eq. (2.16) with these boundary conditions gives $A = B$ and $C = D$ so that in determinant form the problem reduces to

$$\begin{vmatrix} Gb & 2Gs \\ 2Gr & Gb \end{vmatrix} = 0 \qquad (2.18)$$

where $b = 2 - c^2/\beta^2$ or more simply

$$b^2 - 4sr = 0 \qquad (2.19)$$

Expanding the terms b, s and r and factorizing out the quantity c^2/β^2 gives,

$$c^2/\beta^2[c^6/\beta^6 - 8c^4/\beta^4 + c^2(24/\beta^2 - 16/\alpha^2) - 16(1 - \beta^2/\alpha^2)] = 0 \qquad (2.20)$$

which is the form usually found in the literature (e.g. Ewing, Jardetsky and Press, 1957).

For the purpose of illustration it will be assumed that the half-space is a Poisson solid (i.e. $\lambda = G$ or $\alpha = \sqrt{3} \cdot \beta$) . In this case Eq. (2.19) has the following real roots.

$$c^2/\beta^2 = 4 \text{ , } 2 + 2/\sqrt{3} \text{ and } 2 - 2/\sqrt{3} \text{ .}$$

The first two of these roots are usually rejected as they would require that r and s in Eqs. (2.16) become positive imaginary which is not compatible with the requirement that the disturbance decrease rapidly with depth, z , from the surface. The wave corresponding to the last root $(c^2/\beta^2 = 2 - 2/\sqrt{3})$ is a surface wave of the classic type described by Rayleigh (1885). Richter (1943) raised the question

of the physical origin of the alternative roots and this problem was pursued by Fu (1950). For a Poisson solid there are certain angles of incidence to the free surface for which an incident P-wave gives rise to only the reflected S-wave and, similarly, where an incident S-wave produces only a reflected P-wave. These conditions correspond to the "extraneous" roots of Eq. (2.19). For materials other than Poisson solids there may be roots which require that r and/or s become complex which indicates inhomogeneous waves. For a material in which $\alpha/\beta = 1.788$ Walker (1919) found that the reflected P-wave will not vanish but that its amplitude attains a minimum at an angle of incidence near 20°. Miller and Pursey (1955) determined that the distribution of total input energy among P-waves and S-waves in the body and surface waves at the free surface of an elastic half-space is as follows:

Wave Type	% of Total Energy
Rayleigh	67
S	26
P	7

The Rayleigh wave is the surface wave corresponding to the root of Eq. (2.19) which yields real values for the radicals r and s (e.g. $c^2/\beta^2 = 2 - 2/\sqrt{3}$ for a Poisson solid). This wave type is of major concern when dealing with problems involving sources of excitation at the free surface. The relationship between the velocity of this wave, γ, and the velocity of P-waves and S-waves is a function of Poisson's Ratio, ν, for the material comprising the half-space. This relationship is shown in Fig. 2.3. The close approximation between the R-wave and S-wave velocities throughout the range of ν has encouraged the use of the approximation:

$$\gamma \simeq \beta \tag{2.21}$$

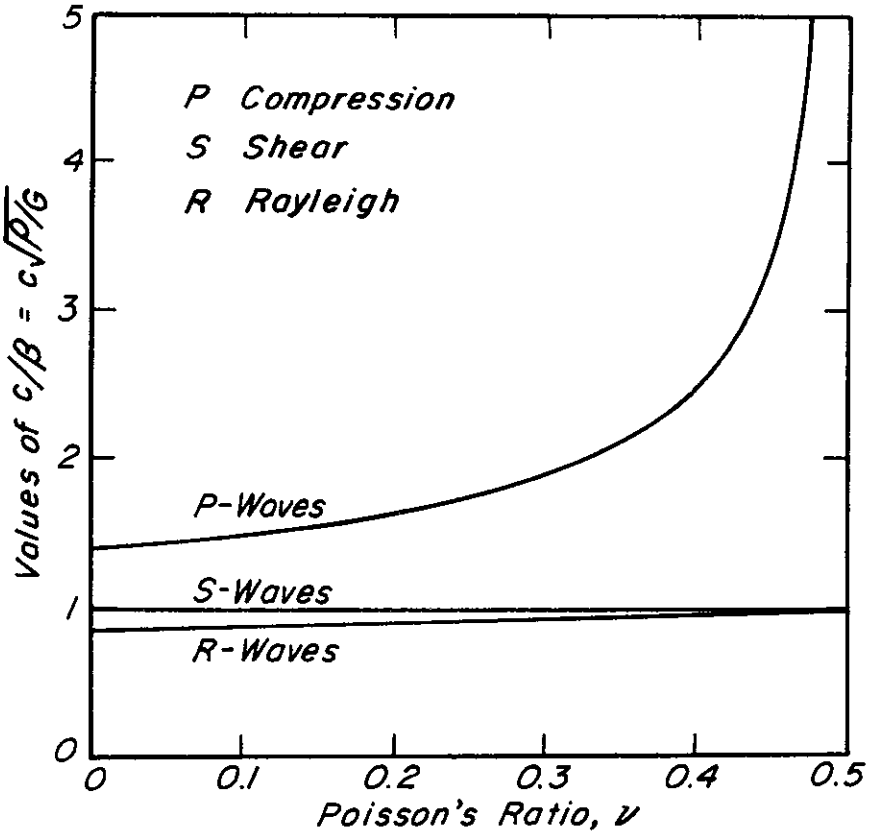

Fig. 2.3 RELATIONSHIP BETWEEN POISSON'S RATIO AND VELOCITIES OF PROPAGATION OF WAVES IN A SEMI-INFINITE ELASTIC MEDIUM (from Richart, 1962)

in many practical applications.

For a Poisson solid the roots of Eq. (2.19) may be represented graphically as shown in Fig. 2.4. It is important to note that, for each curve, the slope $\omega/k = c$ (the phase velocity) is constant and does not vary with the frequency of excitation ω. The significance of this fact will be discussed later.

Single Elastic Layer Over a Rigid Solid

In this case the boundary conditions are zero stress at the surface ($\sigma_{zz} = \sigma_{zx} = 0$) and zero displacement or velocity ($\dot{u} = \dot{w} = 0$) at the interface between the bottom of the elastic layer and the rigid solid, which will be assumed to be in welded contact. Applying these constraints and using Eq. (2.3), Eq. (2.4), Eq. (2.7) and Eq. (2.16) yields a determinant expression:

$$\begin{vmatrix} \text{Sinh}(irkd) + \frac{2rs}{b}\,\text{Sinh}(iskd) & s\text{Cosh}(iskd) - \frac{2s}{b}\,\text{Cosh}(irkd) \\ -r\text{Cosh}(irkd) + \frac{2r}{b}\,\text{Cosh}(iskd) & \text{Sinh}(iskd) + \frac{2rs}{b}\text{Sinh}(irkd) \end{vmatrix} = 0 \quad (2.22)$$

where the variables are as defined previously for Eq. (2.18). There are an infinite number of discrete values of the wave numbers k which satisfy this equation at any particular exciting frequency ω. The relationships between frequency and five of these roots are shown in Fig. 2.5 for a Poisson solid of unit depth over the rigid solid. Curves of the type given in Fig. 2.5 are known as spectral lines. The solid lines lie in the ω-Real(k) plane and represent real wave numbers. The short dashed lines lie in the ω-Imaginary(k) plane and represent purely imaginary wave numbers. The long dashed lines are curves in the ω-Real(k) - Imaginary(k) space which represent complex wave

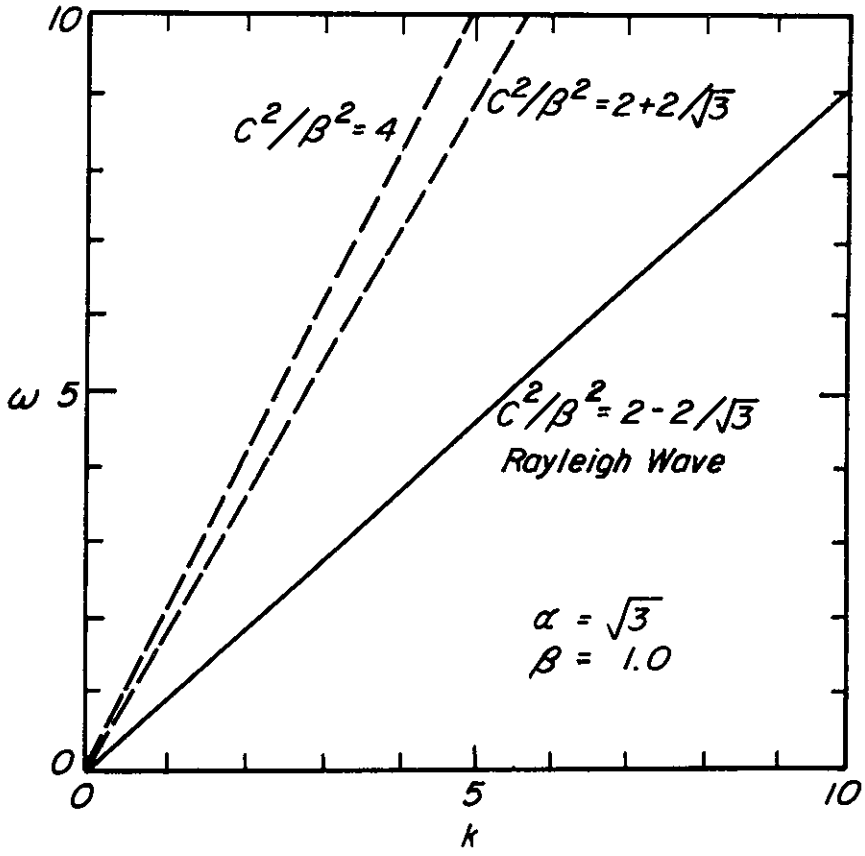

Fig. 2.4 ω/k RELATIONSHIP FOR A HALF-SPACE OF A POISSON SOLID

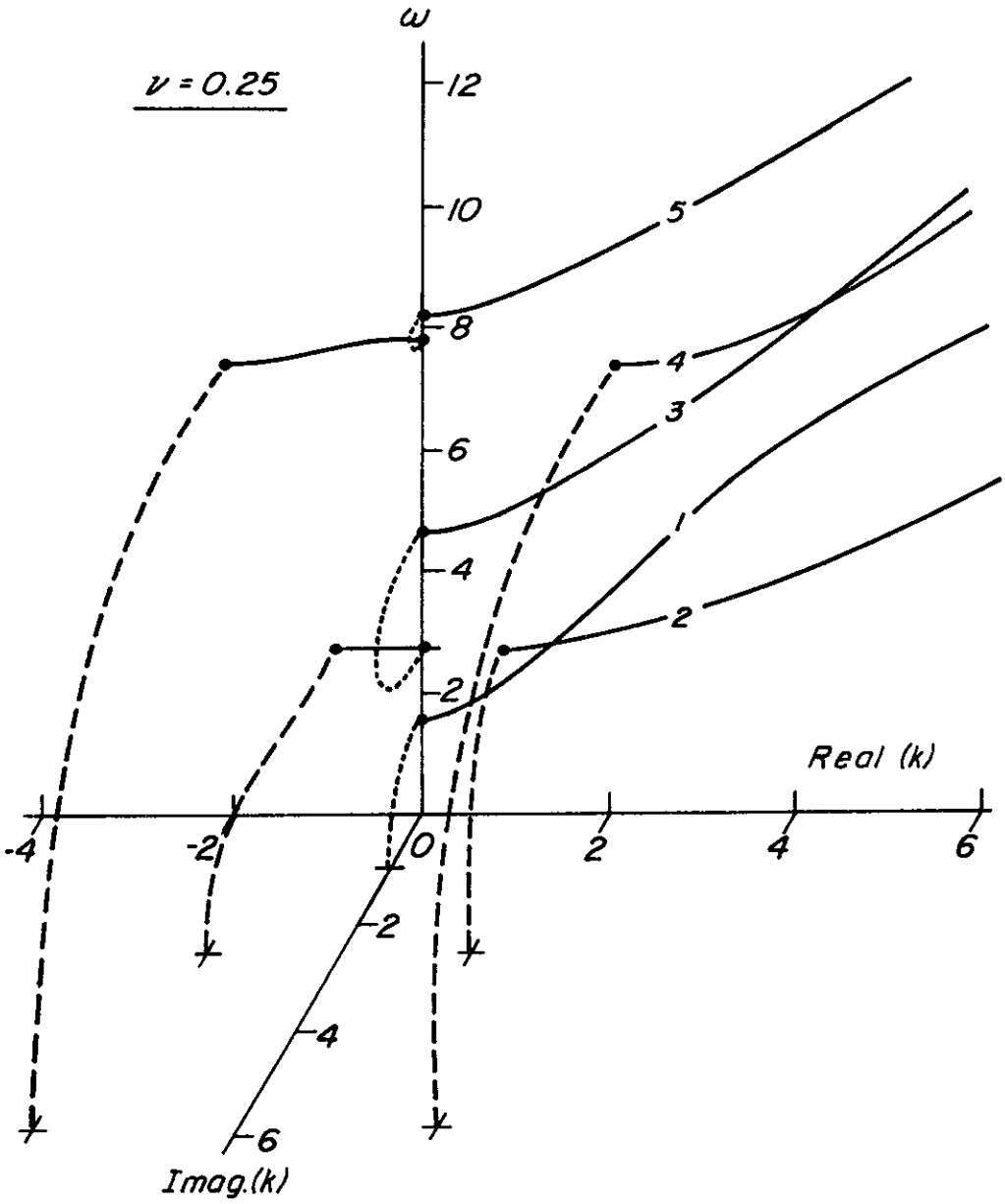

Fig. 2.5 SPECTRAL LINES FOR WAVE NUMBERS OF HOMOGENEOUS ELASTIC LAYER OVER ROUGH RIGID BASE

numbers. Sets of spectral lines with similar characteristics to those in Fig.2.5 have been presented for extensional waves in semi-infinite hollow elastic rods by McNiven and Shah (1966). Since Eq. (2.22) is an analytic function in ω and k it may be proven that the spectral lines intersect the planes $\omega = 0$, Real(k) = 0 , and Imaginary(k) = 0 at right angles. In addition, when a complex branch intersects the real plane it does so at a point on a branch in the real plane where the slope is zero. Appendix 1 outlines a proof of the above conditions in a similar manner to that developed for waves in elastic hollow rods by McNiven, Shah and Sackman (1965) and McNiven, Sackman and Shah (1965) or for solid rods by Onoe, McNiven and Mindlin (1962).

Fig.2.5 implies that at any given frequency, ω , the motion at the free surface may be thought of as resulting from the combined action of an infinite number of waves, each corresponding to a particular root of Eq. (2.22). Thus, although the motion may be extremely complex, it is possible to break it down into component parts the mathematical expressions for which are relatively easy to associate with their physical behavior. Fig. 2.5 contains all four possible conditions for the wave number k . The physical significance of each type is summarized below.

Wave Types

The motion of particles associated with any root of Eq. (2.22) may be expressed as

$$\delta_x = u(z) \cdot \exp(i\omega t - ikx)$$

and

$$\delta_z = w(z) \cdot \exp(i\omega t - ikx) \qquad (2.23)$$

where $u(z)$ and $w(z)$ are the horizontal and vertical displacements respectively, as defined by Eqs. (2.7), the magnitudes of which are a function of the depth, z, below the free surface. As k may be real, imaginary or complex Eq. (2.23) may describe any one of the following wave types.

1. If k is complex

$$\exp(i\omega t - ikx) = \exp(k_2 x) \cdot \exp(i\omega t - ik_1 x) \quad \text{where } k = k_1 + ik_2 . \tag{2.24}$$

Then Eq. (2.23) describes a motion which propagates in the x-direction with the phase velocity $c = \omega/k_1$ but decays or increases in amplitude depending upon the sign of k_2. This type of motion will be called a decaying mode.

2. If k is real

$$\exp(i\omega t - ikx) = \exp(i\omega t - ik_1 x) \quad \text{as } k_2 = 0 . \tag{2.25}$$

This motion propagates in the x direction with constant amplitude and will be called a real mode.

3. If k is imaginary

As $k_1 = 0$

$$\exp(i\omega t - ikx) = \exp(k_2 x) \cdot \exp(i\omega t) . \tag{2.26}$$

This type of motion will be called an exponential mode. There is no propagation in this case.

4. If $k = 0$

Now

$$\exp(i\omega t - ikx) = \exp(i\omega t) . \qquad (2.27)$$

This condition corresponds to a standing P- or S-wave which travels vertically through the elastic layer. Such a mode will be called a pure P-mode or pure S-mode depending on the type of standing wave.

Illustrations of these various wave types are given in Fig. 2.6. The existence of a decaying mode in a perfectly elastic layer bounded at the surface by vacuum and at the base by a rigid solid deserves some explanation. Such a mode would normally indicate that energy is being lost from the system; for example, by conversion of kinetic energy into heat in a medium with material damping. No such energy loss can occur in the system considered here. However, as shown in Fig. 2.5 the complex branches of the spectral lines occur in pairs with wave numbers $k = k_1 - ik_2$ and $k = -k_1 - ik_2$ which are equal in their absolute magnitudes. This means that the net transport of energy to $x = +\infty$ is zero.

Dispersion

It was noted previously that the phase velocity $c = \omega/k$ was a constant in the case of wave propagation in a homogeneous elastic half-space. This is not the case for any of the branches in Fig. 2.5. Here $c = f(\omega)$ and the system is said to be dispersive. Graphical representations of the secular function have traditionally been known as dispersion curves although only the projection of the function on to the real plane are normally presented. Dispersion curves are also

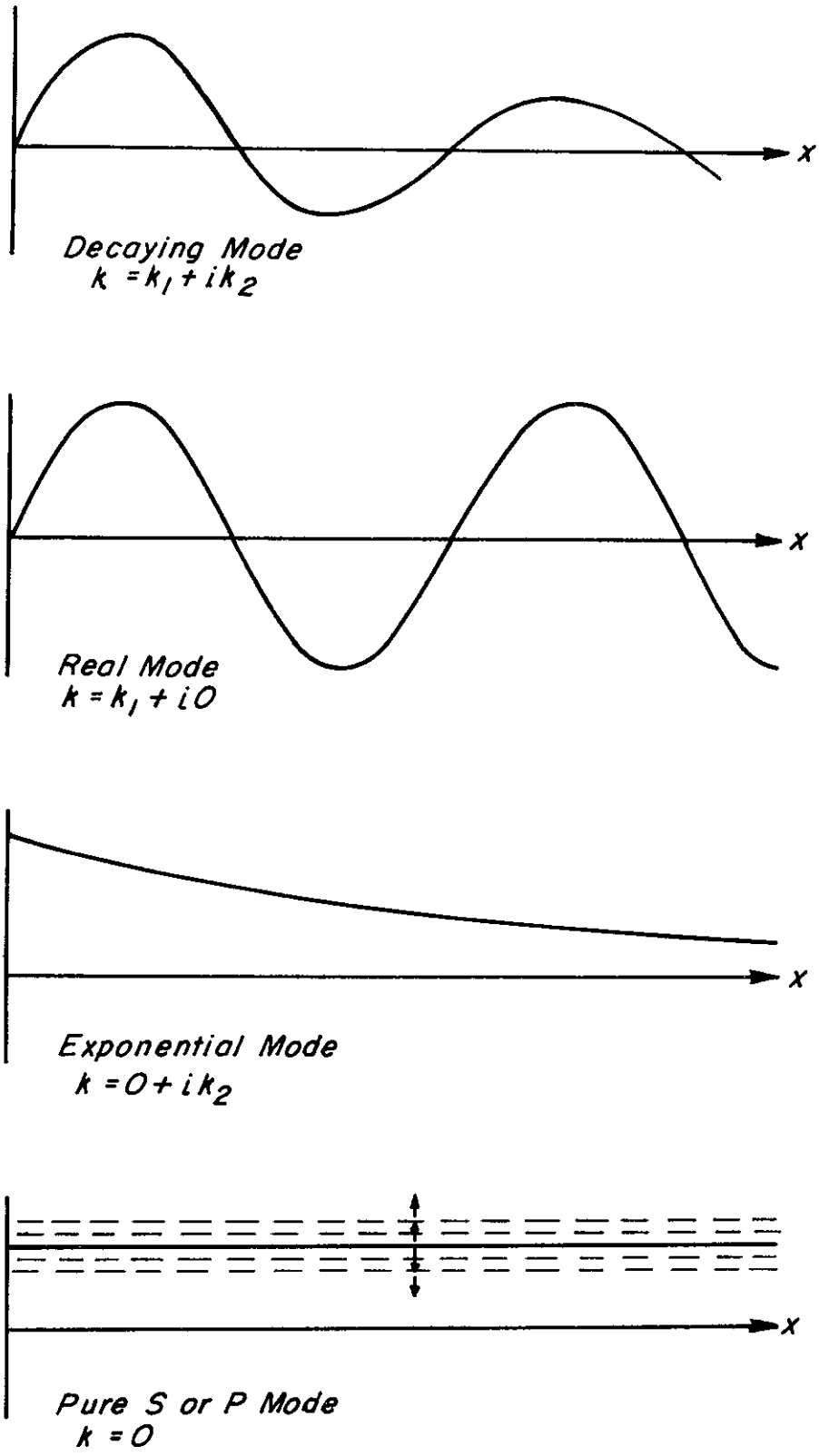

Fig. 2.6 WAVE TYPES WHICH MAY EXIST IN LAYERED ELASTIC MEDIA

commonly plotted on the axes frequency (or period) against phase velocity c.

A Multi-layered Half-space

It is only in a few cases that a homogeneous layer exists whose thickness is so great, compared with the wave length, that the theories for a half space are applicable. Equally, a single layer over a rigid solid is of minimal practical significance, although this model may approximate a soft deposit over a hard rock stratum. However, the principal phenomena described in the previous section are all present in multi-layered systems but are superimposed in a very complex manner. The ability to analyze complex structures, and ideally a generalized multi-layered system, is of great importance to the progress of the wave propagation method of testing in-situ structures. Some approaches to this problem will be discussed in the next chapter.

CHAPTER 3

METHODS FOR THE ANALYSIS OF WAVE PROPAGATION IN LAYERED MEDIA

The desire to understand the mechanism by which seismic tremors propagate through the earth and along its surface led the early geophysicists to attempt the development of analytic methods for the study of these phenomena. The nature of disturbances excited from within an infinite elastic body was well understood by the mid nineteenth century, for example, Stokes (1849), but the first major contribution to the understanding of the transmission of seismic waves was made by Lord Rayleigh (1885). By the application of elastic theory he was able to analyze the nature of waves at the plane surface of a semi-infinite solid. However, the recognition that the earth's crust is composed of layers having marked differences in their properties required investigation of more complex situations. Bromwich (1898) made the first analysis of the case of a plane surface layer bonded to a semi-infinite solid and a comprehensive treatment of this model was presented by Love (1926). Further work on this model has been undertaken by many authors including Fu (1946a and 1946b) who used an approach based on matrix algebra which gives useful insights into some of the basic phenomena in a manner similar to that used in some of the more modern analytic techniques. The efforts of these workers greatly advanced understanding of wave propagation phenomena, such as the effects of surfaces and interfaces on wave propagation. A number of basic ideas have been presented in the previous chapter. The general case of a multi-layered system is so complex, however, that significant advances in understanding could only make for simplified and idealized

models of special cases. Many of these models, nevertheless, contributed greatly to geophysics as they simulated many of the situations actually founded in the earth's crust, such as liquid to solid contracts and surfaces of separation between two solids. See, for example, Stoneley (1924) and Tolstoy and Usdin (1953). Comprehensive reviews of the available method for treating the problems of two and three layered media are to be found in Ewing, Jardetsky and Press (1957), Brekhovskikh (1960) and Červený and Ravindra (1971), who also discuss problems involving the multi-layered case. With the exception of Sezawa (1938), researchers were interested in analyzing systems in which rigidity increased with depth, which is the case in practically all geophysical instances. Sezawa (1938) concluded that above a certain frequency surface waves could not be propagated in systems in which rigidity decreased with depth. The phase velocity corresponding to this limiting frequency was predicted to be that of a shear wave propagating in the softer, deeper material. However, in studies undertaken for the wave propagation testing technique, Jones (1962) showed that this conclusion is untrue and that surface waves can be propagated at velocities greater than the shear wave velocity of the less rigid substratum.

Unlike geophysical problems, many engineering applications involve the propagation of dynamic waves in structures which are stiffer than the materials upon which they are founded. The dynamic testing of pavements poses a classic problem of this type and after Sezawa (1938) the next study of a surface layer bonded to a softer substratum was undertaken by Pickett (1945) in connection with this type of work. A case, in which the ratio of the velocity of propagation of shear waves

in the upper layer to that in the lower layer was 1.41, was analyzed. He showed that at high frequencies the velocity of the surface wave is asymptotic to the velocity of a Rayleigh wave in the upper material; at low frequencies to that of the substratum.

The mathematical difficulties involved in the analyses of multi-layered systems forced engineers to study simplified models and special cases in an approach similar to that taken by the geophysicists. The models studied and the approximations made were influenced by empirical data obtained from field tests, mainly on highway pavements. Some of the work was directed to interpret results from tests with the heavy vibrators used to measure the dynamic stiffness of pavements. Methods based on elastic theory, for rotating mass vibrators on semi-infinite solids, were available (Reissner, 1936 and Sung, 1953). Most of these analyses involved modelling the vibrator/pavement system by various spring, dashpot and mass systems. See, for example, Jones (1958) and Heukelom and Foster (1960). Certain special cases were open to solution by established methods. Noting Pickett's (1945) earlier work Jones (1955) approximated a concrete road slab resting on a soft base to an elastic plate without support. He then applied Lamb's (1916) solution for this case and was able to use this analysis to evaluate the thickness of pavement slabs from the results of wave propagation tests.

Methods for Solution of the General Equations of Motion

Jones (1962) also applied the elastic theory to analyze layered systems which approximate more general pavement structures. His approach is similar to that outlined in Chapter 2 in which the boundary conditions imposed by the surface and the layer interfaces are used to

obtain appropriate forms of the general solution to the equations of motion for wave propagation. Three types of structure were considered:

1. A layer of material over a semi-infinite half-space of lower elastic modulus.
2. As in 1 but with an intermediate layer having elastic properties such that the compressional wave velocity is less than in the underlying medium.
3. As in 2 but with the intermediate layer having elastic moduli comparable with those of the surface layer but considerably greater than those of the underlying medium.

In each case it was assumed that the layers were homogeneous and elastic and infinite in both horizontal directions. Only plane waves were considered. In application to the interpretation of results from the wave propagation method this approximation is reasonable. Although the vibratory source is in practice applied to a circular area of finite radius, the asymmetric waves propagating into the structure become almost identical with plane waves within a very short distance from the source. The general solutions for these multilayered cases take the form of families of secular lines in complex space which exhibit characteristics similar to those illustrated in Fig. 2.5 for a single layer over a rigid half-space. The derivation of quantitative results poses many analytic and numerical differences. However, by making certain simplifying assumptions Jones (1962) was able to obtain approximate solutions for certain frequency ranges which are of considerable practical importance.

For Case 1 the underlying semi-infinite medium was assumed to have a Poisson's ratio of 0.5 and a velocity of propagation of shear waves so low compared to the overlying layer that it could be treated as a liquid. By considering the solutions to this simplified problem in the limiting cases of high frequencies (very short wave lengths) and low frequencies (long wave lengths) and with the aid of techniques developed by Osborne and Hart (1945), for the analysis of submerged plates, the results shown in Fig. 3.1 were obtained.

For Case 2 of a double layer over a half-space Jones (1962) assumed that the intermediate layer as well as the substratum could be treated as a half-space. For Case 3 it was assumed that at high frequencies the two layers responded to excitation independently of the subgrade and the system was analyzed as a composite free plate. Thus, Jones (1962) made simplifying assumptions in each case and, while some experimental results agree well with this approximate theory, the analysis breaks down in the intermediate frequency and velocity ranges and does not explain some of the modes of propagation actually observed in the field. Valuable insights were gained, however, and later work enabled some of the analyses to be refined (Jones and Thrower, 1965b). Jones and Thrower (1965a) were also able to show that an assumption of welded contact between layers was valid in application to analysis of wave propagation testing of pavements.

Jones' work was extended by Vidale (1964) who studied the same basic structures but included the shear rigidities of all layers, including the half-space, and investigated the properties of dispersion curves in the intermediate velocity ranges. Vidale (1964) was able to improve the understanding of some of the basic characteristics of

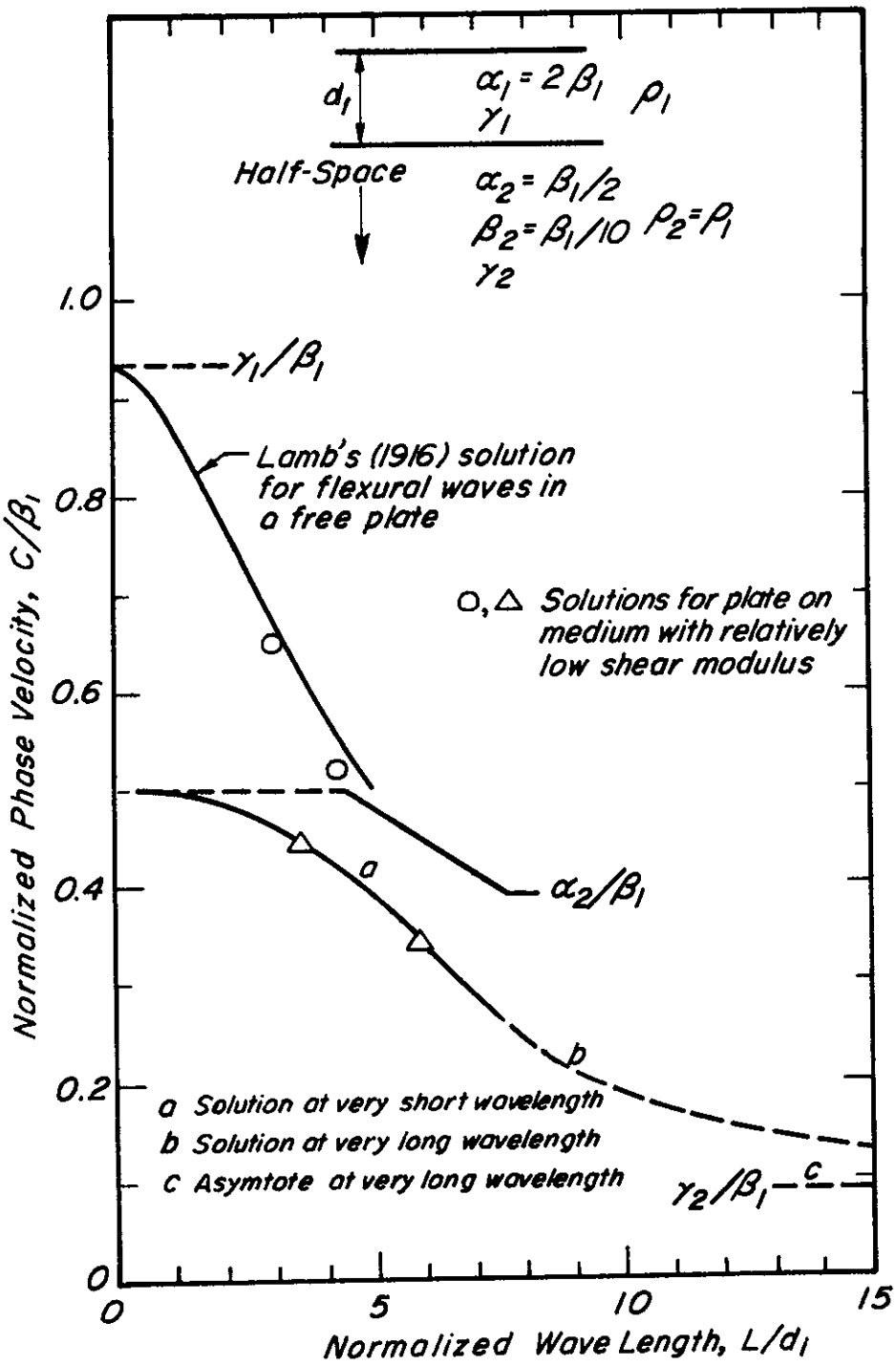

Fig. 3.1 JONES' (1962) RESULTS FOR DISPERSION OF WAVES IN A PLATE OVERLYING A MEDIUM OF LOW SHEAR MODULUS

dispersion curves for a number of typical pavement structures and this work has been used successfully as an aid in the interpretation of wave propagation test data. For the more complex structures, however, a number of uncertainties remain. The problems stem largely from the numerical problems involved in obtaining the roots to the secular equations and the numerous singularities present in the solution. The results obtained will be discussed further in the next chapter.

A method of analysis in which the equation of motion for a generalized system of elastic layers overlying an elastic half-space are formulated in matrix algebra was proposed by Thomson (1950), improved by Haskell (1953) and presented in the form of a computer program by Press, Harkrider and Seafeldt (1961). This formulation is well suited to solution with the aid of a digital computer but there remains a number of difficulties in applying the method directly, particularly to problems involving structures in which rigidity decreases with depth. These difficulties arise primarily from the fact that the analysis involves the use of hyperbolic functions, which may become numerically very large, and the peculiar behavior of solution in certain regions which renders numerical values of the solution very difficult to obtain. The extremely high accuracy required of the computation if details of the displacement field are to be computed is also a disadvantage of the method. Quantitative solutions also require that a first approximation to any desired root (of which there are an infinite number) is used to initiate the procedure. Due to the present limited knowledge of the form of the secular lines for many problems, this can be a severe limitation. Thrower (1965) has discussed many of these problems and proposed a method by which improved numerical results may be obtained for certain cases.

The approximation that practical structures are composed of purely elastic materials is not unreasonable when the empirically observed response of many materials, particularly soils, to dynamic loadings is considered. Theoretical models would, of course, be improved by the addition of factors to account for internal damping. In addition, it has been found that the singularities in the solutions for wave disperson in elastic systems are not present in the secular lines for structures formed of viscoelastic materials. By defining the various moduli of viscoelastic materials in the form of a complex number it is possible to incorporate this improvement in analyses with a minimum of effort. The rheological characteristics of soils and bituminous concrete and the method of complex moduli are discussed in Appendix 6.

A method for the analysis of wave dispersion in generalized, layered, viscoelastic structures resting either on a viscoelastic half-space or a rigid solid is presented in Appendix 2. The method is based on Haskell's (1953) matrix formulation. A discussion of the limitations and numerical difficulties of this method are also discussed in more detail in this appendix. A computer program (HASK) which takes advantage of the complex algebra capability of the FORTRAN language to incorporate the ability to analyze viscoelastic systems defined with the aid of the method of complex moduli is described in Appendix 3. The program is derived from the analytic methods described in Appendix 2.

Despite the increasing sophistication of the analyses discussed above, they are all based on the same fundamental approach. That is, the application of various boundary conditions to the general equations of motion and the solution of the resulting differential equations.

For this reason they all exhibit characteristics which make for serious difficulties in their quantitative solution.

Solutions Using Discretized Models

The establishment of the finite element technique as one of the most powerful numerical methods used in engineering analysis (Zienkiewicz, 1971) has encouraged its application to problems and situations involving dynamic loading. See, for example, Costantino (1967). For most dynamic problems, however, the finite element method involves the manipulation of very large matrices which often demands storage capacity which can only be provided by the largest digital computers, if at all. The computations may also be correspondingly costly. These problems are particularly acute in geotechnical applications. For all practical purposes the earth is of infinite size, while any model of a structure resting on the earth must, by necessity, be bounded at finite distances. Thus, when using discretized models, there is always the need to compromise between the accuracy of the model and the finite capacity of the computing facilities. For the case of wave propagation in layered media this problem was considerably reduced by Lysmer (1970) who developed a method for discretizing a layered structure into a series of layers of infinite horizontal extent. In this manner the discretized models is confined by only one finite boundary; that at the bottom. This model may no longer be strictly referred to as a finite element discretization, as the layers are, by definition, not finite. Based on the fundamental approach employed by the technique this will be designated the "direct stiffness" method. Lysmer and Drake (1972) have illustrated the use of the method for the analysis of both Love and Rayleigh wave propagating in horizontally layered media.

By considering discretized units composed of layers of infinite horizontal extent Lysmer's (1970) direct stiffness method lacks the generality which is one of the strongest features of the finite element method. By considering a model composed of three zones, Waas (1972) was able to restore this ability of the finite element method to deal with very complex geometries while maintaining the advantage of a model extending to infinity in the horizontal dimension. Fig. 3.2 shows a typical structure discretized in this manner. The irregular zone (I) contains all the complex geometry, zones of varying material properties and external loading. It is discretized into finite elements. Zones L and R are simple layered structures (each layer may be composed of a different material) with each layer extending to infinity in the y and left and right x directions respectively. The analysis of the irregular zone follows the established finite element formulation, while Zones L and R are treated in the manner proposed by Lysmer (1970). By considering the boundary conditions at the interfaces between the zones the excitation field for the complete system may be computed. The theoretical development of this method of analysis is outlined in Appendix 4.

This direct stiffness analytic technique offers a number of advantages over the traditional methods for solution of the equations of motion. Due to the discretization of the model and its finite (or semi-infinite) dimensions there are a finite number of solutions to the secular equation for any model. Further, mathematical techniques are available which allow all of the roots to be obtained without ambiguity. The computation of mode shapes is easily performed and does not require numerical accuracy in excess of that required to

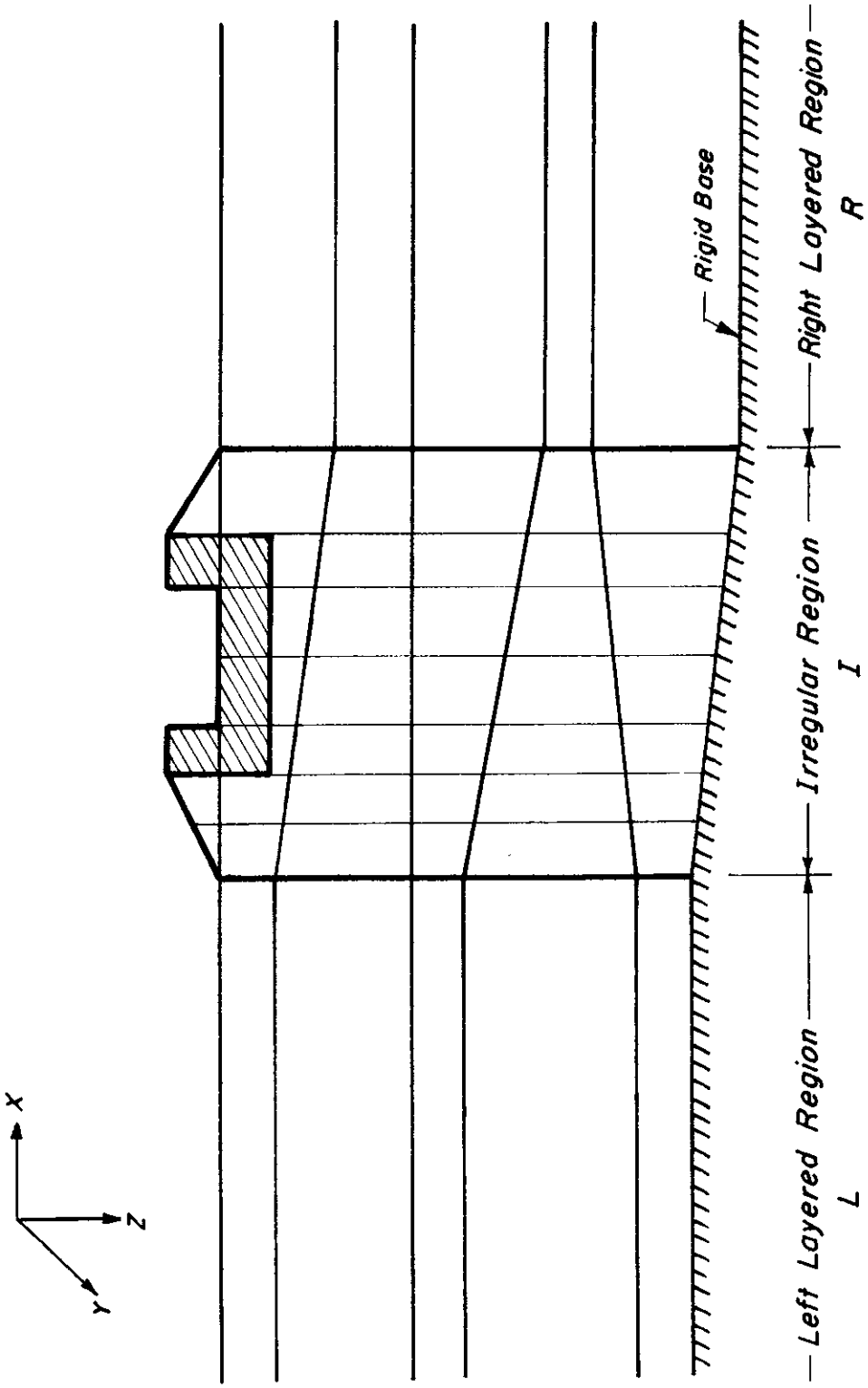

Fig. 3.2 DISCRETIZATION OF A TYPICAL PLANE STRUCTURE

obtain the basic characteristics of the wave form (e.g., the wave number). As it is possible to model the loading of the structure, it is also possible to compute the amplitude of excitation at any point within the field or on the surface at any distance from the source. The contribution of each mode of propagation to the total amplitude may also be computed and this provides the possibility of discriminating between modes which contribute heavily to the surface motion detected by instruments in a vibratory testing situation and those modes which are of little practical significance.

The formulation of this method of analysis is well adapted for use in the form of a computer program and may be used to solve problems involving viscoelastic material properties with no added difficulty. In summary, the direct stiffness method is capable of providing the maximum of detailed information with a minimum of numerical difficulies. A computer program based on this method, designed to analyze plane propagation in horizontally layered systems, is presented in Appendix 5.

However, despite the significant advantages of the direct stiffness technique, it suffers from two major practical limitations. The discretized model is not capable of simulating a prototype composed of layers resting on a semi-infinite half-space. The base of the model will always represent a rigid solid, as shown in Fig. 3.2. In a majority of practical engineering situations, particularly in application to pavement analysis, it is more accurate to assume that the structure rests on a relatively soft material of infinite depth. The rigid base of the model introduces a surface from which impinging energy may be reflected back into the structure when in fact no such reflector exists in nature. While modifications of the rigid boundary have

been proposed (Lysmer and Kuhlemeyer, 1969 and Ang and Newmark, 1971) and have been demonstrated to be successful in absorbing a majority of the impinging energy (Hadala, 1971), no fully satisfactory boundary has been developed which can be used where there is a steady state source of excitation. A discussion of the problem of a finite model of an infinite prototype and a method for minimizing energy reflection from the base of a discretized model will be found in Appendix 4.

The accuracy of the direct stiffness method is dependent upon the size of the elements into which the model is discretized. Shipley, Leistner and Jones (1967) observed that finite element models behave like low pass filters having definite passing bands and cut-off frequencies and that the cut-off frequency depends upon the wave type and finite element mesh. From experience in the use of the finite element method for the solution of wave propagation problems, Kuhlemeyer and Lysmer (1973) recommend that the maximum length of an element (or depth of a layer in the case of Zone L and R in Fig. 3.2) should not exceed one-eighth of the wave length of the slowest body wave propagating in the material for analysis of two- or three-dimensional layered media. Even when Lysmer's (1970) method of discretizing into layers of infinite horizontal extent is used, this restriction often generates linear algebraic equations involving matrices of very large dimension. Models of pavement structures resting on soft materials will thus require extensive computer core for their solution and the cost of the computations will be correspondingly high. This problem is aggravated by the desire to place the artificial rigid base of the model at the maximum possible depth so as to minimize its influence on the surface excitation.

Summary

Thus, there are presently available two basic approaches to the problem of the analysis of wave propagation in layered media. One approach attempts the solution of the basic equations of motion in differential form. These methods result in expression which pose a number of serious difficulties to numerical solution. Secondly, a structure may be simulated by a discretized model which may be analyzed with relative ease to yield a maximum of information about the nature of the excitation. These models, however, may not always provide realistic simulations of practical structures and solutions using this method may be excessively costly.

The wave propagation method of testing relies on the ability to interpret the data obtained in the field so that the characteristics of the structure beneath the surface may be determined. This interpretative ability relies, fundamentally, on comparison of the field data with the expected behavior of typical man-made or natural structures which have been simulated in theoretical analysis. This problem of determining the structure associated with a given set of data (dispersion curve) is very complex, and it seems as yet uncertain under what conditions unique solutions exist (Alekseev, 1962 and Knopoff, 1962). Detailed analytic solutions for many of the more complex, but practically important, structures are lacking but by comparing empirical data with the available analytic solutions a considerable amount of useful information can be obtained. The next chapter discusses these interpretative techniques.

CHAPTER 4

A REVIEW OF DATA INTERPRETATION FOR WAVE PROPAGATION TESTS

The interpretation of data from wave propagation tests has historically lagged advances in equipment design and improvements in field testing techniques. This has, in large part, been due to the limited ability to provide theoretical analyses of typical structures. This has resulted in a significant quantity of field data being rendered redundant due to the inability to utilize it at the interpretation stage. Equipment design has, in turn, been influenced by available interpretation methods. Methods of interpretation may be divided into four broad types, although considerable overlapping may occur and elements of each method type may be used in any given application. The four types may be categorized as follows:

1. Simple asymptote method.
2. Interpretation supplemented by seismic test data.
3. Methods relying on the detailed comparison of empirical dispersion curves with theoretical curves for simplified plate-like structures.
4. Methods dependent upon knowledge of the general characteristics of the spectral lines and dispersion curves of structures similar to those under test.

Simple Asymptote Method

This is the most basic interpretation method and is applicable to only the most simple situations. Fundamentally it is only applicable to the case where the structure may be reliably approximated to a

homogeneous elastic half-space. In this case the surface wave is a single mode propagating with a velocity equal to the velocity of propagation of a Rayleigh wave (see Chapter 2). The wave velocity may then be related to the material properties of the half-space as follows:

$$c = \gamma \simeq \beta = \sqrt{\frac{G}{\rho}} \tag{4.1}$$

where

c = apparent velocity of the surface wave

γ = velocity of propagation of Rayleigh wave

β = velocity of propagation of a shear wave

G = shear modulus

ρ = mass density .

By making suitable assumptions, or from independent determination of the mass density of the material, the shear modulus may be obtained from Eq.(4.1). In addition, if the Poisson's ratio for the material is known, or can be reliably estimated, the approximation that the Rayleigh wave velocity is equal to the shear wave velocity may be eliminated by reference to the relationship given in Fig. 2.3. The Young's modulus (compression modulus) may also be obtained from the relationship:

$$E = 2(1 + \nu)G \tag{4.2}$$

where:

E = Young's modulus

ν = Poisson's ratio

G = Shear modulus

This method of interpretation may be extended to cases involving single surface layers over a half-space. Fig. 4.1 shows a hypothetical dispersion curve obtained from a structure consisting of a relatively rigid layer over a softer half-space $(\beta_1/\beta_2 = 4)$. The portion of the dispersion curve obtained from high frequency (short wave length) vibratory tests is asymptotic to the velocity of propagation of Rayleigh waves in the surface material. This is due to the fact that Rayleigh waves are a boundary phenomenon (see Chapter 2) and the dynamic excitation, both horizontally and vertically, is substantially confined to a zone within about 1.5 wave lengths from the surface and, beyond a depth of about 2.0 wave lengths, the displacements are practically insignificant. Thus, as the wave length of the propagating wave tends toward zero, the influence of the material comprising the half-space has decreasing influence on the velocity of the surface wave. Conversely, at very long wave lengths the volume of material subjected to significant excitation is dominantly composed of the material forming the half-space and the dispersion curve becomes asymptotic to the velocity of propagation of waves in the half-space material. These interpretations allow some information to be gained about material lying beneath structures but, due to limitations in the frequency range capacity of any given vibratory equipment, rather crude approximations are often required to determine the asymptote, especially in cases involving high rigidity surface layers such as concrete pavements.

Vibratory/Seismic Methods

The simple method of interpretation described above actually yields no fundamental properties without the input of assumptions regarding the mass density and Poisson's ratio of the material. This problem

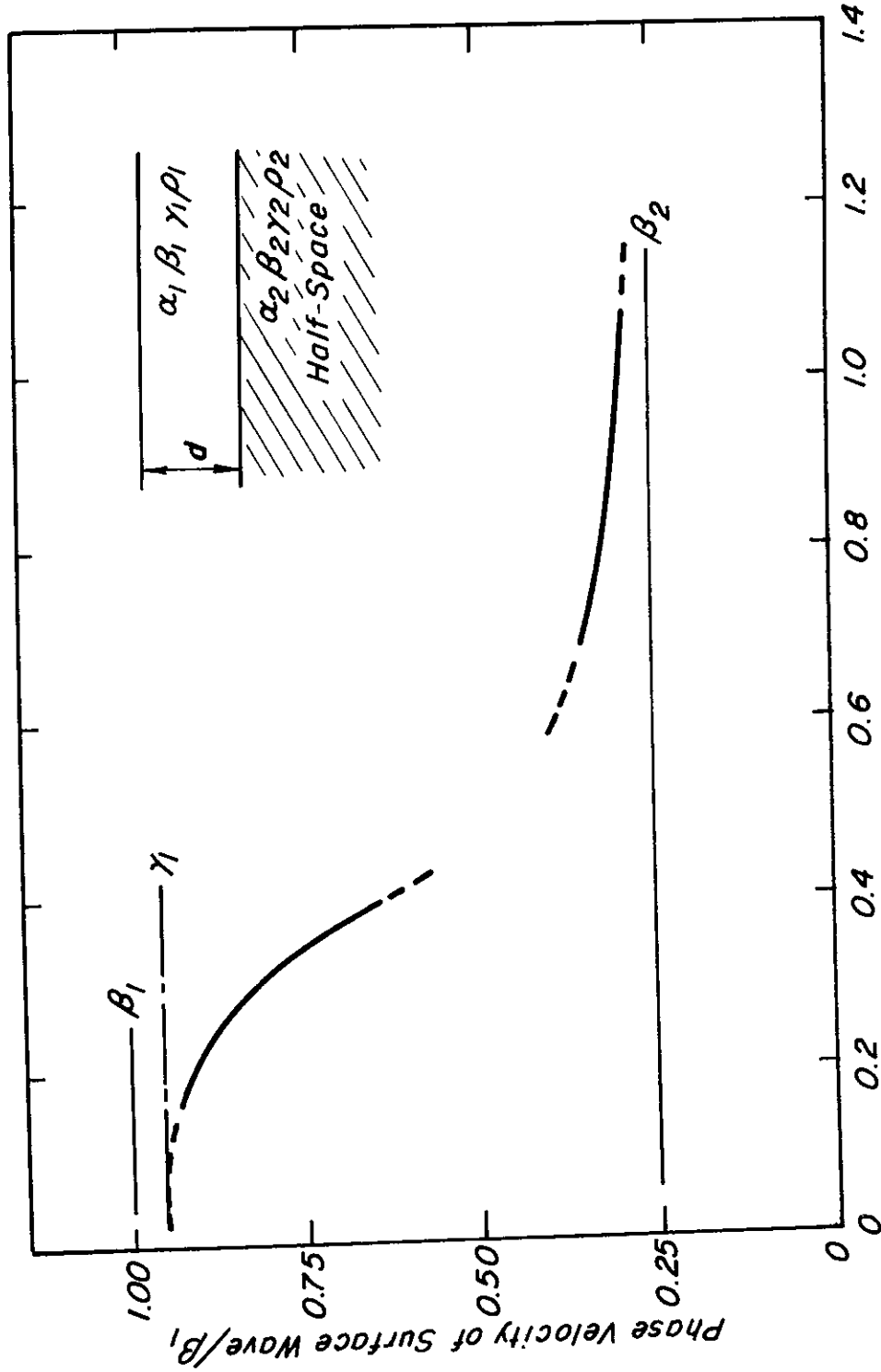

Fig. 4.1 HYPOTHETICAL DISPERSION CURVE OBTAINED FOR A HALF-SPACE BENEATH A LAYER OF GREATER RIGIDITY

limits the utility of the technique. The mass density of common materials can be readily approximated or determined independently without excessive effort. The Poisson's ratio, however, is not easily determined and reliable estimates are not normally readily available. The Young's modulus of materials is often of great interest and thus it would be desirable to achieve some means whereby the Poisson's ratio could be obtained by direct measurement. The velocity of propagation of P-waves (compressional wave) in geologic structures may be obtained by the well established methods of seismic investigation. These methods have been used (Maxwell and Fry, 1967) in conjunction with vibratory testing in situations where data was required for strata at great depth, such as at sites of excavation by nuclear explosives. The velocity of propagation of a P-wave is

$$\alpha = \sqrt{\frac{\lambda + 2G}{\rho}} \tag{4.3}$$

where λ = Lamé's constant,

and the three basic velocities of propagation are related by

$$\gamma = f\left(\frac{\alpha}{\beta}\right) . \tag{4.4}$$

In studies of pavement structures the added information to be gained from the supplementation of the vibratory method by seismic surveys has not been pursued due to the greatly expanded time and expense required to obtain data for each inspection site. There is also the problem of interpretation of seismic test data for such detailed structures as multi-layered pavements and the limited ability to analyze cases in

which accoustic rigidity decreases with depth, as discussed in the previous chapter.

Plate Theory Methods

The development of methods for the theoretical analysis of layered structures, in which the material properties allow the use of simplified models comprising single and double horizontal plates, has been discussed in Chapter 3. Experimental results obtained on highway pavements having a single upper layer of relatively high shear modulus of elasticity have shown that a "free-plate" approximation is justified at phase velocities which are appreciably greater than the velocity of compressional waves in the underlying medium (Jones, 1962). Wave propagation testing techniques for highways, particularly concrete pavements, were developed to take advantage of this fact. The interpretation procedure relies on the short wave length portion of the dispersion curves and thus is well suited to testing with equipment based on light weight, high frequency vibrators.

Consider a single layer of infinite horizontal dimensions resting in welded contact on a half-space as shown in Fig. 4.2. The equations of motion at any point within this system are as defined in Eqs. (2.16). The boundary conditions are, at the free surface the normal and shear stresses are zero, at the interface the stresses and displacements are continuous and at great depth (i.e. $z \to \infty$) the displacements tend to zero. Applying these constraints and using Eqs. (2.16) yields the determinant expression:

$$
\begin{vmatrix}
2kr_1\mathrm{Sinh}(ikr_1d) & 2kr_1\mathrm{Cosh}(ikr_1d) & b_1\mathrm{Cosh}(iks_1d) & b_1\mathrm{Sinh}(iks_1d) & 0 & 0 \\
b_1\mathrm{Cosh}(ikr_1d) & b_1\mathrm{Sinh}(ikr_1d) & 2ks_1\mathrm{Sinh}(iks_1d) & 2ks_1\mathrm{Sinh}(iks_1d) & 0 & 0 \\
1 & 0 & 0 & ks_1 & 1 & -ks_2 \\
0 & kr_1 & 1 & 0 & kr_2 & 1 \\
0 & 2kr_1G_1 & b_1G_1 & 0 & 2kr_2G_2 & b_2G_2 \\
b_1G_1 & 0 & 0 & 2ks_1G_1 & b_2G_2 & -2ks_2G_2
\end{vmatrix} = 0 . \qquad (4.5)
$$

in which the symbols are as previously defined in Chapter 2 and the subscript 1 refers to the surface layer and 2 to the half-space. To make the solution of Eq. (4.5) tractable Jones (1962) proposed that it is reasonably accurate, for many practical cases, to neglect the shear strength of the half-space and deal with a layer resting on a semi-infinite liquid. Then with $G_2 = 0$ (i.e. $\beta_2 = 0$) in Eq. (4.5) the solution to this reduced problem is

$$P\{2Q + \delta \operatorname{Cosh}(\tfrac{1}{2} ikr_1 d) \operatorname{Cosh}(\tfrac{1}{2} iks_1 d\} + Q\,\delta \operatorname{Sinh}(\tfrac{1}{2} ikr_1 d) \operatorname{Sinh}(\tfrac{1}{2} is_1 d_1) = 0 \tag{4.6}$$

where

$$P = b_1^2 \operatorname{Cosh}(\tfrac{1}{2} ikr_1 d) \operatorname{Sinh}(\tfrac{1}{2} iks_1 d) - 4r_1 s_1 \operatorname{Sinh}(\tfrac{1}{2} ikr_1 d) \operatorname{Cosh}(\tfrac{1}{2} iks_1 d)$$

$$Q = b_1^2 \operatorname{Sinh}(\tfrac{1}{2} ikr_1 d) \operatorname{Cosh}(\tfrac{1}{2} iks_1 d) - 4r_1 s_1 \operatorname{Cosh}(\tfrac{1}{2} ikr_1 d) \operatorname{Sinh}(\tfrac{1}{2} iks_1 d)$$

and

$$\delta = \frac{\rho_2}{\rho_1} \frac{r_1}{r_2} \frac{c^4}{\beta_1^4} .$$

Jones (1962) presented a limited number of solutions to Eq. (4.6) but, in the case where the further approximation can be made that the upper layer is a free plate, Lamb's (1916) solution is applicable. In this case for longitudinal waves $P = 0$ and for flexural waves $Q = 0$ in Eq. (4.6) and the two types of solution reduce to:

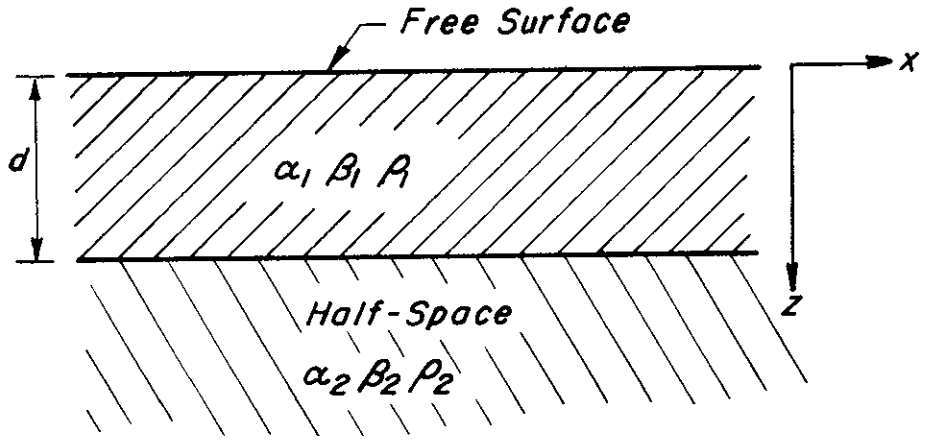

Fig. 4.2 A SINGLE LAYER RESTING ON A HALF-SPACE

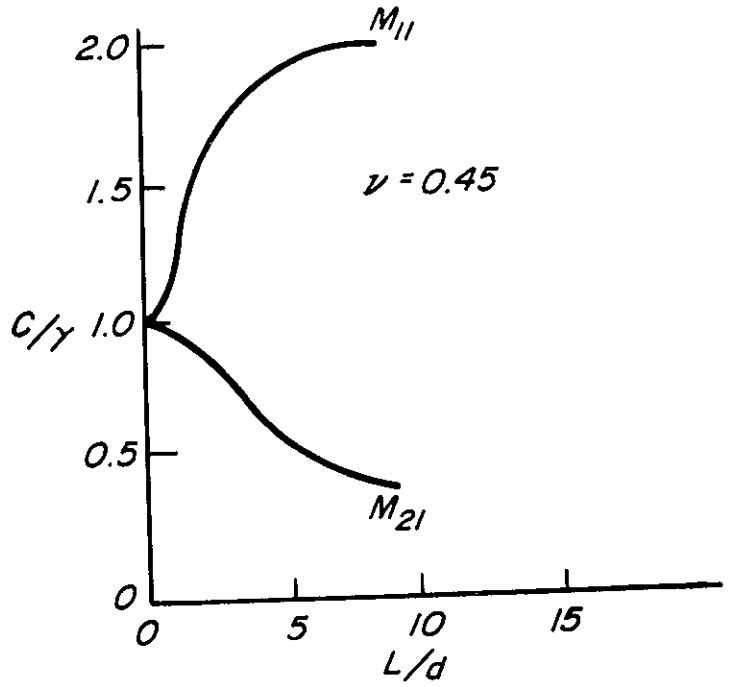

Fig. 4.3 PRINCIPAL BRANCHES OF DISPERSION CURVE FOR A FREE PLATE

$$\frac{\text{Tanh } (\frac{1}{2} \text{ ikr}_1 d)}{\text{Tanh } (\frac{1}{2} \text{ iks}_1 d)} = \frac{b^2}{4rs} \tag{4.7}$$

and

$$\frac{\text{Tanh } (\frac{1}{2} \text{ ikr}_1 d)}{\text{Tanh } (\frac{1}{2} \text{ iks}_1 d)} = \frac{4rs}{b^2} \quad . \tag{4.8}$$

The solutions of Eq. (4.6) for short waves (i.e. $k \to \infty$) are:

$$b_1^2 - 4r_1 s_1 = 0 \tag{4.9}$$

and

$$b_1^2 - 4r_1 s_1 + \delta = 0 \quad . \tag{4.10}$$

Eq. (4.9) corresponds to surface waves propagating along the surface with the Rayleigh wave velocity γ_1 appropriate to the upper layer and is identical to the free plate solution at zero wave length. As the Rayleigh wave velocity is a fundamental property of the plate material it may be conveniently used to normalize dispersion curves. The dispersion curves for a free plate representing the solutions to Eqs. (4.7) and (4.8) plotted on the normalized axes c/γ and L/d (c = phase velocity, γ = Rayleigh wave velocity, L = wave length and d = plate thickness) are shown in Fig. 4.3. An infinite number of solutions to Eqs. (4.7) and (4.8) exist but the higher modes are of little practical significance. In addition there is a separate family of curves for materials of differing Poisson's ratio, ν. Fig. 4.3 is for $\nu = 0.45$. The curve corresponding to Eq. (4.7) is known as the symmetric or longitudinal mode. In some of the literature, particularly in seismology, it may

be designated the M_{11} branch. This branch is of minor importance in vibratory testing as the majority of the energy generated is in the form of asymmetric or flexural waves represented by the M_{21} branch (Eq. 4.8). Fortunately, the shape of the M_{21} branch is affected to only a minor extent by variations in Poisson's ratio so that an error in its selection is not of major consequence.

Normalized free-plate dispersion curves are used in the interpretation of wave propagation test data in the following manner. The test results are reduced to phase velocities and wave lengths for each test frequency and plotted on fully logarithmic axes as shown in Fig. 4.4. These points are compared with the theoretical solutions to the dispersion of waves in a free plate drawn on a transparent material. It is convenient to construct the theoretical curves against the fully logarithmic axes γ/c and L/d so that in this normalized form only one curve is required for each value of Poisson's ratio. In addition, the axes used on the transparency are drawn in a position corresponding to a shift of the axes from the origin to some convenient ordinate and abcissus which allows the curves to be presented in a compact form. Fig. 4.4 represents an example in which the theoretical solution plotted in this form, for a material of Poisson's ratio = 0.25, has been overlaid onto experimental results. The full line represents Lamb's (1916) solution and is referred to the inner set of axes which are drawn at ordinate and abscissus corresponding to 400 m/s and 10 cm respectively. The axial shifts between this set of axes and the corresponding axes against which the experimental results are plotted are:

$$\text{Horizontal Axial Shift} = \text{Log } L + \text{Log } (d/L) = \text{Log } d \qquad (4.11)$$

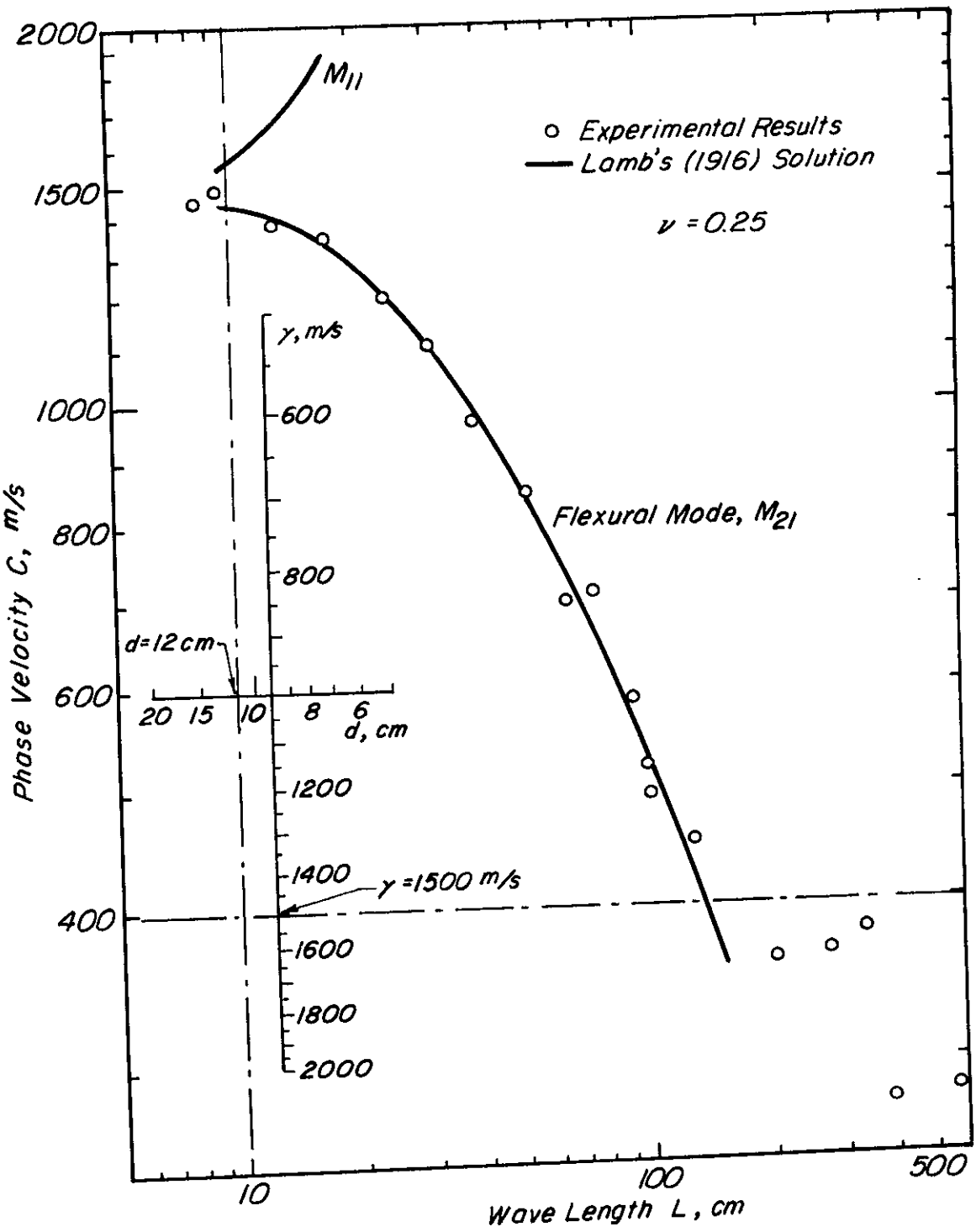

Fig. 4.4 INTERPRETATION BY COMPARISON WITH FREE PLATE SOLUTION

and

$$\text{Vertical Axial Shift} = \text{Log } c + \text{Log } (\gamma/c) = \text{Log } \gamma \ . \qquad (4.12)$$

By suitable annotation of the inner set of axes (associated with the normalized theoretical curve) the value of γ and d may thus be read directly at the point where the 400 m/s ordinate and the 10 cm abscissus of the experimental data plot intersects the inner set of axes. For the example in Fig. 4.4 these values are $\gamma = 1500$ m/s and $d = 12$ cm respectively. A set of transparencies designed for this method of interpretation has been published by Laboratoire Central des Ponts et Chaussées (1971) of France.

Interpretation methods based on the comparison of test data with theoretical dispersion curves for simplified structures may be extended to include structures composed of two surface layers over a half-space. Fig. 4.5 represents a structure of this type. By applying the appropriate boundary conditions and considering the equations of motion, it is possible to express the propagation equation for plane waves in such a structure in the form of an 8×8 determinant, the elements of which contain hyperbolic functions of a kind similar to those given in Eq. (4.5) for the single layer case. There are again an infinite number of discreet roots to the equation and solutions are not readily obtained (Jones, 1962). However, in a number of practical cases highway pavements consisting of two upper layers of relatively rigid materials overlying a soft half-space may be adequately approximated by a two-layer composite plate in free space (Jones and Thrower, 1965b). The solution to the wave propagation equation for this simplified model may be obtained either by methods of the type outlined in Chapter 3 or by the following approximation.

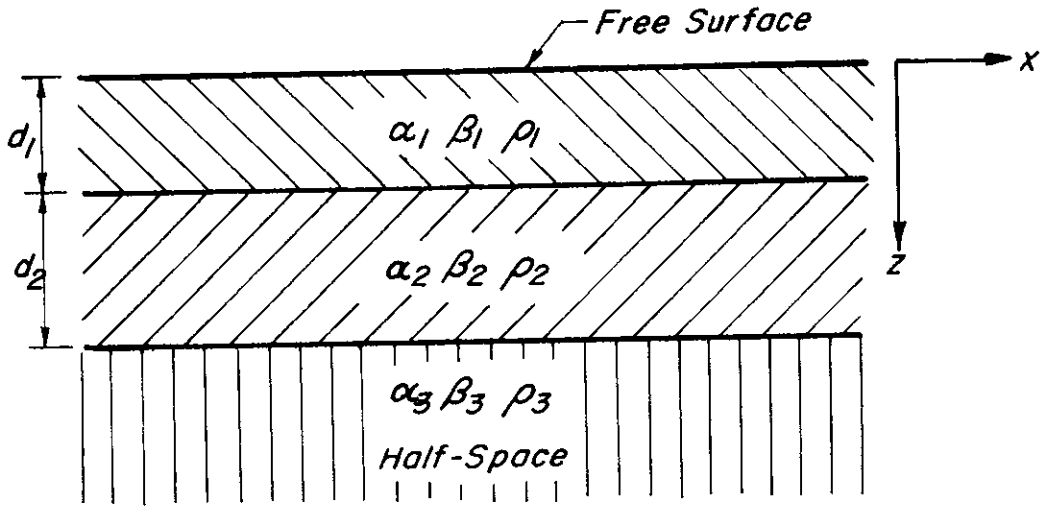

Fig. 4.5 LAYERED STRUCTURE COMPOSED OF TWO LAYERS OVER A HALF-SPACE

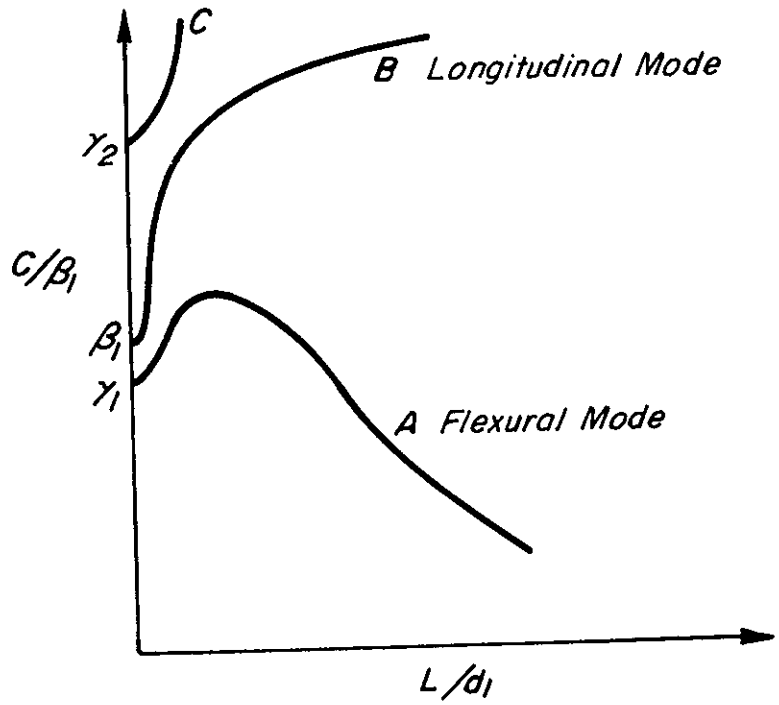

Fig. 4.6 PRINCIPAL BRANCHES OF DISPERSION CURVE FOR TWO-LAYER PLATE ($\beta_1 < \beta_2$)

Consider propagation in a uniform free plate. The dispersion equation is of the form

$$F(c/\beta \ , \ L/d) = 0 \ . \tag{4.13}$$

Thus, the wave length of disturbances propagating at a given phase velocity, in a plate formed by joining two plates of identical elastic properties in welded contact, is obtained by addition of the wave lengths of vibrations of the same velocity in each plate separately. If the components of the two-layer plate are not identical in thickness and elastic properties, this additive method is not accurate but Jones and Thrower (1965b) have shown that, for cases where the elastic properties are within the range $4:1 < G_1 : G_2 > 1:4$, the error involved in applying this method in less than $\pm$ 5%.

A typical dispersion curve obtained for a two-layer free plate is shown in Fig. 4.6. Branch A is similar in shape at long wave length to the principal flexural mode (M_{21}) shown in Fig. 4.3 for a single plate. At a shorter wave length it passes through a velocity maximum and ultimately approaches the lower of the two Rayleigh velocities (γ_1) at zero wave length. This suggests an asymptotic approach to a true Rayleigh wave propagating along the surface of the corresponding material.

Branch B corresponds to the longitudinal mode in a free plate at long wave length and at short wave length approaches the lower of the two shear wave velocities (β_1) .

Branch C approximates the higher of the two Rayleigh wave velocities (γ_2) at near zero wave length and is attributed to a surface wave at the free surface of the material of higher Rayleigh wave velocity. With increasing wave length the velocity tends to infinity and probably repre-

sents a wave resulting from the influence of the internal boundary between the two materials.

Interpretation techniques rely on the characteristics of Branch A alone and in practice points along Branch B or C are rarely obtained from test data. However, even after this simplification, the two-layer free plate approximation is much more difficult to apply to the interpretation problem than the corresponding single plate analogy. This is due to the greatly increased number of parameters involved. By normalization by properties of the surface layer, the two upper layers of the structure shown in Fig. 4.5 may be defined by the following five ratios:

$$\frac{d_2}{d_1}, \frac{\alpha_1}{\beta_1}, \frac{\alpha_2}{\beta_1}, \frac{\beta_2}{\beta_1} \text{ and } \frac{\rho_2}{\rho_1}.$$

It is usual to estimate reasonable values for the mass densities, ρ_1 and ρ_2, and the Poisson's ratios ν_1 and ν_2 for both of the layers by independent methods. These estimates fix the values of the ratios ρ_2/ρ_1 and α_1/β_1 and in addition yield an estimate of α_2/β_2. For any fixed set of values for the ratios, ρ_2/ρ_1 and β_2/β_1 it is possible to plot a family of curves, one curve for each value of the ratio d_2/d_1, of the relationship

$$\frac{c}{\beta_1} = F\{\frac{L}{d_1}\} \tag{4.14}$$

in a manner similar to that for a single free plate as was shown in Fig. 4.4. A typical set of these curves is shown in Fig. 4.7 where the axes are again set to correspond with a $L = 10$ cm, $c = 400$ m/s base on the c/L plot obtained from the field data. Laboratoire Regional D'Autun (1971) of France has published a set of transparencies

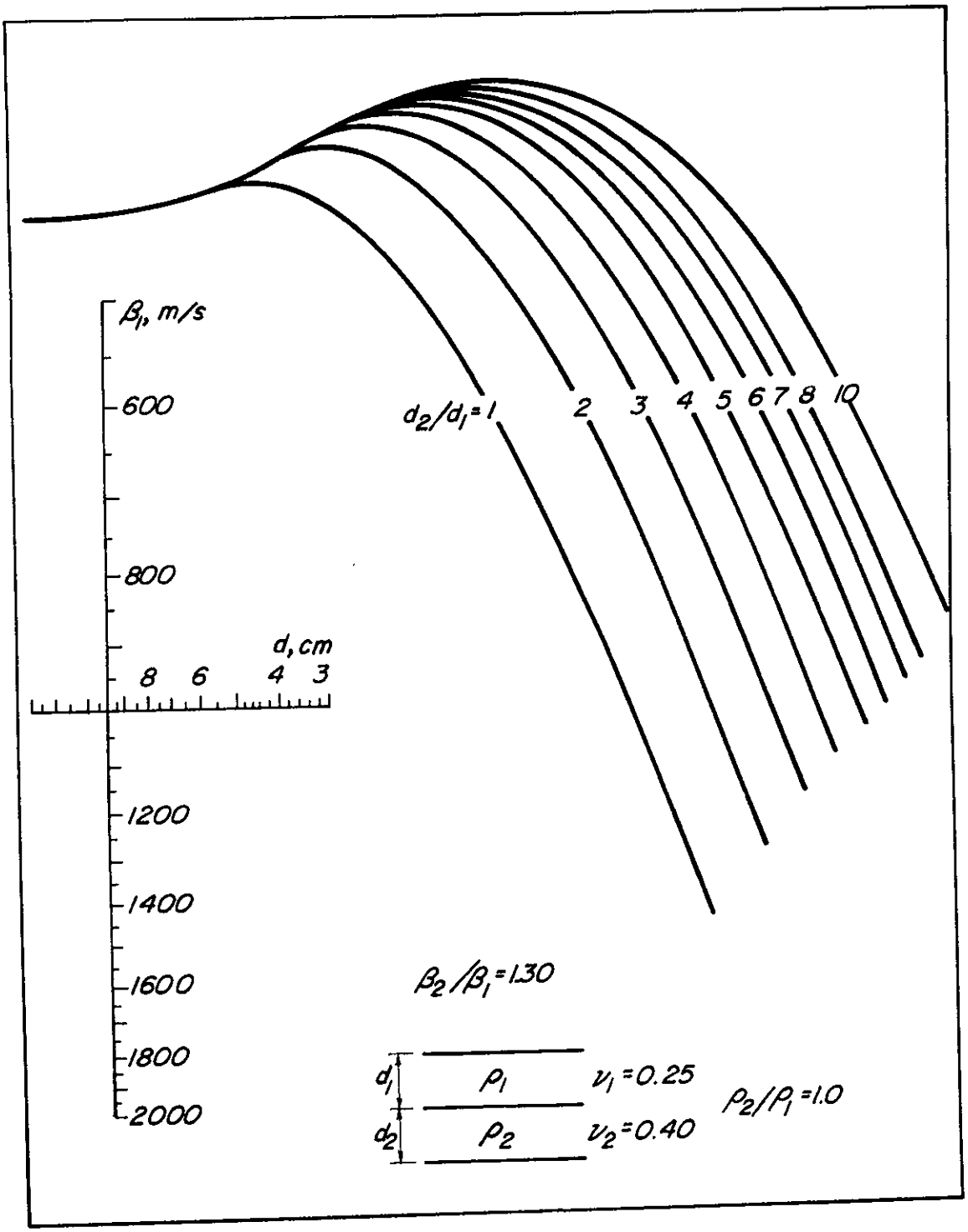

Fig. 4.7 TYPICAL CURVES OF $C/\beta_1 = F(L/d_1)$ USED IN INTERPRETATION OF VIBRATORY TEST DATA

engraved with families of curves of the type shown in Fig. 4.7, suitable for use in the interpretation of vibratory test data from a range of typical highway structures. However, the possible combinations of parameters yields hundreds of individual curves for the dispersion function and as their shapes do not differ radically it is not possible to select the appropriate curve in practice without foreknowledge, or at least a reliable estimate, of some basic properties of the structure. The geometry of an existing highway structure is usually reliably known so that the ratio d_2/d_1 may be available but, due to the form of the dispersion curves, an estimate of the appropriate value of β_2/β_1 is often required. A knowledge of this latter ratio confines the search for the correct curve to the members of a single family which when presented in the form shown in Fig. 4.7 are drawn all together on one sheet.

The peculiar shape of the dispersion curve for the flexural mode of vibration in a composite plate (Branch A in Fig. 4.6) is of assistance in the search for estimates of the ratio β_2/β_1. It is possible to construct curves relating the coordinates of the maximum on this curve to the value of the ratio β_2/β_1. The ordinate, i.e. c/β_1, is a function of β_2/β_1 of the type shown in Fig. 4.8A while the abscissa, L/d_1, is as shown in Fig. 4.8B. Two examples will illustrate the use of these functions in interpretation of wave propagation test data.

Fig. 4.9 gives the hypothetical results obtained from a test of a highway structure known to consist of two relatively stiff layers over a soft substratum. It is known that $d_2/d_1 = 5$. At very short wave length the dispersion curve is asymptotic to $c = 1370$ m/s which, from knowledge of the characteristic shape of dispersion curves in a two-layer composite free plate, can be assumed to approximate the Rayleigh wave

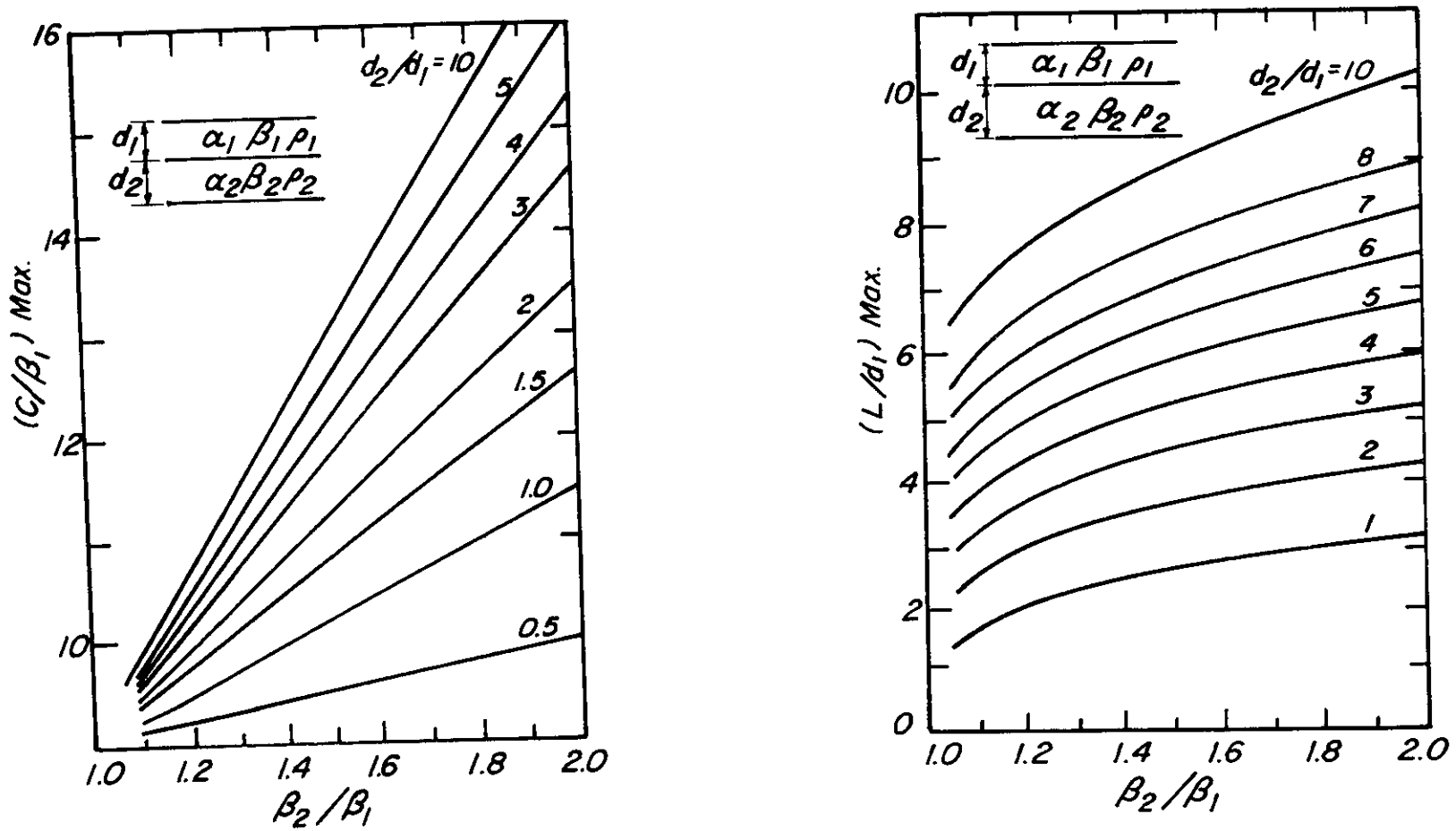

Fig. 4.8 PROPERTIES OF THE FLEXURAL MODE OF DISPERSION IN A COMPOSITE FREE PLATE

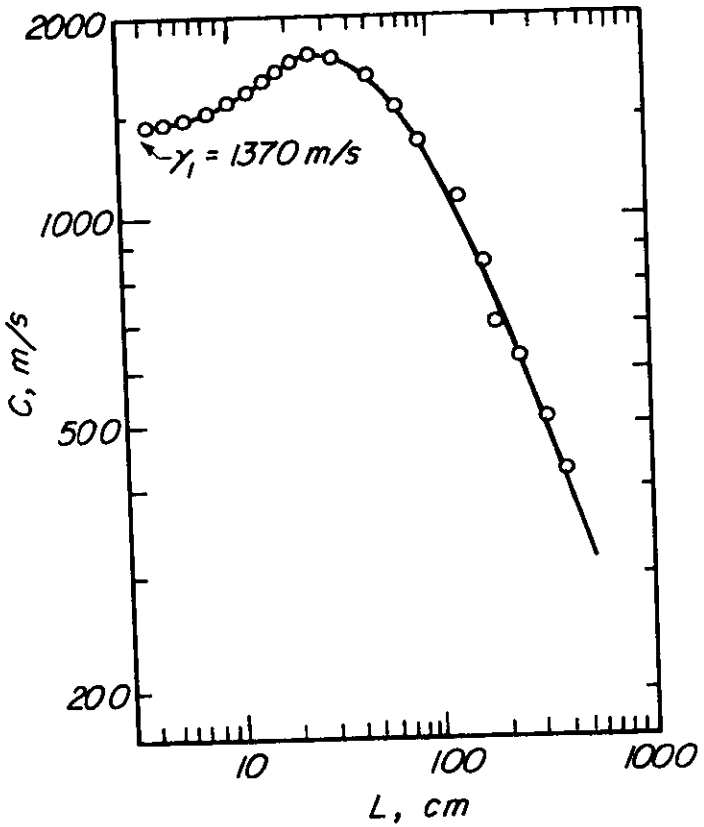

Fig. 4.9 WELL DEFINED DISPERSION CURVE

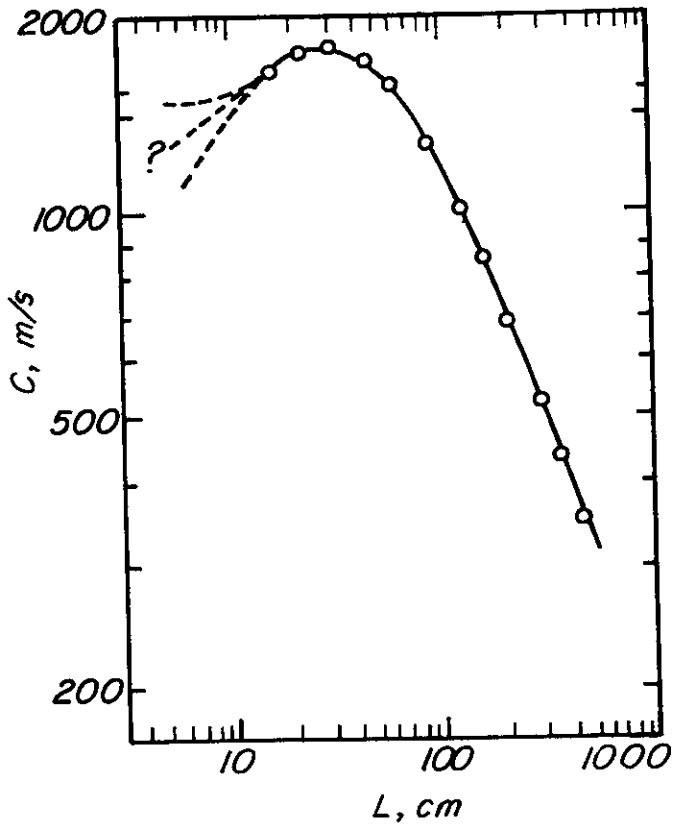

Fig. 4.10 POORLY DEFINED DISPERSION CURVE

velocity, γ_1, in the surface layer. If a Poisson's ratio of 0.25 is assumed for this material, this yields the information $\beta_1 = 1{,}490$ m/s. The maximum point on the dispersion curve (Fig. 4.9) is observed to occur at $c_{max} = 1{,}780$ m/s so that

$$(c/\beta_1)_{max} = \frac{1{,}780}{1{,}490} = 1.19 \ . \tag{4.15}$$

Entering Fig. 4.8A with this value and noting the intersection of this ordinate with the curve for $d_2/d_1 = 5$ yields $\beta_2/\beta_1 = 1.40$. Thus, a reliable estimate of the theoretical dispersion curve which best corresponds to the test data has been obtained and it is now possible to proceed with a more detailed analysis using constructions of the type illustrated in Fig. 4.7.

In other cases test data may be reduced to a dispersion curve of the type shown in Fig. 4.10. Due to the properties of the materials, the limitations of the instrumentation or a combination of both of these factors it is often impossible to obtain points on the dispersion curve in the high frequency, i.e., short wave length, range. As shown in Fig. 4.10 it is then not possible to make a reliable estimate of the value of γ_1 for the surface material. Nevertheless, the abscissa of the maximum point on the curve may be determined to be 28 cm in this case. Assuming $d_1 = 5$ cm and $d_2 = 25$ cm (i.e. $d_2/d_1 = 5$) have been obtained independently, it is now possible to compute $(L/d_1)_{max} = 28/5 = 5.6$. Entering Fig. 4.8B at $(L/d_1)_{max} = 5.6$, then for $d_2/d_1 = 5$, $\beta_2/\beta_1 = 1.40$ and, as for the previous example, it is now possible to proceed with the analysis by comparing the test data with the appropriate theoretical result.

Extension of methods involving detailed comparison of dispersion

curves with those of approximately similar plate structures has not been made beyond the two-layer composite plate analogy. This is due, in part, to the difficulty of obtaining numerate theoretical solutions but also to the fact that the number of variables become unmanageable. Even for the simpler cases discussed above, reliable results can only be expected for structures which sufficiently approximate the assumptions made in developing the theoretical dispersion curves. Such pavements are typically those composed of bituminous surfacing laid on good quality lean concrete bases or concrete slabs on lean concrete bases (Jones and Thrower, 1965b).

In practice it is important to ensure that the structure subject to test complies with the limitations of the interpretative technique or erroneous evaluations may occur. Significant heterogeneities and discontinuities often occur in practical structures and a body of experience with the testing method is required if reliable interpretations are to be obtained. Guillemin (1970) and Guillemin and Gramsammer (1971) have discussed a number of these problems and methods for the statistical analysis of results from typical highways.

Methods Using the General Characteristics of Dispersion Curves

The development of heavy vibratory testing equipment, notably in the United States, has allowed dispersion curves to be obtained from the low frequency range for relatively deep and complex structures. However, for functional reasons, such equipment is not well suited to the production of detailed dispersion curves in the highest frequency range. Some of the practical implications of this will be discussed at greater length in the next chapter, but at present it should be noted that the interpretation methods discussed above rely heavily on a study

of dispersion curves within the high frequency range. Interpretation of dispersion curves obtained from multi-layered structures by tests using the heavy vibrators depends more on an understanding of the general characteristics of the dispersion curves rather than a detailed comparison of the test results with theoretical curves. In this case a knowledge of the properties of the branches representing the higher modes of propagation is important. Chapter 3 includes a discussion of the methods by which analyses of layered structures may be made, but also points out their limitations and the difficulties involved in obtaining numerical data for all but the simplest systems. Some of the basic findings have been reviewed previously and their use in interpretation will be outlined below.

Consider first the case of a single surface layer resting on a half-space of lesser rigidity. Vidale (1964) has presented theoretical dispersion curves for a variety of cases with differing stiffness contrasts between the surface layer and the half-space. Two typical cases are shown in Fig. 4.11. These models include the influence of the shear strength of the material in the half-space but their principal characteristics are similar to those found by Jones (1962) where the shear strength of the half-space was ignored.

In both Case 1 and Case 2 of Fig. 4.11 there is a branch of the dispersion curve similar to that found for the flexural mode (M_{21}) in a free plate. The velocity of waves of this mode approach that of Rayleigh waves in the surface layer (γ_1) in the high frequency, short wave length range. As the wave length increases the curves fall below the free plate solution. The dispersion curves shown in Fig. 4.11 are the projections onto the real plane of the secular lines in complex

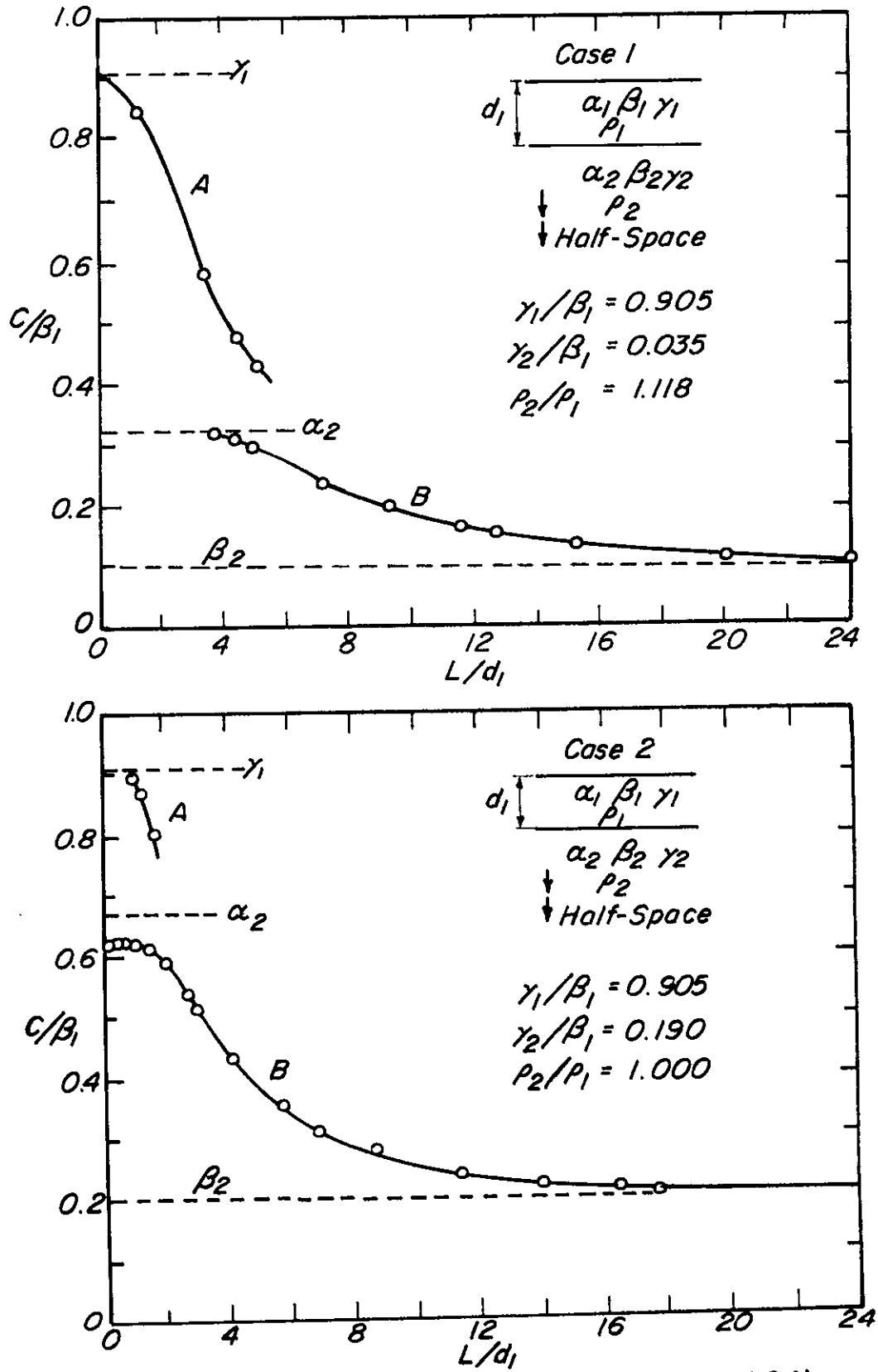

Fig. 4.11 THEORETICAL DISPERSION CURVES (Vidale, 1964)

space. Along Branch A the complex component increases with increasing wave length. Vidale (1964) does not demonstrate that this branch terminates at any definitive upper value of wave length but postulates that the increasing attenuation would make it unlikely that such waves would be measured in practice. This is supported by evidence from the field (Jones, 1962).

Branch B in Case 1 also has a cut-off point as defined by Vidale (1964) but in this case it is at a short wave length limit. Again there is no absolute criterion for the location of this point other than the increasing magnitude of the complex component and the fact that in the field it is observed that the instrumentation detects a sudden large variation in the wave length of the propagating surface motion at frequencies in the vicinity of these points. This short wave length cut-off of Branch B occurs at a phase velocity which is at, or close to, the velocity of compressional waves in the half-space (α_2). This observation has been used to determine the velocity of compressional waves (α_2) in the half-space beneath a single surface layer.

In Case 2 of Fig. 4.11 the mismatch between the stiffness of the surface layer and the half-space is considerably less than in Case 1. Branch A is present but is much more poorly defined than in Case 1. At the short wave length limit Vidale (1964) indicates a cut-off but this occurs at a phase velocity close to the Rayleigh wave velocity for the upper layer (α_1) and thus may be used in interpretation. Branch B in this case does not exhibit a short wave length cut-off, but is continuous to the $L/d_1 = 0$ axis. The short wave length portion is not normally observed in the field as the mode of propagation associated with Branch A begins to dominate in this region. It should be noted

that in the short wave length limit Branch B is not asymptotic to the velocity of compressional waves in the half-space (α_2), but only approximates this value. In interpretation of field data, however, the phase velocity corresponding to the coordinate of this branch at the shortest observed wave length is usually taken as equal to the velocity α_2. Error resulting from these kinds of approximations would appear to be of uncertain magnitude, depending upon the type of structure under investigation.

In all of the cases studied by Vidale (1964) Branch B is asymptotic at long wave lengths to the velocity of Rayleigh waves in the half-space (γ_2). This observation has been used in interpretation on the assumption that the longest wave length coordinate on this branch has an ordinate approximately either β_2 or γ_2.

Vidale's (1964) studies provide some useful insights into the general characteristics of dispersion curves but the material properties which were used are in many cases disimilar to those encountered in the majority of engineering structures. For example, in both Case 1 and Case 2 discussed above, Poisson's ratio for the surface layer is 1/6, which is lower than normally encountered. A thick-lift asphalt pavement on a clay subgrade is a more practical example of a structure composed of a single layer over a half-space. Fig. 4.12 shows the dispersion curves obtained for a pavement structure of this type by an analysis using computer program HASK which is described in Appendix 3. Branch AB corresponds to the propagation of a longitudinal wave in the surface layer (M_{11}) and is not of great practical significance as it is only rarely that this type of wave is observed in the field. Branch AC is similar to those found by Jones (1962) and Vidale (1964) and approximates

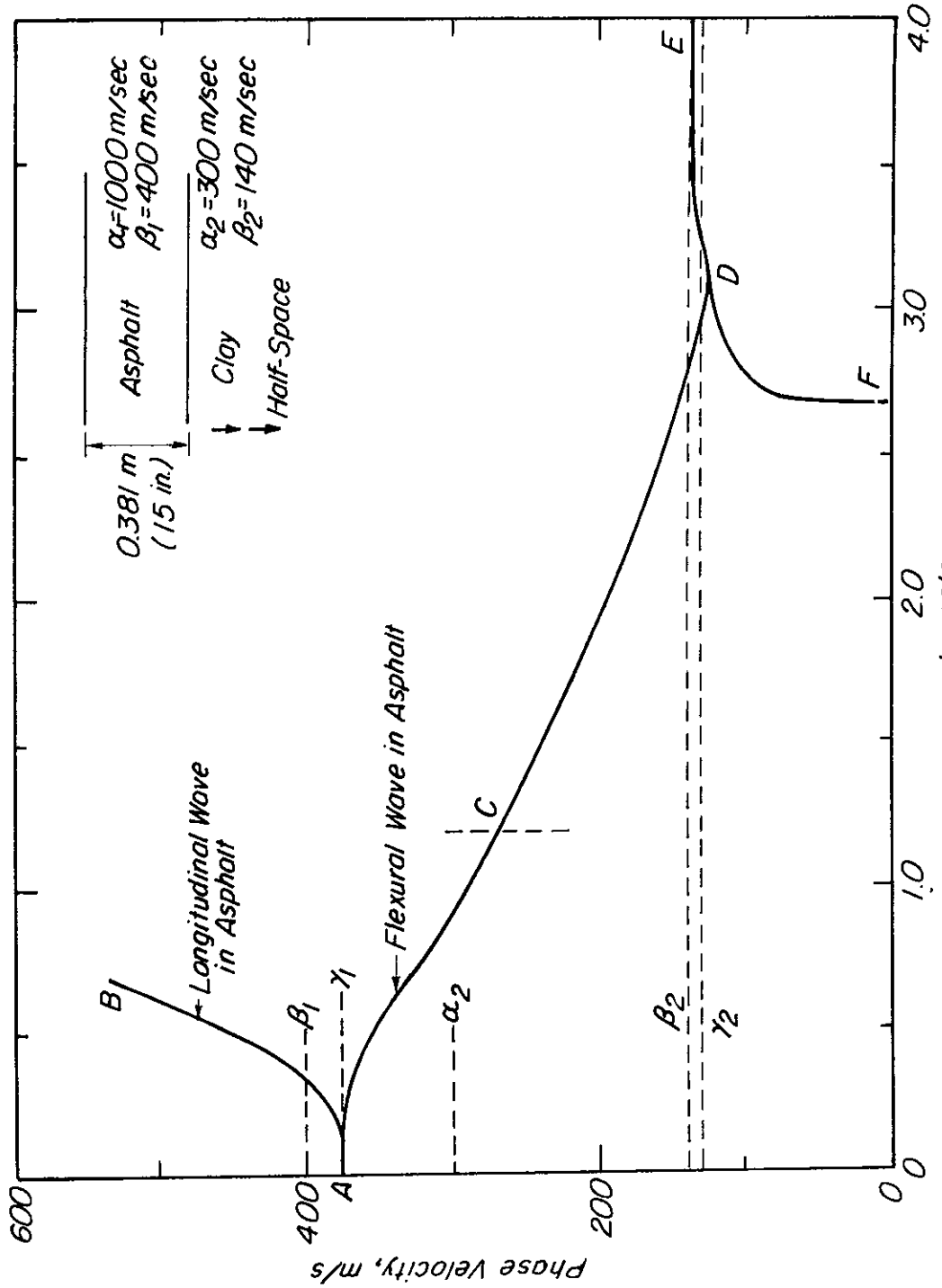

Fig. 4.12 THEORETICAL DISPERSION CURVE FOR A THICK-LIFT ASPHALT PAVEMENT

the flexural wave in a free plate of similar properties to the asphalt surface layer. It is asymptotic to the velocity of Rayleigh waves at the surface of the asphalt (γ_1) in the short wave length limit. As the wave length increases the wave attenuates to a greater and greater degree in a manner similar to that noted by Vidale (1964). However, no arbitrary decision was made to terminate this branch at some predetermined value of the complex component and it was found that a continuous secular line could be constructed through to the long wave length region. At point C the complex component of the attenuating wave reaches a maximum at a wave length of about 1.2 meters (wave numbers $k \simeq 5.20 + i\ 0.81$) and then decreases to zero at point D. A separate branch of a type similar to Branch B in Fig. 4.11 could not be found in this case. In the field it may well be that waves corresponding to points in the vicinity of C would not be detected and the portions of the curve closest to points A and D might be assumed to constitute separate branches. These would have an appearance not unlike Branches A and B in Case 1 of Fig. 4.11 and it might erroneously be concluded that an apparent cut-off point somewhere to the right of point C in Fig. 4.12 coincided with the velocity of compressional waves in the half-space (α_2).

Branches FD and DE in Fig. 4.12 are both in the real plane. That is, they both have zero complex components. A singularity occurs at point D. Branch CD, which is a secular line in complex space, intersects the real plane, represented by the plane of the paper in Fig. 4.12, at right angles to this point. A minimum on the branch DE also occurs at D. These characteristics are similar to those found in the vicinity of singularities in the secular lines for a single layer over a rigid

base discussed in Chapter 2 and Appendix 1. Note, also, that point D is below γ_2 , the velocity of a Rayleigh wave propagating in the half-space but that along Branch DE the phase velocity increases slightly towards β_2 . This tendency of increasing velocity at very long wave lengths has been observed in the field and has been ascribed to increasing stiffness of the sub-strata with depth (Richart, Hall and Lysmer, 1962). As no such increases of stiffness was present in the model studied here, it may be that the field observations are due to a combination of this effect and the basic characters of the dispersion curves in this region. Using the plate approximations, Jones (1962) was unable to obtain points on the dispersion curve in the vicinity of point D in Fig. 4.12, but he was of the opinion that some form of transition zone was to be expected. Vidale (1964) experienced numerical difficulties in obtaining points in this region for some of the structures which he examined but, despite the fact that in a number of cases he found that the complex component of the wave propagation reduced to zero in the long wave limit, he surmised that the dispersion curves were smoothly continuous; through from the zone CE to DE in Fig. 4.12. Neither author reports point associated with a branch similar to FD.

The wave length at which points on dispersion curves constructed from field data transfer from one branch to another, such as from Branch A to Branch B in Case 1 of Fig. 4.11, has been used as an aid to interpretation. Heukelom and Foster (1960) report case histories, from a site where vibratory testing was accompanied by exploratory drilling, in which this wave length coincided with a value equal to about twice the depth of the superficial layer. The case reported involved a site at which the underlying material was stiffer than the surface layer.

This observation led to an interpretation method commonly known as the "half wave length theory." It is assumed that the depth of the surface layer is equal to one-half of the wave length at which the dispersion curve is discontinuous in passing from one branch to another. This idea has been extended to more complex multi-layered situations and in the United States has been widely employed in the interpretation of data from vibratory tests on pavement as well as geologic structures. (See for example Ballard, 1964). An inspection of Figs. 4.11 and 4.12 will show that there is no reliable relationship between the discontinuities between branches of the dispersion curves and the thickness of the surface layer. Vidale (1964) reached the same conclusion and thus, while approximate layer thicknesses may be obtained by this method in certain individidual cases, it cannot be recommended as an interpretation technique, unless supported by independent evidence at a particular site.

In those cases in which there are more than one layer overlying the half-space the numerical difficulties involved in obtaining theoretical dispersion curves are greatly increased. However, some general characteristics of these systems can be recognized. Fig. 4.13 shows dispersion curves obtained by Vidale (1964) for a structure composed of two layers over a half-space. There are three branches. Branch A is similar to those seen for simpler structures (See Figs. 4.11 and 4.12) and represents a high frequency wave propagating along the surface. At the short wave length limit it approaches the velocity of Rayleigh waves in the upper layer (γ_1) . Branch B falls within a velocity range similar to that of Branch B for Case 1 of Fig. 4.11. The short wave length limit approximates α_2 while the long wave limit approaches

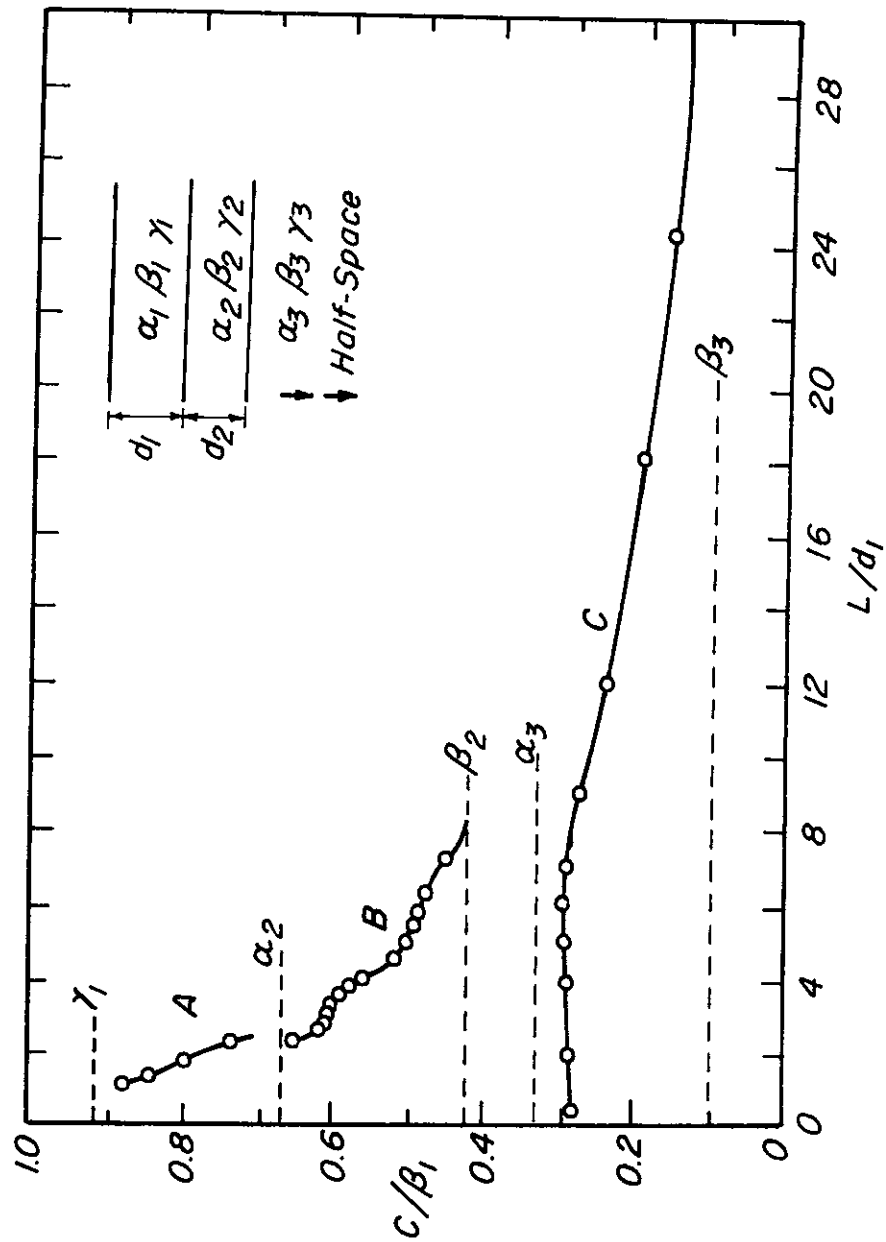

Fig. 4.13 DISPERSION CURVE FOR A DOUBLE SURFACE LAYER OVER A HALF-SPACE (Vidale, 1964)

β_2 . Branches of this type are observed in the field (Rao, 1973) and the coordinates of the limiting points are used in interpretation on the assumption that the phase velocities with which they correspond are reasonable approximations to the velocity of propagation of shear and compressional waves in the second layer. For systems with more than two surface layers a corresponding branch is usually found for each layer.

Another feature commonly observed in field data from multi-layered sites is a branch similar to that designated C in Fig. 4.13. It covers a very wide frequency range, often being present throughout the spectrum of wave lengths. As shown in Fig. 4.13, at short wave lengths it approaches the velocity of compressional waves in the half-space (α_3) and at long wave lengths becomes asymptotic to the velocity of shear waves (β_s) in this materials.

By comparing field data with theoretical dispersion curves of the type discussed above it is possible to obtain some of the characteristic properties of a structure under investigation. Note, however, that while discontinuities in dispersion curves similar to those separating the various branches are observed in field data, there is no absolute evidence to show how closely these points approximate the values which they are assigned in interpretation. For the more complex structures it is often difficult to assign points obtained from the field to any particular branch. Branch B in Fig. 4.13, for example, is very irregular and if the computed points shown were presented as field data, it might not be unreasonable to regard them as associated with two or more separate branches. Problems of this type are resolved in practice by the application of experience on the part of the interpreter and by selecting results according to their "reasonableness."

To illustrate a typical interpretation problem, results obtained by Rao (1973) from the pavement at Nellis Air Force Base, Nevada, will be used. Fig. 4.14 shows the dispersion curve and the results of the interpretation. The cross-section of the site represents what was known prior to the vibratory testing. After plotting the points obtained from the test, the first step is to draw curves through them to form the branches A, B, C and D. The discontinuities between the branches occur where there is a divergence from a continuous smooth curve. It is clear, however, from an inspection of Fig. 4.14 that, based on the plotted data points alone, the curves could be considered discontinuous at a number of places other than those selected here. This problem presents one of the major difficulties posed to the interpreter. With the aid of sophisticated testing equipment, Rao (1973) has observed that at certain frequencies there is a sudden discontinuity in the smooth relationship between the frequency and the phase of the measured surface response relative to the vibratory source. He interprets this as occurring when there is a change from one mode of propagation to another in the dominant surface motion. It is at points on the dispersion curve corresponding to those occurrences that the discontinuities are shown. A fuller discussion of this technique will be found in the next chapter. Where this kind of supplementary data is not available the uncertainties of the interpretation are greatly increased.

Branch A which lies in the short wave length range is considered to approximate the dispersion curve for a flexural wave propagating in a free plate of similar characteristics to the surface layer. Thus, the velocity of Rayleigh waves in this material is assigned a value equal to that corresponding to the short wave length cut-off of this

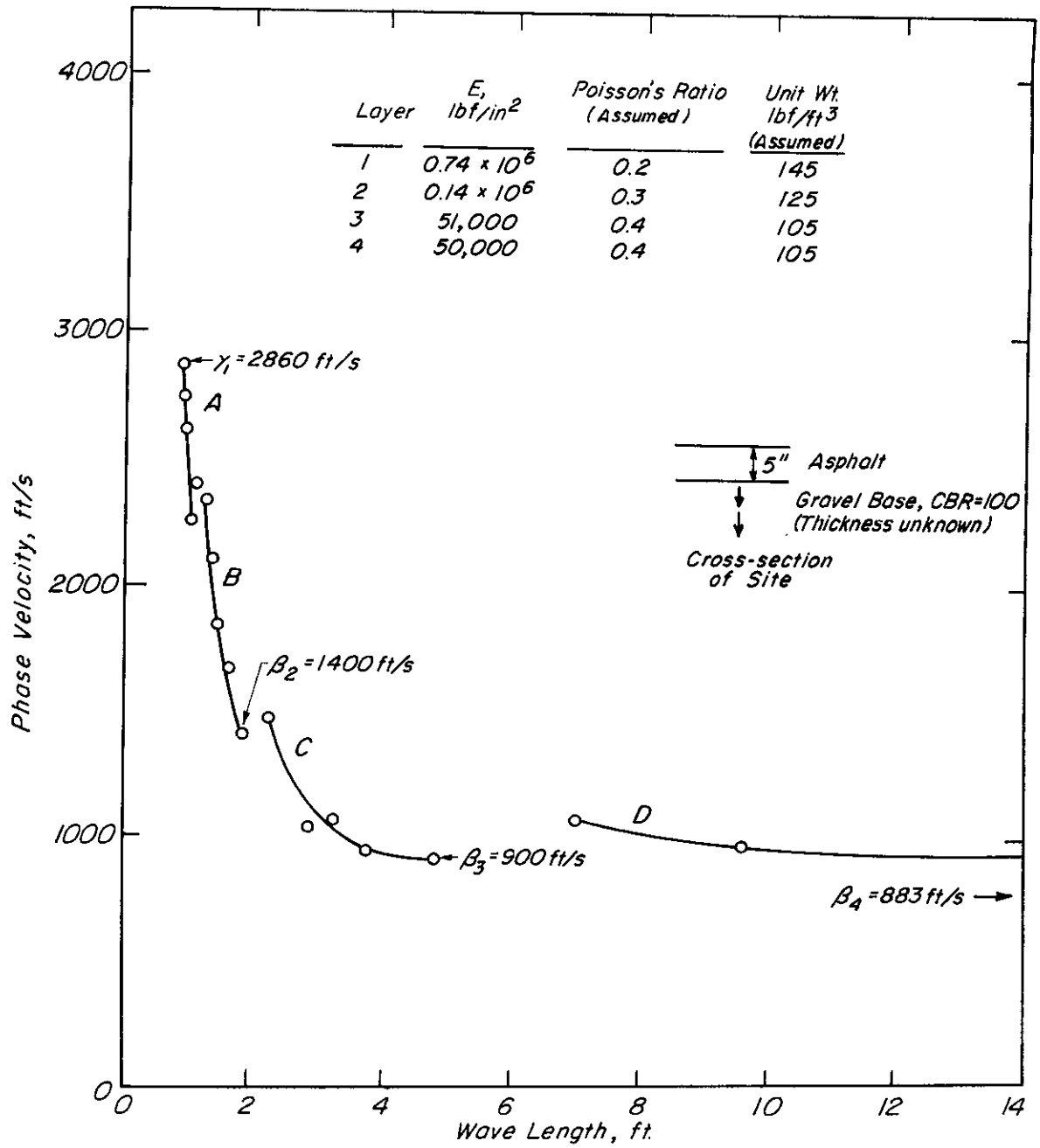

Fig. 4.14 DISPERSION CURVE FROM PAVEMENT AT NELLIS A.F.B.
(after Rao, 1973)

branch, i.e., γ_1 = 2860 ft/sec. Branches B and C are unexpected, as the known cross-section does not predict layering in the gravel base. However, the discontinuities appear distinctive and, relying on the fact that the long wave length cut-off of branches associated with intermediate layers approximates the shear wave velocity in the layer, the interpretation β_2 = 1400 ft/sec and β_3 = 900 ft/sec is made. The usual interpretation is applied to Branch D, i.e., that at very long wave lengths it is asymptotic to the velocity of shear waves in the deepest layer involved in the vibratory excitating. In this case it is assumed that β_4 = 883 ft/sec.

At this stage the shear wave velocities of materials in four distinct layers have been estimated. The depth and thickness of layers beneath the asphalt surfacing are not known, however. To convert these results into Young's moduli it is necessary to know both the Poisson's ratio and the mass density of each of the layers. As is usual, these have been estimated based on the material types known to be present in the pavement structure. The resulting estimates of the moduli are tabulated in Fig. 4.14.

The interpretation method illustrated by this example is typical both of the approach used and the type of results obtained. This dispersion curve was obtained with a relatively heavy vibrator and it is possible that had lighter equipment been available a more detailed picture could have been obtained in the high frequency range. Some of the interpretation methods outlined in the previous section of this chapter may then have been applied to Branch A, so that the Poisson's ratio of the surface material might also have been deduced and the need to introduce an estimate of its value eliminated.

Physical Models

Difficulties with analytic methods used to predict the propagation of wave fronts have encouraged the construction of physical models to simulate natural and man-made structures. Applications in the field of geophysics have been reported by Toksoz and Anderson (1963) and discussed theoretically by Oliver, Press, and Ewing (1954). Models in the form of two-dimensional sheets composed of materials intended to reflect properties similar to those found in highway structures have been constructed by Thomas (1969) and Jones (1968) reports similar studies performed by Tosticorelli. These models have been constructed from aluminum and plexiglass representing a pavement structure and with linoleum simulating a half-space composed of natural soil. These materials have been chosen because they provide model structures in which the stiffness contrast between the different layers is similar to that found in pavements. Linoleum also has a low shear modulus, the shear wave velocity does not change appreciably with frequency and damping of vibrations occurs, which are all characteristics found for many soils.

Results from model testing have been successful in confirming the validity of the theoretical analyses for simple structures and have shown that those modes of propagation which are predicted to dominate the excitation are in fact observed at the free surface. Gramsammer (1969) has reported excellent agreement between dispersion curves obtained from a model composed of a single layer over a half-space and those derived analytically. However, model studies do not appear to have produced results of direct assistance to the problem of interpretation of wave propagation test data.

Application of Results

The interpretative process applied to the dispersion curves obtained from a vibratory testing program yields information about the geometry of a structure and/or the material properties of the component layers in the form of pseudo-elastic moduli; i.e., Young's Modulus, E and Shear Modulus, G . These moduli are usually sought for use in the analysis of existing or projected structures by methods based on some form of elastic or viscoelastic techniques. The loadings used in such analyses are, of course, similar to those encountered in daily use. While the vibratory methods of testing obtain data from the materials in-situ and thus eliminate the need to evaluate the influence of many environmental factors such as confining pressure and water content, the loading imposed by the test vibrator is dissimilar to the in-service loading and is normally much smaller in magnitude. This factor is of major importance, as the moduli of soils and pavement construction materials are sensitive to strain amplitude. Increasing shear strain amplitude is associated with decreasing shear modulus. Moduli obtained from wave propagation tests are typically much higher than those suitable for use in analyses where traffic loading is involved. The influence of confining pressure is also of considerable importance when deep layers are considered, as has been demonstrated by Cunny, Cooper and Fry (1969) in a comparative study of dynamic in-situ and laboratory tests.

Bituminous macadam materials are sensitive to temperature fluctuations, so that it is important to record the climatic conditions prevailing at the time of testing. The frequency of excitation may also be a significant factor influencing the measured properties of these materials.

A discussion of the properties of typical materials involved in highway construction and methods by which wave propagation test results may be modified for use in analysis of in-service structures is presented in Appendix 6.

CHAPTER 5

SOME PRACTICAL ASPECTS OF VIBRATORY TESTING

As the wave propagation method is substantially in the development stage, there exist a variety of instrumentation, equipment and test procedures which have been developed by the various research groups working in the field. The major influence on test configuration is the purpose for which the data obtained from the test is required but also, to a significant extent, the theoretical basis of the method used to interpret the test data and the history of its development affect the design. The principal applications in which the wave propagation method has been used to date are:

Principal Applications of the Wave Propagation Method

1. To obtain in-situ properties of soils and pavement materials. Surface layer only.
2. In quality control of pavement construction.
3. Detection of deteriorating zones in existing pavements.
4. Studies of the influence of changing traffic patterns on pavement stiffness.
5. Seasonal and long term variations in pavement properties.
6. As an exploratory tool to obtain details of the cross-section of existing pavements prior to the design of overlays.

7. In the investigation of sites for the foundations of heavy structures subject to vibration. Principally radar towers subject to oscillatory wind loading.

8. Investigation of rock properties to depths up to 200 ft (60 m). Principally at nuclear cratering sites.

Light and Heavy Vibrators

There are two major divisions into which the equipment types may be divided. These will be designated as the "heavy type" and the "light type." This designation is based upon the size and power of the vibratory source used to excite the structure to be tested. The heavy vibrators have their origin in machines primarily designed to measure the overall stiffness of pavements as discussed in Chapter 1. They are large mechanisms capable of delivering forces of up to approximately 23,000 N (5,000 lbf) at maximum amplitude (Rao, 1973). The mass may attain 3,000 kg, resting on loading plates up to 0.5 m (20 in.) in diameter (Mucci, 1968). Extensive auxiliary equipment, such as hydraulic cooling, is also required and transportation usually involves specially designed vehicles. The light vibrators typically have a mass of less than 50 kg, are supported by compact auxiliary equipment and are easily transported by light vehicles. In their basic form they are simple electro-magnetic oscillators mounted on loading plates of no more than 10 cm (4 in.) diameter.

Some of the equipment based on the light vibrators has been designed for specific applications where its simplicity and mobility are essential. Ideally, however, wave propagation equipment used for general purposes should be capable of operating through a frequency

[illegible] its simplicity but, to date, a single

range from 5 to 50,000 cps (Nair,1971) while generating sufficient energy at the lower frequencies to excite deep structures even when they lie beneath stiff layers such as concrete pavement slabs. Considerable effort has been expended to improve the operating range of equipment while maintaining its simplicity but, to date, a single system capable of operating through the full range has not been perfected.

Light Equipment

Systems designed around light vibrators such as those developed by the Transport and Road Research Laboratory, (TRRL) England (Jones, Thrower and Gatfield, 1967) have frequency ranges of order 30 to 30,000 cps but due to their light weight and small power are not capable of exciting layers at depth beneath pavements. Recent advances in the design of the pick-ups which measure the characteristics of the surface wave have allowed this wide frequency range capability to be utilized with compact auxiliary equipment, rapid test procedures and high system mobility. Early test procedures involved moving the pick-up outward from the vibratory source until the signal from the pick-up recorded on an oscilloscope indicated that the position was coincident with a peak (or trough) of the surface wave. (Maxwell and Fry, 1967). This method is cumbersome and detracts from one of the major advantages of the wave propagation technique which is its speed. The method outlined in Chapter 1 in which the phase difference between the source and the pick-up is measured for arbitrary pick-up position improves the pace considerably. The need for simple and rapid on-site procedures also dictates that the full frequency range required for a test can be covered with a minimum of disruption to the continuity of the test. In the range 25 to 30,000 cps the light vibrator system developed at

TRRL achieves this aim by careful design of the total equipment package so that a maximum number of the components are interchangeable with minimum operator effort.

The TRRL wave propagion equipment is mounted in a four-wheel drive light truck (a long wheel base Land Rover). The vehicle has a power take off (PTO) facility as standard and with minor modification a 5 kw electric generator driven by the PTO is mounted under the passenger seat. All electronics are permanently mounted in the cargo compartment and so arranged that a seated operator may comfortably operate all controls. Electric power cables and electronic leads passing to the instruments on the pavement pass through weatherproof ports and are stored on reels in the specially designed compartments. The small number of items required on the ground during the test is stored in purpose built, floor level racks along each side of the truck floor. This careful design of the test equipment is of vital importance in the field. For example, during a test program conducted by TRRL at Grangemouth, Scotland, in 1972, the method was used to obtain in-situ moduli of the various structural layers of an experimental pavement. Tests were conducted on each of the layers as construction progressed and, due to the needs of numerous other special testing programs, as well as the usual construction activity, it was essential that site occupancy was minimal. TRRL personnel were able to achieve equipment set-up times of 2 or 3 minutes from arrival at the site. The capability of Land Rover type vehicles to convey personnel in comfort on long journeys to site but also to negotiate terrain normally accessible only to tracked vehicles is also of great importance in many practical applications. Similar short site occupancy times are also of advantage when testing airport pavements

where dislocation of operations can be very costly.

TRRL's equipment as presently designed employs two types of vibrator and three pick-up designs to cover the frequency range 25 to 30,000 cps. The systems are matched to the various operating ranges as follows:

TABLE 5.1 - VIBRATORS AND PICK-UPS IN USE BY TRRL

Frequency Range cps	Vibrator	Pick-up
25- 300	Electro-magnetic moving coil	Geophone
300- 5,000	Electro-magnetic moving coil	Salt crystal bi-morph
5,000-30,000	Ferro-electric ceramic cylinder	Ceramic detector matched to vibrator

The frequency range required for any given test will depend upon the purpose and the nature of the material involved. Generally speaking, the deeper the penetration required the lower the frequency range. The various systems employed by TRRL have been designed to facilitate minimum disruption of test continuity when a change from one set to another is required. Vibrators are cemented to the site with quick drying dental cement and testing is usually commenced in the high frequency range to avoid high amplitude oscillations while the cement is setting. The pick-up is moved away from the vibrator in equal steps in distance by an operator guided by a signal lamp controlled by a senior technician who is in charge of the electronic equipment mounted inside the vehicle. Loudspeakers are also provided and these are used where special instructions, such as equipment change, are called for.

It has been found that signal lamps produce less operator fatigue than audio systems, particularly at crowded and noisy sites. With these procedures and with experienced personnel it is possible to obtain the basic data from a test site for a wide range of frequencies and for a considerable areal extent around a vibrator position within the order of one hour for a typical highway pavement application.

Improvements in equipment simplicity and compactness and in speed of operation are, however, the subject of on-going research. TRRL developed the use of the salt crystal bi-morph pick-up principally to simplify operating procedure and to improve accuracy. Geophone type pickups are capable of use beyond the 300 cps limit defined in Table 5.1 but are restricted by their physical dimensions. Typical geophones have a diameter of about 10 cm which is of the same order of magnitude as the wave length of the surface motion in some situations. This makes for errors in the accurate measurement of wave lengths and the physically smaller bi-morph is introduced to avoid this problem. For the very high frequencies required in some applications moving coil vibrators are inadequate. The ferro-electric ceramic cylinder vibrators are then used with matched ceramic detectors. This system, however, has two major disadvantages. In order to transmit sufficient energy into the structure under investigation the system must be operated at selected frequencies at which "resonance" occurs. TRRL's system, for example, operates only at frequencies of approximately 5, 10, 15 and 25 kilocycles per second. This limits the detail which can be obtained for dispersion curves in the high frequency range. Secondly, the control electronics required for this system is not compatible with that required for the moving coil vibrators. The need to provide two

sets of electronics adds considerably to equipment cost and complexity.

Improvements in the design of light equipment have been pursued by workers at Laboratoires Routiers in France. The French designs are based on the original concepts developed by TRRL but, instead of relying upon commercially available moving-coil vibrators, new special purpose equipment has been constructed. Excellent results have been obtained with moving-coil vibrators capable of operation in the ranges 5,000 to 10,000 cps and 10,000 - 20,000 cps. (Dosso and Keryell, 1968). Magneto-strictive devices have also been used for high frequency operation. These systems have the advantage of infinitely variable frequency within the operating range and have auxiliary and control equipment compatible with that used for low frequency testing.

In applications where the speed and mobility of the wave propagation method is the major advantage more specialized equipment has been developed. These applications are typically those in which absolute values of material properties are not required but, rather, only comparison between one site and another or conditions at one time or another are required. Examples are to be found in construction quality control, diagnostic surveys for potential pavement deterioration and studies of environmental and loading effects on highway structures.

Ducloux, Poilane and Guillemin (1968) have described a number of applications of the wave propagation method in the testing of highway pavements including the correlation of test data with the quality and degree of deterioration of bituminous macadam. Their work, however, involved full scale testing. Jones (1964) has discussed a number of applications in which the tests procedure is simplified and tailored to the specific problem at hand. For example, the quality control of

APPENDIX 5

COMPUTER PROGRAM SPRDSP

A program for the computation of dispersion curves for multi-layered media by the Direct Stiffness method. The theoretical methods are described in Appendices 4, 7 and 8.

(1970) has reported on an experimental prototype system mounted on a light vehicle (Chevrolet station wagon). A moving-coil vibrator and an array of three pick-ups are mounted on a hinged cantilever which is capable of being lifted and lowered to and from the operating position by remote control. With the vibrators and pick-ups positioned on the surface, tests are conducted automatically at ten pre-selected frequencies by means of suitable electronic control devices. Five sets of measurement of phase difference are made at each frequency and the mean values selected. This data is recorded on punched tape and may be reduced to the form of dispersion curves by a computer program incorporating a plotting routine. In this way tests can be run at 60 or more sites per working day. The rather limited flexibility of the vibrator/pick-up system when confined to the semi-permanent positions dictated by the cantilever support structure is, however, a serious drawback. As shown above, the range of frequencies and wave lengths which are found in many practical applications of the wave propagation method require the ability to convert from one set of instrumentation to another and to cover a wide variety of surface wave lengths. In typical highway applications wave lengths may vary from a few centimeters to ten or more meters at any given test site. The automated nature of this test procedure while greatly improving speed does not allow the experienced operator the "hands on" approach often required to deal with peculiar site conditions and the not infrequent anomolous results found in practical situations. These problems limited the first experimental equipment built by Statens Väginstitut to applications on base courses of heavy pavement construction but further development is expected to improve the range considerably. The desire to

capitalize on the high speed potential of the method while maintaining the maximum system flexibility is one of the major challenges in equipment design for the wave propagation technique.

Heavy Equipment

The systems based on the heavy vibrators have been largely developed in the United States with a strong accent on application to the testing of airfield pavements. Influenced by the early work at the Royal Dutch Shell Laboratories in Holland (see Chapter 1),a vibrator consisting of counter rotating eccentric weights of fixed mass driven by hydraulic power was constructed in 1962 at the U. S. Army Engineer Waterways Experiment Station (WES), Vicksburg, Mississippi (Fry, 1963). With this equipment soil moduli for material at depths of approximately 10m (30 ft) were determined. The need to achieve penetration to greater depths for site investigation for nuclear cratering experiments and heavy structures led to the development of a large variable-mass vibrator capable of generating a maximum force of 116.2 kn(2,128 lbf) at a frequency of 40 cps (Ballard, 1964). With this vibrator, moduli of various materials including basalt and other rocks were obtained at depths up to the order of 50 m (150 ft).

The need to upgrade airfield pavements to meet the demand of increasing aircraft wheel loads led to the application of the wave propagation method as an aid to the evaluation of pavement geometry and material properties needed for the design of structural overlays. Studies of the variation of pavement properties with time and environment were also made. See, for example, Maxwell and Joseph (1967). In many cases airfield pavements were subjected to a number of other nondestructive tests in addition to the wave propagation test, such

as the plate bearing and Benkleman beam tests (Finn, 1962). The overall complexity of this type of testing program and the near ideal site conditions afforded by airfields encouraged the development of large and highly sophisticated mobile testing laboratories. A major effort in this direction has been made at the Eric H. Wang Civil Engineering Research Facility at the University of New Mexico, Albuquerque (CERF).

The CERF equipment is mounted in a trailer 8 ft (2.44 m) wide by 35 ft (10.67m) long, which is divided into three compartments. The first compartment houses a 100 kw generator capable of supplying 220 volts, 3-phase power. The central compartment houses a field power supply unit, a transformer (220 v to 440 v step-up), the vibrator and a cooling unit. The rear compartment houses the instrumentation and provides operator space. (Rao 1973). Load-deflection tests at selected frequencies, reasonant frequency tests and deflection-basin tests as well as wave propagation test can be made with the equipment available in the mobile laboratory. The vibrator weights 6,750 lbf and consists of armature coils and field coils. The armature is connected through three load cells to a 2 in. thick, 12 in. diameter plate. The vibrator is lowered into position on the pavement through a hatch in the floor of the van.

Fig. 5.1 is a schematic diagram of the equipment arrangement as set-up for the wave-propagation test. Up to six pick-ups are cemented to the pavement in positions matched to the expected range of the wave length. The testing is carried out automatically with a continuous sweep over the desired frequency range. The CERF equipment has a fourteen channel control and data recording system which allows the phase-difference between the vibrator and each of the six pickups,

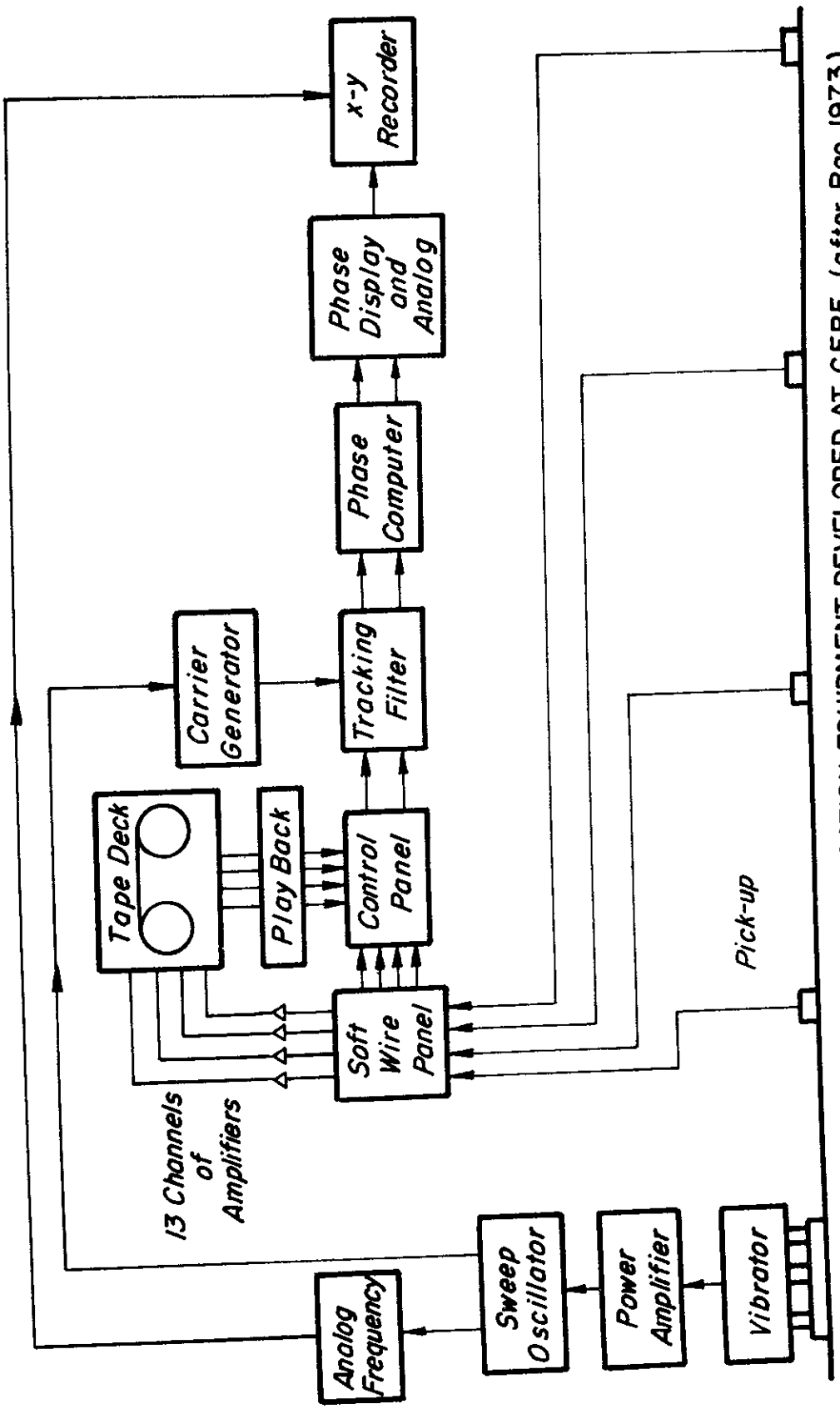

Fig. 5.1 SCHEMATIC OF WAVE PROPAGATION EQUIPMENT DEVELOPED AT CERF (after Rao, 1973)

the operating frequency and other information to be recorded on magnetic tape. Dispersion curves can be constructed from the data recorded on tape with the aid of suitable programs and computer driven plotters. In addition to the basic data which is stored on tape for later analysis, an x - y plotter is provided which continuously traces the relationship between the phase-difference at a selected pickup and the operating frequency. This plot is used by experienced operators as an empirical check on the progress of the test. Fig. 5.2 is a simplified version of one of the plots obtained by Rao (1973) at Nellis Air Force Base, Las Vegas, Nevada. For clarity, certain calibration data has been excluded. The basic form of the plot has characteristics reminiscent of a sine wave but in certain frequency ranges such as at A and B this system breaks down and an irregular pattern develops. CERF operators have observed empirically that these frequencies coincide with situations at which points on the wave length/wave velocity dispersion plot disassociate themselves from a group lying on one branch of the curve and join another group on a second branch. For example, from branch A to branch B in Fig. 1.6. This phenomenon is probably associated with the complex surface wave which occurs at those points in the frequency range where two or more propagating wave modes have significant amplitudes and no single mode dominates. Experienced operators also use these plots as a diagnostic guide to equipment behavior.

Relative Advantages of Heavy and Light Vibrations

The major application of both the heavy vibrators and the light vibrators is in the evaluation of pavements. For this use, both systems have their respective advantages and disadvantages. Basically

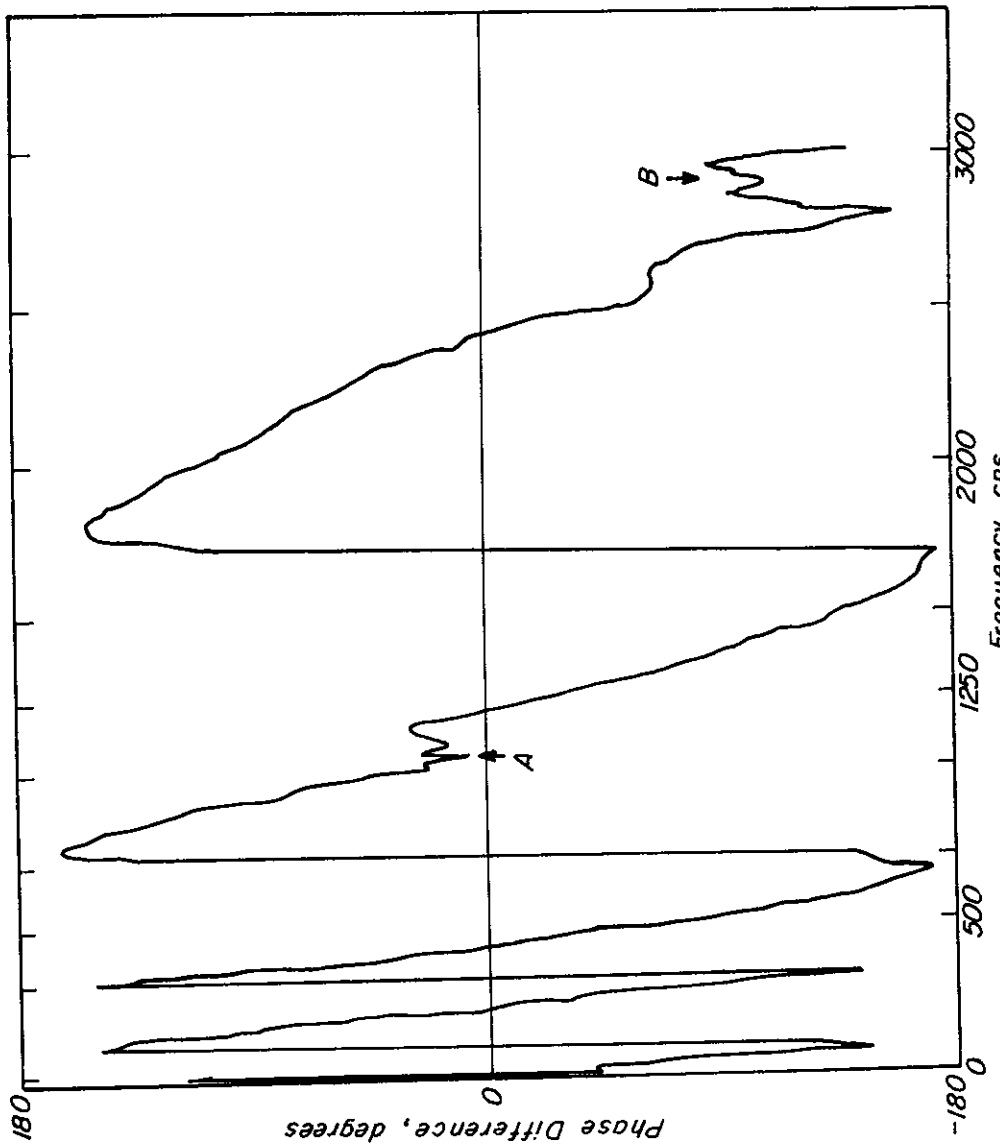

Fig. 5.2 FREQUENCY PHASE DIFFERENCE PLOT FOR A SITE AT NELLIS A.F.B.
(after Rao, 1973)

the heavy vibrators cannot achieve operating frequencies greatly in excess of 3,000 to 5,000 cps while the light vibrations are unable to transmit sufficient energy into the structure to obtain data relating to deeply buried layers; this is particularly the case for structures with very stiff surface layers such as concrete slabs. Both of these respective limitations confine the detail and accuracy of the dispersion curves required to extract the maximum information about the properties of the pavement under test. Simple deep asphalt structures may not require the use of frequencies in excess of 5,000 cps but in some of the more complex, traditional pavement constructions frequencies up to the 30,000 to 50,000 cps range may be needed to define individual layer properties. This is particularly the case if details of wearing courses are required. The method in which the test data is interpreted also influences the degree of importance attached to the high frequency range. Methods which involve detailed comparison of dispersion curves obtained in the field with theoretical curves by means of overlays and similar methods (see Chapter 4) rely heavily on data from the high frequency range. Those which depend more on the general characteristics of the curves and the points of termination of the various branches (Vidale, 1964) suffer less from a lack of high frequency detail but are improved when it is available.

Heavy vibrators and their complex auxiliary equipment reduce system mobility greatly and are obviously not suited to applications requiring access to confined construction sites and rough terrain. Their capital cost is also very great compared to the simple light vibrator systems. Large facilities do, however, provide the opportunity to incorporate a maximum of equipment for the automatic reduction of

test data. Primary reduction of raw frequency/phase difference data may become a heavy burden and even with basically manually operated equipment it has been found advantageous to develop specially designed chart tables and drafting aids to ease this task (Jones, Thower and Gatfield, 1967). The degree to which the test procedure and data interpretation can be fully automated is debatable. The need to monitor the results of field tests as they proceed and thus avoid selection of inappropriate pick-up siting, frequency range or other difficulty, requires an automatic system to be sufficiently flexible that an operator can intervene when it is apparent that an unprogrammed condition has occurred.

Except for special applications the goal of ongoing equipment development research for the wave propagation method is to achieve a system with the maximum operating frequency range, with sufficient power at any frequency to gain sufficient penetration of the field of excitation and with maximum mobility. It is unlikely that the ideal goal will be met in a single model but, with careful attention to both design and operating procedure, it should be possible to produce one or two complimentary systems capable of operating satisfactorily in a wide variety of situations.

Alternate Methods

In recent years a number of innovations in the wave propagation method has been investigated. These have largely been attempts to overcome the problem of data interpretation currently limiting the method's applicability. Workers at Laboratoires Routiers have investigated the possibility of measuring the amplitude of the surface wave propagating away from a vibrator and the utilization of this

data as an aid to interpretation. Gramsammer (1968) has reported on a successful experimental program in which amplitudes at various distances from the source were measured on the surface of simple structures.

The standard wave propagation method involves excitation by means of a vertically oscillating vibrator which produces generalized Rayleigh waves in the structure. Other types of excitation are possible. Jones (1958) used a linear vibrator operating parallel to the surface of the ground and observed Love waves propagating in a layer of silty clay overlying gravel. Cogill(1965) built a torsional vibrator specifically designed for the generation of horizontally polarized shear waves (SH) in soils. Recognizing the somewhat simpler problem of analysis posed by the propagation of SH waves in layered media, Kurzeme (1970a), working at the CSIRO in Australia, built a torsional vibrator capable of exciting SH waves in pavements (Kurzeme, 1970b). In combination with appropriate theoretical studies he was able to use this vibrator to achieve some interpretative ability for data obtained from highway structures (Kurzeme, 1971). However, many similar problems to those found for Rayleigh wave propagation were encountered. In addition, in typical pavement structures, in which the surface layer is more rigid than the underlying layer,no information can be gained about the lower layers with this method. There remain, however, a large number of unexplored areas in the study of alternative procedures for the wave propagation technique.

CHAPTER 6

SUMMARY AND CONCLUSIONS

General

The wave propagation method of nondestructive testing originated in dynamic loading tests of pavements. It has developed into a specialized procedure but the test equipment is generally in prototype form and operated by a limited number of research centers. A review of the literature revealed that the method has been applied in a variety of site investigation situations in addition to pavement evaluation. The method is frequently used in conjunction with other tests on pavements, including those involving other forms of dynamic loading.

The advantages and disadvantages of the method were studied and discussed in Chapter 1. In addition to the nondestructive nature of the test and the speed of operation, its principal advantage is its ability to obtain in-situ properties of a structure. This factor is of increasing importance as greater reliance is being placed on pavement design methods which require the basic moduli of the materials as input. The primary disadvantage of the method is the restricted ability to accurately interpret all of the data obtained during testing. Valuable interpretation of data from simple structures can be made but many practical systems can be only partially evaluated. To obtain an understanding of the basic phenomena of wave propagation in layered structures, a study of simple, plane structures under vibratory loading was undertaken.

Vibratory Excitation of Plane Layered Structures

The results of the study reported in Chapter 2 show that the surface motion on a layered system subjected to vibratory excitation is very complex. It may be considered to be the superposition of an infinite

number of simpler wave motions known as modes. In layered elastic systems, modes were found to have either the form of wave motions which propagated horizontally away from the source without loss of amplitude, or the form of waves which attenuate with increasing distance from the source. In visco-elastic systems all modes are attenuated. The characteristics of the various modes were investigated and the different types are illustrated in Fig. 2.6.

The relationship between the frequency of excitation and the form of the surface waves was studied. There was found to be a separate curve in complex space, relating frequency and wave length (defined in the form of a wave number), for each mode of propagation. These curves, or secular lines, were shown to form families of three dimensional branches. The projection of these functions onto the real plane are known as dispersion curves and are obtained experimentally by the wave propagation test.

The properties of the secular lines for a single elastic layer over a rigid solid were studied in detail. The form of the curves is illustrated in Fig. 2.5 and the nature of the singularities which occur in them is analyzed in Appendix 1.

Methods of Analysis for Multi-layered Structures

The propagation of waves in multi-layered structures poses a difficult analytic problem, particularly if solutions are required in numerical form. The available methods of analysis, some of which originate from the field of seismology, have been reviewed in Chapter 3. Structures which decrease in stiffness with depth have received limited attention because they are of little importance in seismology. They also pose the most difficult analytic problems.

Two approaches to the problem were developed here. The first is based on the solution to the general equations of motion, as constrained by the boundary conditions imposed by the structure. The problem is formulated in a manner which allows it to be reduced to the form of linear algebraic equations. This method was used to prepare a computer program designed to compute dispersion curves for structures resting either on a rigid base or a visco-elastic half-space. (See Program HASK, Appendix 3). This program is an economic means by which simple structures may be analyzed but, in some situations, the functions are difficult to manipulate and the numerical methods used to obtain the solutions break down. These difficulties are a common feature of algorithms based on solutions to the general equations of motion. These problems restrict the utility of the technique, especially if detailed characteristics of the wave propagation phenomenon are to be studied. Nevertheless, the capability of the FORTRAN language to incorporate complex functions makes it possible to use Program HASK to study the three dimensional nature of many of the important secular lines.

The second approach to the analytic problem involved the discretization of the structure into elements of finite, or semi-finite, dimension. The behavior of this discretized model, when subjected to vibratory excitation, has been analyzed by the direct stiffness method (see Appendix 4). A computer program (SPRDSP), described in Appendix 5, has been developed which allows the excitation of models of this type to be studied in considerable detail.

This method has the advantage that there are a finite number of roots to the secular equation, all of which may be determined without ambiguity. In addition, the mode shapes may be studied in detail.

In practical application, however, the direct stiffness method was found to have limitations. The discretized model is an imperfect representation of the actual structure. The base of the model is equivalent to a rigid solid and must be placed at some finite depth. Many pavement structures are more realistically represented by a system resting on a semi-infinite half-space. The presence of the rigid base in the model allows energy to be reflected back into the system. This does not usually occur in the prototype. A modified boundary condition was developed to minimize this difficulty, and is discussed in Appendix 4, but a fully satisfactory solution to this problem has not been found.

The discretized model must conform to the assumptions inherent in the direct stiffness method. This frequently requires that the model be divided into a large number of sub-layers. The number of similtaneous equations which must be solved to obtain the solutions is then also very large. This demands large blocks of computer core and long execution times which may restrict the methods practicality.

Fundamentally, however, the greatest difficulty found in the study of wave propagation in layered media was the complexity of the solutions, the large number of variables and the overwhelming detail involved in all but the simplest cases. Program SPRDSP was used to assist in the interpretation of the secular lines representing dispersion in a single layer over a rigid base. (See Chapter 2). For more complex structures the quantity of data was found to be unmanageable and, with the present limited understanding of many of the basic phenomena, did not materially assist interpretation.

Despite these difficulties, an improved capability for the analysis

of elastic and visco-elastic structures was achieved. To help define the areas of greatest practical interest, there is a need for well documented case histories of field tests. A minimum of this type of information was found in the literature.

Interpretation Techniques

A review of the literature (see Chapter 4) revealed two principal approaches to the interpretation of dispersion curves obtained in wave propagation testing. The first relies on comparison of the high frequency range of the dispersion curve, obtained from the field, with the corresponding portion of the results obtained from an analysis of analogous plate structures. This method is considered to yield reliable values of material properties for simple structure which fall within certain specified limits. In general, it was found to be applicable to stiff, concrete or asphalt pavements resting on soft subgrades but only useful for the determination of the properties of the surface layer of more complex structures.

The second approach was found to have greater generality of application. The complete family of dispersion curve branches is considered. The general characteristics of the various branches, particularly their terminal points, are noted and compared with similar properties obtained in analytic studies. From this, it is possible to interpret the approximate material properties of the various layers in a structure subject to test. While this method allows fairly complex structure to be studied, the precision of the interpretation is somewhat uncertain. An analysis of a simple thick-lift asphalt pavement, made with the aid of the computer programs developed during this study, showed that a number of the assumptions inherent in this type of interpretation are either of uncertain accuracy, of in some cases, unwarranted. This study established the need

for further investigation of the basic characteristics of the secular functions, particularly for systems with properties similar to those of practical structures.

Application of Results

A principal advantage of the wave propagation method of testing is the ability to determine in-situ material properties. Thus, the need to account for a variety of environmental factors is eliminated. However, the loading imposed by the test equipment is dissimilar to that usually imposed by vehicles. The differences in strain amplitude are of major importance.

A review of the rheological response of soils and bituminous materials was undertaken and is presented in Appendix 6. It was shown that soil properties may be represented in the form of complex moduli. While sufficient experimental data is not available for all soils, it is possible to modify moduli obtained from wave propagation tests to yield properties suitable for use in analyses of structures subject to vehicular loading. Bituminous materials are also affected by the frequency of the loading and climatic conditions. These factors must also be considered when reviewing the results of wave propagation tests.

Equipment Design and Test Procedures

Equipment and test procedures for the wave propagation method were reviewed and inspected in the field. The results of this study are presented in Chapter 5. There were found to be a variety of equipment designs, many used in special applications, but two principal catagories can be recognized.

The first catagory includes systems designed around light weight vibrators. They are used in a number of applications where simplicity

and high mobility are an advantage. In many cases absolute material properties are not required. This occurs when the investigation can be limited to a comparison of relative conditions from site to site or over a period of time. Light weight equipment has the potential to produce data from which detailed dispersion curves for the high frequency range may be constructed. Light weight systems are suitable for use in conjunction with interpretation techniques which rely upon this portion of the curves. Their energy production is low, however, and they are restricted in their ability to reveal the properties of buried materials.

The second catagory of equipment is less mobile and considerably more expensive to develop than the light weight equipment. Based on heavy vibrators, these systems generate high energy excitations which are capable of penetrating to considerable depths beneath pavement structures. They are well suited to the testing of exiting pavements, preparatory to the design of overlays, but tend to be restricted to the moderate to low frequency range. Theoretical considerations, which have been discussed in Chapters 3 and 4, indicate that this limitation may prevent the application of some of the available interpretation methods to data obtained with this type of equipment.

The field investigations, which formed part of the research program, demonstrated the importance of careful equipment design and procedural organization. Simplicity of design, versatility and mobility of the equipment together with reliable procedures, which minimize operator fatigue and allow rapid execution, are essential. The interpretative technique to be applied to the field data should be considered in the design of equipment. Some methods require a high frequency capability while, for others, the equipment should be capable of producing excitation at great depth.

Recommendations

From the investigations reported here, three major divisions of the factors involved in wave propagation testing can be recognized. These are; the nature of the basic phenomena of wave propagation in layered systems, the practical interpretation of dispersion curves obtained from field tests and the design of testing equipment.

Many of the basic phenomena have been studied here and analytic tools have been developed. These studies should be extended to other simple structures which have characteristics similar to practical systems. Particular attention should be paid to singularities in the secular lines and their form in complex space. Program HASK, or a similar algorithm, should provide an economic aid in conducting these studies and the detailed results which can be obtained from the direct stiffness method may be of assistance. Improved understanding at this level would assist in interpretation of the more complex features of dispersion curves.

Due to the unmanageable quantity of data output from the analysis of models of the more complex types of pavement structure, it is recommended that future studies of this type should be conducted in close conjunction with carefully monitored field testing. In this way, those partions of the theoretical results which are of practical importance could be isolated and the problem reduced to manageable proportions. There are, at present, insufficient fully documented case histories available in the literature to be of assistance in this respect.

The theoretical studies presented have demonstrated, that in designing wave propagation testing equipment, close attention should be given to the interpretation method to be used in reducing the data. Close cooperation between analytic research and equipment design studies is

recommended. In this way, the most appropriate data can be obtained in the field and theoretical research may be concentrated in areas likely to yield the most practically fruitful results.

APPENDIX 1

PROPERTIES OF THE SPECTRAL LINES FOR AN ELASTIC LAYER OVER A RIGID SOLID

The spectral lines for an elastic solid layer in welded contact with a rigid solid are of the type shown in Fig. 2.5 which were obtained from Eq. (2.22). Eq. (2.22)is, in general, complex and may be expressed in the form:

$$F(k\ ,\ \omega) = F_1(k_1\ ,\ k_2\ ,\ \omega) + iF_2(k_1\ ,\ k_2\ ,\ \omega) \tag{A1.1}$$

where $k = k_1 + ik_2$.

At any point in the real plane $k_2 = 0$ and $F(k\ ,\ \omega)$ is real so that:

$$F_2(k_1\ ,\ 0\ ,\ \omega) = 0\ . \tag{A1.2}$$

For a point in close proximity to the real plane, i.e., at $F(k_1 + i\Delta k_2\ ,\ \omega)$ Eq. (A1.2) may be expanded into a Taylor series:

$$F(k_1 + ik_2\ ,\ \omega) = F_1(k_1\ ,\ 0\ ,\ \omega) + i\frac{\Delta k_2}{1!}\frac{\partial F_2}{\partial k_2}(k_1\ ,\ 0\ ,\ \omega) + \ldots \tag{A1.3}$$

For a point on a complex spectral line both the imaginary and real parts of this expression must be zero in accordance with the requirements of Eq. (2.22), i.e.,

$$F_1(k_1\ ,\ 0\ ,\ \omega) = 0 \tag{A1.4}$$

and

$$\Delta k_2 \frac{\partial F_2}{\partial k_2}(k_1\ ,\ 0\ ,\ \omega) = 0$$

if only the leading terms of Eq. (A1.3) are retained.

As Eq. (2.22) is an analytic function, the real and imaginary parts must satisfy the Cauchy-Riemann condition:

$$\frac{\partial F_2}{\partial k_2} = \frac{\partial F_1}{\partial k_1} \tag{A1.5}$$

and as $\Delta k_2 \neq 0$ on a complex spectral line Eq. (A1.5) may be written:

$$F(k_1 , \omega) = 0 \tag{A1.6}$$

and

$$\frac{\partial F}{\partial k_2} (k_1 , \omega) = 0 .$$

Let any pair of roots of the first equation of Eqs. (A1.6) be k_1^* and ω^* then from the first equation of Eqs. (A1.6) and the value of the function in close proximity to the real plane:

$$F(k_1^* , \omega^*) = 0 \tag{A1.8}$$

and

$$F(k_1^* + i\Delta k_2 , \omega^*) = 0 .$$

Eqs. (A1.7) indicate that a small movement away from the point (k_1^* , ω^*) perpendicular to the real plane is a movement along a complex branch. Thus, near the real plane each complex branch is contained in a plane perpendicular to the real plane.

Expanding

$$F(k_1^* + i\Delta k_2 , \omega^* + \Delta\omega)$$

in a Taylor series about (k_1^* , ω^*) and applying the same methods as before gives:

$$\frac{\partial \omega}{\partial (ik_2)} = \lim_{\Delta k_2 \to 0} \frac{\Delta \omega}{(i \Delta k_2)} = \frac{-\frac{\partial F}{\partial k_1}(k_1^* , \omega^*)}{\frac{\partial}{\partial \omega}(k_1^* , \omega^*)} \tag{A1.8}$$

In general $\frac{\partial F}{\partial \omega}(k_1^* , \omega^*)$ is not zero but from the second equation of Eqs. (A1.6) $\frac{\partial F}{\partial k_1}(k_1^* , \omega^*)$ is zero so that:

$$\frac{\partial \omega}{\partial (ik_2)} (k_1^* , \omega^*) = 0 \tag{A1.9}$$

Thus, the projections of the complex branches on the imaginary plane are perpendicular to the real plane so that Eqs. (A1.7) and Eq. (A1.9) together prove that the complex branches are perpendicular to the real plane where they intersect it. Similar arguments can be applied to the purely imaginary branches.

The method of expansion into a Taylor series may also be applied to

$$\frac{\partial F}{\partial \omega} \cdot \frac{\partial \omega}{\partial k_1} + \frac{\partial F}{\partial k_1} = 0 \tag{A1.10}$$

to show that

$$\frac{\partial \omega}{\partial k_1}(k_1 , \omega^*) = 0 \ . \tag{A1.11}$$

Therefore, the complex branches intersect the real plane at points on the real branches where their slope is zero. Again this argument can be applied equally to the purely imaginary branches.

Noting that if

$$F(k , \omega) = 0 \quad \text{on a branch line}$$

then $G(k^2 , \omega^2) = 0$. Thus all branches have mirror images about the plane $\omega = 0$. Assuming that $G(k^2 , \omega^2)$ is continuously differentiable

with respect to ω even at $\omega = 0$, $k \neq 0$ it may be concluded that the branches must be perpendicular to the plane $\omega = 0$.

All of the above conclusions are supported by the numerical values obtained for the roots of Eq. (2.22).

APPENDIX 2

THE THOMSON-HASKELL METHOD FOR THE ANALYSIS OF SURFACE WAVES ON MULTI-LAYERED MEDIA

Thomson (1950) presented a method for the analysis of waves transmitted through a stratified solid medium which formulates the problem in terms of matrices. This type of formulation is well suited for computation using a digital computer. However, there is an error in Thomson's presentation involving the boundary conditions at the interface between two layers. Thomson's analysis implies that shear strain must be continuous across an interface when in fact the correct boundary condition requires the shearing stress be continuous across the boundary. This error was noted by Haskell (1953) who also simplified the notation used by Thomson (1950).

The method used here closely follows Haskell's (1953) notation with minor revisions and further simplifications but is also extended to include the case where the layered media rest on a rigid solid.

Consider a layered system of the type shown in Fig. A2.1 which consists of layers extending infinitely in both the x and y directions in the horizontal plane. The system is excited by the forcing function $Pe^{i\omega t}$ which is constant in the y direction. Thus the model describes a plane system.

This disturbance in any layer m may be described in the form of displacement potentials as:

$$\begin{aligned} \phi_m &= [A_m \operatorname{Sinh}(r_m kz) + B_m \operatorname{Cosh}(r_m kz)] \exp[ik(ct - x)] \\ \psi_m &= [C_m \operatorname{Cosh}(s_m kz) + D_m \operatorname{Sinh}(s_m kz)] \exp[ik(ct - x)] \end{aligned} \qquad \text{(A2.1)}$$

where

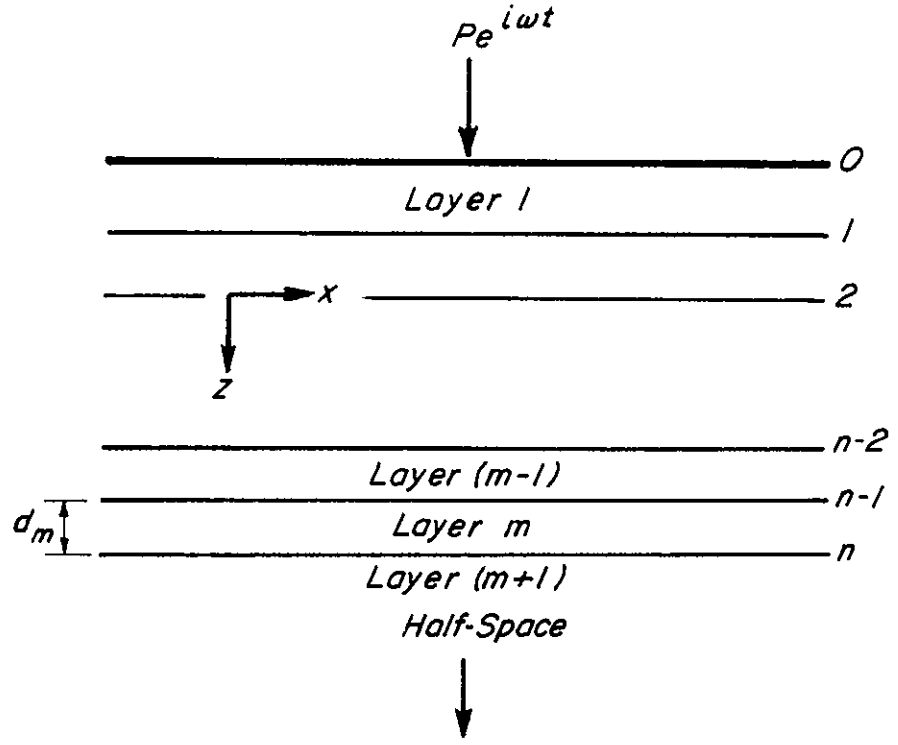

a. Layers Over an Elastic Half-Space

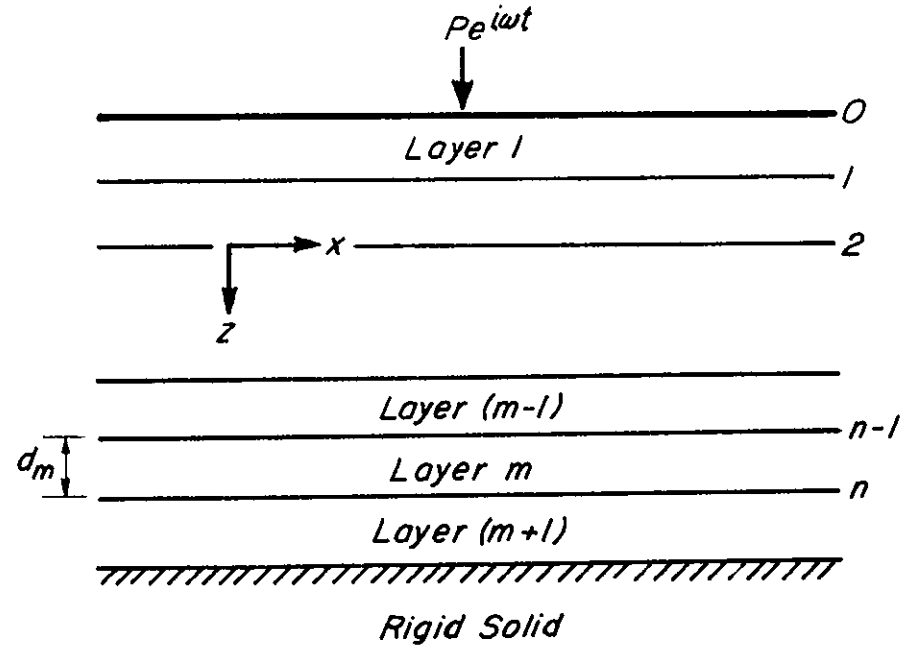

b. Layers Over a Perfectly Rigid Solid

Fig. A2.1 NOTATION FOR ANALYSIS OF WAVES IN LAYERED MEDIA BY THOMSON-HASKELL METHOD

$$r_m = ir = \sqrt{1 - c^2/\alpha^2}$$

$$s_m = is = \sqrt{1 - c^2/\beta^2}$$

The velocities and stresses at the bottom of the m^{th} layer ($z = d_m$) can be expressed in the matrix form.

$$\begin{bmatrix} \dot{u}/c \\ \dot{w}/c \\ \sigma_{zz} \\ \sigma_{zx} \end{bmatrix}_n = [F_m] \begin{bmatrix} A_m \\ B_m \\ C_m \\ D_m \end{bmatrix} \qquad \text{(A2.2)}$$

where $[F_m] =$

$$k^2 \begin{bmatrix} \text{Sinh}(r_m k d_m) & \text{Cosh}(r_m k d_m) & -is_m \text{Sinh}(s_m k d_m) & -is_m \text{Cosh}(s_m k d_m) \\ ir_m \text{Cosh}(r_m k d_m) & ir_m \text{Sinh}(r_m k d_m) & \text{Cosh}(s_m k d_m) & \text{Sinh}(s_m k d_m) \\ G_m b_m \text{Sinh}(r_m k d_m) & G_m b_m \text{Cosh}(r_m k d_m) & -2iG_m s_m \text{Sinh}(s_m k d_m) & -2iG_m s_m \text{Cosh}(s_m k d_m) \\ -2iG_m r_m \text{Cosh}(r_m k d_m) & -2iG_m r_m \text{Sinh}(r_m k d_m) & -G_m b_m \text{Cosh}(s_m k d_m) & -G_m b_m \text{Sinh}(s_m k d_m) \end{bmatrix}$$

where

$b_m = 2 - c^2/\beta^2$

$k = \omega/c$

G_m = shear modulus

d_m = layer thickness

m = layer number

n = interface number at bottom of m^{th} layer

At the top of the layer $(z = 0)$ the velocities and stresses are given by:

$$\begin{bmatrix} A_m \\ B_m \\ C_m \\ D_m \end{bmatrix} = [E_{n-1}]^{-1} \begin{bmatrix} \dot{u}/c \\ \dot{w}/c \\ \sigma_{zz} \\ \sigma_{zx} \end{bmatrix}_{n-1} \tag{A2.3}$$

where

$$[E_{n-1}]^{-1} = \frac{1}{k^2(b_m - 1)} \begin{bmatrix} 0 & -ib_m/r_m & 0 & -i/G_m r_m \\ -2 & 0 & 1/G_m & 0 \\ 0 & -2 & 0 & -1/G_m \\ ib_m/s_m & 0 & -i/G_m s_m & 0 \end{bmatrix}$$

and $n - 1$ refers to the interface at the top of the m^{th} layer.

Substituting Eq. (A2.3) into Eq. (A2.2) yields the following relationship between interface velocities and stresses at the top and bottom of the m^{th} layer.

$$\begin{bmatrix} \dot{u}/c \\ \dot{w}/c \\ \sigma_{zz} \\ \sigma_{zx} \end{bmatrix}_n = [g_m] \begin{bmatrix} \dot{u}/c \\ \dot{w}/c \\ \sigma_{zz} \\ \sigma_{zx} \end{bmatrix}_{n-1} \tag{A2.4}$$

where

$$[g_m] = [F_m][E_{n-1}]^{-1} .$$

Similarly for the $(m-1)^{th}$ layer.

$$\begin{bmatrix} \dot{u}/c \\ \dot{w}/c \\ \sigma_{zz} \\ \sigma_{zx} \end{bmatrix}_{n-1} = [g_{m-1}] \begin{bmatrix} \dot{u}/c \\ \dot{w}/c \\ \sigma_{zz} \\ \sigma_{zx} \end{bmatrix}_{n-2} \tag{A2.5}$$

Imposing the boundary condition that there must be continuity of stresses and displacements across the interface between the m^{th} and $(m-1)^{th}$ layer and combining Eq. (A2.4) and Eq. (A2.5) gives:

$$\begin{bmatrix} \dot{u}/c \\ \dot{w}/c \\ \sigma_{zz} \\ \sigma_{zx} \end{bmatrix}_{n} = [g_m][g_{m-1}] \begin{bmatrix} \dot{u}/c \\ \dot{w}/c \\ \sigma_{zz} \\ \sigma_{zx} \end{bmatrix}_{n-2} \tag{A2.6}$$

Noting that at the free surface the boundary condition is $\sigma_{zz} = \sigma_{zx} = 0$, the relationship between the velocities and stresses at the n^{th} interface and those at the free surface is thus:

$$\begin{bmatrix} \dot{u}/c \\ \dot{w}/c \\ \sigma_{zz} \\ \sigma_{zx} \end{bmatrix}_{n} = [g_m][g_{m-1}] \cdots [g_1] \begin{bmatrix} \dot{u}/c \\ \dot{w}/c \\ 0 \\ 0 \end{bmatrix}_{0} \tag{A2.7}$$

By substituting Eq. (A2.7) into Eq. (A2.3) an expression for the constants is obtained.

$$\begin{bmatrix} A_{m+1} \\ B_{m+1} \\ C_{m+1} \\ D_{m+1} \end{bmatrix} = [J] \begin{bmatrix} \dot{u}/c \\ \dot{w}/c \\ 0 \\ 0 \end{bmatrix}_0 \tag{A2.8}$$

where $[J]$ is the 4×4 matrix:

$$[J] = [E_n]^{-1}[g_m][g_{m-1}] \cdots [g_1] .$$

Note at this point that the n^{th} interface is at the top of the deepest elastic layer for the case of a system resting on a rigid solid but at top of the half-space where the system rests on an elastic half-space.

Eq. (A2.8) is perfectly general but for solution the boundary conditions at the bottom of the $(m + 1)^{th}$ layer must be considered and each case must be treated separately.

Layered System Resting on an Elastic Half-space

The boundary conditions at the bottom of the $(m + 1)^{th}$ layer are zero displacements and stresses at infinite depth. In addition, because no energy can be reflected back from the bottom of an infinitely deep layer, r and s must both be imaginary in the half-space. Under these conditions,

$$\begin{aligned} A_{m+1} &= B_{m+1} \\ C_{m+1} &= D_{m+1} \end{aligned} \tag{A2.9}$$

and Eq. (A2.8) becomes

$$\begin{bmatrix} A_{m+1} \\ A_{m+1} \\ C_{m+1} \\ C_{m+1} \end{bmatrix} = [J] \begin{bmatrix} \dot{u}/c \\ \dot{w}/c \\ 0 \\ 0 \end{bmatrix}_0 \tag{A2.10}$$

which gives:

$$(\dot{u}/\dot{w})_0 = \frac{J_{22} - J_{12}}{J_{11} - J_{21}} . \tag{A2.11}$$

and

$$(\dot{u}/\dot{w})_0 = \frac{J_{42} - J_{32}}{J_{31} - J_{41}} . \tag{A2.12}$$

Equating these expressions and presenting the result in determinant form gives:

$$\begin{vmatrix} (J_{22} - J_{12}) & (J_{42} - J_{32}) \\ (J_{11} - J_{21}) & (J_{31} - J_{41}) \end{vmatrix} = 0 \tag{A2.13}$$

The value of the wave number k which satisfies Eq. (A2.13) for any particular value of frequency ω may be found by trial and error.

Layered System Resting on a Rigid Plane

All energy incident to the rigid base will be perfectly reflected and there will be zero displacement at the bottom of the $(m + 1)^{th}$ layer.

$$\text{i.e.} \quad \text{At} \quad z = d_{m+1} \qquad \dot{u}/c = \dot{w}/c = 0 \ .$$

Enforcement of these boundary conditions results in the matrix equation

$$\begin{bmatrix} F_{11} & F_{12} & F_{13} & F_{14} \\ F_{21} & F_{22} & F_{23} & F_{24} \end{bmatrix}_{m+1} \begin{bmatrix} A_{m+1} \\ B_{m+1} \\ C_{m+1} \\ D_{m+1} \end{bmatrix} = 0 \qquad \text{(A2.14)}$$

Rewriting Eq. (A2.8) in the form:

$$\begin{aligned} A_{m+1} &= \frac{J_{11}J_{22} - J_{12}J_{21}}{J_{22}} \left(\frac{\dot{u}}{c}\right)_0 + \frac{J_{12}}{J_{22}} B_{m+1} \\ C_{m+1} &= \frac{J_{22}J_{31} - J_{21}J_{32}}{J_{22}} \left(\frac{\dot{u}}{c}\right)_0 + \frac{J_{32}}{J_{22}} B_{m+1} \qquad \text{(A2.15)} \\ D_{m+1} &= \frac{J_{22}J_{41} - J_{21}J_{42}}{J_{22}} \left(\frac{\dot{u}}{c}\right)_0 + \frac{J_{42}}{J_{22}} B_{m+1} \end{aligned}$$

which on substituting into Eq. (A2.14) results in two equations which may be put into the determinant form:

$$\begin{vmatrix} a_{11} & a_{12} \\ a_{21} & a_{22} \end{vmatrix} = 0 \qquad \text{(A2.16)}$$

where

$$\begin{aligned} a_{11} &= F_{11}(J_{12}J_{21}-J_{11}J_{22}) + F_{13}(J_{32}J_{21}-J_{31}J_{22}) + F_{14}(J_{42}J_{21}-J_{41}J_{22}) \\ a_{21} &= F_{21}(J_{12}J_{21}-J_{11}J_{22}) + F_{23}(J_{32}J_{21}-J_{31}J_{22}) + F_{24}(J_{42}J_{21}-J_{41}J_{22}) \\ a_{12} &= F_{11}J_{12} + F_{12}J_{22} + F_{13}J_{32} + F_{14}J_{42} \\ a_{22} &= F_{21}J_{12} + F_{22}J_{22} + F_{23}J_{32} + F_{24}J_{42} \end{aligned}$$

in which

F_{jk} are elements of the matrix $[F]_{m+1}$.

Thus a wave number k which satisfies Eq. (A2.16) must be obtained by trial and error for each excitation frequency ω .

The method as developed to this stage is a complete solution of the problem and is a very versatile technique. By application of the particular boundary conditions to Eq. (A2.8) many different systems (e.g. a multi-layered free plate) may be studied. However, from a practical point of view there are a number of difficulties.

Numerical Difficulties

The matrices involve hyperbolic functions, some of which may become very large in relation to others. If $c < \beta < \alpha$ both r_m and s_m are real and $r_m > s_m$. When $r_m kd_m$ is large $\text{Cosh}(r_m kd_m)$ and $\text{Sinh}(r_m kd_m)$ both become very large in relation to $\text{Cosh}(s_m kd_m)$ and $\text{Sinh}(s_m kd_m)$. In this case, as the matrix multiplications imply addition and subtraction, those elements which involve s_m are swamped by those involving r_m and tend to have no effect on the values stored by a digital computer.

Thrower (1965) has discussed these problems at length and has proposed a method which prevents terms involving s_m being overwhelmed. However, the new method introduces other precision problems which involve the risk of underflow when low phase velocities are considered. This difficulty can also be eliminated at the expense of some computational effort.

The general problem of accuracy is always present in computations involving exponentiation and in this case the advantage to be gained by the use of multiple-length arithmetic is not great compared to the

added difficulties created, especially when complex functions are involved. There are two simple steps which may be taken to reduce the severity of the problem. The elements of matrix [F] in Eq. (A2.2) may each be divided by whichever hyperbolic function is large and the model of the layered system may also be normalized in relation to the properties of one of the layers; usually the surface layer. Another approach is based on the fact that $\mathrm{Cosh}(r_m kd_m) \simeq \mathrm{Sinh}(r_m kd_m)$ and $\mathrm{Cosh}(s_m kd_m) \simeq \mathrm{Sinh}(s_m kd_m)$ if $r_m kd_m$ and $s_m kd_m$ are sufficiently large. Thower (1965) has shown that it is possible to obtain the characteristic determinant of wave modes which arise from interfaces above the layer in which this condition occurs by terminating the sequence of matrix multiplications in Eq. (A2.8) at the matrix [g] corresponding to this layer and treated the layer as a half-space. This result may be used to reduce the numbers of computations and thus reduce the risk of overflow in some cases but it is limited in scope and cannot be used in regions where $r_m kd_m$ is large but $s_m kd_m$ is not or where r_m is real and s_m is imaginary.

The accuracy of computation required to obtain reliable displacement vectors is much greater than that required if only the characteristics of the wave motion at the free surface are to be studied. Detailed information on the variation of displacements with depth below the surface may also require the introduction of additional layers formed by subdivision of the natural layering. This requires additional matrix multiplication with a resulting loss of accuracy. For these reasons it is not advisable to compute displacement vectors with a program designed to generate dispersion curves.

The computation of a dispersion curve requires that values of the

parameters ω and k be found for which the characteristic determinant is zero. Other equivalent pairs of parameters could also be chosen; such are phase velocity c and wave length L. However, since an iterative technique is required to find the combination of the pair of parameters for which the determinant is zero, the correct choice is of importance. One parameter is usually held constant and the other is varied in steps until a satisfactory result is obtained. This requires that there be a monotonical relationship between the parameters and in addition the path of the iteration should approximate as closely as possible a normal to the dispersion curve if difficulties are to be avoided. Harkrider, Hales and Press (1963) used c as the independent variable and were unable to obtain values of L for certain regions. Thrower (1965) demonstrated that the use of L as the independent variable avoids these problems.

The interpolation method used to find the root is constrained by the amount of information available as to the characteristics of the function. While it would be possible to generate the necessity derivatives by methods similar to those outlined previously to generate the determinant itself the extra work involved far outweights any advantages. In these circumstances some form of Regula-Falsi method is indicated. These methods require a pair of approximations, one on each side of the root and thus some initial procedure is required to search for the general region enclosing the root. These methods tend to be arbitrary and difficult to control.

The writer has found that the choice of the frequency ω and the wave number k with ω held constant and the search for a zero determinant made by varying k is very effective. The iteration in k is

controlled by Newton's method but with numerical differentiation. For the cases investigated, the relationship between ω and k was well suited to this technique if the usual requirement of the Newton method, that the first approximation is sufficiently close to the root to allow monotonical convergence, was observed. The Newton method also avoids the necessity for a dual procedure as required by Regula-Falsi methods. It is also rapidly convergent.

A major problem encountered in generating dispersion curves is "mode jumping." In general there are an infinite number of roots to the secular equation and many may be closely packed in space and they often cross at very acute angles. In these cases the first approximation to a root must be of very high quality if the iteration scheme is not to converge to a point on a dispersion curve associated with a mode other than that originally being followed. If mode jumping occurs there is often the danger that the error will pass unrecognized with resulting misrepresentation of the form of the dispersion curves.

Methods for the computation of dispersion do not usually yield reliable values of group velocity, $(d\omega/dk)$, with practical economy and this requires that predictor methods for curve following rely upon numerical differentiation with its attendant unreliability. Thus the basic method available to minimize the risk of mode jumping is the use of appropriately small step sizes. Thrower (1972) has suggested an interesting alternative method to reduce the mode jumping problem.

A point on a dispersion curve must satisfy the condition:

$$\Delta(k\ ,\ \omega) = 0 \qquad \text{(A2.17)}$$

where:

Δ = the characteristic determinant of the secular equation

k = the wave number

ω = the frequency

Consider instead curves satisfying:

$$\Delta(k\ ,\ \omega) = \text{constant} \tag{A2.18}$$

Differentiating gives:

$$\frac{d\,\omega}{dk} = \frac{\partial\Delta}{\partial\omega}\Big/\frac{\partial\Delta}{\partial k}\ . \tag{A2.19}$$

This is a differential equation for curves satisfying Eq. (A2.18). Eq. (A2.19) may be solved by the choice of some initial conditions and the use of an appropriate numerical method and contours of Δ may be obtained. A dispersion curve corresponds to the contour $\Delta = 0$. Such a method would be expected to suffer less from mode jumping than predictor corrector methods but again Eq. (A2.19) involves differentiation with attendant difficulties.

The secular equation for wave propagation in layered media composed of elastic materials contains may singularities at points where the dispersion curves move from one plane to another in complex space. It is not possible to follow a dispersion curve through those points by any of the methods described above and it is necessary to treat each branch of the curve separately.

In summary, the generation of dispersion curves for waves propagating in layered media poses a difficult numerical problem requiring a critical review of computational results if erroneous conclusions as to the nature of the phenomenon are to be avoided.

APPENDIX 3

COMPUTER PROGRAM HASK

A program for the computation of dispersion curves for multi-layered media by the Thomson-Haskell method. The theoretical methods employed are described in Appendices 2 and 8.

PROGRAM HASK

SECTION 1:	PROGRAM IDENTIFICATION
Title:	Wave Dispersion By Thomson-Haskell Method
Program Code Name:	HASK
Writer:	D. J. Watkins
Organization:	Department of Civil Engineering, University of California, Berkeley, California, 94720, U.S.A.
Date:	May 1973
Updates:	None, Version 0
Source Language:	FORTRAN IV (CDC 6400)
Availability:	Complete program listing Fig. A3.1
Abstract:	Program computes wave numbers and phase velocity of the surface wave as roots of the secular equation for wave propagation in multi-layered media. The layered system may rest on a half-space or a rigid solid. Up to 20 layers may be modeled. Material damping within layers may be simulated by the use of complex body wave velocities. Imaginary, real or complex roots may be computed.

SECTION 2: ENGINEERING DOCUMENTATION

Narrative Description

Program HASK -- "Wave Dispersion by Thomson-Haskell Method" -- computes dispersion curves for waves propagating in layered media. Up to 20 layers can be included in the input. Each must be described in terms of its mass density, thickness, and velocity of propagation of P- and S—waves in the material of which it is composed. Material damping in any layer may be input in the form of complex P- and S— wave velocities. The program calculates and prints coordinates of frequency, wave number and phase velocity and the characteristic determinant of the secular equation. The user is called upon to critically review the results and check that a continuous spectral line has been followed.

Method of Solution

The program uses the matrix formulation of the secular equation to compute dispersion curves for waves propagating in layered media. This formulation is variously known as Thomson or Haskell method and the program uses the modified form presented in Appendix 2.

The following assumptions are implicit.

1. The layers are of infinite lateral extent and are homogeneous and isotropic.
2. The materials forming the layers are either linearly elastic or visco-elastic.
3. The layers are in welded contact.

Curve following is achieved by a predictor-corrector method. The first root is obtained by iteration from an initial value supplied at

input. The second iteration to a root uses the first root as an initial value and is displaced from the first by an arbitrary shift along the frequency axis. Successive points are predicted by Newton's divided difference extrapolation of increasing order up to the third. The correction is performed in all cases by Newton's method of iteration. The step-size along the frequency axis is optimized by the method given in Appendix 8.

Program Capabilities

A maximum of 20 layers may be included in the model. The system may rest either on a half-space or a rigid solid. Complex, imaginary, or real branches of the dispersion curves may be analyzed. The curve following technique is designed to adjust its accuracy as the complexity of the curves requires but "mode-jumping" cannot be avoided altogether. No attempt is made to negotiate signularities which occur in curves for purely elastic systems.

The computations involve exponentiation and are therefore subject to loss of accuracy under certain conditions. There are two variables,

$$\text{RMKD} = d\sqrt{k^2 - \omega^2/\alpha^2} \quad \text{and} \quad \text{SMKD} = d\sqrt{k^2 - \omega^3/\beta^2}$$

where

α = P-wave velocity

β = S-wave velocity

k = wave number

d = depth of layer

for each layer which are subject to exponentiation. Depending upon the capability of the system, if either of these values exceeds approximately

740.0 the computation cannot be performed by the commonly available library subroutines. The program detects the occurrence of this condition and prints a warning.

To avoid misinterpretation of the results, the user is called upon to review the output critically to ensure that mode-jumping has not occurred and that the roots obtained by the iteration are reasonable. Loss of the curve being followed can usually be rectified by choosing a narrower range of frequency for the computations and building up the curve in stages. The maximum allowable step-size in the curve following algorithm is closely related to the range of frequency; small for small frequency range, larger for wider range.

Data Inputs

The data are input from punched cards using the format shown below. Any compatible system of units may be used but the frequency must be in radians/second.

CARD GROUP	FORMAT	COLUMN	DESCRIPTION
A	2I10, 2F10.0	1 - 10	NL - No. layers in the system (including the half-space if present)
		11 - 20	MOP - Set as follows: 1 if system rests on a half-space 2 if system rests on a rigid solid
		21 - 30	OMF - The excitation frequency at which the curve is to be initiated
		31 - 40	OML - The excitation frequency at which computation is to be terminated

B	8F10.0	1 - 10 11 - 20	D(I, 1) - The real and imaginary parts of the complex P-wave velocity
		21 - 30 31 - 40	D(I, 2) - The real and imaginary parts of the complex S-wave velocity
		41 - 50	D(I, 3) - The mass density
		51 - 60	Leave blank
		61 - 70	D(I, 4) - The depth of the layer
		71 - 80	Leave blank

Group B consists of NL cards, one for each layer commencing with the surface layer. If the system rests on a half-space include a card giving its properties but with columns 61-70 set to 1.0.

C	2F10.0	1 - 10 11 - 20	KG - the value of the wave number (which may be complex, real or imaginary) to be used to start the iteration to find a root at the initial frequency OMF

Program Options:

There are no special options other than that controlled by the option switch MOP described in Card Group A above. The program terminates upon receipt of a zero value for the number of layers NL .

Printed Output:

The printed output consists of a reformatted playback of the input data and a tabulation of the results. See Fig. A3.4.

Other Outputs:

All output is produced on the line printer. No special messages other than those on the printed output are produced.

Sample Run:

A sample problem for program HASK is shown in Fig. A3.2. The input data is shown in Fig. A3.3 and the resulting output in Fig. A3.4.

SECTION 3: SYSTEM DOCUMENTATION

Computer Equipment

Program HASK was developed on a CDC 6400 computer with 65 k core memory. The computer uses a 60-bit word length with floating point arithmetic performed in single words. The core cycle time is 1.0 μ sec. per memory bank but interlacing of up to 10 memory banks is possible.

Peripheral Equipment

The following peripheral equipment was used during development of this program: CDC 405 card reader. CDC 501 or IBM 1403 line printer.

Source Program

The source listings for HASK and subroutines DETER, SECNT and EXTRAP are given in Fig. A3.1.

Variables and Subroutines

The principal variables in the program are as follows:

OM - frequency (real)

K - phase velocity (complex)

KG - wave number approximating a root of the secular equation (complex)

C - phase velocity (complex)

D(I, 1) - P-wave velocity in layer I (complex)

D(I, 2) - S-wave velocity in layer I (complex)

D(I, 3) - mass density of layer I (real no. treated as complex)

D(I, 4) - depth of layer I (real no. treated as complex)

DET - characteristic determinant (complex)

NL - number of layers (integer)

MOP - option switch for base of system (integer)

OMF - initial frequency (real)

OML - final frequency (real)

The program consists of the following parts:

1. HASK. Main program for input, output and curve following. Calls DETER, SECNT and EXTRAP
2. Subroutine DETER. Computes the characteristic determinant.
3. Subroutine SECNT. Iterates to a root of the secular equation by Newton's method with numerical differentiation. Calls DETER.
4. Subroutine EXTRAP. Predicts next root along dispersion curve and optimizes step size in frequency.
5. Library Subroutines. Subroutines for computation of a complex number from two real arguments (CMPLX), extraction of the real part of a complex number (REAL), extraction of the imaginary part of a complex number (AIMAG), complex absolute (CABS), complex exponentiation (CEXP), absolute (ABS) and integer to real conversion (FLOAT) are required and are supplied by the system.

Data Structure

No files are created by the program. Data is read from file INPUT. Output is written on file OUTPUT.

Storage Requirements

This program requires less than 50,000 octal words of storage.

Maintenance and Updates

None to date.

SECTION 4: OPERATING DOCUMENTATION

Operator Instructions

There are no special operator instructions.

Run Time

Execution time depends upon the number of soil layers used and other problem parameters. The sample problem with a single layer over a half-space was executed in approximately 1.8 secs on the CDC 6400 computer.

FIG. A3.1

LISTING OF PROGRAM HASK

(The next three pages form Fig. A3.1)

FIG. A3.1 LISTING OF PROGRAM HASK

```
      PROGRAM HASK(INPUT,OUTPUT)
C
C-----DISPERSION OF WAVES IN LAYERED MEDIA BY THOMSON-HASKELL METHOD
C
      COMMON/BLOCKA/D(20,4),MOP,NL
      COMMON/BLOCKB/OMF,OML,SK(4),SOM(4)
      COMPLEX C,D,DET,K,KG,SK
      DATA HS/10HHALF SPACE/
      PI2=6.2831853072
C
C-----READ INPUT DATA AND PRINT PROPERTIES OF STRUCTURE
C
   10 READ 100,NL,MOP,OMF,OML
      IF(NL.EQ.0) STOP
      PRINT 400
      DO 15 I=1,NL
      READ 200,(D(I,N),N=1,4)
      RHO=REAL(D(I,3))
      IF(I.EQ.NL.AND.MOP.NE.2) GO TO 11
      DEPTH=REAL(D(I,4))
   15 PRINT 500,I,(D(I,N),N=1,2),RHO,DEPTH
      GO TO 12
   11 PRINT 550,I,(D(NL,N),N=1,2),RHO,HS
   12 GO TO (16,17),MOP
   16 PRINT 700
      GO TO 18
   17 PRINT 800
   18 PRINT 600
C
C-----COMPUTE FIRST TWO POINTS ON DISPERSION CURVE
C
      READ 200,KG
      CALL DETER(OMF,KG,DET)
C
      K=KG
      CALL SECNT(K,DET,OMF)
      C=CMPLX(OMF,0.0)/K
      WL=PI2/REAL(K)
      PRINT 300,OMF,K,C,WL,DET
      SK(1)=K
      SOM(1)=OMF
      OM=OMF-(OMF-OML)/100.0
      SOM(2)=OM
      CALL DETER(OM,K,DET)
      CALL SECNT(K,DET,OM)
      C=CMPLX(OM,0.0)/K
      WL=PI2/REAL(K)
      PRINT 300,OM,K,C,WL,DET
      SK(2)=K
      NP=0
C
C-----FOLLOW DISPERSION CURVE BY PREDICTION AND CORRECTION
C
   20 NP=NP+1
      IF(NP.GT.4) NP=4
      CALL EXTRAP(K,KG,OM,NP)
      CALL DETER(OM,KG,DET)
      K=KG
      CALL SECNT(K,DET,OM)
      C=CMPLX(OM,0.0)/K
      WL=PI2/REAL(K)
      PRINT 300,OM,K,C,WL,DET
      IF(OM.EQ.OML) GO TO 10
      GO TO 20
  100 FORMAT(2I10,2F10.0)
  200 FORMAT(8F10.0)
  300 FORMAT(2X,E12.5,2(5X,2E12.5),5X,F12.5,5X,2E12.5)
  400 FORMAT(1H1,41X,27HDISPERSION IN LAYERED MEDIA,////,
     14X,9HLAYER NO.,13X,5HALPHA,30X,4HBETA,23X,3HRHO,13X,5HDEPTH)
  500 FORMAT(4X,I5,6(5X,E12.5))
  550 FORMAT(4X,I5,5(5X,E12.5),7X,A10)
  600 FORMAT(//,5X,9HFREQUENCY,12X,11HWAVE NUMBER,17X,14HPHASE VELOCITY,
     110X,11HWAVE LENGTH,14X,11HDETERMINANT,/)
  700 FORMAT(/,4X,32HTHE SYSTEM RESTS ON A HALF SPACE)
  800 FORMAT(/,4X,33HTHE SYSTEM RESTS ON A RIGID SOLID)
      END


      SUBROUTINE DETER(OM,K,DET)
C
C-----COMPUTES CHARACTERISTIC DETERMINANT OF SECULAR EQUASION FOR
C     WAVES PROPOGATING IN LAYERED MEDIA
C
      COMMON/BLOCKA/D(20,4),MOP,NL
      COMPLEX AJ(4,4),BM,CCA,CCB,COSHR,COSHS,D,DET,E(4,4),EXP,EXS,F(4,4)
     1,G(4,4),GM,K,KBT,KS,RM,RMKD,RMKS,S(4,4),SINHR,SINHS,SM,SMKD,EXR1,E
     2XS1
      ND=0
      DO 10 I=1,NL
      J=NL+1-I
C
C-----INITIALIZE ELEMENTS
C
      DO 20 L=1,4
      DO 20 M=1,4
      AJ(L,M)=(0.0,0.0)
      E(L,M)=(0.0,0.0)
      F(L,M)=(0.0,0.0)
   20 G(L,M)=(0.0,0.0)
      GO TO 150
   30 J=NL
      ND=1
C
C-----COMPUTE THE BASIC FUNCTIONS
C
  150 CCA=(CMPLX(OM,0.0)/D(J,1))**2
      CCB=(CMPLX(OM,0.0)/D(J,2))**2
```

```
      KS=K**2
      GM=D(J,2)**2*D(J,3)
      RM=CSQRT(KS-COA)
      SM=CSQRT(KS-COB)
      RM=KS+KS-COB
      RMKD=RM*D(J,4)
      SMKD=SM*D(J,4)
      IF(CABS(RMKD).GT.740.0.OR.CABS(SMKD).GT.740.0) GO TO 200
      EXR=CEXP(RMKD)
      EXR1=CEXP(-RMKD)
      EXS=CEXP(SMKD)
      EXS1=CEXP(-SMKD)
      SINHR=(0.5,0.0)*(EXR-EXR1)
      SINHS=(0.5,0.0)*(EXS-EXS1)/SINHR
      COSHR=(0.5,0.0)*(EXR+EXR1)/SINHR
      COSHS=(0.5,0.0)*(EXS+EXS1)/SINHR
      SINHR=SINHR/SINHR
      IF(ND.EQ.1) GO TO 170
C
C-----COMPUTE THE ELEMENTS OF MATPIX E
C
      E(1,2)=-(0.0,1.0)*BM/RM/K/COB
      E(1,4)=-(0.0,1.0)/GM/RM/COB*K
      E(2,1)=-(2.0,0.0)/COB
      E(2,3)=(1.0,0.0)/GM/COB
      E(3,2)=E(2,1)
      E(3,4)=-E(2,3)
      E(4,1)=(0.0,1.0)*BM/SM/K/COB
      E(4,3)=-(0.0,1.0)/GM/SM/COB*K
      IF(I.EQ.1.AND.ND.EQ.0) GO TO 80
C
C-----COMPUTE THE ELEMENTS OF MATRIX F
C
  170 F(1,1)=SINHR*KS
      F(1,2)=COSHR*KS
      F(1,3)=-(0.0,1.0)*SM*SINHS*K
      F(1,4)=-(0.0,1.0)*SM*COSHS*K
      F(2,1)=(0.0,1.0)*RM*COSHR*K
      F(2,2)=(0.0,1.0)*RM*SINHR*K
      F(2,3)=COSHS*KS
      F(2,4)=SINHS*KS
      F(3,1)=GM*BM*SINHR
      F(3,2)=GM*BM*COSHR
      F(3,3)=-(0.0,2.0)*GM*SM*SINHS*K
      F(3,4)=-(0.0,2.0)*GM*SM*COSHS*K
      F(4,1)=-(0.0,2.0)*GM*RM*COSHR*K
      F(4,2)=-(0.0,2.0)*GM*RM*SINHR*K
      F(4,3)=-GM*BM*COSHS
      F(4,4)=-GM*BM*SINHS
      IF(ND.EQ.1) GO TO 110
C
C-----COMPUTE MATRIX G=F*E
C
      DO 40 L=1,4
      DO 40 M=1,4
      DO 40 N=1,4
   40 G(L,M)=G(L,M)+F(L,N)*E(N,M)
C
C-----COMPUTE MATRIX J
C
      DO 50 L=1,4
      DO 50 M=1,4
      DO 50 N=1,4
   50 AJ(L,M)=AJ(L,M)+S(L,N)*G(N,M)
      GO TO 100
   80 CONTINUE
      DO 90 L=1,4
      DO 90 M=1,4
   90 AJ(L,M)=E(L,M)
  100 CONTINUE
      DO 70 L=1,4
      DO 70 M=1,4
   70 S(L,M)=AJ(L,M)
      IF(I.EQ.NL.AND.MOP.EQ.2) GO TO 30
   10 CONTINUE
      IF(MOP.EQ.2) GO TO 110
C
C-----ELEMENTS OF DETERMINANT FOR SYSTEM ON A HALF SPACE
C
      E(1,1)=AJ(2,2)-AJ(1,2)
      E(1,2)=AJ(4,2)-AJ(3,2)
      E(2,1)=AJ(1,1)-AJ(2,1)
      E(2,2)=AJ(3,1)-AJ(4,1)
      GO TO 120
  110 IF(NL.EQ.1) GO TO 180
C
C-----ELEMENTS OF DETERMINANT FOR SYSTEM ON A RIGID SOLID
C
      S(1,1)=AJ(1,2)*AJ(2,1)-AJ(1,1)*AJ(2,2)
      S(1,2)=(0.0,0.0)
      S(1,3)=AJ(3,2)*AJ(2,1)-AJ(3,1)*AJ(2,2)
      S(1,4)=AJ(4,2)*AJ(2,1)-AJ(4,1)*AJ(2,2)
      DO 160 L=1,4
      DO 160 M=1,4
  160 E(L,M)=(0.0,0.0)
      DO 130 L=1,2
      DO 130 M=1,4
  130 E(L,1)=E(L,1)+F(L,M)*S(1,M)
      DO 140 L=1,2
      DO 140 M=1,4
  140 E(L,2)=E(L,2)+F(L,M)*AJ(M,2)
      GO TO 120
C
C-----SPECIAL CASE FOR SINGLE LAYER OVER A RIGID SOLID
C
  180 DO 190 L=1,2
      E(L,1)=E(L,1)-(0.0,2.0)*RM/BM*E(L,3)*K
  190 E(L,2)=E(L,4)+(0.0,2.0)*SM/BM*E(L,2)*K
C
C-----COMPUTE CHARACTERISTIC DETERMINANT
C
  120 DET=E(1,1)*E(2,2)-E(1,2)*E(2,1)
```

```
      RETURN
  200 PRINT 300,OM,K
  300 FORMAT(10X,52HRESIGNED AFTER ATEMPT TO EXPONENTIATE LARGE ARGUMENT
     1,/,10X,3HOM=,1X,E12.5,1X,2HK=,2(1X,E12.5))
      STOP
      END



      SUBROUTINE SECNT(K,DET,OM)
C
C-----ITERATION TO FIND THE ROOT OF AN EQUATION BY NEWTON METHOD
C     WITH NUMERICAL DIFFERENTIATION
C
      COMPLEX K,K1,K2,DET,DET1,DET2,AC,SL,SL1
      NC=0
C
C-----OBTAIN FIRST TWO VALUES
C
      K1=K
      DET1=DET
      K2=K1+K1/(100.0,0.0)
      CALL DETER(OM,K2,DET)
      DET2=DET
C
C-----ITERATE TO ROOT
C
   10 IF(CABS(K2-K1).LT.1.0E-10) RETURN
      SL=(K2-K1)/(DET2-DET1)
      K=K2-DET2*SL
      NC=NC+1
      CALL DETER(OM,K,DET)
      K1=K2
      K2=K
      DET1=DET2
      DET2=DET
      IF(CABS(DET2-DET1).EQ.0.0) RETURN
      IF(NC.EQ.50) GO TO 20
      GO TO 10
   20 PRINT 100
      PRINT 200,OM,K,DET
      STOP
  100 FORMAT(10X,53HRESIGNED AFTER 50 ITERATIONS TO FIND ZERO DETERMINAN
     1T)
  200 FORMAT(10X,3HOM=,1X,E12.5,1X,2HK=,2(1X,E12.5),1X,4HDET=,2(1X,E12.5
     1))
      END



      SUBROUTINE EXTRAP(K,KG,OM,NP)
C
C-----NEWTON DIVIDED DIFFERENCE PREDICTOR - 3RD ORDER
C
      COMMON/RLOCKA/OMF,OML,SK(4),SOM(4)
      COMPLEX D10,D21,D210,D32,D321,D3210,K,KG,P(3),SK
      DIMENSION EST(3)
      OD=100.0
      GO TO(13,12,11,10) NP
C
C-----STORE COORDINATES OF POINTS
C
   10 SOM(1)=SOM(2)
      SOM(2)=SOM(3)
      SOM(3)=SOM(4)
      SOM(4)=OM
      SK(1)=SK(2)
      SK(2)=SK(3)
      SK(3)=SK(4)
      SK(4)=K
      OD=10.0
      GO TO 13
   11 SOM(4)=OM
      SK(4)=K
      OD=10.0
      GO TO 13
   12 SOM(3)=OM
      SK(3)=K
      OD=50.0
   13 IF(NP.GT.3) NP=3
C
C-----COMPUTE OPTIMAL STEP SIZE
C
      EST(1)=0.59
      EST(2)=0.39
      EST(3)=0.24
      OMX=(OML-OMF)/OD
      DOM=(OM-SOM(NP))*((EST(NP)/CABS(K-KG))**(1.0/FLOAT(NP+1)))
      IF(ABS(DOM).GT.ABS(OMX)) DOM=OMX
      OM=OM+DOM
      IF((OML-OM)*OMX.LT.0.0) OM=OML
C
C-----COMPUTE DIFFERENCES AND PREDICT ROOT
C
      D10=(SK(2)-SK(1))/CMPLX((SOM(2)-SOM(1)),0.0)
      P(1)=SK(1)+CMPLX((OM-SOM(1)),0.0)*D10
      IF(NP.EQ.1) GO TO 20
      D21=(SK(3)-SK(2))/CMPLX((SOM(3)-SOM(2)),0.0)
      D210=(D21-D10)/CMPLX((SOM(3)-SOM(1)),0.0)
      P(2)=P(1)+CMPLX((OM-SOM(1))*(OM-SOM(2)),0.0)*D210
      IF(NP.EQ.2) GO TO 20
      D32=(SK(4)-SK(3))/CMPLX((SOM(4)-SOM(3)),0.0)
      D321=(D32-D21)/CMPLX((SOM(4)-SOM(2)),0.0)
      D3210=(D321-D210)/CMPLX((SOM(4)-SOM(1)),0.0)
      P(3)=P(2)+CMPLX(((OM-SOM(3))*(OM-SOM(2))*(OM-SOM(1))),0.0)*D3210
   20 KG=P(NP)
      RETURN
      END
```

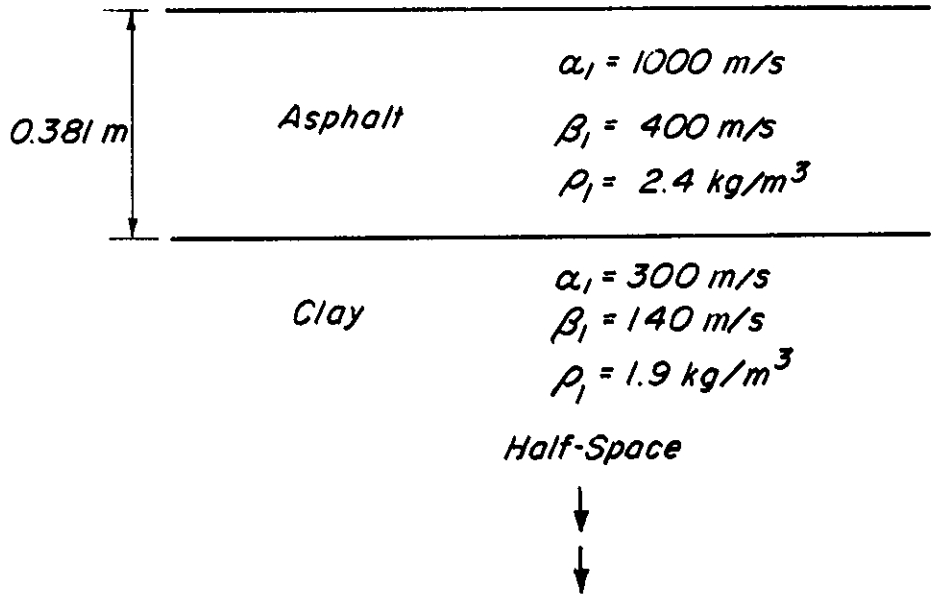

Fig. A 3.2 SAMPLE PROBLEM FOR PROGRAM HASK

Column Number

1	10	20	30	40	50	60	70	80
	2	1	1000.0	500.0				
	1000.0	0.0	400.0	0.0	2.4		0.381	
	300.0	0.0	140.0	0.0	1.9		1.0	
	5.0	0.0						

Total of 4 cards

Fig. A 3.3 INPUT FOR SAMPLE PROBLEM FOR PROGRAM HASK

FIG. A3.4

SAMPLE OUTPUT FROM PROGRAM HASK

(The next page forms Fig. A3.4)

DISPERSION IN LAYERED MEDIA

LAYER NO.	ALPHA		BETA		RHO	DEPTH
1	.10000E+04	0.	.40000E+03	0.	.24000E+01	.38100E+00
2	.30000E+03	0.	.14000E+03	0.	.19000E+01	HALF SPACE

THE SYSTEM RESTS ON A HALF SPACE

FREQUENCY	WAVE NUMBER		PHASE VELOCITY		WAVE LENGTH	DETERMINANT	
.10000E+04	.40824E+01	.75069E+00	.23694E+03	-.43570E+02	.15391E+01	.10658E-13	.38192E-13
.99500E+03	.40692E+01	.75025E+00	.23648E+03	-.43600E+02	.15441E+01	-.71054E-14	.11546E-13
.99149E+03	.40600E+01	.74994E+00	.23615E+03	-.43621E+02	.15476E+01	-.35527E-14	-.22204E-13
.98149E+03	.40336E+01	.74904E+00	.23521E+03	-.43679E+02	.15577E+01	.35527E-14	-.71054E-14
.93149E+03	.39015E+01	.74399E+00	.23037E+03	-.43931E+02	.16104E+01	.31974E-13	-.61284E-13
.88149E+03	.37687E+01	.73795E+00	.22526E+03	-.44107E+02	.16672E+01	.14211E-13	.42633E-13
.83149E+03	.36353E+01	.73069E+00	.21985E+03	-.44189E+02	.17284E+01	.71054E-14	.31974E-13
.78149E+03	.35010E+01	.72195E+00	.21411E+03	-.44152E+02	.17947E+01	-.49738E-13	.88818E-14
.73149E+03	.33660E+01	.71138E+00	.20803E+03	-.43965E+02	.18667E+01	.63949E-13	-.13323E-13
.68149E+03	.32300E+01	.69847E+00	.20156E+03	-.43587E+02	.19453E+01	-.14211E-12	-.76383E-13
.63149E+03	.30929E+01	.68257E+00	.19469E+03	-.42965E+02	.20315E+01	-.85265E-13	.38014E-12
.58149E+03	.29548E+01	.66275E+00	.18737E+03	-.42027E+02	.21265E+01	-.14211E-12	.33573E-12
.53149E+03	.28152E+01	.63767E+00	.17958E+03	-.40676E+02	.22319E+01	-.45475E-12	-.70344E-12
.50000E+03	.27265E+01	.61832E+00	.17441E+03	-.39553E+02	.23045E+01	.22737E-12	.67857E-12

APPENDIX 4

THE DIRECT STIFFNESS METHOD FOR THE ANALYSIS OF WAVES IN MULTI-LAYERED MEDIA

The direct stiffness method for the analysis of waves in multi-layered media was developed by Lysmer (1970) and is based upon discretization of the half-space into finite elements. The finite element method in its general form is well known (Zienkiewicz, 1971), so that the full development will not be shown here. The principal steps of Lysmer's (1970) method as outlined below follow the original with only minor changes in notation and sign convention according to the system used by Lysmer and Drake (1972).

Harmonic displacements in the layered system of the type shown in Fig. (A4.1) may be expressed as:

$$\begin{aligned} \delta_x &= u(z) \cdot \exp(i\omega t - ikx) \\ \delta_z &= w(z) \cdot \exp(i\omega t - ikx) \end{aligned} \qquad \text{(A4.1)}$$

where

δ_x and δ_z are the displacement with respect to the coordinate x and z respectively

ω = frequency of the motion

k = wave number

u(z) and w(z) are the horizontal and vertical amplitude functions respectively.

The sign conventions are as shown in Fig. A4.1. Note that the layered system rests upon a rigid solid half-space. The structure consists of n layers, each of which may have its own mass density ρ_j,

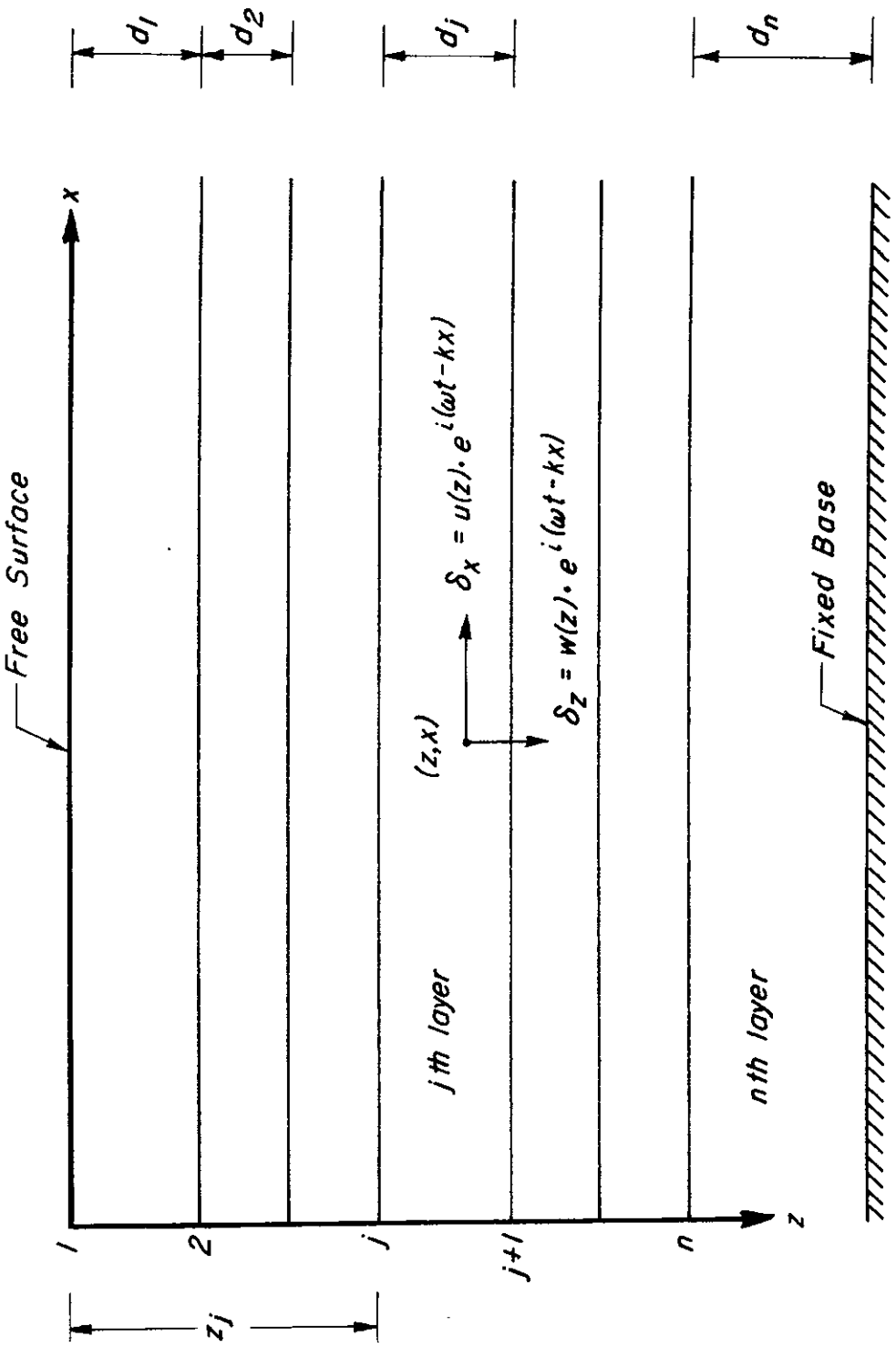

Fig. A4.1 TYPICAL LAYERED STRUCTURE

shear modulus G_j and Lame's constant $\lambda_j = 2G_j\nu_j/(1 - 2\nu_j)$ where ν_j is Poisson's ratio.

The basic assumption of Lysmer's method is that all displacements vary linearly with z within each layer. In order for this assumption to be reasonable, the thicknesses, d_j, of the layers shown in Fig. 4.1 must be chosen small compared to the wave length of shear waves in the layers. For this reason the number, n, of layers in the discrete system is usually chosen larger than the original number of layers which is being modeled. This is easily accomplished by subdivision of the original layering. The importance of this restriction is discussed by Lysmer and Waas (1972) and Lysmer and Kuhlemeyer (1969) suggested that the depth of a layer be restricted to 1/12 of the length of a shear wave in the medium.

With the above assumption the displacement field of the layered structure is completely defined by the $2n$ displacements δ_{xj} and δ_{zj}, $j = 1, \ldots n$, of the interfaces between layers. They will be collected in the vector

$$\{\delta\} = \begin{Bmatrix} \delta_{x1} \\ \delta_{z1} \\ \delta_{x2} \\ \delta_{z2} \\ \vdots \\ \delta_{xn} \\ \delta_{zn} \end{Bmatrix} \qquad \text{(A4.2)}$$

and will be referred to as the displacements of the structure. Similarly by

Eqs. (A4.1), the displacements are defined by the frequency, ω , the wave number, k , and the $2n$ complex numbers

$$\left.\begin{aligned} v_{2j-1} &= u(z_j) \\ v_{2j} &= w(z_j) \end{aligned}\right\} \; j = 1 \; , \; \ldots \; , \; n \tag{A4.3}$$

which will be referred to as the amplitudes of the wave and will be collected in a column vector $\{v\}$. With the introduction of this notation, the displacements of a wave can be written in the simple form

$$\{\delta\} = \{v\} \exp(i\omega t - ikx) \; . \tag{A4.4}$$

The Equations of Motion

By application of the finite element method to the layered structure in Fig. A4.1 Lysmer (1970) obtained the following equation of motion for generalized Rayleigh waves

$$([A]k^2 + i[B]k + [G] - \omega^2[M])\{v\} = \{0\} \; . \tag{A4.5}$$

In this equation the $2n \times 2n$ matrices $[A]$, $[B]$, $[G]$, and $[M]$ are assembled by addition of layer submatrices as indicated in Fig. A4.2. The submatrices to be substituted for $[X]_j$ in Fig. A4.2 are:

$$[A]_j = \frac{d_j}{6}\begin{bmatrix} 2(2G_j+\lambda_j) & 0 & (2G_j+\lambda_j) & 0 \\ 0 & 2G_j & 0 & G_j \\ (2G_j+\lambda_j) & 0 & 2(2G_j+\lambda_j) & 0 \\ 0 & G_j & 0 & 2G_j \end{bmatrix}, \quad j=1,\ldots,n \qquad (A4.6)$$

$$[B]_j = \frac{1}{2}\begin{bmatrix} 0 & (G_j-\lambda_j) & 0 & (G_j+\lambda_j) \\ -(G_j-\lambda_j) & 0 & (G_j+\lambda_j) & 0 \\ 0 & -(G_j+\lambda_j) & 0 & -(G_j-\lambda_j) \\ -(G_j+\lambda_j) & 0 & (G_j-\lambda_j) & 0 \end{bmatrix}, \quad j=1,\ldots,n \qquad (A4.7)$$

$$[G]_j = \frac{1}{d_j}\begin{bmatrix} G_j & 0 & -G_j & 0 \\ 0 & (2G_j+\lambda_j) & 0 & -(2G_j+\lambda_j) \\ -G_j & 0 & G_j & 0 \\ 0 & -(2G_j+\lambda_j) & 0 & (2G_j+\lambda_j) \end{bmatrix}, \quad j=1,\ldots,n \qquad (A4.8)$$

for matrices [A], [B], and [G], respectively. These matrices are obviously related to the stiffness of the layered structure. They will therefore be referred to as stiffness matrices.

The mass matrix [M] may be assembled from the submatrices

$$[M]_j = \rho_j d_j \begin{bmatrix} 1/2 & 0 & 0 & 0 \\ 0 & 1/2 & 0 & 0 \\ 0 & 0 & 1/2 & 0 \\ 0 & 0 & 0 & 1/2 \end{bmatrix}, \quad j = 1 , \ldots , n \qquad (A4.9)$$

These matrices correspond to lumping of all masses at the interfaces between layers. An improvement in accuracy can be obtained by using the submatrices

$$[M]_j = \rho_j d_j \begin{bmatrix} 1/3 & 0 & 1/6 & 0 \\ 0 & 1/3 & 0 & 1/6 \\ 1/6 & 0 & 1/3 & 0 \\ 0 & 1/6 & 0 & 1/3 \end{bmatrix} , \quad j = 1 , \ldots , n \tag{A4.10}$$

which correspond to Archer's (1963) consistent mass matrix. Alternatively some combination of submatrices Eqs. (A4.9) and Eqs. (A4.10) may be used.

The submatrices defined by Eqs. (A4.6) to (A4.10) correspond to individual layers of the structure. The matrices $[A]_j$, $[G]_j$ and $[M]_j$ are symmetric and $[B]_j$ is skew symmetric. The assembled matrices will therefore also have these properties.

As the motion is harmonic with the frequency ω the equation of motion reduces to

$$([A]k^2 + i[B]k + [C])\{v\} = \{0\} \tag{A4.11}$$

where $[C]$ is the symmetric matrix

$$[C] = [G] - \omega^2[M] . \tag{A4.12}$$

Eq. (A4.11) constitutes a set of $2n$ linear homogeneous equations which have solutions $\{v\}$ if, and only if, the determinant of the coefficient matrix vanishes. Hence, for any given ω , the secular equation

$$\left|[A]k^2 + i[B]k + [C]\right| = 0 \tag{A4.13}$$

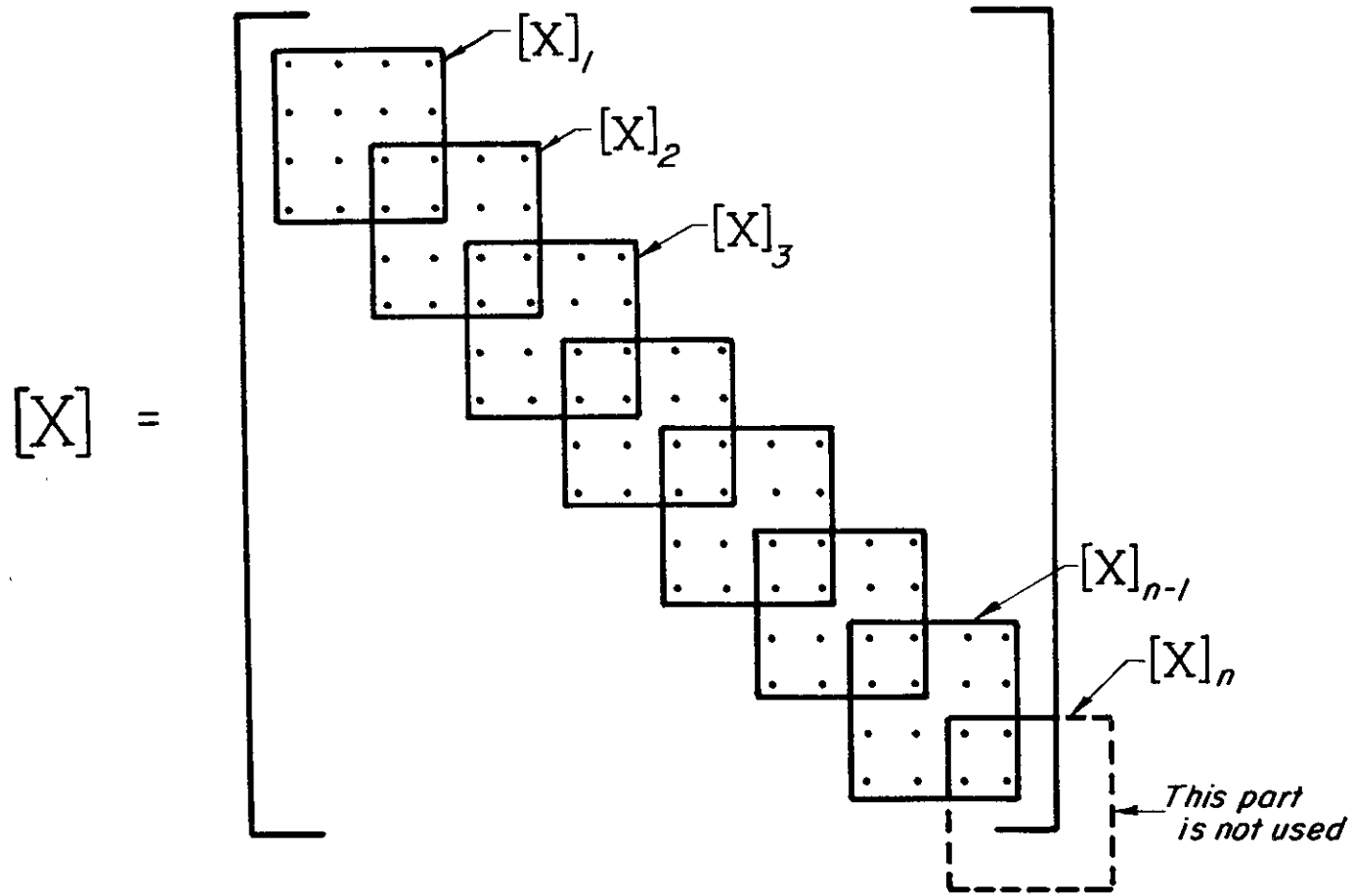

Fig. A4.2 STRUCTURE OF MATRICES [A], [B], [G] AND [M]

defines the possible wave numbers for Rayleigh waves in the layered system.

Eqs. (A4.11) and (A4.13) state an algebraic eigenvalue problem. It can be shown, Wilkinson (1965), that Eq. (A4.13) has exactly $4n$ real or complex roots k_s , $s = 1 , 2 , \ldots , 4n$, called eigenvalues. The corresponding solution vectors $\{v\}_s$, $s = 1 , \ldots , 4n$, Eq. 4.11 are called eigenvectors or mode shapes. A numerical technique for finding the eigenvalues and the corresponding eigenvectors is given by Waas (1972).

Group Velocity

The slopes of the secular lines are known as the group velocities and are defined by:

$$U = \frac{d\omega}{dk} = c + k\frac{dc}{dk} . \qquad \text{(A4.14)}$$

These are usually computed in conjunction with phase velocity dispersion curves by some method which directly or indirectly involves a numerical differentiation of the phase velocity dispersion curve. The method outlined here avoids this difficulty.

Consider a solution $(\omega^2 , \{v\})$ to the eigenvalue problem in Eq. (4.11) and the slightly different solution $(\omega^2 + d(\omega^2) , \{v\} + d\{v\})$ corresponding to the slightly different wave number $k + dk$. The later solution on substitution into Eq. (4.11) gives:

$$([A](k + dk)^2 + i[B](k + dk) + [G] - [M](\omega + d\omega)^2)(\{v\} + \{dv\}) = \{0\} . \qquad \text{(A4.15)}$$

Premultiplying by $\{v\}^T$ and neglecting small terms of the second order gives:

$$\{v\}^T([A]k^2 + i[B]k + [G] - \omega^2[M])(\{v\} + d\{v\}) + \{v\}^T(2kdk[A] - 2\omega d\omega[M])\{v\} = \{0\}. \quad \text{(A4.16)}$$

The first term vanishes since it contains the transpose of the left-hand side of Eq. (4.11) and the last term gives, after normalization:

$$U = \frac{d\omega}{dk} = \frac{k/\omega}{\{v\}^T[M]\{v\}} . \quad \text{(A4.17)}$$

(See Lysmer and Drake, 1972).

Amplitudes of Excitation

The solutions to Eq. (A4.11) yield the basic characteristics of the excitation propagated along the surface of a layered structure in the form of wave numbers k and the eigenvectors $\{v\}$ give the relationship between relative displacement and depth (z) for each node of propagation. However, the absolute amplitudes of displacements at the surface, or at any point within the field, cannot be computed from this information alone. By including the loading in the mathematical model, Waas (1972) was able to overcome this difficulty. Waas' (1972) procedure provides the capability to deal with generalized situations but for present purposes it will be sufficient to consider the case of a horizontally layered structure subjected to a plane oscillatory line loading. Such a system is shown in Fig. A4.3. It may be thought of as consisting of two zones: Zone L on the left and Zone R on the right.

Simulating the reaction supplied by Zone L to excitation in Zone R by a series of forces applied at node points at the interfaces of the layers it is possible to model the forces acting on the region $x > 0$ in the manner shown in Fig. A4.4 in which the factor $\exp(i\omega t)$ is implied. These forces may be collected in a force amplitude vector $\{P\}$

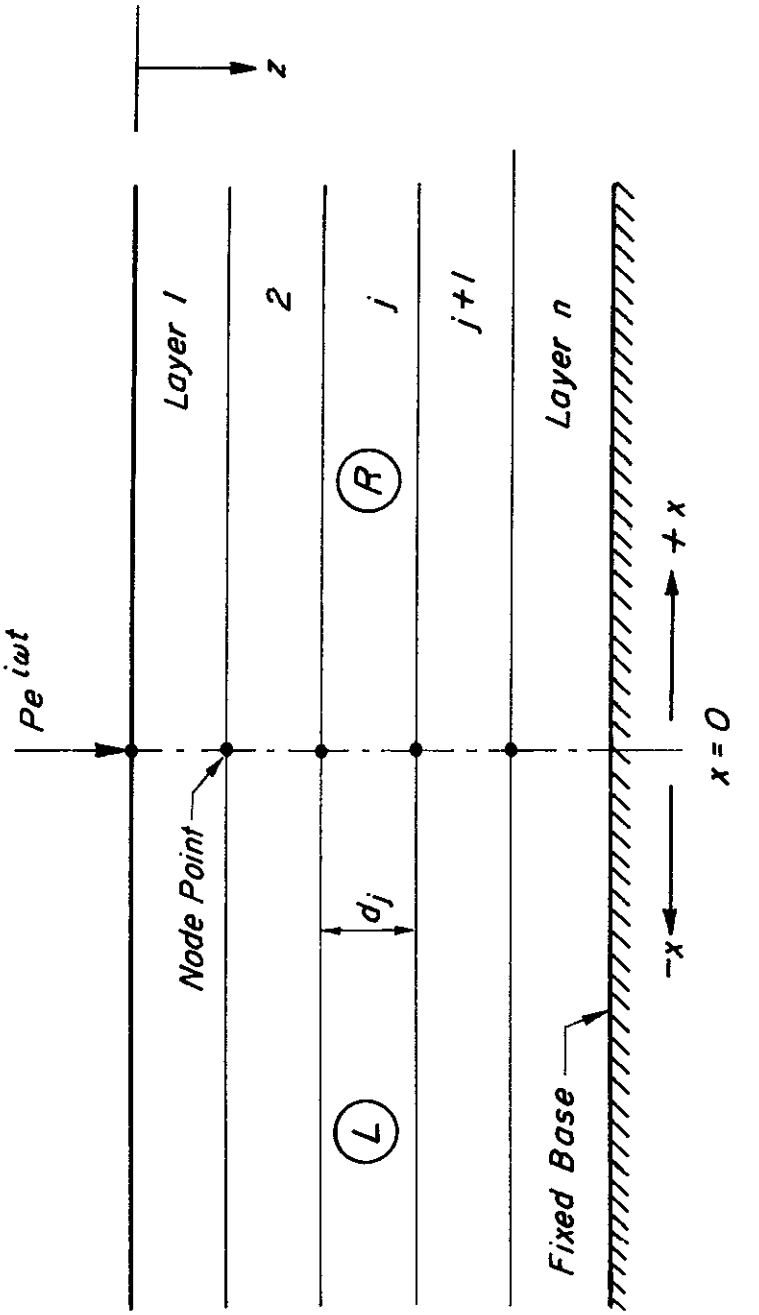

Fig. A4.3 MODEL FOR A HORIZONTALLY LAYERED STRUCTURE SUBJECT TO A PLANE OSCILLATORY LINE LOAD

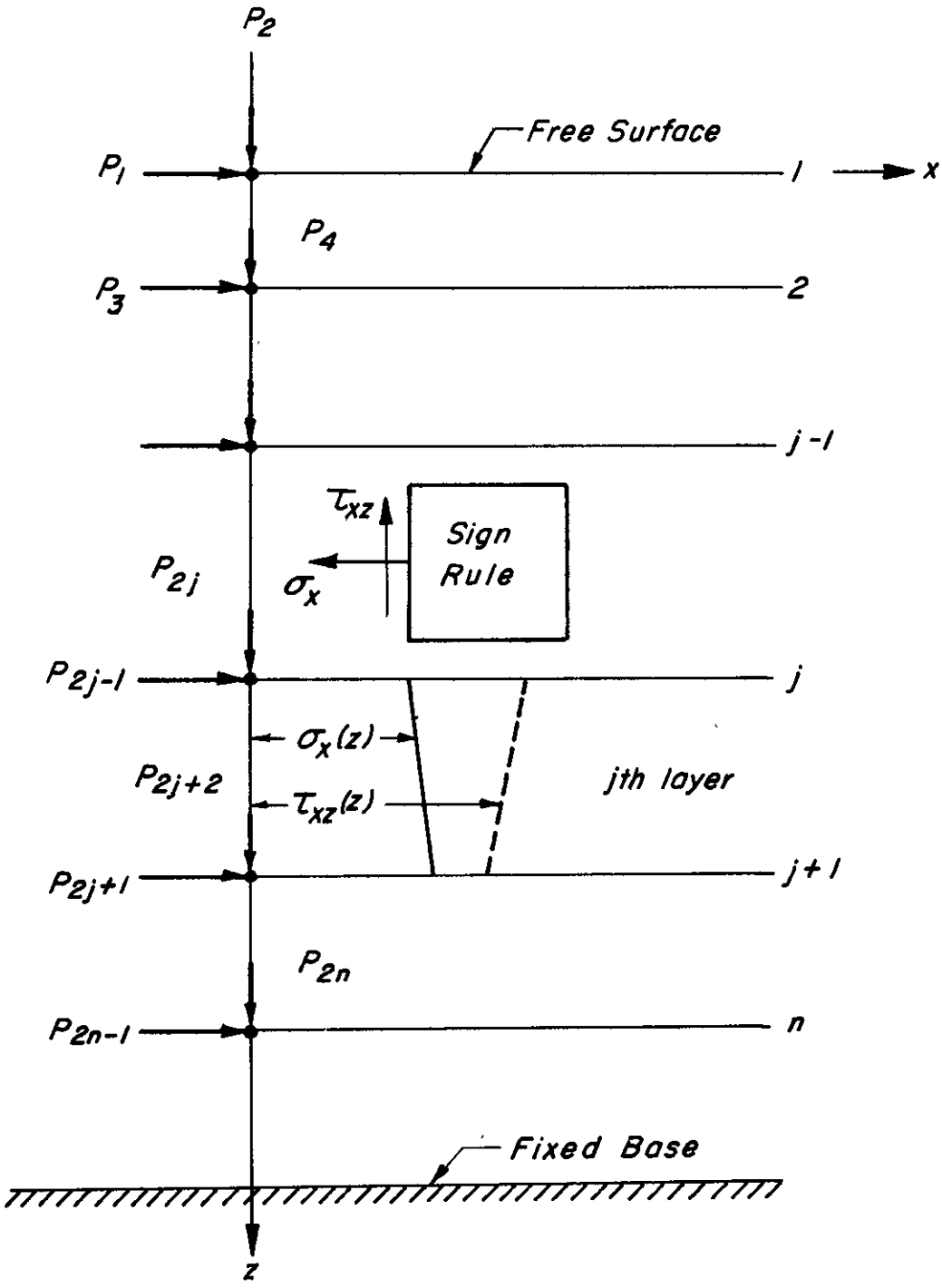

Fig. A4.4 FORCES ON THE VERTICAL PLANE, x = 0

comprising $2n$ components ordered in a similar manner to the displacements $\{\delta\}$ in Eq. A4.2. The particular forces corresponding to the normalized s^{th} mode being denoted $\{P\}_s$. These forces can be computed by considering the stresses and strains in a typical layer. The strains in the j^{th} are, by differentiation of Eqs. A4.1 and recalling Lysmer's (1970) assumption $u(z)$ and $w(z)$ vary linearly within the layer

$$\varepsilon_x = -ik_s u(z) = -\frac{ik_s}{d_j}(z_{j+1} - z)v_{2j-1} + (z - z_j)v_{2j+1})$$

$$\varepsilon_z = \frac{dw(z)}{dz} = \frac{1}{d_j}(v_{2j+2} - v_{2j}) \tag{A4.18}$$

$$\gamma_{xz} = \frac{du(z)}{dz} - ik_s w(z)$$

$$= \frac{1}{d_j}(v_{2j+1} - v_{2j-1} - ik_s((z_{j+1} - z)\, v_{2j} + (z - z_j)\, v_{2j+2})) \,.$$

In the present formulation Hooke's law for the case of plane strain may be stated

$$\begin{Bmatrix} \sigma_x \\ \sigma_z \\ \tau_{xz} \end{Bmatrix} = \begin{bmatrix} (\lambda + 2G) & \lambda & 0 \\ \lambda & (\lambda + 2G) & 0 \\ 0 & 0 & G \end{bmatrix} \begin{Bmatrix} \varepsilon_x \\ \varepsilon_z \\ \varepsilon_{xz} \end{Bmatrix} . \tag{A4.19}$$

The resulting stresses also vary linearly with z as shown in Fig. A4.4 and the discretized forces which are in equilibrium with these stresses are:

$$\begin{Bmatrix} P_{2j-1} \\ P_{2j} \\ P_{2j+1} \\ P_{2j+2} \end{Bmatrix} = (ik_s[A]_j + [D]_j) \begin{Bmatrix} v_{2j-1} \\ v_{2j} \\ v_{2j+1} \\ v_{2j+2} \end{Bmatrix} \tag{A4.20}$$

in which $[A]_j$ is the matrix defined by Eq. A4.6 and

$$[D]_j = \begin{bmatrix} 0 & 1/2\lambda_j & 0 & -1/2\lambda_j \\ 1/2G_j & 0 & -1/2G_j & 0 \\ 0 & 1/2\lambda_j & 0 & -1/2\lambda_j \\ -1/2G_j & 0 & -1/2G_j & 0 \end{bmatrix} \tag{A4.21}$$

The complete force system on the plane $x = 0$ due to the action of the s^{th} mode may be formed by combining the matrix results of the sum $(k_s[A]_j + [D]_j)$ in the manner shown in Fig. A4.2 to give:

$$\{P\}_s = [R]_s\{v\}_s \tag{A4.22}$$

in which

$$[R]_s = (ik_s[A] + [D])\{v\}_s \, . \tag{A4.23}$$

The total motions resulting from all modes which propagate energy or decay in the x^{+ve} direction is by superposition:

$$\{\delta\}^R = \sum_{s=1}^{2n} \alpha_s\{v\}_s \exp(i\omega t - ik_s x) \tag{A4.24}$$

in which the wave numbers k_s and corresponding mode shapes $\{v\}_s$ are chosen according to the rules:

1. If $\pm k_s$ is complex or purely imaginary, choose the sign which give a negative imaginary past.
2. If $\pm k_s$ is real, choose the positive sign if the vertical components of $\{v\}_s$ are real and the negative sign is they are imaginary.

The superscript R in Eq. (A4.24) signifies propagation and amplitude decay to the right in Fig. A4.4. The amplitudes of motion at $x = 0$ are, by Eq.(A4.24):

$$\{u\}^R = \sum_{s=1}^{2n} \alpha_s \{v\}_s = [V]\ \{\alpha\} \tag{A4.25}$$

in which $\{\alpha\}$ is a column vector containing the "mode participation factors" α_s , $s = 1$, ... , $2n$, and $[V]$ is a matrix containing the mode shapes in column order.

Eq. 4.25 may be inverted to give:

$$\{\alpha\} = [V]^{-1}\{u\}^R \tag{A4.26}$$

from which the mode participation factors for each of the Rayleigh modes may be computed.

The force amplitudes at $x = 0$ may be similarly derived from Eqs. A4.22 and A4.23 and are:

$$\begin{aligned} \{P\}^R &= \sum_{s=1}^{2n} \alpha_s (ik_s[A] + [D])\{v\}_s \\ &= (i[A][V][k] + [D][V])\{\alpha\} \end{aligned} \tag{A4.27}$$

or, from Eq. (A4.26),

$$\{P\}^R = [R]\{u\}^R \tag{A4.28}$$

in which $[R]$ is the symmetric matrix:

$$[R] = i[A][V][k][V]^{-1} + [D] \tag{A4.29}$$

where $[K]$ is the diagonal matrix containing the wave numbers k_s, $s = 1, \ldots, 2n$.

The forces $\{P\}^L$ which act on region L in Fig. A4.3 ($x < 0$) for the case when waves propagate or decay toward the left may be similarly shown to be related to the displacement amplitudes $\{u\}^L$ through,

$$\{P\}^L = [L]\{u\}^L \tag{A4.30}$$

in which $[L]$ is identical to matrix $[R]$ except for a sign change of all coefficients for which the sum of the subscripts is an odd number. This sign change concerns the coefficients which relate horizontal forces to vertical displacements or vertical forces to horizontal displacements such that all signs are compatible with the global coordinate for the complete structure shown in Fig. A4.3.

Considering the nodes on the plane $x = 0$ in Fig. A4.3, the equilibrium between the externally applied forces $\{P\}^I$ and the reactions supplied by zones L and R may be expressed as follows:

$$\{P\}^I = \{P\}^R + \{P\}^L \tag{A4.31}$$

and from Eq. (A4.28) and (A4.30),

$$\{P\}^I = [R]\{u\}^R + [L]\{u\}^L \ . \tag{A4.32}$$

For continuity of displacements at $x = 0$ in Fig. A4.3

$$\{u\}^L = \{u\}^R = \{u\} \tag{A4.33}$$

and by observing the signs of the coefficients Eq. A4.32 may be reduced to:

$$\{P\}^I = 2i[A][V][K][V]^{-1}\{u\} \tag{A4.34}$$

The vector $\{P\}^I$ for the case illustrated in Fig. A4.3 contains only a single non-zero coefficient; that corresponding to the plane vertical loading applied at the surface. The solution of Eq. A4.34 for the displacements $\{u\}$ is simplified further by observing that, due to the symmetry of the structure in Fig. A4.3 about the plane $x = 0$, all horizontal displacement on this plane are zero. Thus the solution of the set of linear equations defined by Eq. (4.34) may be reduced to a problem of half the original size.

Summary of Procedure

The analysis of a plane layered structure subjected to plane dynamic loading proceeds in the following manner:

A. DISCRETIZATION AND IDEALIZATION

1. Subdivide the structure into layers of suitably small thickness.
2. Define all materials properties; if necessary in the form of complex moduli.
3. Define the angular frequency ω.
4. Define the loading on the plane $x = 0$, i.e. $\{P\}^I$.

B. ASSEMBLY AND SOLUTION OF THE SECULAR EQUATION

1. Form the matrices [A], [B] and [C] -- Fig. A4.2 and Eqs. (A4.6), (A4.7) and (A4.12).

2. Solve the eigenvalue problem in Eq. A4.11 to yield the matrices [K] and [V].

C. DISPLACEMENTS

1. Compute the displacements on the plane $x = 0$ $\{u\}$, Eq. A4.34.

2. Find the mode participation factors - Eq. (A4.26).

3. Compute the displacements at any desired point on the surface or in the interior of the structure - Eq. (A4.24).

The procedure outlined above is designed for the analysis of the special case of a plane horizontally layered structure. However, the theoretical method is not restricted to this case. Solutions for axisymmetric systems have been presented by Waas (1972) and for nonhorizontally layered structures by Lysmer and Drake (1972).

A Finite Dynamic Model for a Semi-infinite Layered Medium

The application of the direct stiffness method to steady-state wave propagation problems in an infinite medium is restricted by the finite number of nodal points or sub-layers which can be considered and thus the discrete model is confined to a finite region. This poses the problem as to how wave reflections can be prevented at an artificial boundary which is introduced to limit the size of the model. Lysmer's (1970) method eliminates two of these boundaries as shown in Fig. A4.1 in which the layers extend laterally to infinity in either direction. The finite

depth of the model, however, remains. Such a model would accurately simulate a system of soft layers over a rigid half-space, e.g., soil over hard rock, but does not accurately represent a semi-infinite elastic system.

Lysmer and Kuhlemeyer (1969) developed a viscous boundary which absorbs a major portion of the impinging energy. Viscous forces may be applied at the boundary designed to absorb the energy contained in P-waves and S-waves if the incident angles of the waves are known. However, the incident angles are usually unknown and must be anticipated. If the actual incident angles differ from the anticipated angle by not more than about 60° the viscous boundary is very effective. Lysmer and Kuhlemeyer (1969) obtained good results with finite element models of steady-state vertical vibrations of circular footings embedded in a homogeneous elastic half space. Kuhlemeyer (1969) extended the method to the case of a layered half space. Good results were obtained in the low frequency range for cases in which the elastic moduli of the layers decreased with depth. However, it was observed that in general it is difficult to predict the incident angles of P- and S-waves at the artificial boundary because the P- and S-waves undergo multiple reflections and refractions at the layer interfaces and the free surface. In addition, the incident angles often change radically with frequency.

In the case of Lysmer's (1970) model for a layered system the viscous boundary proposed by Lysmer and Kuhlemeyer (1969) may be conveniently simulated by a layer of viscous material at the base of the layered system.

Viscous Boundary Layer

Lysmer and Kuhlemeyer's (1969) boundary condition may be expressed as

$$\sigma_{zz} = a\rho\alpha\dot{w}$$
$$\sigma_{zx} = b\rho\beta\dot{u} \qquad \text{(A4.35)}$$

in which

σ_{zz} and σ_{zx}	are the normal and shear stresses respectively
$\dot{w}$ and $\dot{u}$	are the normal and tangential velocities respectively
α and β	are the velocities of P-waves and S-waves in the half space respectively
a and b	are dimensionless constants

Consider an artificial boundary introduced at the bottom of a semi-infinite layered medium which consists of a liquid layer over a rigid solid as shown in Fig. A4.5. A typical element of the liquid will be as shown in Fig. A4.6 in which it is assumed that the distribution of the displacements u and w in the vertical direction z are linear, as shown to the right of the diagram, in accordance with the assumption of Lysmer's (1970) lumped mass method. The liquid is assigned the material properties G^*, ρ^* and λ^*.

The forces F_z and F_x at the top of the element in the z and x directions respectively will be

$$F_z = \frac{h}{2d}(\lambda^* + 2G^*)w\cdot\exp(i\omega t) - \frac{h\rho^* b w^2\cdot\exp(i\omega t)}{3} \qquad \text{(A4.36)}$$

and

$$F_x = \frac{h}{2d}G^* u\cdot\exp(i\omega t) - \frac{h\rho^* b u^2\cdot\exp(i\omega t)}{3}$$

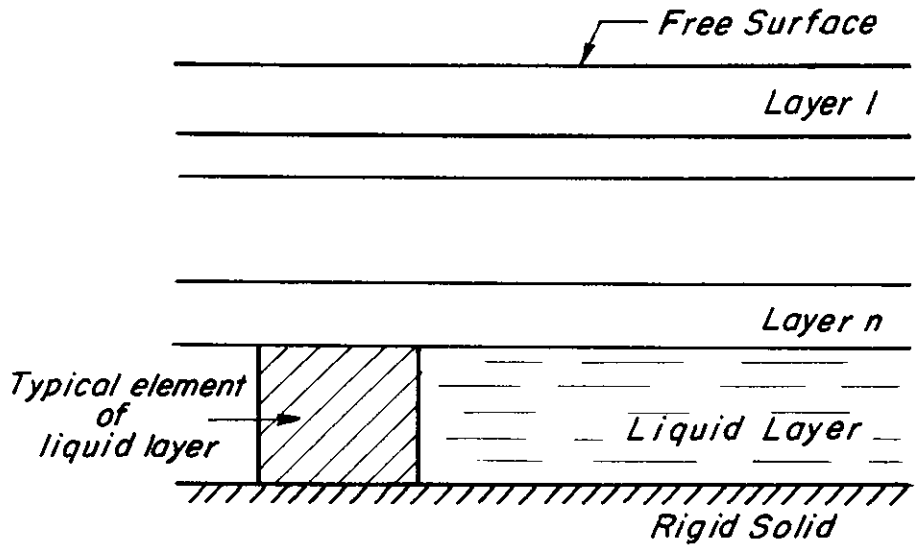

Fig. A4.5 LIQUID LAYER BOUNDARY FOR FINITE MODEL OF SEMI-INFINITE LAYERED MEDIA

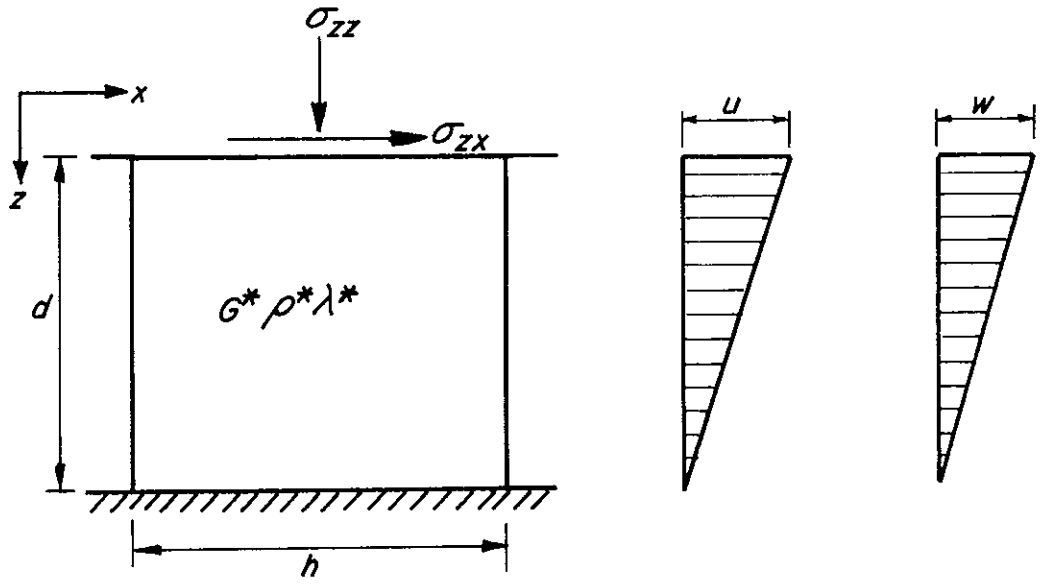

Fig. A 4.6 TYPICAL ELEMENT OF LIQUID LAYER

when the system is subjected to a harmonic excitation. These forces must be equal to those obtained from Eqs. (A4.35) if Lysmer and Kuhlemeyer's (1969) boundary condition is to be satisfied. Thus,

$$i\omega a\rho\alpha \cdot \exp(i\omega t) \cdot wh = h(\lambda^* + 2G^*)\frac{w \exp(i\omega t)}{2d} - \rho^*\frac{d}{3}w^2\exp(i\omega t)$$

and

(A4.37)

$$i\omega b\rho\beta \cdot \exp(i\omega t) \cdot uh = \frac{hG^*}{2d} u \cdot \exp(i\omega t) - \frac{\rho^* d}{3}u^2 \cdot \exp(i\omega t)$$

in which the superscript refers to properties of the liquid and terms without superscripts refer to properties of the infinite medium beyond the artificially imposed boundary. Now assigning the following arbitrary values:

$$\rho^* = 0$$
$$h = 1.0 \qquad \text{(A4.38)}$$
$$d = 1.0$$

Eqs. (A4.36) yield

$$G^* = ib\omega\rho\beta \qquad \text{(A4.39)}$$

and

$$\lambda^* = ia\omega\sqrt{\rho}\,(\sqrt{\lambda + 2G} - 2\sqrt{G}) \qquad \text{(A4.40)}$$

both of which are imaginary which is as is to be expected for a liquid layer. The result provides a simple method by which Lysmer and

Kuhlemeyer's (1969) viscous boundary may be added to models of the type shown in Fig. (A4.1). A layer of unit thickness is simply added to the bottom of the model and is assigned the material properties defined by Eqs. (A4.39) and (A4.40).

Ang and Newmark (1971) developed a "transmitting boundary" to deal with the problem of the finite model for the infinite prototype. It also requires some advance knowledge of the incident angles and in essence is the same as that proposed by Lysmer and Kuhlemeyer. Ang and Newmark (1971) used the transmitting boundary in the analysis of ground shock waves caused by nuclear blasts. The boundary was effective in cases in which the wave motion was mainly one-dimensional. However, studies by Hadala (1971) show that the transmitting boundary is useful in certain two-dimensional shock wave problems in layered semi-infinite media, when only a short time period after the blast is considered.

Another method of analyzing wave propagation in infinite media is to employ a very large model with significant damping. Waves generated at a source are strongly attenuated before they reach the artificial boundary and are further attenuated on reflection. This approach is physically justified if the damping is a reasonable measure of the natural damping of the materials being modeled and the model is sufficiently large. In practice, however, it is usually prohibitively expensive in computational time and memory requirements even for the most advanced digital computers.

Steady-state problems such as those posed by the vibratory loading used in the wave-propagation method of testing are particularly difficult to deal with in respect to the boundaries of finite models. Unlike the case of shock loading, in which interest is usually confined to

the magnitude of the short lived maximum displacements and loads, these problems require accurate solutions to be obtained in the case when time tends to infinity. In these circumstances even minor amounts of energy reflected into the interior of a structure from an artificially imposed boundary may result in misleading solutions. This difficulty is one of the major limitations in the application of the direct stiffness method to steady-state dynamic problems.

APPENDIX 5

COMPUTER PROGRAM SPRDSP

A program for the computation of dispersion curves for multi-layered media by the Direct Stiffness method. The theoretical methods are described in Appendices 4, 7 and 8.

PROGRAM SPRDSP

SECTION 1:	PROGRAM IDENTIFICATION
Title:	Wave Dispersion by Direct-Stiffness Method
Program Code Name:	SPRDSP
Writer:	D. J. Watkins
Organization:	Department of Civil Engineering, University of California, 94720, U.S.A.
Date:	June 1974
Updates:	None, Version 0
Source Language:	FORTRAN IV (CDC 6400)
Availability:	Complete program listing Fig. A5.1
Abstract:	The program computes the wave numbers, mode shapes and other characteristics of waves propagating in plane, elastic or viscoelastic layered structures which are modeled by a system of finite depth consisting of a finite number of layers obtained by subdividing the natural layering of the structure. The base of the model is either rigid or energy absorbing. The dispersion curves for a pre-selected number of the modes of propagation may be constructed. The degree of detail obtained as output may be selected according to a number of available options.

SECTION 2: ENGINEERING DOCUMENTATION

Narrative Description

Program SPRDSP -- "Wave Dispersion by Direct Stiffness Method" -- is designed to produce dispersion curves for wave propagation in a plane elastic or viscoelastic structure. In addition, various options may be used to obtain details of mode shapes and other characteristics of the propagating waves.

The structure to be studied must be idealized as a system of plane horizontal layers of infinite lateral extent. Each layer is described in terms of its thickness, mass density and the velocity of propagation of P and S waves in the material of which it is composed. Material damping in any layer may be input in the form of the percentage of critical damping in both shear and compression.

The base of the model is a rigid plane but a layer with properties similar to a viscous fluid may be superimposed on this plane so that the model better approximates a system resting on a half-space.

The program calculates and prints coordinates of frequency and wave number in the real plane. These may be converted to graphical form.

Method of Solution

The program is based on the direct stiffness method for the analysis of waves in multi-layered media which is described in Appendix 4. At any given frequency the problem is reduced to the solution of the eigenvalue problem:

$$([A]k^2 + [\hat{B}]k + [G] - \omega^2[M])\{w\} = \{0\} \qquad (A5.1)$$

which is the modified form of the secular equation for generalized Rayleigh waves in a multi-layered system obtained by Waas (1972), where,

k = the eigenvalue in the form of the wave number

ω = the frequency

$[A]$, $[\hat{B}]$, $[G]$ and $[M]$ are symmetric matrices whose elements depend upon the geometry and material properties of the layered system.

$\{w\}$ = the eigenvector which is a modified form of the mode shape.

Equation (5.1) has a finite number of discrete solutions, equal to twice the number of layers in the model after subdivisions, all or part of which may be obtained by the program, depending upon the option chosen. Waas' (1972) method is used to solve (Eq. A5.1) numerically.

Dispersion curves are produced by a process of prediction and correction. When a sufficient number of initial values have been obtained, approximate solutions to Eq. (A5.1) are made by means of the predictor described in Appendix 7. Accurate roots to Eq. (A5.1) are then found from these approximations. This predictor-corrector curve following is optimized by the method described in Appendix 8.

The order of procedure within the program is as follows:

1. Input problem parameters.
2. Convert input data and compute the elements of the matrices in the secular equation.
3. Solve the eigenvalue problem, Eq. (A5.1) above, for the first frequency. All roots are obtained.
4. Order the eigenvalues and eigenvectors in ascending order of the imaginary parts of the eigenvalues (wave-number).
5. Compute characteristics of the modes of propagation at the surface.
6. Select the first NDC eigenvalues according to input specifications and compute coordinates of the dispersion curves for these modes over the specified frequency range using the method of prediction and correction described in Appendices 7 and 8.

6a. If required, at each coordinate along the dispersion curve the eigenvectors $\{w\}$ may be modified to yield the mode shapes $\{v\}$.

7. At the final specified frequency obtain the full set of roots to the secular equation.

8. Compute characteristics at the modes of propagation at the surface.

9. Output the results in the format required by the specified option.

Minor variations in the above procedure occur when some options are selected.

Program Capabilities

The program can solve wave propagation problem in structures which reasonably approximate the following conditions:

1. The layers are of infinite lateral extent and are homogeneous and isotropic.

2. The materials forming the layers are either linearly elastic or viscoelastic.

3. The layers are in welded contact.

4. The base of the structure is a rigid plane. Less reliable solutions may also be obtained for structures resting on a non-rigid half-space.

A basic assumption of the direct stiffness method is that the discretized model of the structure is such that it is reasonable to assume that all displacements vary linearly with depth within each layer. To achieve this, the program allows the user to specify the number of sublayers into which the natural layering of the structure is to be subdivided. Lysmer and Kuhlemeyer (1969) have suggested that the maximum depth be restricted to 1/12 of the length of a shear wave propagating in the layer. The user should review the output and, by inspection of the mode shapes, satisfy himself that the layering is sufficiently refined.

The choice of either the lumped or consistent form of the mass matrix [M] is open to the user. A mass matrix which is a combination of the two types may also be specified. (Ref. Kuhlemeyer and Lysmer, 1973).

An option is available which allows the base of the model to simulate a viscous fluid, the properties of which are such that energy arriving at its upper boundary is largely absorbed rather than reflected back into the overlying structure. This option may be used when a structure resting on a half-space is to be modelled. The theoretical basis for this analogy is given in Appendix 4. Not all of the impinging energy is absorbed, however, and results obtained should be critically reviewed.

Eq. (5.1) has twice as many roots as there are discrete layers in the sub-divided structure. These roots are obtained by the equation solving routine in an order unrelated to the participation of the corresponding mode in the total surface motion. As secular lines are followed through the frequency range the modes which are represented may change their contribution to the total motion. Thus, a fully consistent scheme for sorting the roots is not possible. At each initial frequency roots are sorted in ascending order of the imaginary parts. In many cases this allows the dominant modes to appear first in the list and a pre-selected number may be chosen for further analysis. This simplified system does not guarantee that all modes of primary interest will be at the head of the tabulation so that the user should review the results to check for the presence of other significant modes in the body of the list.

The secular lines defining the dispersion of waves in elastic

structures contain a large number of singularities and consist of families of curves in complex space. The curve following method used by the program is modified to accommodate a number of singularity types which occur in this type of problem, but difficulties may be encountered. If this is the case, the problem should be approached on a piece by piece basis using a small frequency range at each step. The dispersion curves are presented at output in the form of the projection of the secular lines onto the real plane.

Dynamic storage is used so that the program may be run for a model containing a number of layers limited only by the capacity of the computer. However, the reliability of the numerical results for systems with an excess of about 40 layers in uncertain. The number of layers used should be kept as small as is compatible with the other requirements of the discretization.

Data Inputs

The data are input from punched cards using the format shown below. Any compatible system of units may be used but the frequency must be in radians/second.

CARD GROUP	FORMAT	COLUMN	DESCRIPTION
A	7I10	1 - 10	LAYERS - No. of layers in the model before subdivision.
		11 - 20	NLT - Total no. of layers after subdivision.
		21 - 30	NBAS - Set as follows: 0 if base of model is rigid. 1 if base of model is energy absorbing viscous layer.

31 - 40	NOP - Set as follows: 0 if standard output is required 1 if dispersion curve for a single curve is required. 2 to obtain characteristics of surface waves at a single specified frequency.
41 - 50	NVEC - Set as follows: 0 if mode shapes are not required as output 1 if mode shapes are required as output.
51 - 60	NDAR - Set as follows: 0 if dispersion curves are to be plotted on line printer or Calcomp plotter. 1 if graphical display is not required.
61 - 70	NTC - Set as follows: 0 if graphical plotting best suited to Calcomp plotter is required. 1 if graphical plotting best suited to line-printer is required.

Note: Depending upon the option chosen the following modifications to this card may be made.

OPTION SWITCH	SETTING	Fields which may be left blank
NOP	2	41 - 50 NVEC 51 - 60 NDAR 61 - 70 NTC
NDAR	1	61 - 70 NTC

B	2E10.5	1 - 10	WLP - the percentage of the matrix [M] which is equivalent to the lumped mass matrix
		11 - 20	WCP - the percentage of matrix [M] which corresponds to a consistent mass matrix
C	3E10.5, I10	1 - 10	OMF - The initial frequency at which the analysis is commenced.
		11 - 20	OML - The frequency at which the dispersion curves are terminated.
		21 - 30	DOM - Maximum step size control. The maximum range between frequencies at which coordinates of the dispersion curve are computed is $(\lvert OML-OMF \rvert)/DOM$
		31 - 40	NDC - The number of modes whose dispersion curves are to be followed. NDC $\leq 2 \times$ NLT. If NOP in card group A = 1 then NDC = 1.

Note: Depending upon the option chosen the following modifications to this card may be made.

OPTION SWITCH	SETTING	Fields which may be left blank
NOP	2	11 - 20 OML
		21 - 30 DOM
		31 - 40 NDC

D	I10,6E10.5	1 - 10	NL - No. of sub-layers into which main layer is to be divided.
		11 - 20	DL - Thickness of main layer.
		21 - 30	VS - Velocity of S-wave in layer.
		31 - 40	VP - Velocity of P-wave in layer.
		41 - 50	BS - Percentage of critical damping in shear for layer material.
		51 - 60	BP - Percentage of critical damping in compression for layer material.
		61 - 70	RH - mass density of material in layer.

Note: Card group D contains one card for each main layer of the model; i.e., No. of cards = LAYERS.

E.	2E10.5	1 - 10	S(MA) - the real part of the complex number which approximates the wave-number of the mode whose dispersion curve is required.
		11 - 20	S(MA+1) - The imaginary part of the above complex number.

Note: If NOP in Card Group A is 0 or 2, this card is omitted.

Note: A new model may be analyzed by continuing the input data cards commencing again at card group A.

Program Options

The options available in the program mainly control the detail of the printed output. Their operation has been described under Data Inputs.

If a dispersion curve for a single mode is to be constructed, the option switch NOP is Card Group A above is set equal to 1. In this

case an approximation to the desired root at the initial frequency is obtained from input (Card Group E). Because the eigenvector is an important factor in influencing the trend of iteration, the desired root may not be reached in all cases. The user should check to ensure that a satisfactory result has been obtained.

Printed Output

The printed output consists of a reformated playback of the input data and a tabulation of the results according to the chosen option. See sample output Fig. A5.4.

Other Outputs

If the Calcomp graphical display unit is used the postprocessor produces a deck of cards in binary code. These are used as input to the Calcomp plotter.

Sample Run

A sample problem for program SPRDSP is shown in Fig. A5.2. The input data is shown in Fig. A5.3 and the resulting output in Fig. A5.4.

SECTION 3: SYSTEM DOCUMENTATION

Computer Equipment

Program SPRDSP was developed on a CDC 6400 computer with k core memory. The computer uses 60-bit word length with floating point arithmetic performed in single words. The core cycle time is 1.0 μ sec. per memory bank but interlacing up to 10 memory banks is possible.

Peripheral Equipment

The following peripheral equipment was used during development of this program: CDC 405 card reader, IBM 1403 line printer, Model 663 Calcomp Plotter and a CDC 415 card punch.

Source Program

The source listing for SPRDSP and subroutines SETUP, ASMBL, MLTYSOL, EIGSOL, FLES, SORT, CHARIC, CURVS, GRPVL, MODSH and DARLUN are shown in Fig. A5.1.

Variables and Subroutines

The principal variables in the program are as follows:

LAYERS - the number of layers in the prototype (integer)

NLT - the total number of layers in the model after subdivision of the prototype layers (integer)

NL2 - 2 × NLT (integer)

OM - frequency

OMF - the initial frequency (real)

OML - the final frequency (real)

DL - depth of a prototype layer (real)

TH(I) - depth of model layer I (real)

VS - velocity of propagation of shear waves (real)

VP - velocity of propagation of compressional waves (real)

BS - percent of critical damping in shear (real)

BP - percent of critical damping in compression (real)

RHO - mass density (real)

G(I) - shear modulus of layer I (complex)

ALAM(I) - Lamé's constant for layer I (complex)

A1(I) - element of matrix [A] (complex)

A3(I) - element of matrix [A] (complex)

B2(I) - element of matrix $[\hat{B}]$ (complex)

B4(I) - element of matrix $[\hat{B}]$ (complex)

W1(I) - element of matrix [M] (real)

W3(I) - element of matrix [M] (real)

G1(I) - element of matrix [G] (complex)

G3(I) - element of matrix [G] (complex)

C1(I) - element of matrix [C] (complex)

C3(I) - element of matrix [C] (complex)

E - array containing eigenvalues (wave numbers) (complex)

VA - array containing eigenvectors (complex)

V - array containing mode shapes (complex)

GV - group velocity (complex)

P(I) - array containing coordinates of the dispersion curves (real)

D - step-size in frequency for curve following predictor (real)

S - general storage array (real)

The following utility storage arrays are used: V1, V2, U1, U2, R1, R2, S1, S2, X .

The program consists of the following parts:

1. SPRDSP. Main program for input, output and storage allocation. Calls SETUP, ASMBL, MLTYSOL, SORT, CHARIC, CURVS and DARLUN.

2. Subroutine SETUP. Converts input prototype layer properties into elastic constants and subdivides layers.

3. Subroutine ASMBL. Computes elements of matrices [A], $[\hat{B}]$ and [C] .

4. Subroutine MLTYSOL. Finds the NL2 eigenvalues and eigenvectors of the secular equation $([A]k^2 + [\hat{B}]k + [C])\{w\} = \{0\}$. Calls EIGSOL.

5. Subroutine EIGSOL. Finds individual eigenvalues and eigenvectors of $([A]k^2 + [\hat{B}]k + [C])\{w\} = \{0\}$ by method described by Waas (1972). Calls FLES.

6. Subroutines FLES. Solves set of symmetric simultaneous equations.

7. Subroutine SORT. Sorts eigenvalues in ascending order of their imaginary parts.

8. Subroutine CHARIC. Computes characteristics of modes of propagation of the surface wave. Calls GRPVL.

9. Subroutine CURVS. Produces coordinates of the projection onto the real plane (dispersion curves) of selected modes of propagation. An optimized predictor is used as described in Appendices 7 and 8. The corrector is Waas' (1972) method for finding eigenvalues of $([A]k^2 + [\hat{B}]k + [C])\{w\} = \{0\}$.

Special modifications are used to deal with certain singularities which may occur. Calls ASMBL, EIGSOL, MODSH and GRPVL.

10. Subroutine GRPVL. Computes the group velocity of modes of surface wave propagation.

11. Subroutine MODSH. Obtains the modes shapes {v} from the eigenvectors {w} .

12. Subroutine DARLUN. Prepares output for use with graphical display systems. Cal University of California library package GDSLIB. The graphical display post-processor is an absolute overlay which takes data produced by a subroutine DARLUN as input and produces control data for graphical display units as output.

13. Library Subroutines. Subroutines for integer to real conversion (FLOAT), computation of square roots (SQRT), a complex number from two real arguments (CMPLX), complex square roots (CSQRT), absolute (ABS), complex absolute (CABS), the real part of a complex number (REAL), the imaginary part of a complex number (AIMAG), and the minimum of a series of real numbers (AMIN1) are required and are supplied by the system.

Data Structure

Input is read from file INPUT. Output is written on file OUTPUT. The program creates the file TAPE 99 which is used to store the output of the graphical display post-processor.

Storage Requirements

The program uses dynamic storage. The principal arrays form part of the blank common S . The required length of S depends upon the size of the problem to be analyzed. The length may be adjusted by replacing card No. 5 in the program (See listing Fig. A5.1). The length of S should be approximately no shorter than defined by the longer of:

$$\text{Length of } S = 8\ NLT^2 + 96\ NLT + 200 \qquad \text{(A5.2)}$$

$$\text{Length of } S = 16\ NLT^2 + 58\ NLT + 200 \qquad \text{(A5.3)}$$

where NLT is the total number of sub-layers in the model.

The length of S as defined in card No. 5 is in decimal units. Excluding the blank common the program requires about 60,000 octal words of storage.

SECTION 4: OPERATING DOCUMENTATION

Operator Instructions

There are no special operator instructions.

Run Time

Execution time depends upon the number of layer in the model, the output option chosen and other problem parameters. The sample problem with two main layers and a total of ten sublayers over a rigid base was executed in approximately 30 secs on the CDC 6400 computer.

FIG. A5.1

LISTING OF PROGRAM SPRDSP

(The next eleven pages form Fig. A5.1)

FIG.A5.1 LISTING OF PROGRAM SPRDSP

```
      PROGRAM SPRDSP(INPUT,OUTPUT,TAPE99)
C
C-----WAVE DISPERSION IN LAYERED MEDIA BY THE DIRECT STIFFNESS METHOD
C
      COMMON S(25000)

      COMMON/STARTS/NA1,NA3,NB2,NB4,NC1,NC3,NX,NMVB,NS1,NS2,NW1,NW3,NV1,
     1NO,NR,NG,NL,NG1,NG3,NU1,NU2
      COMMON/SPECS/LAYERS,NLT,NL2,NBAS,OMF,OML,DOM,WL,WC,NDC,NOP,ENC
      COMMON/MISS/KSP,KRT,KABRT,RDF,NVEC
      COMMON/CHAR/WLI,C,WLT,CI,DCRM,DF,IRL
      COMPLEX RDF,GV
      DATA ENC/3HENC/
C
C-----INPUT PROBLEM SPECIFICATIONS AND DIMENSIONS
C
   10 READ 1000,LAYERS,NLT,NBAS,NOP,NVEC,NDAR,NTC
      IF(LAYERS.EQ.0) STOP
      READ 5000,WLP,WCP
      READ 5000,OMF,OML,DOM,NDC
      PRINT 2000
      PRINT 3000,LAYERS,NLT
      WL=WLP/100.0
      WC=WCP/100.0
      KSP=0
      KABRT=0
C
C-----DEFINE BLOCK LENGTHS FOR PARAMETER STORAGE
C
      IF(NBAS.EQ.1) NLT=NLT+1
      NL2=2*NLT
      NL4=4*NLT
      NL6=6*NLT
      NL16=16*NLT
      NL21=NL2-1
      ND=1
      NR=ND+NLT
      NG=NR+NLT
      NL=NG+NL2
      NA1=NL+NL2
      NA3=NA1+NL4
      NB2=NA3+NL4
      NB4=NB2+NL4
      NG1=NB4+NL4
      NG3=NG1+NL4
      NW1=NG3+NL4
      NW3=NW1+NL2
      NC1=NW3+NL2
      NC3=NC1+NL4
      NV1=NC3+NL4
      NV2=NV1+NL4
      NU1=NV2+NL4
      NU2=NU1+NL4
      NR1=NU2+NL4
      NR2=NR1+NL4
      NS1=NR2+NL4
      NS2=NS1+NL4
      NMVB=NS2+NL4
      NX=NMVB+NL21
      NE=NX+NL16
      NEX=NU2+NL2*NL4
      IF(NEX.GT.NE) NE=NEX
      NVA=NE+NL4
      NP=NVA+NL2*NL4
      PRINT 4000
C
C-----CONVERT INPUT DATA AND DEVELOP MATRICIES FOR SECULAR
C     EQUASION
C
      CALL SETUP(S(ND),S(NR),S(NG),S(NL))
      IF(KSP.EQ.1) GO TO 45
      PRINT 3500,WLP,WCP
      OMS=OMF**2
      KRT=0
      CALL ASMBL(OMS,S(ND),S(NR),S(NG),S(NL),S(NA1),S(NA3),S(NB2),S(NB4)
     1,S(NC1),S(NC3),S(NG1),S(NG3),S(NW1),S(NW3))
      IF(NOP.EQ.1) GO TO 56
C
C-----COMPUTE AND PRINT CHARACTERISTICS OF
C     WAVE MODES OF FIRST FREQUENCY
C
      CALL MLTYSOL(OMS,S(NE),S(NA1),S(NC1),S(NR1),S(NR2),S(NS1),S(NS2),S
     1(NVA),S(NV1),S(NV2),S(NU1),S(NU2))
      IF(KABRT.EQ.1) GO TO 40
      CALL SORT(NL2,S(NE),S(NVA))
      PRINT 7000,NL2,OMF
      PRINT 7500
      DO 55 N=1,NL2
      NTSE=NE+(N-1)*2
      NTSV=NVA+NL4*(N-1)
      CALL CHARIC(OMF,S(NTSE),S(NTSV),S(NV2))
      GO TO(50,51,52),IRL
   50 PRINT 8000,N,S(NTSE),S(NTSE+1),WLT,WLI,C,CI,DF,DCRM,S(NV2),S(NV2+1
     1)
      GO TO 55
   51 PRINT 8600,N,S(NTSE),S(NTSE+1),WLT,WLI,C,CI,DCRM,S(NR1),S(NR1+1)
      GO TO 55
   52 PRINT 8500,N,S(NTSE),S(NTSE+1),S(NR1),S(NP1+1)
   55 CONTINUE
      IF(NOP.EQ.2) GO TO 10
      GO TO 58
C
C-----SPECIAL CASE FOR FOLLOWING SINGLE CURVES
C
   56 NE1=NE+2*NDC-1
      READ 9800,(S(MA),MA=NE,NE1)
      NVA2=NVA+NDC*NL4-1
      DO 57 MA=NVA,NVA2,2
      S(MA)=1.0
```

```
   57 S(MA+1)=0.0
C
C-----FOLLOW DISPERSION CURVES BY PREDICTION AND CORRECTION
C     AND OUTPUT COORDINATES OF PROJECTION ONTO REAL PLANE
C
   58 CALL CURVS(S(NV1),S(NV2),S(NVA),S(NE),S(NP))
      PRINT 9000
      T=0
      DO 130 N=1,NDC
      PRINT 9500,N
  100 K=0
  101 IF(S(NP+I).EQ.ENC) GO TO 120
      S(NR1+K)=S(NP+I)
      S(NP1+K+1)=S(NP+I+1)
      I=I+2
      IF(K.EQ.16) GO TO 121
      K=K+2
      GO TO 101
  120 KE=K-1
      IF(K.EQ.0) GO TO 130
      GO TO 122
  121 KE=K+1
  122 NRJ=NR1-1
      PRINT 9600,(S(NRJ+J),J=1,KE,2)
      PRINT 9700,(S(NR1+J),J=1,KE,2)
      GO TO 100
  130 I=I+1
      IF(NOP.EQ.1) GO TO 66
C
C-----COMPUTE AND PRINT CHARACTERISTICS OF
C     WAVE MODES OF LAST FREQUENCY
C
      OMS=OML**2
      CALL MLTYSOL(OMS,S(NE),S(NA1),S(NC1),S(NR1),S(NR2),S(NS1),S(NS2),S
     1(NVA),S(NV1),S(NV2),S(NU1),S(NU2))
      IF(KABRT.EQ.1) GO TO 40
      CALL SORT(NL2,S(NE),S(NVA))
      PRINT 7000,NL2,OML
      PRINT 7500
      DO 65 N=1,NL2
      NTSE=NE+(N-1)*2
      NTSV=NVA+NL4*(N-1)
      CALL CHARIC(OMF,S(NTSE),S(NTSV),S(NV2))
      GO TO(60,61,62)IRL
   60 PRINT 8000,N,S(NTSE),S(NTSE+1),WLT,WLI,C,CI,DF,DCRM,S(NV2),S(NV2+1
     1)
      GO TO 65
   61 PRINT 8600,N,S(NTSE),S(NTSE+1),WLT,WLI,C,CI,DCRM,S(NP1),S(NP1+1)
      GO TO 65
   62 PRINT 8500,N,S(NTSE),S(NTSE+1),S(NR1),S(NR1+1)
   65 CONTINUE
   66 IF(NDAR.EQ.1) GO TO 10
C
C-----PLOT DISPERSION CURVES ON GRAPHICAL DISPLAY UNIT
C
      NX=1
      NY=NS1
      CALL DAPLUNIS(NP),S(NX),S(NY),NTC)
      GO TO 10
   40 PRINT 6000
      GO TO 10
   45 PRINT 6500
      STOP
C
C-----FORMAT STATEMENTS
C
 1300 FORMAT(7I10)
 2000 FORMAT(1H1,15X,94HDISPERSION CURVES FOR GENERALIZED RAYLEIGH WAVES
     1 IN A MULTILAYERED SYSTEM WITH VISCOUS DAMPING)
 3000 FORMAT(////,5X,27HNUMBER OF MAIN LAYERS     =,I10,//,5X,27HTOTAL N
     1UMBER OF SUBLAYERS =,I10,///)
 3500 FORMAT(/,5X,21HPERCENT LUMPED MASS =,F6.2,10X,25HPERCENT CONSISTEN
     1T MASS =,F6.2)
 4000 FORMAT(4X,12HLAYER  DEPTH,8X,2HVS,9X,2HVP,9X,2HBS,9X,2HBP,8X,3HRHO
     1,9X,13HSHEAR MODULUS,8X,14HLAMES CONSTANT,/,5X,3HNO.,69X,18HREAL
     2   IMAGINARY,4X,18HREAL     IMAGINARY)
 5000 FORMAT(3E10.5,I10)
 6000 FORMAT(//,10X,79HFAILED TO FIND AN EIGENVECTOR ORTHOGONAL TO THOSE
     1 FOUND PREVIOUSLY. JOB ABORTED)
 6500 FORMAT(///,10X,64HJOB ABORTED SUM OF SUBLAYERS NOT EQUAL TO TOTAL
     1NUMBER OF LAYERS)
 7000 FORMAT(////,4X,19HCHARACTERISTICS OF ,I2,35H WAVES GENERATED AT A
     1FREQUENCY OF ,E11.5)
 7500 FORMAT(/,11X,11HWAVE NUMBER,15X,11HWAVE LENGTH,12X,14HPHASE VELOCI
     1TY, 9X,5HDECAY, 6X,11HLOGARITHMIC, 5X,14HGROUP VELOCITY,/,7X,7HREA
     2L(K),5X,8HIMAG.(K), 8X,1HL,10X,3H1/L,11X,1HC,10X,3H1/C, 9X,6HREACTO
     3R, 6X,9HDECREMENT, 4X,7HREAL(U),5X,8HIMAG.(U))
 8000 FORMAT(1X,I2,2X,E11.5,1X,E11.5,2X,E11.5,1X,E11.5,2X,E11.5,1X,E11.5
     1,2X,E11.5,2X,E11.5,2X,E11.5,1X,E11.5)
 8500 FORMAT(1X,I2,2X,E11.5,1X,E11.5,78X,E11.5,1X,E11.5)
 8600 FORMAT(1X,I2,2X,E11.5,1X,E11.5,2X,E11.5,1X,E11.5,2X,E11.5,1X,E11.5
     1,4X,8HV. LARGE,3X,E11.5,2X,E11.5,1X,E11.5)
 9000 FORMAT(////,50X,32HCOORDINATES OF DISPERSION CURVES,//)
 9500 FORMAT(//,4X,21HDISPERSION CURVE NO. ,I2)
 9600 FORMAT(/,1X,9HFREQUENCY,4X,9(2X,E11.5))
 9700 FORMAT(1X,11HWAVE NUMBER,2X,9(2X,E11.5))
 9800 FORMAT(2E10.5)
      END


      SUBROUTINE SETUP1B,RHO,G,ALAM)
C
C     OBTAINS LAYER PROPERTIES IN TERMS OF ELASTIC CONSTANTS
C     FROM BODY WAVE VELOCITIES
C
      COMMON/SPECS/LAYERS,NLT,NL2,NBAS,OMF,OML,DOM,WL,WC,NDC,NOP,ENC
      COMMON/MISS/KSP,KRT,KABRT,RDF,NVEC
      COMPLEX G(1),ALAM(1),RDF
      DIMENSION B(1),RHO(1)
      N1=1
      N2=0
```

```
C
C-----INPUT LAYER PROPERTIES
C
      DO 10 I=1,LAYERS
      READ 1000,NL,DL,VS,VP,BS,BP,RH
      N2=N2+NL
      DL=DL/FLOAT(NL)
C
C-----COMPUTE G AND LAMDA FOR EACH LAYER AND PRINT LAYER PROPERTIES
C
      DO 20 I2=N1,N2
      B(I2)=DL
      RHO(I2)=RH
      GMOD=RH*VS**2
      GRL=GMOD/SQRT(1.0+4.0*BS**2)
      GIM=2.0*BS*GRL
      G(I2)=CMPLX(GRL,GIM)
      TMOD=RH*VP**2
      TRL=TMOD/SQRT(1.0+4.0*BP**2)
      TIM=2.0*BP*TRL
      ALRL=TRL-2.0*GRL
      ALIM=TIM-2.0*GIM
      ALAM(I2)=CMPLX(ALRL,ALIM)
   20 PRINT 2000,I2,DL,VS,VP,BS,BP,RH,GRL,GIM,ALRL,ALIM
   10 N1=N2+1
C
C-----PROPERTIES OF SPECIAL VISCOUS BOUNDARY LAYER
C
      IF(N2.NE.NLT) KSP=1
      IF(NBAS.EQ.0) GO TO 15
      IF(N2.EQ.NLT-1) KSP=0
      RHO(NLT)=0.0
      B(NLT)=1.0
      G(NLT)=CMPLX(0.0,1.0)*CMPLX(SQRT(RHO(NLT-1)),0.0)*CSQRT(G(NLT-1))
      ALAM(NLT)=(0.0,1.0)*CMPLX(SQRT(RHO(NLT-1)),0.0)*(CSQRT(ALAM(NLT-1)
     1+(2.0,0.0)*G(NLT-1))-(2.0,0.0)*CSQRT(G(NLT-1)))
   15 RETURN
 1000 FORMAT(I10,6E10.5)
 2000 FORMAT(2X,I5,1X,10(E10.4,1X))
      END



      SUBROUTINE ASMBL(OMS,TH,RHO,SM,LAM,A1,A3,B2,B4,C1,C3,G1,G3,W1,W3)
C
C-----COMPUTES ELEMENTS OF MATRICIES A,B AND C
C
      COMMON/SPECS/LAYERS,NLT,NL2,NBAS,OMF,OML,DOM,WL,WC,NDC,NOP,ENC
      COMMON/MISS/KSP,KRT,KABRT,RDF,NVEC
      COMPLEX A1(1),A3(1),B2(1),B4(1),C1(1),C3(1),G1(1),G3(1),SM(1),LAM(
     11),AH,AHO,AV,AVO,BH,BHO,BV,GH,GHO,GV,GVO,AL,RDF
      DIMENSION TH(1),RHO(1),W1(1),W3(1)
      IF(NBAS.EQ.0.AND.KRT.EQ.1) GO TO 30
C
C-----INITIALIZATION
C
      AHO=(0.0,0.0)
      AVO=(0.0,0.0)
      BHO=(0.0,0.0)
      GHO=(0.0,0.0)
      GVO=(0.0,0.0)
      WHO1=0.0
      WHO3=0.0
      I=0
      IF(KRT.EQ.1) GO TO 15
C
C-----COMPUTE ELEMENTS OF MATRICIES A,B,G AND M(W)
C
      DO 10 J=1,NLT
      TH3=TH(J)/3.0
      AL=(2.0,0.0)*SM(J)+LAM(J)
      WM1=WL*RHO(J)*TH(J)/2.0+WC*RHO(J)*TH3
      WM3=WC*RHO(J)*TH3
      AH=AL*CMPLX(TH3,0.0)
      AV=SM(J)*CMPLX(TH3,0.0)
      GV=AL/CMPLX(TH(J),0.0)
      GH=SM(J)/CMPLX(TH(J),0.0)
      BH=(SM(J)-LAM(J))*(0.5,0.0)
      BV=(SM(J)+LAM(J))*(0.5,0.0)
      I=I+1
      A1(I)=AH+AHO
      A3(I)=AH*(0.5,0.0)
      B2(I)=BH-BHO
      B4(I)=BV
      G1(I)=GH+GHO
      G3(I)=-GH
      W1(I)=WM1+WHO1
      W3(I)=WM3/2.0
      I=I+1
      A1(I)=AV+AVO
      A3(I)=AV*(0.5,0.0)
      B2(I)=-BV
      B4(I)=(0.0,0.0)
      G1(I)=GV+GVO
      G3(I)=-GV
      W1(I)=WM1+WHO1
      W3(I)=WM3/2.0
      AHO=AH
      AVO=AV
      BHO=BH
      GHO=GH
      GVO=GV
      WHO1=WM1
   10 WHO3=WM3
C
C-----SPECIAL CASE FOR VISCOUS BOUNDARY LAYER
C
      IF(KRT.EQ.0) GO TO 35
      IF(NBAS.EQ.0) GO TO 30
   15 XOM=SQRT(OMS)
      A1(NL2-1)=((2.0,0.0)*SM(NLT-1)+LAM(NLT-1))*CMPLX(TH(NLT-1)/3.0,0.0
     1)+((2.0,0.0)*SM(NLT)+LAM(NLT))/(3.0,0.0)
```

```
      A1(NL2)=SM(NLT-1)*CMPLX(TH(NLT-1)/3.0,0.0)+SM(NLT)/(3.0,0.0)
      B2(NL2-1)=-(0.5,0.0)*(SM(NLT-1)-LAM(NLT-1))+(0.5,0.0)*(SM(NLT)-LAM
     1(NLT))
      G1(NL2-1)=SM(NLT-1)/CMPLX(TH(NLT-1),0.0)+CMPLX(XOM,0.0)*SM(NLT)
      G1(NL2)=((2.0,0.0)*SM(NLT-1)+LAM(NLT-1))/CMPLX(TH(NLT-1),0.0)+CMPL
     1X(XOM,0.0)*((2.0,0.0)*SM(NLT)+LAM(NLT))
C
C-----ELEMENTS OF MATRIX C=G-OMS**2*M
C
   30 DO 20 L=1,NL2
      C1(L)=G1(L)-CMPLX(OMS*W1(L),0.0)
   20 C3(L)=G3(L)-CMPLX(OMS*W3(L),0.0)
   35 RETURN
      END



      SUBROUTINE MLTYSOL(OMS,E,A1,C1,R1,R2,S1,S2,VA,V1,V2,U1,U2)
C
C-----COMPUTES ALL NL2 EIGENVALUES AND EIGENVECTORS
C
      COMMON S(1)
      COMMON/STARTS/NA1,NA3,NB2,NB4,NC1,NC3,NX,NMVB,NS1,NS2,NW1,NW3,NV1,
     1ND,NR,NG,NL,NG1,NG3,NU1,NU2
      COMMON/SPECS/LAYERS,NLT,NL2,NRAS,OMF,OML,DOM,WL,WC,NDC,NDP,ENC
      COMMON/MTSS/KSP,KPT,KABRT,RDF,NVEC
      COMPLEX A1(1),C1(1),E(1),R1(1),R2(1),S1(1),S2(1),VA(1),V1(1),V2(1)
     1,U1(1),U2(1),EV,CE,RDF,C,D
      DATA EPS1/1.0E-5/,EPS2/1.0E-10/
      KRT=1
C
C-----OBTAIN BASIC ELEMENTS OF SECULAR EQUATION
C
      CALL ASMBL(OMS,S(ND),S(NR),S(NG),S(NL),A1,S(NA3),S(NB2),S(NB4),C1,
     1S(NC3),S(NG1),S(NG3),S(NW1),S(NW3))
C
C-----OBTAIN ARBITRARY INITIAL APPROXIMATION TO VECTOR
C
      XN=0.0
      DO 20 J=1,NL2
      XX=C1(J)/A1(J)
   20 XN=XN+ABS(XX)
      XN=SQRT(XN/FLOAT(NL2))
      C=CMPLX(XN,XN+XN)
      DO 30 J=1,NL2
      S1(J)=(1.0,0.0)
      S2(J)=C
      V1(J)=S1(J)
      V2(J)=S2(J)
      R1(J)=(0.0,0.0)
   30 R2(J)=(0.0,0.0)
C
C-----INITIAL ESTIMATE OF AN EIGENVALUE
C
      EV=XN/FLOAT(NL2)
      ISW=0
      KC=0
      MC=0
   40 KC=KC+1
      IF(ISW.EQ.1) GO TO 50
      ISW=0
      XX=CABS(EV)/2.0
      EV=CMPLX(XX,XX+XX)
      GO TO 60
   50 EV=CONJG(EV)
   60 ISW=2
C
C-----ITERATE TO AN EIGENVALUE
C
      CALL EIGSOL(A1,S(NA3),S(NB2),S(NB4),C1,S(NC3),S(NX),V1,V2,U1,U2,EV
     1)
      E(KC)=EV
      ICR=0
      XX=ABS(REAL(EV))
      Y=ABS(AIMAG(EV))
      Z=XX+Y
      IF(Y/Z.LT.EPS2) ICR=1
      IF(Y/Z.LT.EPS2) ICR=1
      IF(XX/Z.LT.EPS2) ICR=2
      IF(ICR.EQ.1) E(KC)=CMPLX(REAL(EV),0.0)
      IF(ICR.EQ.2) E(KC)=CMPLX(0.0,AIMAG(EV))
C
C-----NORMALIZE VECTOR
C
      KCV=KC-1
      DO 80 N=1,NL2
      V2(N)=V2(N)*RDF
      VA(NL2*KCV+N)=V1(N)
      U1(N)=U1(N)*RDF
   80 U2(N)=U2(N)*RDF
C
C-----CHOOSE EIGENVALUE OF APPROPRIATE SIGN
C
      IF(ICR.NE.1) GO TO 102
      X=(V1(1)**2+V1(2)**2)*EV
      IF(X.GT.0.0) GO TO 101
      E(KC)=-E(KC)
      DO 90 N=2,NL2,2
   90 VA(NL2*KCV+N)=-VA(KCV*NL2+N)
      GO TO 101
  102 IF(ICR.NE.2) GO TO 103
      XX=AIMAG(E(KC))
      IF(XX.LT.0.0) GO TO 101
      E(KC)=CMPLX(0.0,-XX)
      DO 92 N=2,NL2,2
   92 VA(NL2*KCV+N)=-VA(NL2*KCV+N)
      GO TO 101
  103 XX=AIMAG(E(KC))
      IF(XX.LT.0.0) GO TO 101
      E(KC)=-E(KC)
      DO 91 N=2,NL2,2
   91 VA(KCV*NL2+N)=-VA(KCV*NL2+N)
```

```
C
C-----CHECK ORTHOGONALITY OF NEW EIGENVECTOR
C     AND SUM OF EIGENVECTORS PREVIOSLY FOUND
C
  101 CE=(0.0,0.0)
      DO 110 N=1,NL2
  110 CE=CE-R1(N)*U1(N)+R2(N)*U2(N)
      XX=ABS(REAL(CE))+ABS(AIMAG(CE))
      IF(XX.LT.EPS1) GO TO 115
      KABRT=1
      RETURN
  115 DO 120 N=1,NL2
      R1(N)=R1(N)+V1(N)
  120 R2(N)=R2(N)+V2(N)
C
C-----OBTAIN AN INITIAL EIGENVECTOR ORTHAGONAL TO
C     THOSE FOUND PREVIOUSLY
C
      C=(0.0,0.0)
      D=(0.0,0.0)
      DO 130 N=2,NL2,2
      M=N-1
      C=C-U1(M)*S1(M)+U2(N)*S2(N)
  130 D=D-U1(N)*S1(N)+U2(M)*S2(M)
      C=C*(2.0,0.0)
      D=D*(2.0,0.0)
      DO 140 N=2,NL2,2
      M=N-1
      S1(M)=S1(M)-C*V1(M)
      S1(N)=S1(N)-D*V1(N)
      S2(M)=S2(M)-D*V2(M)
      S2(N)=S2(N)-C*V2(N)
      V1(M)=S1(M)
      V1(N)=S1(N)
      V2(M)=S2(M)
  140 V2(N)=S2(N)
      IF(ICR+ISW.EQ.0) ISW=1
      MC=MC+1
      IF(MC.GE.NL2) RETURN
      GO TO 40
      END



      SUBROUTINE EIGSOL(A1,A3,B2,B4,C1,C3,X,V1,V2,U1,U2,EV)
C
C-----GENERALIZED RAYLEIGH QUOTIENT ITERATION FOR SINGLE EIGENVALUES
C
      COMMON S(1)
      COMMON/STARTS/NA1,NA3,NB2,NB4,NC1,NC3,NX,NMVB,NS1,NS2,NW1,NW3,NV1,
     1ND,NR,NG,NL,NG1,NG3,NU1,NU2
      COMMON/SPECS/LAYERS,NLT,NL2,NBAS,OMF,OML,DOM,WL,WC,NDC,NOP,ENC
      COMMON/MISS/KSP,KRT,KABRT,RDF,NVEC
      COMPLEX A1(1),A3(1),B2(1),B4(1),C1(1),C3(1),V1(1),V2(1),U1(1),U2(1
     11),X(1),CE,RDF,RQ,EV,EVS,CHK
      DATA EPS1/1.0E-5/,EPS2/1.0E-10/
      NL4=2*NL2
      NL6=3*NL2
      IT=0
      IK=0
      RDF=(1.0,0.0)
C
C-----COMPUTE ELEMENTS OF R.H.S.
C
      DO 20 N=1,NL2
      U1(N)=C1(N)*V1(N)
   20 U2(N)=A1(N)*V2(N)
      DO 30 N=3,NL2
      L=N-2
      U1(L)=U1(L)+C3(L)*V1(N)
      U1(N)=U1(N)+C3(L)*V1(L)
      U2(L)=U2(L)+A3(L)*V2(N)
   30 U2(N)=U2(N)+A3(L)*V2(L)
C
C-----COMMENCE ITERATION
C
  200 EVS=EV**2
C
C-----COMPUTE ELEMENTS OF L.H.S.
C
      DO 40 N=1,NL2
      X(N)=EVS*A1(N)+C1(N)
      X(NL2+N)=EV*B2(N)
      X(NL4+N)=EVS*A3(N)+C3(N)
      X(NL6+N)=EV*B4(N)
   40 V2(N)=(U1(N)-EV*U2(N))*RDF
C
C-----SOLVE SET OF LINEAR EQUASIONS
C
      CALL FLES(NL2,S(NMVB),X,V2)
C
C-----COMPUTE RAYLEIGH QUOTIENT
C
      CE=(0.0,0.0)
      DO 90 N=1,NL2
      V1(N)=(V2(N)-V1(N)*RDF)/EV
      CE=CE-U1(N)*V1(N)+U2(N)*V2(N)
      U1(N)=C1(N)*V1(N)
   90 U2(N)=A1(N)*V2(N)
      CE=CE*RDF
C
C-----COMPUTE ELEMENTS OF R.H.S.
C
      DO 100 N=3,NL2
      L=N-2
      U1(L)=U1(L)+C3(L)*V1(N)
      U1(N)=U1(N)+C3(L)*V1(L)
      U2(L)=U2(L)+A3(L)*V2(N)
  100 U2(N)=U2(N)+A3(L)*V2(L)
C
C-----NEW ESTIMATE FOR EIGENVALUE
C
```

```
      RDF=(0.0,0.0)
      DO 110 N=1,NL2
  110 RDF=RDF-U1(N)*V1(N)+U2(N)*V2(N)
      RQ=CE/RDF
      IF(IT.GT.15) RQ=(0.5,0.0)*RQ
      EV=EV+RQ
      RDF=(1.0,0.0)/CSQRT(RDF)
C
C-----CHECK FOR CONVERGENCE
C
      CHK=RQ/EV
      CHS=ABS(REAL(CHK))+ABS(AIMAG(CHK))
      IF(IK.EQ.1.AND.CHS.LT.EPS2) GO TO 120
      IF(CHS.LT.EPS1) IK=1
      IT=IT+1
      GO TO 200
C
C-----NORMALIZE VECTOR
C
  120 DO 130 N=1,NL2
  130 V1(N)=V1(N)*RDF
      RETURN
      END



      SUBROUTINE FLES(NL2,MVB,X,V2)
C
C-----SOLVES SET OF SYMETRIC SIMILTANEOUS EQUATIONS
C
      DIMENSION MVB(1)
      COMPLEX X(1),V2(1),C
      NL4=2*NL2
      NL6=3*NL2
      N1=NL2-1
      N2=NL2-2
      DO 5 N=1,N2
      MVB(N)=N+NL6
      N=N+1
    5 MVB(N)=N+NL4
      MVB(N1)=N1+NL2
C
C-----REDUCE MATRIX AND VECTOR
C
      DO 30 N=1,N1
      I=N
      J=N+NL2
      M=MVB(N)
      DO 20 L=J,M,NL2
      C=X(L)/X(N)
      I=I+1
      J=I
      DO 10 K=L,M,NL2
      X(J)=X(J)-C*X(K)
   10 J=J+NL2
      X(L)=C
   20 V2(I)=V2(I)-C*V2(N)
   30 V2(N)=V2(N)/X(N)
C
C-----BACK SUBSTITUTION
C
      N=NL2
      V2(N)=V2(N)/X(N)
      DO 40 K=1,N1
      N=N-1
      I=N
      J=N+NL2
      M=MVB(N)
      DO 40 L=J,M,NL2
      I=I+1
   40 V2(N)=V2(N)-X(L)*V2(I)
      RETURN
      END



      SUBROUTINE SORT(NL2,E,VA)
C
C-----ARRANGES EIGENVALUES IN ASCENDING ORDER OF IMAGINARY PARTS
C     OF DECENDING ORDER OF REAL PARTS WHERE IMAGINARY PART .LT. 10/100
C
      COMPLEX E(1),VA(1),ST1,ST2
      DO 10 I=2,NL2
      M=I-1
      DO 20 N=1,M
      ARI=ABS(0.1*REAL(E(I)))
      ARN=ABS(0.1*REAL(E(N)))
      IF(ABS(AIMAG(E(I))).LT.ARI.AND.ABS(AIMAG(E(N))).LT.ARN)
     1GO TO 25
      IF(ABS(AIMAG(E(I))).LE.ABS(AIMAG(E(N)))) GO TO 30
      GO TO 20
   25 IF(ABS(REAL(E(I))).GE.ABS(REAL(E(N)))) GO TO 30
   20 CONTINUE
      GO TO 10
   30 ST1=E(N)
      E(N)=E(I)
      K=I-1
      DO 40 J=N,K
      ST2=E(J+1)
      E(J+1)=ST1
   40 ST1=ST2
      KN=(N-1)*NL2
      KI=(I-1)*NL2
      DO 60 L=1,NL2
      ST1=VA(KN+L)
      VA(KN+L)=VA(KI+L)
      DO 60 J=N,K
      KJ=J*NL2
      ST2=VA(KJ+L)
      VA(KJ+L)=ST1
   60 ST1=ST2
   10 CONTINUE
```

```
      RETURN                                                            651
      END                                                               652


      SUBROUTINE CHARIC(OM,E,V1,GV)                                     653
C                                                                       654
C-----COMPUTES CHARACTERISTICS OF SURFACE WAVES                         655
C                                                                       656
      COMMON S(1)                                                       657
      COMMON/STARTS/NA1,NA3,NB2,NB4,NC1,NC3,NX,NMVB,NS1,NS2,NW1,NW3,NV1,658
     1ND,NR,NG,NL,NG1,NG3,NU1,NU2                                       659
      COMMON/SPECS/LAYERS,NLT,NL2,NBAS,OMF,OML,DOM,WL,WC,NDC,NOP,ENC    660
      COMMON/CHAR/WLI,C,WLT,CI,DCRM,DF,IRL                              661
      COMPLEX E,GV                                                      662
      IF(REAL(E).EQ.0.0) GO TO 10                                       663
      IRL=1                                                             664
      PI2=6.2831853072                                                  665
      WLT=PI2/REAL(E)                                                   666
      WLI=1.0/WLT                                                       667
      C=OM/REAL(E)                                                      668
      CI=1.0/C                                                          669
      DCRM=PI2*AIMAG(E)/REAL(E)                                         670
      IF(-DCRM.GT.740.0) GO TO 15                                       671
      DF=EXP(-DCRM)                                                     672
      GO TO 20                                                          673
   15 IRL=2                                                             674
      GO TO 20                                                          675
   10 IRL=3                                                             676
   20 CALL GRPVL(NL2,S(NS1),S(NW1),S(NW3),V1,OM,E,GV)                   677
      RETURN                                                            678
      END                                                               679


      SUBROUTINE CURVS(V1,V2,VA,E,P)                                    680
C                                                                       681
C-----FOLLOWS DISPERSION CURVE BY PREDICTION AND CORRECTION             682
C                                                                       683
      COMMON S(1)                                                       684
      COMMON/STARTS/NA1,NA3,NB2,NB4,NC1,NC3,NX,NMVB,NS1,NS2,NW1,NW3,NV1,685
     1ND,NR,NG,NL,NG1,NG3,NU1,NU2                                       686
      COMMON/SPECS/LAYERS,NLT,NL2,NBAS,OMF,OML,DOM,WL,WC,NDC,NOP,ENC    687
      COMMON/MISS/KSP,KRT,KABRT,RDF,NVEC                                688
      COMPLEX VA(1),V1(1),V2(1),E(1),EV,GV,AL(4,4),SGV(3),ST1,ST2,EVS,EV689
     1S1,RDF,CN,VD1,VD2                                                 690
      DIMENSION SD(4),EST(4),P(1)                                       691
      KRT=1                                                             692
      IF(NVEC.EQ.0) GO TO 1                                             693
      PRINT 100                                                         694
C                                                                       695
C-----INITIALIZE COEFFICIENTS                                           696
C                                                                       697
    1 DO 5 M=1,4                                                        698
      DO 5 N=1,4                                                        699
    5 AL(M,N)=CMPLX(0.0,0.0)                                            700
      AL(1,1)=CMPLX(1.0,0.0)                                            701
C                                                                       702
C-----OPTIMAL ERROR FACTORS                                             703
C                                                                       704
      EST(1)=0.59                                                       705
      EST(2)=0.39                                                       706
      EST(3)=0.24                                                       707
      EST(4)=0.13                                                       708
      L=0                                                               709
C                                                                       710
C-----MAXIMUM STEP SIZE IN FREQUENCY                                    711
C                                                                       712
      RNG=OML-OMF                                                       713
      DOM=RNG/DOM                                                       714
C                                                                       715
C-----START CURVE FOLLOWING                                             716
C                                                                       717
      DO 60 J=1,NDC                                                     718
      IF(NVEC.EQ.1) PRINT 200,J                                         719
      C=DOM                                                             720
      KEND=0                                                            721
      KO=1                                                              722
      KW=0                                                              723
      ERR=EST(1)                                                        724
C                                                                       725
C-----INITIALIZATION                                                    726
C                                                                       727
      SGV(1)=1.0                                                        728
      SGV(2)=1.0                                                        729
      SGV(3)=1.0                                                        730
      SD(1)=0.0                                                         731
      SD(2)=0.0                                                         732
      SD(3)=0.0                                                         733
C                                                                       734
C-----COMPUTE FIRST POINT ON CURVE                                      735
C                                                                       736
      KJ=NL2*(J-1)                                                      737
      OM=OMF                                                            738
      EV=E(J)                                                           739
      EVS=E(J)                                                          740
      EVS1=E(J)                                                         741
      DO 10 N=1,NL2                                                     742
      V1(N)=VA(KJ+N)                                                    743
   10 V2(N)=EV*V1(N)                                                    744
      IF(NOP.EQ.0) GO TO 6                                              745
      OMS=OM**2                                                         746
      CALL ASMBL(OMS,S(ND),S(NR),S(NG),S(NL),S(NA1),S(NA3),S(NB2),S(NB4)747
     1,S(NC1),S(NC3),S(NG1),S(NG3),S(NW1),S(NW3))                       748
      CALL EIGSCL(S(NA1),S(NA3),S(NB2),S(NB4),S(NC1),S(NC3),S(NX),V1,V2,749
     1S(NU1),S(NU2),EV)                                                 750
C                                                                       751
C-----PRINT DISPLACEMENT VECTORS                                        752
C                                                                       753
    6 IF(NVEC.EQ.0) GO TO 16                                            754
      PRINT 300,OM,EV                                                   755
      CALL MODSHP(NL2,EV,V1)                                            756
```

```
      M2=0
      N4=0
   81 M1=M2+1
      M2=M1+1
      N1=N4+1
      N2=N1+1
      N3=N2+1
      N4=N3+1
      IF(M1.EQ.NLT) GO TO 14
      VD1=V1(N2)
      V1(N2)=V1(N2)/(0.0,-1.0)
      VD2=V1(N4)
      V1(N4)=V1(N4)/(0.0,-1.0)
      PRINT 400,M1,VD1,M2,VD2,M1,V1(N1),M2,V1(N3)
      IF(M2.EQ.NLT) GO TO 16
      GO TO 81
   14 VD1=V1(N2)
      V1(N2)=V1(N2)/(0.0,-1.0)
      PRINT 500,M1,VD1,M1,V1(N1)
   16 IF(NOP.EQ.0) GO TO 15
      CALL GRPVL(NL2,S(NS1),S(NW1),S(NW3),V1,OM,EV,GV)
   15 L=L+1
      P(L)=OM
      L=L+1
      P(L)=REAL(EV)
C
C-----COMPUTE COEFFICIENTS
C
   20 CALL GRPVL(NL2,S(NS1),S(NW1),S(NW3),V1,OM,EV,GV)
   21 GO TO(25,2,3,4),KO
    2 AL(2,2)=CMPLX(-0.5*D/SD(1),0.0)
      AL(2,1)=CMPLX(1.0,0.0)-AL(2,2)
      ERR=EST(2)
      GO TO 25
    3 AL(3,3)=CMPLX(D/6.0/SD(2)*((2.0*D+3.0*SD(1))/(SD(1)+SD(2))),0.0)
      AL(3,2)=CMPLX(-D/6.0/SD(1)/SD(2)*(2.0*D+3.0*(SD(1)+SD(2))),0.0)
      AL(3,1)=CMPLX(1.0,0.0)-AL(3,2)-AL(3,3)
      ERR=EST(3)
      GO TO 25
    4 AL(4,4)=CMPLX(-D/12.0*(6.0*SD(1)**2+3.0*D**2+8.0*D*SD(1)+4.0*D*SD(
     12)+6.0*SD(1)*SD(2))/(SD(3)*(SD(3)+SD(2))*(SD(3)+SD(2)+SD(1))),0.0)
      AL(4,3)=CMPLX(D/12.0*(6.0*SD(1)**2+3.0*D**2+8.0*D*SD(1)+4.0*(D*SD(
     12)+D*SD(3))+6.0*(SD(1)*SD(2)+SD(1)*SD(3)))/SD(3)/SD(2)/(SD(2)+SD(1
     2)),0.0)
      AL(4,2)=-(CMPLX(0.5*D/SD(1),0.0)+CMPLX((SD(2)+SD(1))/SD(1),0.0)*AL
     1(4,3)+CMPLX((SD(1)+SD(2)+SD(3))/SD(1),0.0)*AL(4,4))
      AL(4,1)=CMPLX(1.0,0.0)-AL(4,2)-AL(4,3)-AL(4,4)
      ERR=EST(4)
   25 OM=OM+D
C
C-----ESTIMATE NEXT EIGENVALUE
C
      EV=EV+CMPLX(D,0.0)*(AL(KO,1)/GV+AL(KO,2)/SGV(1)+AL(KO,3)/SGV(2)+AL
     1(KO,4)/SGV(3))+CMPLX(1.0E-5,-1.0E-5)
      IF(REAL(EVS)*AIMAG(EVS)*REAL(EV)*AIMAG(EV).LT.-1.0E-10.AND.D.GT.DO
     1M) GO TO 41
      EVS=EV
   26 OMS=OM**2
C
C-----COMPUTE EIGENVALUE
C
      CALL ASMBL(OMS,S(ND),S(NR),S(NG),S(NL),S(NA1),S(NA3),S(NB2),S(NB4)
     1,S(NC1),S(NC3),S(NG1),S(NG3),S(NW1),S(NW3))
      CALL EIGSOL(S(NA1),S(NA3),S(NB2),S(NB4),S(NC1),S(NC3),S(NX),V1,V2,
     1S(NU1),S(NU2),EV)
      IF(AMIN1(ABS(REAL(EV)),ABS(REAL(EVS1)),ABS(AIMAG(EV)),ABS(AIMAG(EV
     1S1))).LT.1.0E-10) GO TO 40
   31 EVS1=EV
C
C-----PRINT DISPLACEMENT VECTORS
C
      IF(NVEC.EQ.0) GO TO 82
      PRINT 300,OM,EV
      CALL MODSH(NL2,EV,V1)
      M2=0
      N4=0
   83 M1=M2+1
      M2=M1+1
      N1=N4+1
      N2=N1+1
      N3=N2+1
      N4=N3+1
      IF(M1.EQ.NLT) GO TO 84
      VD1=V1(N2)
      V1(N2)=V1(N2)/(0.0,-1.0)
      VD2=V1(N4)
      V1(N4)=V1(N4)/(0.0,-1.0)
      PRINT 400,M1,VD1,M2,VD2,M1,V1(N1),M2,V1(N3)
      IF(M2.EQ.NLT) GO TO 82
      GO TO 83
   84 VD1=V1(N2)
      V1(N2)=V1(N2)/(0.0,-1.0)
      PRINT 500,M1,VD1,M1,V1(N1)
C
C-----STORE COORDINATE DATA
C
   82 L=L+1
      P(L)=OM
      L=L+1
      P(L)=REAL(EV)
      IF(KEND.EQ.1) GO TO 50
      KO=KO+1
      DS1=SD(1)
      SD(1)=D
      DS2=SD(2)
      SD(2)=DS1
      SD(3)=DS2
      ST1=SGV(1)
      SGV(1)=GV
      ST2=SGV(2)
      SGV(2)=ST1
      SGV(3)=ST2
```

```
C
C-----OBTAIN OPTIMUM STEP SIZE
C
      D=D*(ERR/CABS(EV-EVS))**(1.0/FLOAT(KO))
      IF(KO.GT.4) KO=4
      EVS=EV
      IF(ABS(D).GT.ABS(DOM)*FLOAT(KO+1)) D=DOM*FLOAT(KO+1)
      IF(ABS(D).GT.ABS(OML-OM)) GO TO 43
      GO TO 20
C
C-----SPECIAL CASES FOR PASSING THROUGH SINGULARITIES
C
   40 IF(AMIN1(ABS(REAL(EV)-REAL(EVS1)),ABS(AIMAG(EV)-AIMAG(EVS1))).GT.1
     1.0E-10) GO TO 32
      IF(AIMAG(EV)*AIMAG(EVS1).LT.-1.0E-10.AND.ABS(AIMAG(EV)).GT.1.0E-10
     1) GO TO 75
      IF((REAL(EV)-REAL(EVS1))*RNG.GT.-1.0E-10.AND.REAL(EV)*REAL(EVS1).G
     1T.-1.0E-10) GO TO 31
      GO TO 44
   32 IF(D.LT.DOM) GO TO 42
      OM=OM-D
      D=D/4.0
      EV=EVS1
      GO TO 21
   42 IF((REAL(EV)-REAL(EVS1))*RNG.GT.0.0) GO TO 35
   44 KW=KW+1
      EV=CMPLX(REAL(EVS1)+ABS(REAL(EV)-REAL(EVS1)),AIMAG(EV))
      IF(KW.GT.1) EV=CMPLX(REAL(EVS)+ABS(REAL(EVS)/2.0),AIMAG(EVS))
      IF(KW.GT.2.AND.REAL(EVS1).LT.-1.0E-10) EV=CMPLX(0.0,REAL(EVS1))
      IF(KW.GT.7) GO TO 50
      EVS=EV
      GO TO 26
   75 KW=KW+1
      EV=CMPLX(AIMAG(EVS1),0.0)
      IF(KW.GT.4) GO TO 50
      EVS=EV
      GO TO 26
   35 KO=1
      KW=0
      ERR=EST(1)
C
C-----INITIALIZATION
C
      SGV(1)=1.0
      SGV(2)=1.0
      SGV(3)=1.0
      SD(1)=0.0
      SD(2)=0.0
      SD(3)=0.0
C
C-----STORE COORDINATE DATA
C
      L=L+1
      P(L)=OM
      L=L+1
      P(L)=REAL(EV)
      EVS1=EV
      EVS=EV
      CALL GRPVL(NL2,S(NS1),S(NW1),S(NW3),V1,OM,EV,GV)
      IF(KEND.EQ.1) GO TO 50
C
C-----RESET STEP SIZE
C
      D=DOM
      OM=OM+D
      GO TO 26
   41 OM=OM-D
      D=D/4.0
      EV=EVS
      GO TO 21
   43 D=OML-OM
      KEND=1
   45 GO TO 20
   50 L=L+1
   60 P(L)=ENC
      RETURN
  100 FORMAT(///,57X,20HDISPLACEMENT VECTORS,//,30X,8HVERTICAL,60X,10HHO
     1RIZONTAL,/)
  200 FORMAT(//,3X,9HCURVE NO.,I3)
  300 FORMAT(/,3X,4HDOM =,1X,E11.5,2X,3HK =,1X,E11.5,1X,E11.5,/)
  400 FORMAT(1X,I3,2X,E11.5,1X,E11.5,3X,I3,2X,E11.5,1X,E11.5,10X,I3,2X,E
     111.5,1X,E11.5,3X,I3,2X,E11.5,1X,E11.5)
  500 FORMAT(1X,I3,2X,E11.5,1X,E11.5,41X,I3,2X,E11.5,1X,E11.5)
      END



      SUBROUTINE GRPVL(NL2,S1,W1,W3,V1,OM,EV,GV)
C
C-----COMPUTES GROUP VELOCITY
C
      COMPLEX S1(1),V1(1),DN,EV,GV
      DIMENSION W1(1),W3(1)
      DO 10 N=1,NL2
   10 S1(N)=V1(N)*CMPLX(W1(N),0.0)
      DO 20 N=3,NL2
      L=N-2
      S1(L)=S1(L)+V1(N)*CMPLX(W3(L),0.0)
   20 S1(N)=S1(N)+V1(L)*CMPLX(W3(L),0.0)
      DN=(0.0,0.0)
      DO 30 N=1,NL2
   30 DN=DN+S1(N)*V1(N)
      GV=(0.5,0.0)/CMPLX(OM,0.0)/DN/EV
      RETURN
      END



      SUBROUTINE MODSH(NL2,E,V)
C
C-----OBTAINS MODE SHAPE FROM EIGENVECTOR
C
```

```
      COMPLEX E,V(1)
      DATA EPS2/1.0E-10/
      ICR=0
      X=ABS(REAL(E))
      Y=ABS(AIMAG(E))
      Z=X+Y
      IF(Y/Z.LT.EPS2) ICR=1
      IF(X/Z.LT.EPS2) ICR=2
      IF(ICR.EQ.1) E=CMPLX(REAL(E),0.0)
      IF(ICR.EQ.2) E=CMPLX(0.0,AIMAG(E))
      IF(ICR.NE.1) GO TO 30
      X=ABS(REAL(V(1)))+ABS(REAL(V(2)))
      IF(X.GT.EPS2) GO TO 15
      DO 10 J=1,NL2
   10 V(J)=CMPLX(AIMAG(V(J)),0.0)
      GO TO 30
   15 DO 20 J=1,NL2
   20 V(J)=CMPLX(REAL(V(J)),0.0)
   30 DO 40 J=2,NL2,2
   40 V(J)=V(J)*(0.0,-1.0)
      IF(ICR.NE.2) GO TO 50
      X=ABS(REAL(V(1)))+ABS(REAL(V(2)))
      IF(X.GT.EPS2) GO TO 45
      DO 35 J=1,NL2
   35 V(J)=CMPLX(AIMAG(V(J)),0.0)
      GO TO 50
   45 DO 55 J=1,NL2
   55 V(J)=CMPLX(REAL(V(J)),0.0)
   50 RETURN
      END



      SUBROUTINE DARLUN(P,X,Y,NTC)
C
C-----GRAPHICAL DISPLAY INTERFACE ROUTINE
C
      COMMON/SPECS/LAYERS,NLT,NL2,NBAS,CMF,CML,DOM,WL,WC,NDC,NOP,ENC
      DIMENSION SPECS(30),GIVEN(3),P(1),X(1),Y(1),BUFX(500),BUFY(500)
C
C-----LAYOUT SPECIFICATIONS
C
      SPECS(1)=1.5
      SPECS(2)=1.0
      SPECS(7)=9.25
      SPECS(8)=5.75
      SPECS(11)=1.0
      SPECS(12)=99.0
      I=1
      GIVEN(1)=0.0
      GIVEN(2)=0.0
      DO 10 N=1,NDC
   15 IF(P(I).EQ.ENC) GO TO 10
      IF(P(I+1).GT.GIVEN(1)) GIVEN(1)=P(I+1)
      IF(P(I+1).LT.GIVEN(2)) GIVEN(2)=P(I+1)
      I=I+2
      GO TO 15
   10 I=I+1
      GIVEN(3)=9.0
      CALL FABLIX(GIVEN,SPECS)
      GIVEN(1)=AMAX1(CMF,CML)
      GIVEN(2)=AMIN1(CMF,CML)
      GIVEN(3)=10.0
      CALL FABLIY(GIVEN,SPECS)
      CALL AXLILI(SPECS)
      SPECS(14)=1.0
      SPECS(15)=1.0
      SPECS(17)=0.1
      SPECS(18)=0.1
C
C-----REDUCE COORDINATE DATA TO FORM SUITABLE FOR PLOTING
C
      I=1
      DO 40 N=1,NDC
      K=1
   20 IF(P(I).EQ.ENC) GO TO 30
      X(K)=P(I+1)
      IF(ABS(X(K)).LT.1.0E-10) X(K)=0.0
      Y(K)=P(I)
      I=I+2
      K=K+1
      GO TO 20
   30 SPECS(13)=K-1
      I=I+1
      SPECS(16)=FLOAT(N)
      IF(NTC.EQ.0) GO TO 35
C
C-----PARABOLIC CURVE FITTING
C
      CALL PSLILI(X,Y,SPECS)
      GO TO 40
   35 CALL PFLILI(X,Y,BUFX,BUFY,SPECS)
C
C-----CONSTRUCT AXES ETC.
C
   40 SPECS(13)=2.0
      X(1)=SPECS(3)
      Y(1)=SPECS(5)
      X(2)=SPECS(4)
      Y(2)=SPECS(5)
      CALL SLLILI(X,Y,SPECS)
      X(2)=SPECS(3)
      Y(1)=SPECS(5)
      Y(2)=SPECS(6)
      CALL SLLILI(X,Y,SPECS)
      X(1)=0.0
      X(2)=0.0
      Y(2)=0.0
      CALL SLLILI(X,Y,SPECS)
      SPECS(19)=0.0
      SPECS(21)=1.0
      SPECS(24)=0.1
```

```
      SPECS(29)=2.0                                                     1084
C                                                                       1085
C-----AXIS NOTATION                                                     1086
C                                                                       1087
      CALL NOSLIB(SPECS)                                                1088
      SPECS(20)=90.                                                     1089
      SPECS(26)=0.1                                                     1090
      SPECS(28)=1.0                                                     1091
      CALL NOSLIL(SPECS)                                                1092
C                                                                       1093
C-----TITLES                                                            1094
C                                                                       1095
      SPECS(17)=0.2                                                     1096
      SPECS(18)=0.15                                                    1097
      SPECS(19)=0.1                                                     1098
      SPECS(25)=0.1                                                     1099
      SPECS(26)=0.2                                                     1100
      CALL TITLET(17HDISPERSION CURVES,SPECS)                           1101
      SPECS(17)=0.15                                                    1102
      SPECS(18)=0.15                                                    1103
      SPECS(19)=0.0                                                     1104
      CALL TITLEL(9HFREQUENCY,SPECS)                                    1105
      CALL TITLEB(11HWAVE NUMBER,SPECS)                                 1106
      CALL GOSEND(SPECS)                                                1107
      RETURN                                                            1108
      END                                                               1109
```

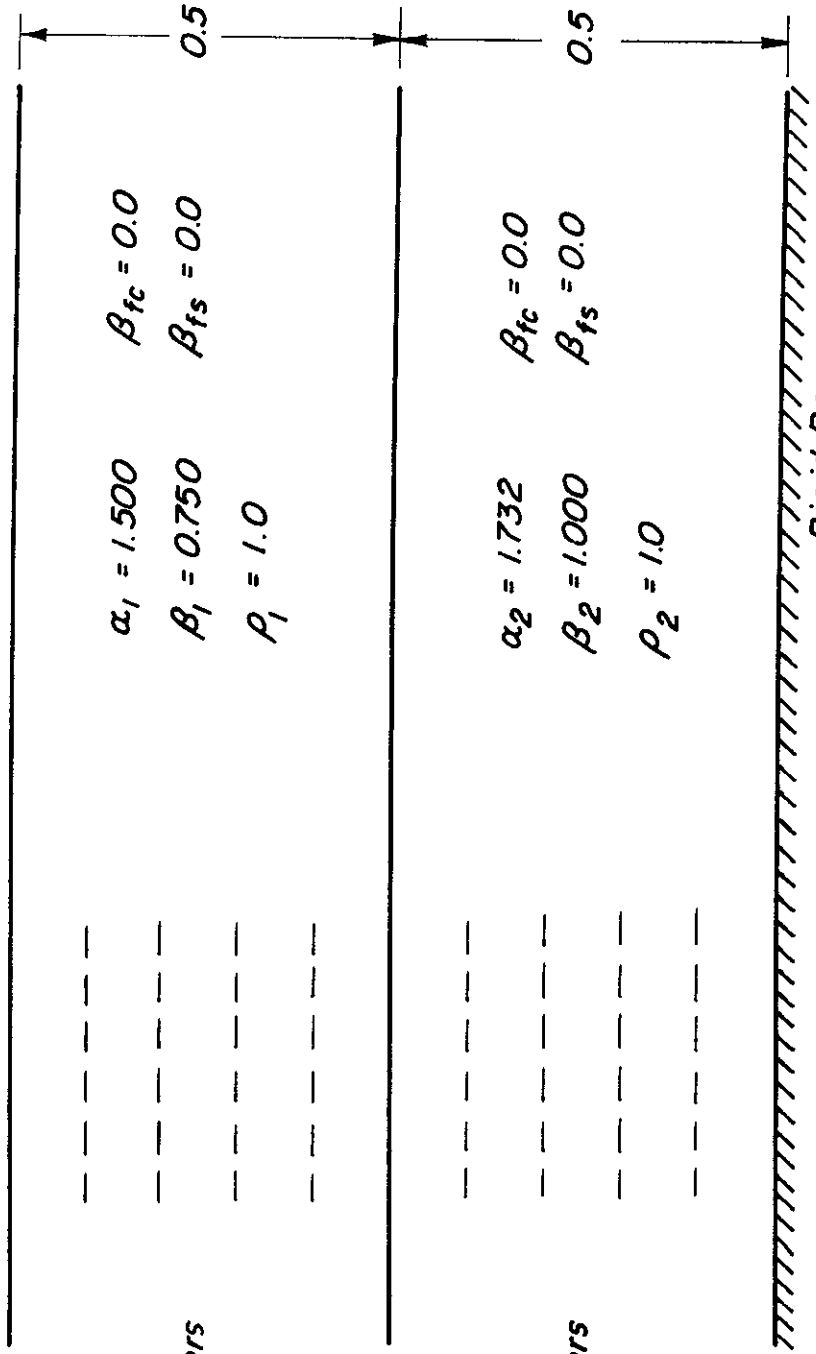

Fig. A5.2 SAMPLE PROBLEM FOR PROGRAM SPRDSP

	Column No.							
1	10	20	30	40	50	60	70	80
	2	10	0	0	1	0	0	
	0.0	100.0						
	1.0	10.0	10.0	2				
	5	0.5	0.75	1.732	0.0	0.0	1.0	
	5	0.5	1.0	1.5	0.0	0.0	1.0	

Total of 5 cards

Fig. A5.3 INPUT FOR SAMPLE PROBLEM FOR PROGRAM SPRDSP

FIG. A5.4

SAMPLE OUTPUT FROM PROGRAM SPRDSP

(The next eight pages form Fig. A5.4)

DISPERSION CURVES FOR GENERALIZED RAYLEIGH WAVES IN A MULTILAYERED SYSTEM WITH VISCOUS DAMPING

NUMBER OF MAIN LAYERS = 2

TOTAL NUMBER OF SUBLAYERS = 10

LAYER NO.	DEPTH	VS	VP	BS	BP	RHO	SHEAR MODULUS REAL	SHEAR MODULUS IMAGINARY	LAMES CONSTANT REAL	LAMES CONSTANT IMAGINARY
1	.1000E+00	.7500E+00	.1500E+01	0.	0.	.1000E+01	.5625E+00	0.	.1125E+01	0.
2	.1000E+00	.7500E+00	.1500E+01	0.	0.	.1000E+01	.5625E+00	0.	.1125E+01	0.
3	.1000E+00	.7500E+00	.1500E+01	0.	0.	.1000E+01	.5625E+00	0.	.1125E+01	0.
4	.1000E+00	.7500E+00	.1500E+01	0.	0.	.1000E+01	.5625E+00	0.	.1125E+01	0.
5	.1000E+00	.7500E+00	.1500E+01	0.	0.	.1000E+01	.5625E+00	0.	.1125E+01	0.
6	.1000E+00	.1000E+01	.1732E+01	0.	0.	.1000E+01	.1000E+01	0.	.9998E+00	0.
7	.1000E+00	.1000E+01	.1732E+01	0.	0.	.1000E+01	.1000E+01	0.	.9998E+00	0.
8	.1000E+00	.1000E+01	.1732E+01	0.	0.	.1000E+01	.1000E+01	0.	.9998E+00	0.
9	.1000E+00	.1000E+01	.1732E+01	0.	0.	.1000E+01	.1000E+01	0.	.9998E+00	0.
10	.1000E+00	.1000E+01	.1732E+01	0.	0.	.1000E+01	.1000E+01	0.	.9998E+00	0.

PERCENT LUMPED MASS = 0. PERCENT CONSISTENT MASS =100.00

CHARACTERISTICS OF 20 WAVES GENERATED AT A FREQUENCY OF .10000E+01

	WAVE NUMBER REAL(K)	WAVE NUMBER IMAG.(K)	WAVE LENGTH L	WAVE LENGTH 1/L	PHASE VELOCITY C	PHASE VELOCITY 1/C	DECAY FACTOR	LOGARITHMIC DECREMENT	GROUP VELOCITY REAL(U)	GROUP VELOCITY IMAG.(U)
1	0.	-.78628E+00							-.15935E+00	-.97904E+00
2	-.11824E+01	-.27306E+01	-.53138E+01	-.18819E+00	-.84571E+00	-.11824E+01	.40955E-06	.14510E+02	-.38241E+00	-.24089E+01
3	.11824E+01	-.27306E+01	.53138E+01	.18319E+00	.84571E+00	.11824E+01	.20018E+07	-.14510E+02	.38241E+00	-.24089E+01
4	.26011E+01	-.56351E+01	.24156E+01	.41398E+00	.38445E+00	.26011E+01	.81586E+06	-.13612E+02	-.23023E-01	-.62024E+01
5	-.26011E+01	-.56351E+01	-.24156E+01	-.41398E+00	-.38445E+00	-.26011E+01	.12257E-05	.13612E+02	.23023E-01	-.62024E+01
6	0.	-.81485E+01							-.15935E+00	-.97904E+00
7	-.21577E+01	-.11645E+02	-.29120E+01	-.34341E+00	-.46345E+00	-.21577E+01	.19745E-14	.33910E+02	.13200E+01	-.11537E+02
8	.21577E+01	-.11645E+02	.29120E+01	.34341E+00	.46345E+00	.21577E+01	.53349E+15	-.33910E+02	-.13200E+01	-.11537E+02
9	.27074E+01	-.13183E+02	.23207E+01	.43090E+00	.36935E+00	.27074E+01	.19337E+14	-.30593E+02	.91269E+00	-.14599E+02
10	-.27074E+01	-.13183E+02	-.23207E+01	-.43090E+00	-.36935E+00	-.27074E+01	.51715E-13	.30593E+02	-.91269E+00	-.14599E+02
11	0.	-.14785E+02							-.15935E+00	-.97904E+00
12	0.	-.16816E+02							-.15935E+00	-.97904E+00
13	0.	-.17582E+02							-.15935E+00	-.97904E+00
14	0.	-.19238E+02							-.15935E+00	-.97904E+00
15	0.	-.20972E+02							-.15935E+00	-.97904E+00
16	0.	-.27393E+02							-.15935E+00	-.97904E+00
17	0.	-.38289E+02							-.15935E+00	-.97904E+00
18	0.	-.47009E+02							-.15935E+00	-.97904E+00
19	0.	-.56101E+02							-.15935E+00	-.97904E+00
20	0.	-.64983E+02							-.15935E+00	-.97904E+00

DISPLACEMENT VECTORS

CURVE NO. 1

	VERTICAL			HORIZONTAL		
OM = .10000E+01 K = 0. -.78528E+00						
1	.13251E+00 0.	2	.93114E-01 0.	1	-.10134E+01 0.	2 -.98630E+00 0.
3	.55717E-01 0.	4	.22414E-01 0.	3	-.82654E+00 0.	4 -.83596E+00 0.
5	-.48557E-02 0.	6	-.24369E-01 0.	5	-.71719E+00 0.	6 -.57362E+00 0.
7	-.31392E-01 0.	8	-.33023E-01 0.	7	-.48038E+00 0.	8 -.37416E+00 0.
9	-.28629E-01 0.	10	-.17729E-01 0.	9	-.25710E+00 0.	10 -.13154E+00 0.
OM = .12250E+01 K = -.11215E-27 -.59271E+00						
1	-.13513E+00 0.	2	-.95471E-01 0.	1	.13466E+01 0.	2 .13150E+01 0.
3	-.57523E-01 0.	4	-.23576E-01 0.	3	.12369E+01 0.	4 .11152E+01 0.
5	.42639E-02 0.	6	.24144E-01 0.	5	.95381E+00 0.	6 .75805E+00 0.
7	.31283E-01 0.	8	.32923E-01 0.	7	.63141E+00 0.	8 .49922E+00 0.
9	.28499E-01 0.	10	.17604E-01 0.	9	.33442E+00 0.	10 .17022E+00 0.
OM = .24190E+01 K = .14358E+01 -.38963E-44						
1	0. .21758E+00	2	0. .17660E+00	1	-.52875E+00 0.	2 -.54540E+00 0.
3	0. .13177E+00	4	0. .87303E-01	3	-.53192E+00 0.	4 -.48785E+00 0.
5	0. .47282E-01	6	0. .15385E-01	5	-.41517E+00 0.	6 -.31813E+00 0.
7	0. -.47278E-04	8	0. -.94914E-02	7	-.25680E+00 0.	8 -.19275E+00 0.
9	0. -.12643E-01	10	0. -.94261E-02	9	-.12754E+00 0.	10 -.62756E-01 0.
OM = .30640E+01 K = .20180E+01 -.10315E-31						
1	0. -.75828E-01	2	0. -.31215E-01	1	.43191E+00 0.	2 .43284E+00 0.
3	0. .12378E-01	4	0. .49486E-01	3	.40536E+00 0.	4 .35184E+00 0.
5	0. .75441E-01	6	0. .86951E-01	5	.27785E+00 0.	6 .19140E+00 0.
7	0. .83596E-01	8	0. .71799E-01	7	.13601E+00 0.	8 .87564E-01 0.
9	0. .52321E-01	10	0. .28265E-01	9	.47842E-01 0.	10 .15307E-01 0.
OM = .37189E+01 K = .26150E+01 .95518E-30						
1	0. .11697E+00	2	0. .70977E-01	1	-.32171E+00 0.	2 -.33879E+00 0.
3	0. .21286E-01	4	0. -.24388E-01	3	-.32758E+00 0.	4 -.28789E+00 0.
5	0. -.58962E-01	6	0. -.77196E-01	5	-.22458E+00 0.	6 -.14671E+00 0.
7	0. -.77021E-01	8	0. -.67010E-01	7	-.95776E-01 0.	8 -.54009E-01 0.
9	0. -.49146E-01	10	0. -.25884E-01	9	-.23264E-01 0.	10 -.49665E-02 0.
OM = .43539E+01 K = .32139E+01 .22415E-30						
1	0. .13247E+00	2	0. .85310E-01	1	-.24993E+00 0.	2 -.27966E+00 0.
3	0. .29543E-01	4	0. -.24276E-01	3	-.28071E+00 0.	4 -.24986E+00 0.
5	0. -.66237E-01	6	0. -.88368E-01	5	-.19150E+00 0.	6 -.11668E+00 0.
7	0. -.88088E-01	8	0. -.75625E-01	7	-.65270E-01 0.	8 -.26053E-01 0.
9	0. -.54162E-01	10	0. -.27537E-01	9	-.11602E-02 0.	10 .78206E-02 0.

OM = .49391E+01 K = .38095E+01 .16800E-28

1	0.	.14227E+00	2	0.	.95166E-01	1	-.19157E+00	0.	2	-.23394E+00	0.
3	0.	.33347E-01	4	0.	-.29677E-01	3	-.24772E+00	0.	4	-.22565E+00	0.
5	0.	-.79791E-01	6	0.	-.10618E+00	5	-.17125E+00	0.	6	-.97824E-01	0.
7	0.	-.10525E+00	8	0.	-.89052E-01	7	-.43368E-01	0.	8	-.42258E-02	0.
9	0.	-.62292E-01	10	0.	-.30562E-01	9	.17181E-01	0.	10	.18970E-01	0.

OM = .61172E+01 K = .52301E+01 -.12716E-28

1	0.	-.14099E+00	2	0.	-.10156E+00	1	.78639E-01	0.	2	.14290E+00	0.
3	0.	-.32493E-01	4	0.	.46626E-01	3	.18151E+00	0.	4	.17877E+00	0.
5	0.	.11249E+00	6	0.	.14684E+00	5	.13611E+00	0.	6	.71644E-01	0.
7	0.	.14359E+00	8	0.	.11824E+00	7	.11348E-01	0.	8	-.28061E-01	0.
9	0.	.79342E-01	10	0.	.36430E-01	9	-.44409E-01	0.	10	-.35950E-01	0.

OM = .82445E+01 K = .81533E+01 -.18554E-28

1	0.	-.91619E-01	2	0.	-.68499E-01	1	-.18616E-02	0.	2	.57586E-01	0.
3	0.	-.80764E-02	4	0.	.63506E-01	3	.92462E-01	0.	4	.91321E-01	0.
5	0.	.11760E+00	6	0.	.13820E+00	5	.62192E-01	0.	6	.31574E-01	0.
7	0.	.12683E+00	8	0.	.97680E-01	7	-.11481E-01	0.	8	-.31559E-01	0.
9	0.	.61295E-01	10	0.	.25777E-01	9	-.36344E-01	0.	10	-.27241E-01	0.

OM = .98858E+01 K = .10327E+02 -.26377E-32

1	0.	-.78254E-01	2	0.	-.56570E-01	1	-.11654E-01	0.	2	.44495E-01	0.
3	0.	.54634E-02	4	0.	.72824E-01	3	.70948E-01	0.	4	.61004E-01	0.
5	0.	.11289E+00	6	0.	.11654E+00	5	.30033E-01	0.	6	.13254E-01	0.
7	0.	.98243E-01	8	0.	.70013E-01	7	-.15734E-01	0.	8	-.23940E-01	0.
9	0.	.41285E-01	10	0.	.16383E-01	9	-.23213E-01	0.	10	-.16445E-01	0.

OM = .10000E+02 K = .10478E+02 .92544E-28

1	0.	.77889E-01	2	0.	.56131E-01	1	.12035E-01	0.	2	-.44107E-01	0.
3	0.	-.62842E-02	4	0.	-.73549E-01	3	-.70091E-01	0.	4	-.59516E-01	0.
5	0.	-.11268E+00	6	0.	-.11510E+00	5	-.28269E-01	0.	6	-.12211E-01	0.
7	0.	-.96328E-01	8	0.	-.68198E-01	7	.15889E-01	0.	8	.23428E-01	0.
9	0.	-.40309E-01	10	0.	-.15809E-01	9	.22422E-01	0.	10	.15804E-01	0.

CURVE NO. 2

OM = .10000E+01 K = -.11824E+01 -.27306E+01

1	.28943E+00	.76944E-01	2	.29252E+00	.10752E+00	1	-.93923E-01	.22546E+00	2	-.17688E-01	.13770E+00
3	.29581E+00	.12402E+00	4	.29027E+00	.12369E+00	3	.28440E-01	.11491E+00	4	.41565E-01	.25893E-01
5	.26888E+00	.10766E+00	6	.22749E+00	.79759E-01	5	.24535E-01	-.62376E-01	6	-.15862E-01	-.13656E+00
7	.18559E+00	.55504E-01	8	.13828E+00	.30750E-01	7	-.10163E-01	-.16388E+00	8	-.18415E-02	-.16533E+00
9	.89599E-01	.99847E-02	10	.42895E-01	-.18509E-02	9	.63279E-02	-.13745E+00	10	.92474E-02	-.80713E-01

OM = .19000E+01 K = -.12440E+01 -.21218E+01

1	.39859E+00	.93637E-01	2	.39807E+00	.12347E+00	1	-.14813E+00	.26028E+00	2	-.61195E-01	.20550E+00
3	.39181E+00	.13722E+00	4	.37326E+00	.13312E+00	3	.14534E-02	.11568E+00	4	.34691E-01	.12145E-01
5	.33785E+00	.11316E+00	6	.28350E+00	.62274E-01	5	.38061E-01	-.85105E-01	6	.14433E-01	-.15986E+00

```
7   .23223E+00  .56762E-01     8   .17490E+00  .31454E-01      7   .24094E-01 -.19836E+00     8   .30511E-01 -.18752E+00
9   .11511E+00  .10601E-01    10   .56092E-01 -.13035E-02      9   .31491E-01 -.15449E+00    10   .23099E-01 -.90274E-01

OM =  .22496E+01  K = -.12403E+01 -.16591E+01

1   .53876E+00  .12180E+00     2   .53534E+00  .15130E+00      1  -.20648E+00  .29747E+00     2  -.10784E+00  .22360E+00
3   .51962E+00  .16306E+00     4   .48704E+00  .15576E+00      3  -.27111E-01  .11887E+00     4   .27525E-01  .84756E-03
5   .43499E+00  .13190E+00     6   .36309E+00  .96959E-01      5   .51741E-01 -.10587E+00     6   .44334E-01 -.18253E+00
7   .29805E+00  .68540E-01     8   .22583E+00  .40414E-01      7   .58936E-01 -.21264E+00     8   .64340E-01 -.20998E+00
9   .14999E+00  .16777E-01    10   .73860E-01  .19545E-02      9   .58522E-01 -.17207E+00    10   .38383E-01 -.10028E+00

OM =  .38156E+01  K =  .14601E-36 -.63762E+00

1   .24781E+00 0.               2   .21265E+00 0.           1  -.96332E+00 0.              2  -.82473E+00 0.
3   .17520E+00 0.               4   .14568E+00 0.           3  -.47586E+00 0.              4  -.79466E-02 0.
5   .12877E+00 0.               6   .12262E+00 0.           5   .45781E+00 0.              6   .80104E+00 0.
7   .11759E+00 0.               8   .10714E+00 0.           7   .87852E+00 0.              8   .81997E+00 0.
9   .86224E-01 0.              10   .51050E-01 0.           9   .63341E+00 0.             10   .34598E+00 0.

OM =  .49523E+01  K =  .18318E+01 -.35067E-32

1  0.           .14482E+00     2  0.           .11108E+00   1  -.31679E+00 0.              2  -.28771E+00 0.
3  0.           .77065E-01     4  0.           .56945E-01   3  -.15824E+00 0.              4   .30862E-01 0.
5  0.           .56506E-01     6  0.           .71104E-01   5   .21647E+00 0.              6   .33618E+00 0.
7  0.           .81010E-01     8  0.           .83161E-01   7   .34411E+00 0.              8   .30129E+00 0.
9  0.           .71874E-01    10  0.           .44038E-01   9   .21757E+00 0.             10   .11013E+00 0.

OM =  .55418E+01  K =  .24655E+01 -.33916E-30

1  0.           .11391E+00     2  0.           .79095E-01   1  -.24802E+00 0.              2  -.22675E+00 0.
3  0.           .46798E-01     4  0.           .33424E-01   3  -.11648E+00 0.              4   .43443E-01 0.
5  0.           .44016E-01     6  0.           .70088E-01   5   .19182E+00 0.              6   .27200E+00 0.
7  0.           .85746E-01     8  0.           .89942E-01   7   .26259E+00 0.              8   .21629E+00 0.
9  0.           .77366E-01    10  0.           .46466E-01   9   .14558E+00 0.             10   .67578E-01 0.

OM =  .61591E+01  K =  .31218E+01 -.23859E-31

1  0.          -.84761E-01     2  0.          -.44028E-01   1   .24806E+00 0.              2   .22141E+00 0.
3  0.          -.13693E-01     4  0.          -.13304E-01   3   .10285E+00 0.              4  -.57399E-01 0.
5  0.          -.44331E-01     6  0.          -.89320E-01   5  -.18835E+00 0.              6  -.23415E+00 0.
7  0.          -.11207E+00     8  0.          -.11518E+00   7  -.20153E+00 0.              8  -.14368E+00 0.
9  0.          -.95052E-01    10  0.          -.54060E-01   9  -.78740E-01 0.             10  -.25855E-01 0.

OM =  .67952E+01  K =  .39212E+01 -.91557E-30

1  0.           .62959E-01     2  0.           .84660E-02   1  -.28554E+00 0.              2  -.25000E+00 0.
3  0.          -.23112E-01     4  0.          -.79018E-02   3  -.11577E+00 0.              4   .50816E-01 0.
5  0.           .48946E-01     6  0.           .11608E+00   5   .16631E+00 0.              6   .17820E+00 0.
7  0.           .14507E+00     8  0.           .14340E+00   7   .12127E+00 0.              8   .53573E-01 0.
9  0.           .11154E+00    10  0.           .58668E-01   9  -.10120E-02 0.             10  -.22377E-01 0.

OM =  .73841E+01  K =  .47150E+01 -.23341E-31

1  0.           .72029E-01     2  0.           .10405E-01   1  -.25570E+00 0.              2  -.23610E+00 0.
3  0.          -.30869E-01     4  0.          -.23089E-01   3  -.12603E+00 0.              4   .17365E-01 0.
5  0.           .30475E-01     6  0.           .96637E-01   5   .11658E+00 0.              6   .12302E+00 0.
```

7	0.	.12549E+00	8	0.	.12416E+00	7	.70479E-01	0.	8	.13444E-01	0.
9	0.	.94641E-01	10	0.	.47755E-01	9	-.27075E-01	0.	10	-.34186E-01	0.

OM = .79887E+01 K = .54638E+01 -.13686E-31

1	0.	-.88350E-01	2	0.	-.23507E-01	1	.21076E+00	0.	2	.21216E+00	0.
3	0.	.29308E-01	4	0.	.35800E-01	3	.12856E+00	0.	4	.35780E-02	0.
5	0.	-.85931E-02	6	0.	-.71541E-01	5	-.89400E-01	0.	6	-.98901E-01	0.
7	0.	-.10126E+00	8	0.	-.10317E+00	7	-.54302E-01	0.	8	-.62497E-02	0.
9	0.	-.79008E-01	10	0.	-.39234E-01	9	.27419E-01	0.	10	.31962E-01	0.

OM = .85586E+01 K = .61428E+01 .20196E-30

1	0.	.10066E+00	2	0.	.34111E-01	1	-.17283E+00	0.	2	-.19190E+00	0.
3	0.	-.29974E-01	4	0.	-.47580E-01	3	-.12748E+00	0.	4	-.12444E-01	0.
5	0.	-.86647E-02	6	0.	.55064E-01	5	.79583E-01	0.	6	.90726E-01	0.
7	0.	.87266E-01	8	0.	.92289E-01	7	.49855E-01	0.	8	.58237E-02	0.
9	0.	.71499E-01	10	0.	.35252E-01	9	-.25340E-01	0.	10	-.29815E-01	0.

OM = .92885E+01 K = .70309E+01 .27388E-30

1	0.	-.11114E+00	2	0.	-.44156E-01	1	.12857E+00	0.	2	.16745E+00	0.
3	0.	.32431E-01	4	0.	.62640E-01	3	.12302E+00	0.	4	.15898E-01	0.
5	0.	.26681E-01	6	0.	-.42095E-01	5	-.77067E-01	0.	6	-.87667E-01	0.
7	0.	-.78646E-01	8	0.	-.86903E-01	7	-.47735E-01	0.	8	-.56873E-02	0.
9	0.	-.68177E-01	10	0.	-.33312E-01	9	.24219E-01	0.	10	.28858E-01	0.

OM = .10000E+02 K = .79523E+01 -.70662E-28

1	0.	-.11502E+00	2	0.	-.49989E-01	1	.89260E-01	0.	2	.14350E+00	0.
3	0.	.36051E-01	4	0.	.75493E-01	3	.11507E+00	0.	4	.14409E-01	0.
5	0.	.39276E-01	6	0.	-.36217E-01	5	-.78264E-01	0.	6	-.85863E-01	0.
7	0.	-.76571E-01	8	0.	-.86458E-01	7	-.44786E-01	0.	8	-.39742E-02	0.
9	0.	-.67944E-01	10	0.	-.32746E-01	9	.24580E-01	0.	10	.28841E-01	0.

COORDINATES OF DISPERSION CURVES

DISPERSION CURVE NO. 1

FREQUENCY	.10000E+01	.12250E+01	.15190E+01	.24190E+01	.30640E+01	.37189E+01	.43539E+01	.49391E+01	.61172E+01
WAVE NUMBER	0.	0.	.28733E+00	.14358E+01	.20180E+01	.26150E+01	.32139E+01	.38095E+01	.52301E+01

FREQUENCY	.82445E+01	.93858E+01	.10100E+02
WAVE NUMBER	.81533E+01	.10327E+02	.10478E+02

DISPERSION CURVE NO. 2

FREQUENCY	.10000E+01	.19000E+01	.22496E+01	.29156E+01	.38156E+01	.40523E+01	.49523E+01	.55419E+01	.61591E+01
WAVE NUMBER	-.11824E+01	-.12440E+01	-.12403E+01	.73579E-27	0.	.45679E+00	.18318E+01	.24655E+01	.31213E+01

FREQUENCY	.67952E+01	.73841E+01	.79387E+01	.85586E+01	.92386E+01	.10000E+02
WAVE NUMBER	.39212E+01	.47150E+01	.54638E+01	.61428E+01	.70309E+01	.79523E+01

CHARACTERISTICS OF 20 WAVES GENERATED AT A FREQUENCY OF .10000E+02

	WAVE NUMBER		WAVE LENGTH		PHASE VELOCITY		DECAY	LOGARITHMIC	GROUP VELOCITY	
	REAL(K)	IMAG.(K)	L	1/L	C	1/C	FACTOR	DECREMENT	REAL(U)	IMAG.(U)
1	.13871E+02	0.	.45298E+00	.22076E+01	.72095E-01	.13871E+02	.10000E+01	0.	.72472E+01	.86811E-14
2	.10478E+02	0.	.59968E+00	.16676E+01	.95442E-01	.10478E+02	.10000E+01	0.	.75652E+01	.84336E-16
3	.79523E+01	0.	.79011E+00	.12656E+01	.12575E+00	.79523E+01	.10000E+01	0.	.74597E+01	-.33260E-25
4	.59076E+01	0.	.10636E+01	.94022E+00	.16927E+00	.59076E+01	.10000E+01	0.	.11518E+02	.40955E-18
5	.40554E+01	0.	.15493E+01	.64544E+00	.24658E+00	.40554E+01	.10000E+01	0.	.73088E+01	-.16195E-16
6	.13545E+01	0.	.46387E+01	.21558E+00	.73827E+00	.13545E+01	.10000E+01	0.	.14107E+01	-.95330E-22
7	0.	-.58441E+01							.67003E+00	.18213E+00
8	0.	-.80909E+01							.67003E+00	.18213E+00
9	.23591E+01	-.98556E+01	.26634E+01	.37546E+00	.42389E+00	.23591E+01	.25115E+12	-.26249E+02	-.47645E+01	-.13775E+02
10	-.23591E+01	-.98556E+01	-.26634E+01	-.37546E+00	-.42389E+00	-.23591E+01	.39817E-11	.26249E+02	.47645E+01	-.13775E+02
11	0.	-.13098E+02							.67003E+00	.18213E+00
12	0.	-.15860E+02							.67003E+00	.18213E+00
13	-.66898E+00	-.17186E+02	-.93922E+01	-.10647E+00	-.14948E+01	-.66898E+00	.79477E-70	.16141E+03	-.11345E+02	-.12170E+02
14	.66898E+00	-.17186E+02	.93922E+01	.10647E+00	.14948E+01	.66898E+00	.12582E+71	-.16141E+03	.11345E+02	-.12170E+02
15	0.	-.18312E+02							.67003E+00	.18213E+00
16	0.	-.25119E+02							.67003E+00	.18213E+00
17	0.	-.36673E+02							.67003E+00	.18213E+00
18	0.	-.45534E+02							.67003E+00	.18213E+00
19	0.	-.54989E+02							.67003E+00	.18213E+00
20	0.	-.63705E+02							.67003E+00	.18213E+00

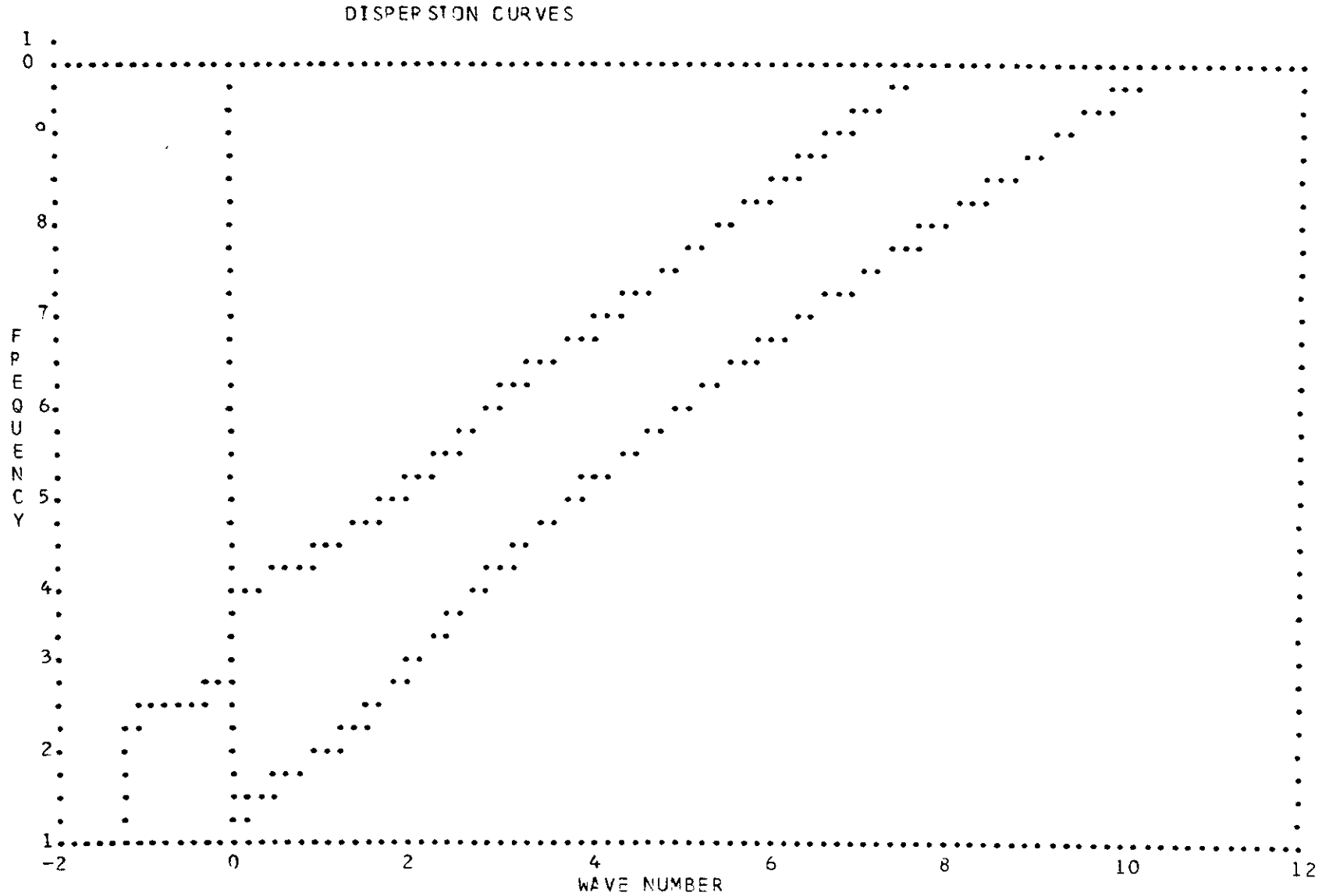
DISPERSION CURVES
FREQUENCY
10
9
8
7
6
5
4
3
2
1
-2
0
2
4
6
8
10
12
WAVE NUMBER

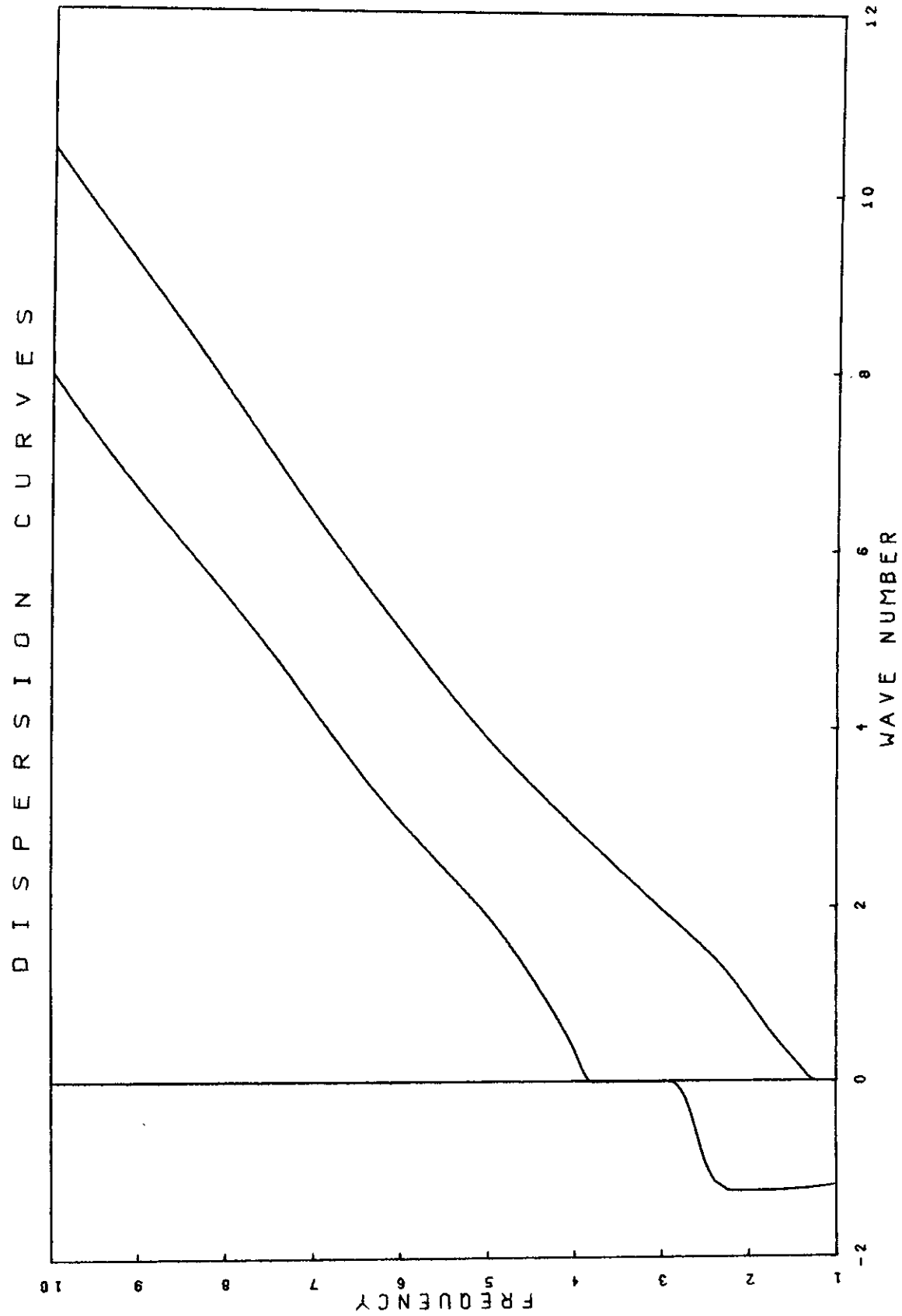
DISPERSION CURVES
FREQUENCY
WAVE NUMBER
1
2
3
4
5
6
7
8
9
10
-2
0
2
4
6
8
10
12

APPENDIX 6

RHEOLOGICAL RESPONSE OF SOILS AND BITUMINOUS CONCRETE SUBJECTED TO DYNAMIC LOADING

Soils, rocks, bituminous concrete and stabilized natural materials are, in general, complex multi-phase systems whose behavior may be dependent upon a large number of environmental factors including: pressure, stress history, loading conditions and temperature. In addition, the theoretical analysis of structures composed of these materials is often difficult, especially if results suitable for practical application are to be obtained. To simplify analysis it has been traditionally assumed that the rheological properties of these materials are elastic. The limitations of this approximation, particularly in situations involving dynamic loading, has encouraged experimental work to determine more realistic descriptions of materials properties. Experience has shown that some form of viscoelastic model, such as the Kelvin-Voigt (Hardin, 1965) or the Maxwell (Freudenthal, 1950) type, can satisfactorily represent these materials. This does not imply that these materials, especially soils, are in fact viscoelastic material, or that they necessarily exhibit internal damping which is the result of viscous behavior. The models are simply convenient tools with which to characterize their empirically observed behavior.

Complex Modulus Representation

If the rheologic behavior of a material can be characterized by a viscoelastic model, its stress strain behavior, when subjected to loads varying harmonically in time, may be represented by complex moduli.

The stress-strain relation under uniaxial conditions may be expressed as

$$\sigma \exp(i\omega t) = E\, \varepsilon \exp(i\omega t) \qquad \text{(A6.1)}$$

where:

$$\sigma = \sigma_1 + i\sigma_2$$
$$\varepsilon = \varepsilon_1 + i\varepsilon_2$$
$$E(\omega) = E_1(\omega) + i\, E_2(\omega)$$

are the complex stress, the complex strain and the complex modulus respectively, ω is the angular frequency and $i = \sqrt{-1}$. The subscript 1 denotes the real component and the subscript 2 the imaginary component. The complex stress and strain may be represented by a pair of vectors rotating at the frequency ω about the origin of the complex plane as shown in Fig. A6.1. At any instant in time, the actual stress and strain are the projections of the vectors onto the real axis. The real component E_1 of the complex modulus is the modulus of strain which is in phase with the stress and its imaginary component E_2 is the modulus of strain which is 90° out of phase with the stress. E_1 is associated with the elastic phenomenon in which stored energy is recoverable and E_2 is associated with the internal damping phenomenon (modeled here as a viscous behavior) in which energy is dissipated.

Due to the internal dissipation of energy the strain vector lags behind the stress vector by an angle ϕ_L, known as the "loss angle" the tangent of which is known as the "loss tangent;" from its association with energy loss. The loss tangent is defined by:

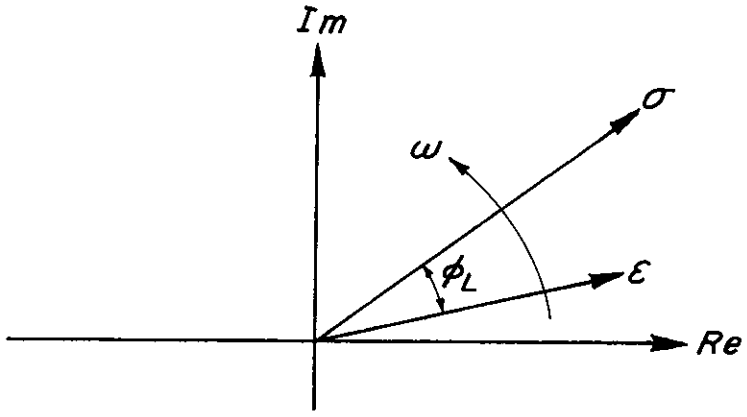

Fig. A 6.1 REPRESENTATION OF STRESS AND STRAIN IN THE COMPLEX PLANE

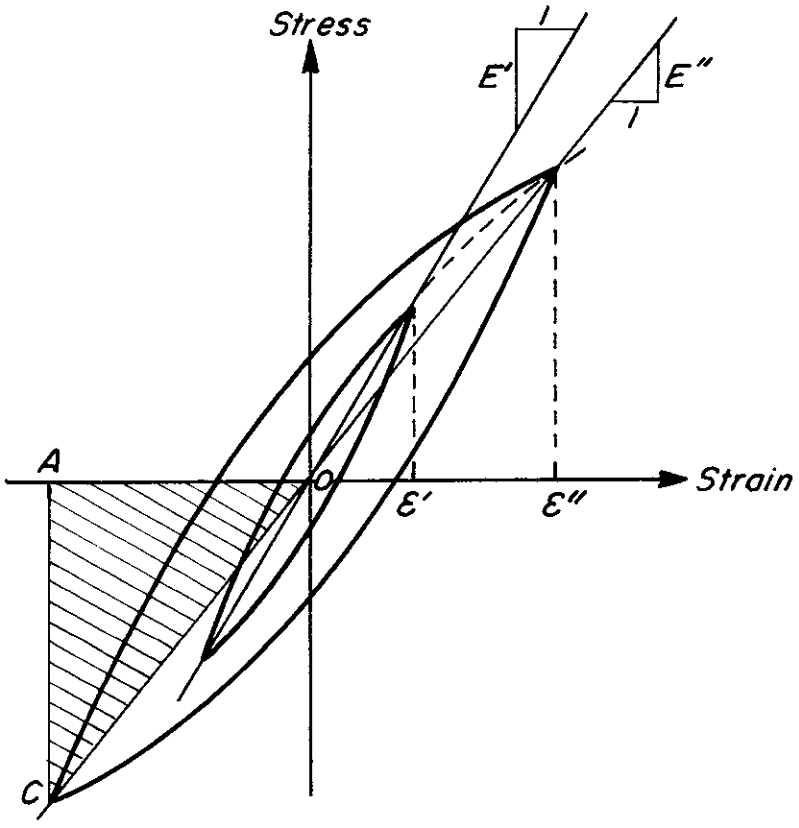

Fig. A 6.2 HYSTERETIC STRESS-STRAIN RELATIONSHIP AT DIFFERENT AMPLITUDES

$$\text{Tan } \phi_L = E_2/E_1 \tag{A6.2}$$

In addition to Young's modulus, E, the complex representation may be employed with any of the other usual moduli. This allows the relationships between the complex moduli of a material, which may be approximated by an isotropic, linearly viscoelastic system, to be defined in a manner analogous to that for elastic materials, e.g.,

$$\lambda = \lambda_1 + i\lambda_2 = \frac{G(E - 2G)}{(3G - E)} \tag{A6.3}$$

and

$$\nu = \nu_1 + i\nu_2 = \frac{E}{2G} - 1 \tag{A6.4}$$

in which λ is the complex Lame's constant and ν is the complex Poisson's ratio and the moduli G and E are both in the complex form.

The wave velocities α and β, of P and S-waves respectively, may also be expressed in the complex form:

$$\alpha = \alpha_1 + i\alpha_2 = \sqrt{\frac{\lambda + 2G}{\rho}} \tag{A6.5}$$

$$\beta = \beta_1 + i\beta_2 = \sqrt{\frac{G}{\rho}}\,. \tag{A6.6}$$

If the imaginary components of both λ and G are equal to zero then α_2 and β_2 vanish and Eqs. (A6.5) and (A6.6) define the velocities of propagation of body waves in a linearly elastic media.

Values of the complex moduli E and G are commonly obtained from longitudinal and torsional vibration test on cyclindrical samples and are related to parameters obtained from these tests as follows:

Logarithmic Decrement (Richart, Hall and Woods, 1970),

$$\delta = \ln \left\{ \frac{Z_1}{Z_2} \right\} \tag{A6.7}$$

where Z_1 and Z_2 are successive amplitudes of motion.

For small damping

$$\delta \simeq 2\pi\beta_{fc} \tag{A6.8}$$

where β_{fc} is the fraction of critical damping.

Decay Factor,

$$\text{Decay Factor} = \exp(-\delta) \tag{A6.9}$$

Loss Angle,

$$\text{Tan } \phi_L = \delta/\pi \tag{A6.10}$$

For small damping

$$\text{Tan } \phi_L \simeq 2\beta_{fc} \tag{A6.11}$$

Complex Shear Modulus,

For small damping

$$G = G_1 (1 + 2i\beta_{fc}) \tag{A6.12}$$

Specific Damping Capacity (Richart, Hall and Woods, 1970),

$$\Delta_{cd} = \frac{\text{Energy absorbed in one cycle}}{\text{Potential energy at maximum strain}} \tag{A6.13}$$

By reference to Fig. A6.12,

$$\Delta_{cd} = \frac{\text{Area enclosed within hysteresis loop}}{\text{Area } \Delta AOC} \qquad \text{(A6.14)}$$

Hysteretic Damping or Damping Ratio (Jacobson, 1930),

$$\lambda_d = \Delta_{cd}/4\pi \qquad \text{(A6.15)}$$

For small damping

$$\lambda_d \simeq \beta_{fc}/\pi \ . \qquad \text{(A6.16)}$$

Attenuation

It is important to note that an attenuation of an amplitude of motion is not necessarily due to internal damping. There are three possible reasons for attenuation.

1. Geometric Attenuation

   This results from the dissipation of energy away from a localized source into a body. With increasing distance from the source the energy density is reduced as more volume becomes involved in the excitation.

2. Internal Damping

   Due to conversion of transmitted energy from a potential or kinetic form into some other form. Energy is usually dissipated by conversion into heat energy.

3. Interference Attenuation

   In certain circumstances wave modes may interact in such a way as to produce a surface wave which attenuates with increasing distance from the source. No energy is lost in this case.

In all practical situations internal damping is present to some degree so that attenuation will always be observed.

Dynamic Soil Properties

The stress-strain relationships of most soils subjected to symmetric cyclic loading are curvilinear as shown in Fig. A6.2. This behavior is represented by the secant modulus, which is determined by the extreme points on the hysteresis loop, and the damping factor, which is proportional to the area inside the loop. If complex moduli are used to define the behavior then the actual hystersis loop is approximated by an elliptical loop enclosing an area equal to that of the actual loop and with a principal axis of the same slope. Thus the secant modulus of the type illustrated in Fig. A6.2 is equivalent in the real component of the corresponding complex modulus.

A study of the factors affecting the shear moduli and damping factors of soils was undertaken by Hardin and Drnevich (1970). They suggested that the following factors are of primary importance:

Strain amplitude

Effective mean principal stress

Void ratio

Number of cycles of loading

Degree of saturation of cohesive soils

and that the following are less important factors:

Octahedral shear stress

Overconsolidation ratio

Effective stress strength parameters

Time effects

The interrelationship of the parameters is very complex and presents

a difficult problem if definitive and comprehensive expressions are sought to describe the behavior of soils subjected to dynamic loading. Laboratory programs have been conducted using forced and free longitudinal, tortional, shear and triaxial compression vibratory testing. All investigations have shown that the modulus values and damping factors for soils are strongly influenced by the strain amplitude. While many of the other factors listed above, especially confining pressure and void ratio, are of great importance in laboratory studies, in-situ vibratory testing in the field has the advantage that the need to account for the influence of a majority of these parameters is eliminated. The effects of sample disturbance is also eliminated. This fact is of major importance when saturated clays are involved.

However, in many applications, the strain amplitudes induced by vibratory testing are very much smaller than those generated by the loads to which the structure is subjected during use. Thus, results from vibratory in-situ tests can be expected to yield higher values of moduli and indicate less damping than would be appropriate for use in the functional evaluation of structures.

Some typical strain ranges are given in Table A6.1.

Table A6.1
Strains Induced by Various Dynamic Loads

Loading Condition	Approximate Strain Range
Laboratory tests to determine hysteretic stress-strain relationships	10^{-2} to 5%
Laboratory forced vibration tests	10^{-4} to 10^{-2}%
Laboratory free vibration tests	10^{-3} to 1%
Vibratory field tests	$\simeq 5 \times 10^{-4}$%
Highway structures subjected to traffic load	10^{-3} to 10^{-1}%

Seed and Idriss (1970) have made a comprehensive review of data available from a wide variety of dynamic tests on soils and have proposed a method by which the moduli and damping properties obtained from in-situ vibratory tests may be used to obtain similar properties for the description of behavior at strain amplitudes greater than those induced by the test. Fig. A6.3 shows the variation with shear strain of the ratio of shear modulus at strain γ to shear modulus at a shear strain of 10^{-4}%. As the results fall within a relatively narrow band a reasonable approximation to the modulus versus shear strain relationship for any sand may be obtained by determining the modulus at a very low strain level, such as by wave propagation methods in the field, and then reducing this value for other strain levels in accordance with the average (full) line in Fig. A6.3.

A similar method may be used in the case of damping. Fig. A6.4 shows the result of Seed and Idriss, (1970) study of data relating damping ratios to shear strain for sands.

Information about the dynamic response (particularly the damping) of soils other than sand is severely limited. Data gathered for saturated clays by Seed and Idriss (1970) are summarized in Figs. A6.5 and A6.6. It seems likely that moduli and damping factors for gravelly soil will decrease, with increasing strain amplitude, in a manner similar to that for sands. While further data is lacking, it is suggested that moduli obtained from a test on gravelly soils may be modified to approximate values at other strain amplitudes by extrapolation in accordance with the method proposed for sands.

The fraction of critical damping observed for soils subjected to many practical loading situations (e.g., soils beneath foundations of

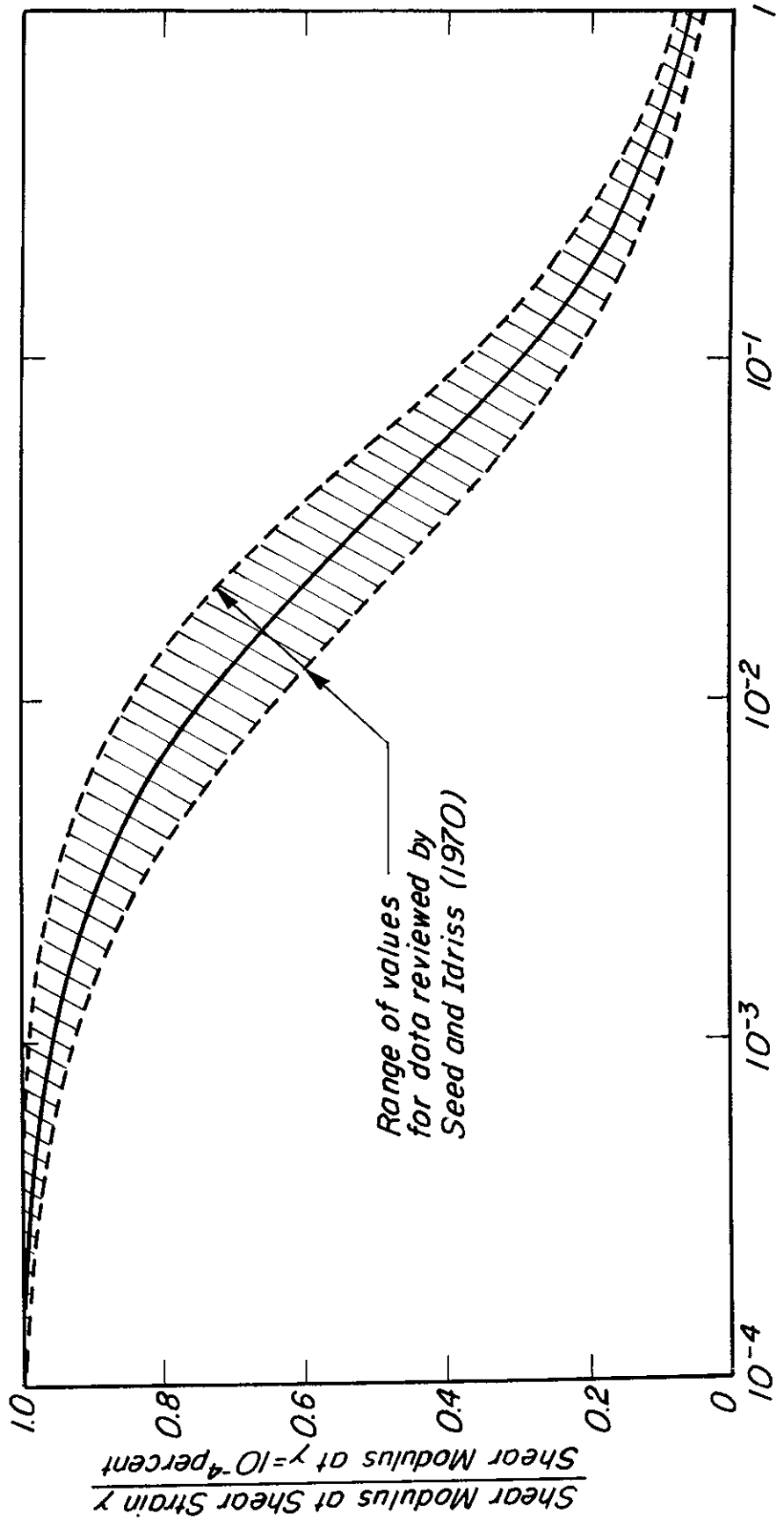

Fig. A6.3 VARIATION OF SHEAR MODULUS WITH SHEAR STRAIN FOR SANDS

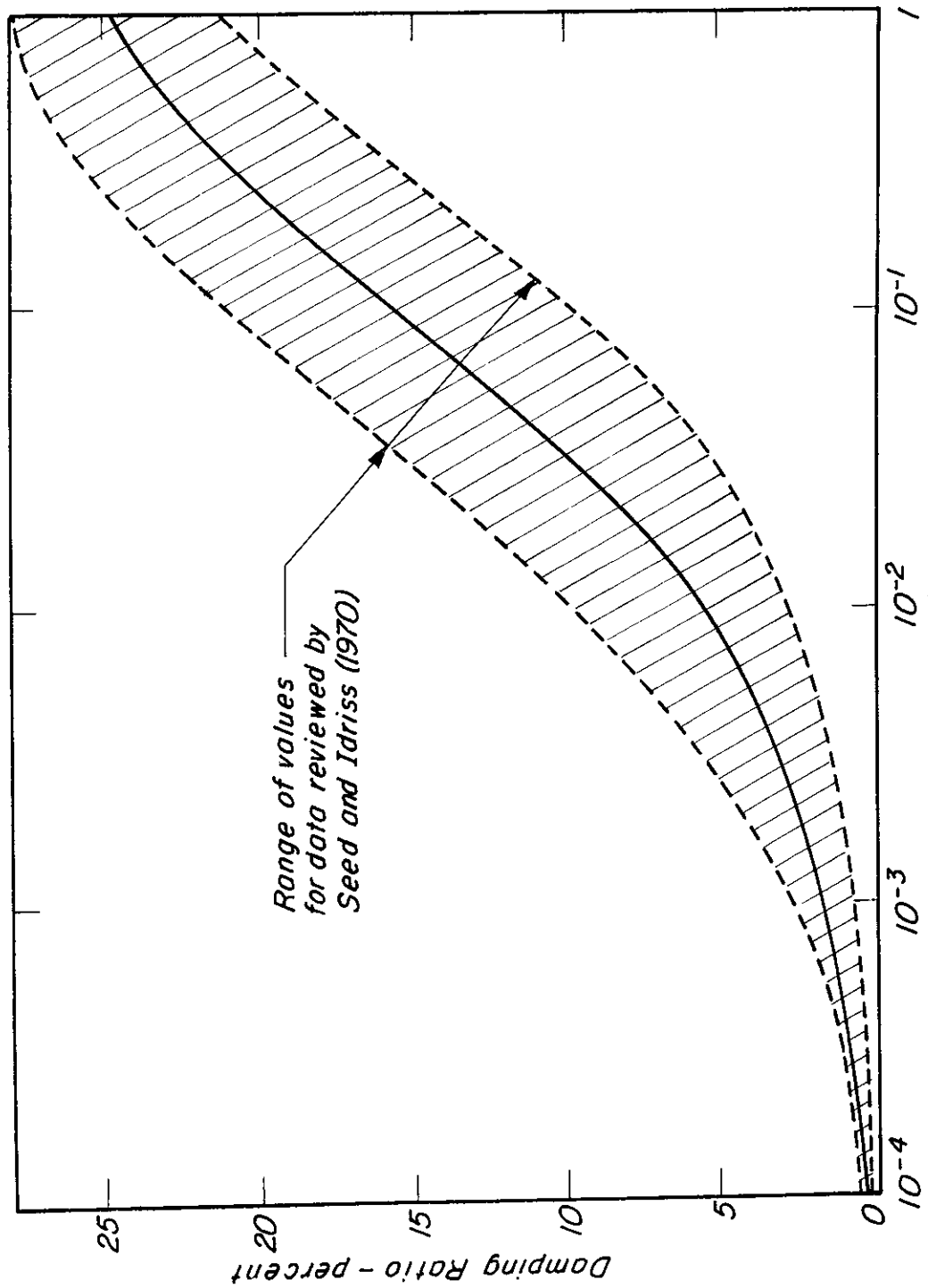

Fig. A 6.4 DAMPING RATIOS FOR SANDS

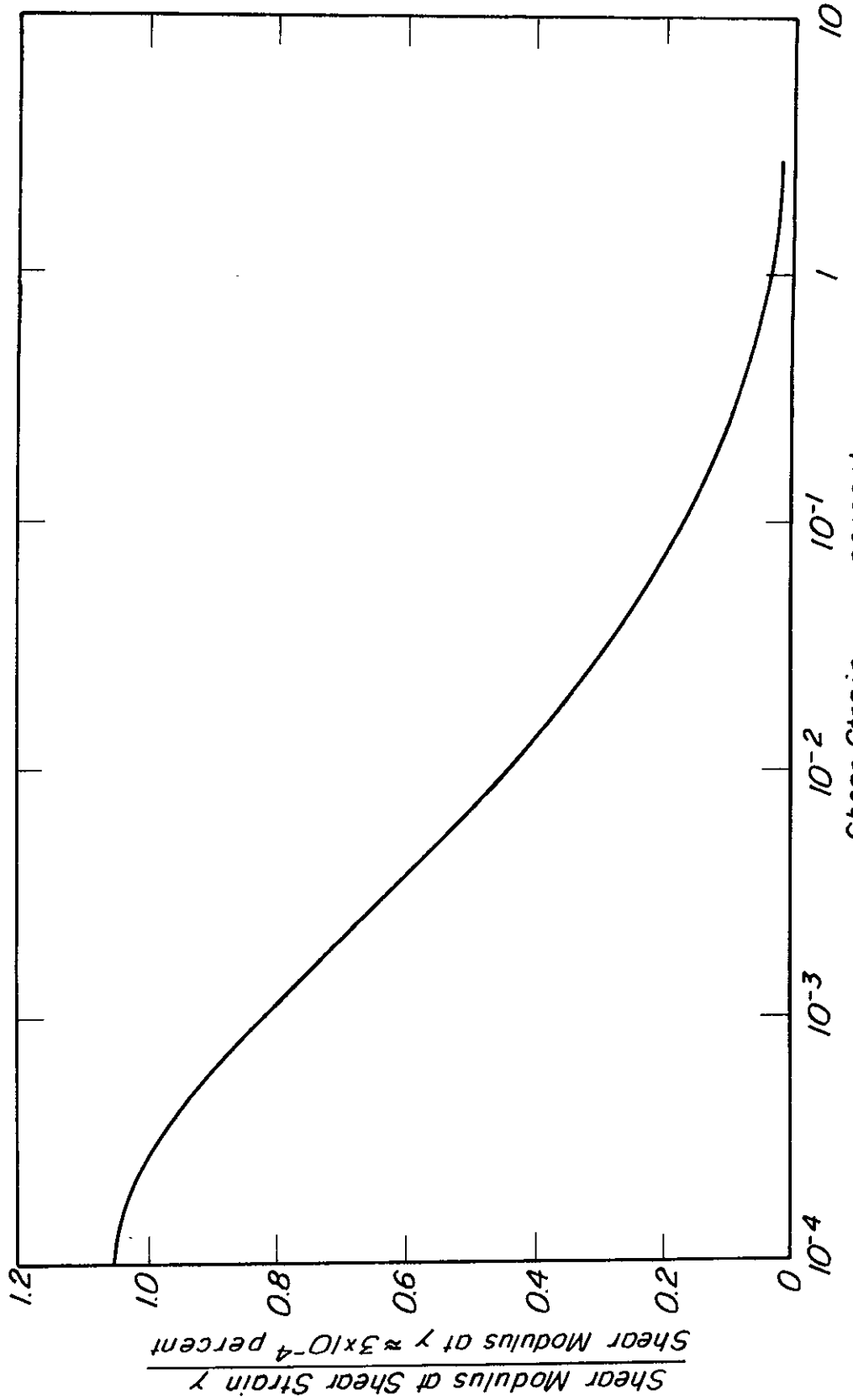

Fig. A 6.5 TYPICAL REDUCTION OF SHEAR MODULUS WITH SHEAR STRAIN FOR SATURATED CLAYS

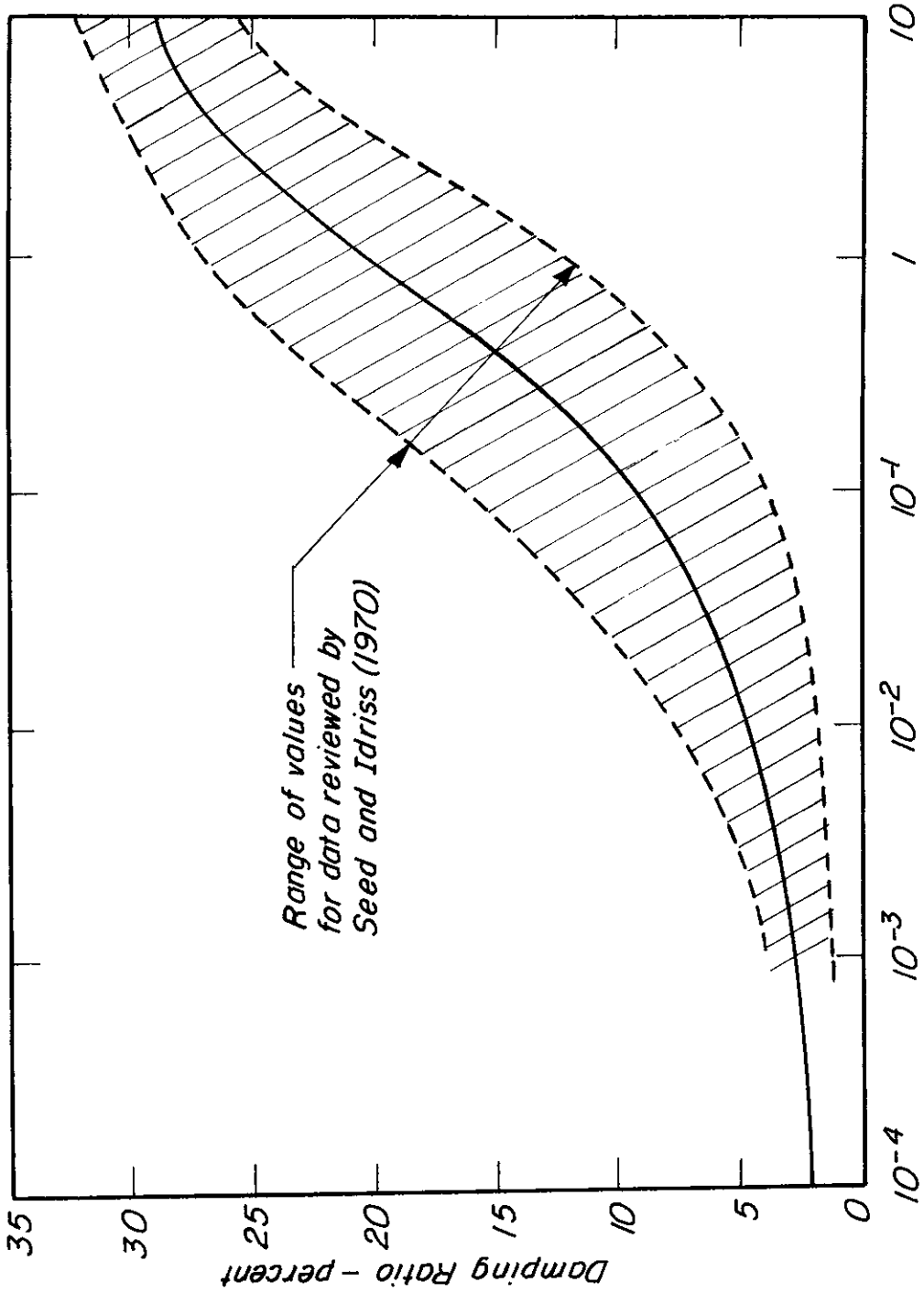

Fig. A 6.6 DAMPING RATIOS FOR SATURATED CLAYS

vibratory machines) is very small. Values for shear deformations may typically vary from 2 to 5% and for compressional deformations are even less. Therefore, the use of viscoelastic theory for analysis may be considered unwarranted, especially as determination of the scant modulus may involve errors of the order 10 to 20%. However, the convenient method of complex moduli provides a simple means to provide a more realistic model and the inclusion of damping eliminates certain singularities which may occur in the analysis.

Rheologic Response of Bituminous Concrete

The rheologic behavior of bituminous concrete is also complex and it exhibits particular sensitivity to duration of loading, frequency of loading and temperature. Material properties obtained in the field by wave propagation methods again have the advantage that the need to consider the influence of a majority of the variables is eliminated. There remain, however, three major areas which must be accounted for when applying the results obtained from these tests to the analysis of structures under working loads.

Temperature

Bituminous concretes are very sensitive to temperature (Monismith, Secor and Secor, 1965) and the temperature variations within a structure are themselves dependent upon many of the elements of climate, such as air temperature, wind conditions and cloud cover (Monismith, 1970). For this reason, accurate records of climatic condition at a site should be made at the time of testing.

Creep

Although the wave-propagation method involves steady-state dynamic

loading, neither the duration of the test nor, in general, the magnitude of the loading is sufficient to stimulate creep behavior in bituminous concrete. In use, however, particularly at high temperature, these materials often exhibit significant time dependent behavior. (Pagen, 1965).

Frequency

A study by Pagen (1965) has shown that the moduli and damping of asphaltic materials are sensitive to the frequency of dynamic loading. Although early applications of the wave-propagation method involved an attempt to simulate actual loading conditions (Van der Poel, 1951), most modern techniques involve a wide frequency range which is designed to meet the requirements of the test itself. Fig. A6.7 shows the results of tests conducted by Pagen (1965) relating Young's modulus (in terms of the absolute $|E|$ of the complex modulus E) and the damping (in terms of the loss angle ϕ_L) to frequency for a typical bituminous concrete.

The ability to predict complex moduli for bituminous concretes at some functional loading and temperature conditions from tests conducted under some other conditions is the goal of continuing research. (e.g., Dehlen, 1969, Pagen, 1963, and Secor, 1961).

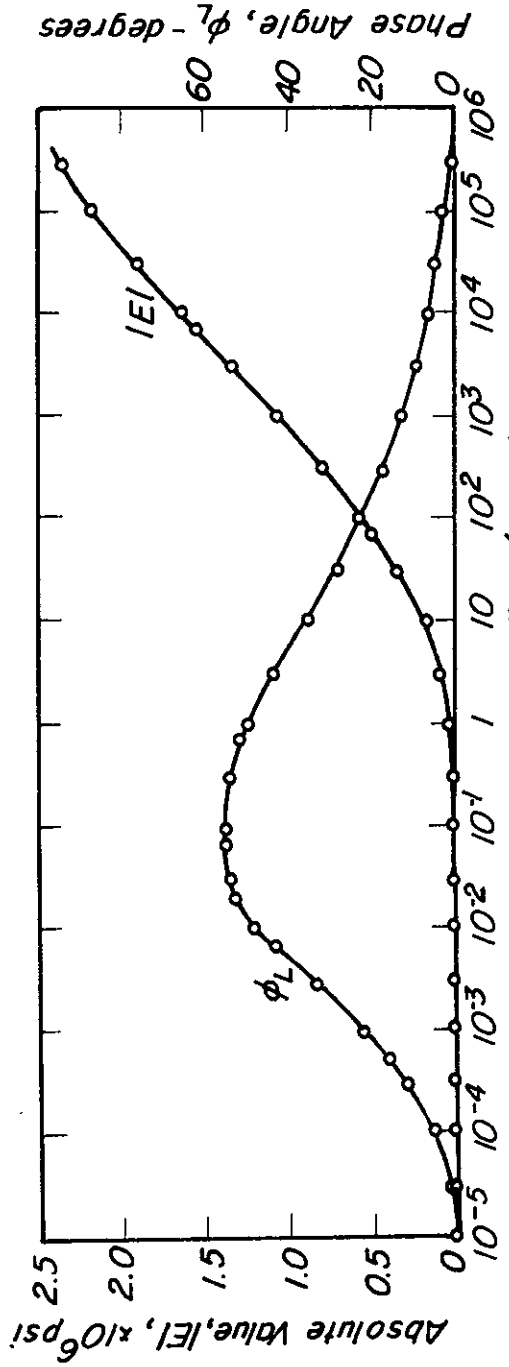

Fig. A 6.7 MAGNITUDE AND PHASE ANGLE OF COMPLEX ELASTIC MODULUS, E, AS A FUNCTION OF ANGULAR FREQUENCY AT 77 °F

APPENDIX 7

A NUMERICAL PREDICTOR FOR CURVE FOLLOWING USING SLOPES

In some cases the slope at a point on a curve may be determined by a method which does not rely upon numerical differentiation using the coordinates of adjacent points. In these cases high order predictors may be designed, which take advantage of the accuracy with which slopes can be calculated, to improve the performance of numerical curve following methods. Such a predictor, of varying order up to the fourth, with the capability to deal with varying step-size is developed below.

Consider the point (x_{k+1}, y_{k+1}) on the curve shown in Fig. A7.1. The ordinate y_{k+1} may be expressed in the form of the Taylor expansion

$$y_{k+1} = y_k + \frac{\bar{h}_0}{1!} y'_k + \frac{\bar{h}_0^2}{2!} y''_k \cdots \tag{A7.1}$$

where

$$y'_k = \frac{dy_k}{dx_k}, \quad y''_k = \frac{d^2 y_k}{dx_k^2}, \text{ etc.}$$

In general

$$y'_{k-n} = y'_k - \frac{\bar{h}_n y''_k}{1!} + \frac{\bar{h}_n^2 y'''_k}{2!} - \frac{\bar{h}_n^3}{3!} y''''_k + \cdots \tag{A7.2}$$

for $n = 1, 2, 3, \ldots$

A method is required which yields an approximation $\bar{y}_{k+1}$ to the ordinate y_{k+1}. The order n of the approximation will depend upon the point at which the expansion is terminated. This approximation may be expressed in the form:

$$\bar{y}_{k+1} = y_k + \bar{h}_0 \{\alpha_0 y'_k + \alpha_1 y'_{k-1} \cdots + \alpha_n y'_{k-n}\} \tag{A7.3}$$

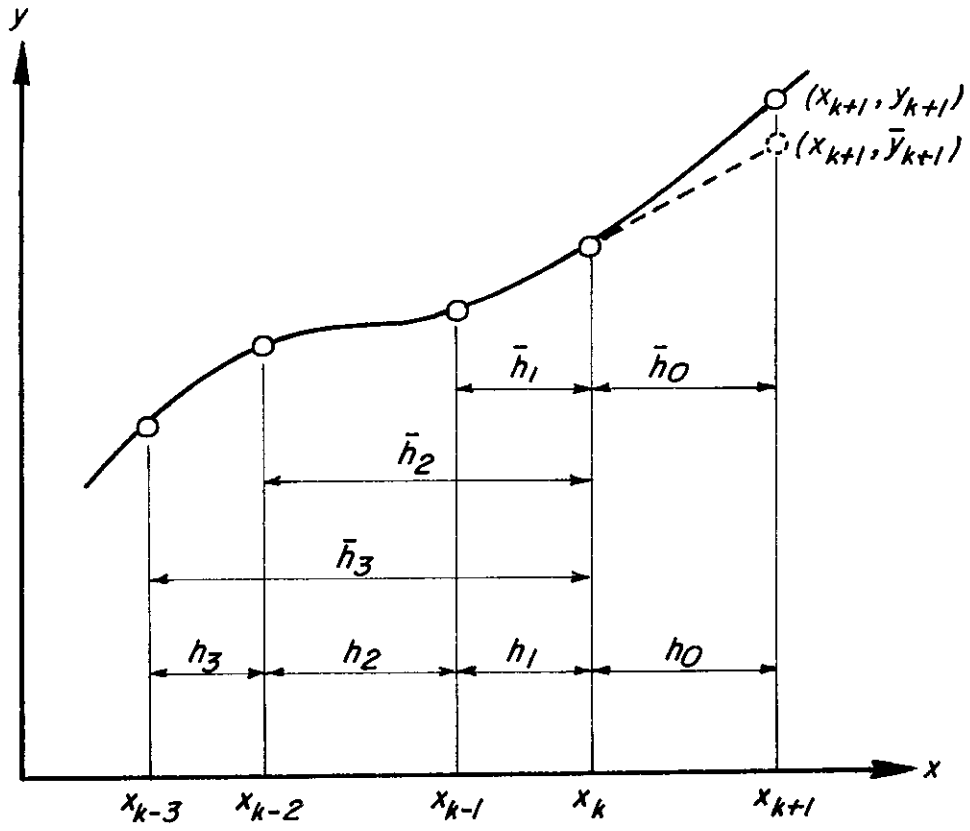

Fig. A 7.1 ILLUSTRATION OF THE USE OF THE PREDICTOR

and using (A7.2) and (A7.3)

$$\begin{aligned}\bar{y}_{k+1} &= y_k + \bar{h}_0\alpha_0 y'_k \\ &+ \bar{h}_0\alpha_1\left\{y'_k - \frac{\bar{h}_1 y''_k}{1!} + \frac{\bar{h}_1^2 y'''}{2!} - \frac{\bar{h}_1^3 y''''_k}{3!} + \ldots\right\} \\ &+ \bar{h}_0\alpha_2\left\{y'_k - \frac{\bar{h}_2 y''_k}{1!} + \frac{\bar{h}_2^2 y'''_k}{2!} - \ldots\ldots\ldots\right\} \qquad \text{(A7.4)} \\ \ldots\ldots &+ \bar{h}_0\alpha_n\left\{y'_k - \frac{\bar{h}_n y''_k}{1!} + \frac{\bar{h}_n^2 y'''_k}{2!} - \ldots\ldots\ldots\right\}\end{aligned}$$

The terms α_j are unknowns which may be evaluated by a comparison of Eq. (A7.1) and (A7.4). For $\bar{y}_{k+1}$, defined by Eq. (A7.4), to approximate y_{k+1} in Eq. (A7.1) the coefficients of the similar terms y'_k, y''_k, etc., must be identical. This comparison yields the following set of equation.

$$\begin{aligned}\alpha_0 + \alpha_1 + \alpha_2 \ldots + \alpha_n &= 1 \\ \bar{h}_1\alpha_1 + \bar{h}_2\alpha_2 \ldots + \bar{h}_n\alpha_n &= -\frac{\bar{h}_0}{2} \qquad \text{(A7.5)} \\ \bar{h}_1^2\alpha_1 + \bar{h}^2\alpha_2 \ldots + \bar{h}_n^2\alpha_n &= \frac{\bar{h}_0^2}{3}\end{aligned}$$

and so on to

$$\bar{h}_1^n\alpha_1 + \bar{h}_2^n\alpha_2 \ldots + \bar{h}_n^n\alpha_n = \frac{(-1)^n\,\bar{h}_0^n}{n+1} \; .$$

Eqs. (A7.5) may be solved for any order n to yield values of α for use with Eq. (A7.3).

At this stage it is convenient to redefine the parameters involving

the step size as follows (see Fig. A7.1):

$$\begin{aligned} h_0 &= x_{k+1} - x_k &&= \bar{h}_0 \\ h_1 &= x_k - x_{k-1} &&= \bar{h}_1 \\ h_2 &= x_{k-1} - x_{k-2} &&= \bar{h}_2 - h_1 \\ &\text{and so on} \end{aligned} \tag{A7.6}$$

so that

$$\begin{aligned} \bar{h}_0 &= h_0 \\ \bar{h}_1 &= h_1 \\ \bar{h}_2 &= h_1 + h_2 \\ \bar{h}_3 &= h_1 + h_2 + h_3 \\ &\text{and so on} \end{aligned} \tag{A7.7}$$

This redefinition when used with Eq. (A7.5) gives the following expressions for the terms α_j in Eq. (A7.3):

2nd Order

$$\begin{aligned} \alpha_0 &= 1 - \alpha_1 \\ \alpha_1 &= -1/2 \{h_0/h_1\} \end{aligned} \tag{A7.8}$$

3rd Order

$$\begin{aligned} \alpha_0 &= 1 - \alpha_1 - \alpha_2 \\ \alpha_1 &= -\frac{1}{6}\frac{h_0}{h_1 h_2}\left\{2h_0 + 3h_1 + 3h_2\right\} \\ \alpha_2 &= \frac{1}{6}\frac{h_0}{h_2}\left\{\frac{2h_0 + 3h_1}{h_1 + h_2}\right\} \end{aligned} \tag{A7.9}$$

4th Order

$$\alpha_0 = \quad 1 - \alpha_1 - \alpha_2 - \alpha_3$$

$$\alpha_1 = - \left\{ \frac{h_0}{2h_1} + \frac{\alpha_2(h_2 + h_1)}{h_1} + \frac{\alpha_3(h_1 + h_2 + h_3)}{h_1} \right\}$$

$$\alpha_2 = \frac{h_0}{12} \left\{ \frac{6h_1^2 + 3h_0 + 8h_0h_1 + 4h_0h_2 + 4h_0h_3 + 6h_1h_2 + 6h_1h_3}{h_3h_2(h_2 + h_1)} \right\} \quad \text{(A7.10)}$$

$$\alpha_3 = -\frac{h_0}{12} \left\{ \frac{6h_1^2 + 3h_0^2 + 8h_0h_1 + 4h_0h_2 + 6h_1h_2}{h_3(h_3 + h_2)(h_3 + h_2 + h_1)} \right\}$$

With the values of α_0 , α_1 ... etc. known, it is now possible to use Eq. (A7.3) to approximate the value of the function at a point $(x_{k+1}$, $y_{k+1})$ when the value of the function is known at a point $(x_k$, $y_k)$ together with y' at this point and for a number of preceding points. For example, if this information is available for two points prior to that defined by $(x_k$, $y_k)$ in Fig. A7.1 then the appropriate values of α_0 , α_1 and α_2 may be computed as shown in Eqs. (A7.9) and used in Eq. (A7.3), together with the slopes y'_k , y'_{k-1} and y'_{k-2} and the ordinate y_k , to give the approximation $\bar{y}_{k+1}$ to the ordinate at x_{k+1} which is a distance h_0 beyond x_k .

APPENDIX 8

A METHOD FOR THE OPTIMIZATION OF THE STEP SIZE IN PREDICTOR-CORRECTOR CURVE FOLLOWING

The computational cost of curve following by predictor-corrector methods is a function of the step size in the independent variable. Large steps reduce the number of corrector cycles to be performed but tend to increase the number of iterations per cycle. Small steps tend to minimize the number of iterations in each corrector cycle but increase the total number of cycles. For any problem there is an optimum balance between step size and corrector iteration length which minimizes the overall computational cost. In general terms, to achieve such an optimization a method is required which distributes points at which the function is to be computed in such a way as to take advantage of the predictor's ability to perform well in regions where the function is well behaved (e.g. nearly linear) and to recognize zones where the predictor requires a small step size (e.g. regions of high curvature). A method which uses the past performance of the predictor as a guide to the optimal size of a future step is developed below.

Step-size Variation

Assume that an initial approximation $\bar{y}_k$ to a root is obtained by a predictor of order p_k. Then if y_k is the exact root, the error ε_k is given by

$$\varepsilon_k = |y_k - \bar{y}_k| = C_k h_k^{p_k+1} \tag{A8.1}$$

where h is the step in the independent variable and C_k is a constant. Since ε_k, h_k and p_k are known, C_k may be obtained from

$$C_k = \frac{\varepsilon_k}{h_k^{p_k+1}} \quad . \tag{A8.2}$$

If it is desired to use the predictor to make an initial approximation, $\bar{y}_{k+1}$ for the next step, which results in a predetermined error ε_c, then a step size h_{k+1} must chosen so that

$$\varepsilon_c = C_{k+1} h_{k+1}^{p_k+1} \tag{A8.3}$$

C_{k+1} is obtained by assuming that

$$C_{k+1} = C_k \tag{A8.4}$$

within a reasonably small zone.

From Eq. (A8.2), (A8.3) and (A8.4) the required stepsize is given by:

$$h_{k+1} = h_k \{\varepsilon_c/\varepsilon_k\}^{\frac{1}{p_k+1}} . \tag{A8.5}$$

Eq. (A8.5) has the following properties.

1. If the error ε_k obtained by the predictor at step k was larger than the desired error ε_c

$$h_{k+1} < h_k$$

2. If ε_k was smaller than ε_c

$$h_{k+1} > h_k$$

Eq. (A8.5) provides a means by which the stepsize of a predictor-corrector curve following method may be varied to maintain an error in the prediction which closely approximates some predetermined criterion ε_c. The choice of this criterion will affect the overall economy of the curve following and it is desirable to obtain an optimization of the magnitude of ε_c.

Step-size Optimization

Let g be the cost of performing the correction from a predicted root to the actual root. This cost is proportional to the number of iterations I required to perform the correction, i.e.

$$g = aI \tag{A8.6}$$

where a is a constant related to the cost of one iteration step.

To optimize locally it is necessary to minimize the cost per unit step in the independent variable. Thus if h is the step in the independent variable, g/h must be minimized. This will be achieved locally if

$$\frac{d(g/h)}{dh} = 0 \tag{A8.7}$$

From Eq. (A8.6) and Eq. (A8.7)

$$\frac{d(aI/h)}{dh} = 0$$

or

$$\frac{a}{h}\frac{dI}{dh} - \frac{aI}{h^2} = 0$$

or

$$\frac{dI}{dh} = \frac{I}{h}$$

or

$$\frac{dI}{d(\ell n\ h)} = I\ . \tag{A8.8}$$

Now, assume the iterative process used by the corrector converges at a rate n. If ε is the initial error (due to the error in the

initial value provided by the predictor), the error after one iteration is ε^n and after two iterations ε^{n^2} ... etc. Thus after I iterations the error will be ε^{n^I}. Thus to approach the correct root to within an allowable error of ε_0 iteration must be performed until

$$\varepsilon^{n^I} = \varepsilon_0$$

which may also be expressed as

$$I = \frac{\ell n\{\ell n\ \varepsilon_0/\ell n\ \varepsilon\}}{\ell n(n)} \quad . \tag{A8.9}$$

If the initial value is provided by a predictor of order p then the error in the initial guess is given by

$$\varepsilon = Ch^{(p+1)} \tag{A8.10}$$

where C is assumed to be a constant.

From Eq. (A8.10)

$$\ell n\ \varepsilon = \ell n\ C + (p + 1)\ell n\ h$$

and differentiating

$$\frac{d(\ell n\ \varepsilon)}{d(\ell n\ h)} = p + 1 \ . \tag{A8.11}$$

From Eq. (9)

$$\frac{dI}{d(\ell n\ h)} = \frac{-\ 1}{(\ell n\ n)(\ell n\ \varepsilon)} \cdot \frac{d(\ell n\ \varepsilon)}{d(\ell n\ h)} \tag{A8.12}$$

Using Eq. (11)

$$\frac{dI}{d(\ell n\ h)} = \frac{-\ (p + 1)}{(\ell n\ n)(\ell n\ \varepsilon)} \tag{A8.13}$$

The LHS of Eq. (A8.13) is equal to the LHS of Eq. (A8.8), so that

$$I = \frac{-(p+1)}{(\ell n\ n)(\ell n\ \varepsilon)} \tag{A8.14}$$

From Eq. (A8.9) and (A8.14)

$$\ell n\ (\ell n\ \varepsilon_0) - n\ (\ell n\ \varepsilon) = \frac{p+1}{\ell n\ \varepsilon}\ .$$

Let $x = \ell n\ \varepsilon$, $x_0 = \ell n\ \varepsilon_0$ and $y = \ell n\ (x_0/x)$ then

$$y = \{(p+1)/-x_0\}\ \exp\cdot y \tag{A8.15}$$

The value y is related to the error ε , created by the initial approximation resulting from the use of the predictor, as follows:

$$y = \ell n(x_0/x) \tag{A8.16}$$

where $x_o = \ell n\ \varepsilon_o$ and $x = \ell n\ \varepsilon$.

The value of ε obtained from Eq. (A8.16) is that which the predictor will achieve when a step size is used which satisfies the requirements of Eq. (A8.7). If the term ε_c in Eq. (A8.5) is set equal to this value the step size computed will be optimal.

Summary

Eqs. (A8.5) and (A8.15) provide a technique for varying the step size in a predictor-connector curve following method in such a way as to minimize the overall cost. The procedure is as follows.

1. Establish an allowable bound ε_0 on the error permitted in the roots.

2. Compute the value of y from:

$$y = \{(p+1)/-x_0\}\ \exp\cdot y \tag{A8.15}$$

where p = the order of the predictor and $x_0 = \ell n\ \varepsilon_0$.

3. Compute the optimum error ε_c in the approximation to the root provided by the predictor from

$$y = \ell n(x_0/x) \tag{A8.16}$$

where

$$x = \ell n\ \varepsilon_c\ .$$

ε_c is a constant for any combination of allowable error in the root ε_0, and order of the predictor p. Where the order of the predictor changes from step to step, a new computation of ε_c must be made for each case.

4. Select the optimal step size for the next step of the curve following from

$$h_{k+1} = h_k\{\varepsilon_c/\varepsilon_k\}^{\frac{1}{p_k+1}} \tag{A8.5}$$

where

h_k = step size of step just completed

h_{k+1} = step size of step to be performed next

ε_c = optimal error is the predictor established in 3. above

ε_k = actual error, measured as difference between predicted and actual root, in step just completed

p_k = order of the predictor used for the step just completed

It should be noted that the step size computed by this method

depends upon the history of the curve-following prior to the step in question. The method does not have power of foresight to predict the performance of the predictor in the future. In some cases, such as in regions of near linearity, very large steps may be proposed. If such a region is followed by a region of very high curvature, without an intermediate transition zone, the method may be unable to reduce the size of the steps sufficiently to prevent serious loss of predictor accuracy. Thus it is advisable to limit the maximum allowable step size. Of course, in practical application, other constraints may be involved such as the need to obtain sufficient points to allow accurate graphical representation of the function.

Example

To illustrate the method, the following example will be used:

Assume a function is to be plotted by a predictor corrector method consisting of the following parts.

a. A Newton Divided-Difference Interpolating Polynomial used in extrapolation as the predictor.

b. A Newton method iteration scheme as the corrector.

The allowable error on the root is $\pm 10^{-11}$.

The predictor will be used in orders 1, 2, and 3 with the highest order possible being employed depending upon the availability of points.

Eqs. (A.15) and (A.16) yield the following values for ε_c

Order of predictor, p	ε_c
1	0.59
2	0.39
3	0.24

and the step size will be calculated from the following forms of Eq. (A8.5).

$$h_{k+1} = h_k\{0.59/\varepsilon_k\}^{1/2} \quad \text{for 1st order}$$
$$h_{k+1} = h_k\{0.39/\varepsilon_k\}^{1/3} \quad \text{for 2nd order}$$
$$h_{k+1} = h_k\{0.24/\varepsilon_k\}^{1/4} \quad \text{for 3rd order}$$

REFERENCES

Alekseev, A. S., (1962), "Some Converse Problems in Wave Propagation Theory," Bulletin of the Academy of Science of the U.S.S.R., Vol. 11 (English Ed. Am. Geophys. Union)

Andersson, O. (1970), A System for Automatic Assessment of Stability in Road Construction by the Wave Propagation Method, Internrapport Nr. 1, Statens Väginstitut, Stockholm.

Ang, A. H. S. and Newmark, N. M. (1971), Development of a Transmitting Boundary for Numerical Wave Motion Calculations, Report to Defence Atomic Support Agency, Contract DASA-01-69-0040, Washington, D. C.

Archer, J. S. (1963), "Consistent Mass Matrix for Distributed Mass Systems," Journal of the Structures Division of ASCE, Vol. 89, No. ST4, pp. 161-178.

Ballard, R. F., Jr. (1964), Determination of Soil Shear Moduli at Depths by In-situ Vibratory Techniques, Miscellaneous Paper No. 4-691. U. S. Army Engineer Waterways Experiment Station, Vicksburg, December.

Bergstrom, S. G., and Linderholm, S. (1946). A Dynamic Method for Determining Average Elastic Properties of Surface Soil Layers, Swedish Cement and Concrete Institute at the Royal Technical University, Stockholm.

Bernhard, R. K. (1939), "Highway Investigation by Means of Induced Vibrations," Pennsylvania State Engineering Experiment Station Bulletin, No. 49.

Brekhovskikh, L. M. (1960), Waves in Layered Media, Academic Press Inc., (London) Ltd., London.

Bromwich, T. J. L'A. (1898), "On the Influence of Gravity on Elastic Waves, and, in Particular, on the Vibrations of an Elastic Globe," Proceeding of the London Mathematical Society, Vol. 30, pp. 98-120.

Červený, V., and Ravindra, R. (1971), Theory of Seismic Head Waves, University of Toronto Press, Toronto.

Cogill, W. H. (1965), "A Torsional Vibrator for Soils," Geophysical Magazine, Vol. 32, p. 285.

Costantino, C. J. (1967), "Finite Element Approach to Stress Wave Problems," Journal of the Engineering Mechanics Division, ASCE, Vol. 93, No. EM2, pp. 153-176, April.

Crawford, J. E. (1972), An Analytical Model for Airfield Pavements Analysis, Technical Report No. AFWL-TR-71-70, Air Force Weapons Laboratory, Kirtland Air Force Base, New Mexico, May .

Cunny, R. W., Cooper, S. S., and Fry, A. B., Jr. (1969), Comparison of Results of Dynamic In-situ and Laboratory Tests for Determination of Soil Moduli, Miscellaneous Paper S-69-48, U. S. Army Engineer Waterways Experiment Station, Vicksburg, October.

Dehlen, G. L. (1969), The Effect of Non-Linear Material Response in the Behaviour of Pavements Subjected to Traffic Loads, Ph.D. Dissertation, University of California, Berkeley.

Deutsche Forschungsgesellschaft für Bodenmechanik (1933), Veroffentlichungen des Instituts Degebo der Technischen Hochschule, No. 1 Berlin.

Deutsche Forschungsgesellschaft für Bodenmechanik (1936), Veröffentlichgen des Instituts Degebo der Technischen Hochschule, No. 4, Berlin.

Deutsche Forschungsgesellschaft fur Bodenmechanik (1938), Veröffentlichgen des Institute Degebo der Technischen Hochschule, No. 6, Berlin.

Dosso, N., and Keryell, P. (1968), "Etude et réalisation des étages 10.000 et 20.000 Hz du vibreur Goodman," Bulletin de Liaison des Laboratoires Routiers, Special J, pp. 146-159, Ministere de L'Équipment et du Logement, Paris, July.

Ducloux, A., Poilane, J., and Guillemin, R. (1968), "Un an d'utilization du vibreur Goodman au Laboratoire Régional d'Autun," Bulletin de Liaison des Laboratoires Routiers, Special J, pp. 108-129, Ministère de L'Équipment et du Logement, Paris, July.

Duncan, J. M., Monismith, C. L., and Wilson, E. L. (1968), "Finite Element Analyses of Pavements," Highway Research Record No. 228, pp. 18-33, Highway Research Board, Washington, D. C.

Ewing, W. M., Jardetzky, W. S., and Press, F. (1957), Elastic Waves in Layered Media, McGraw-Hill, New York.

Finn, F. N. (1962), "Symposium of Flexible Pavement Behaviour as Related to Part I -- Methods of Measurement," Proceedings of the Association of Asphalt Paving Technologists, Vol. 31.

Freudenthal, A. M. (1950), The Inelastic Behaviour of Engineering Materials and Structures, John Wiley and Sons, New York.

Fry, Z. B. (1963), A Procedure for Determining Elastic Moduli of Soils by Field Vibratory Techniques, Miscellaneous Paper no. 4-577, U. S. Army Waterways Experiment Station, Vicksburg, Mississippi, June.

Fu, C. Y. (1946a), "Studies on Seismic Waves: I. Reflection and Refraction of Plane Waves," Geophysics, Vol. 11, No. 1, pp. 1-9, Jan.

Fu, C. Y. (1946b), "Studies on Seismic Waves: II. Rayleigh Waves in a Superficial Layer," Geophysics, Vol. 11, No. 1, pp. 10-23, Jan.

Fu, C. Y. (1950), "Some Problems of the Propagation of Elastic Waves in a Horizontally Stratified Medium," Journal of the Chinese Geophysical Society, Vol. 2, No. 1, pp. 40-59, June.

Fung, Y. C. (1965), Foundations of Solid Mechanics, Prentice-Hall, Englewood Cliffs.

Gramsammer, J. C. (1968), "Première étude expérimentale de la variation de l'amplitude au vibreur Goodman," Bulletin due Liaison des Laboratoires Routiers, Special J, pp. 171-178, Ministère de L'Equipment et du Logement, Paris, July.

Gramsammer, J. C. (1969), Rapport sur l'exploitation des courbes de phase présent des oscillations, Fiche programme 1-01-05-9, Laboratoire Central des Ponts et Chaussees, Ministère de L'Équipment et due Logement, Paris, November.

Guillemin, R. (1970), Interprétation des vibrations de surface sur les structures routières, Rapport de recherche No. 9, Laboratoire Central des Ponts et Chaussees, Ministere de L'Equipment et due Logement, Paris.

Guillemin, R. and Gramsammer, J. C. (1971), Auscultation dynamique des Chaussées a l'aide du vibreru léger, Note D'Information Technique, Laboratoire Central des Ponts, et Chaussees, Ministère de L'Équipment et du Logement, Paris, Nov.

Hadala, P. F. (1971), Evaluation of a Transmitting Boundary for a Two-Dimensional Wave Propagation Computer Code, Technical Report S-71-16, U. S. Army Engineer Waterways Experiment Station, Vicksburg.

Hardin, B. O. (1965), "The Nature of Damping in Soils," J. Soil Mech. and Found. Div. of ASCE, Vol. 91, No. SM 1, pp. 63-97, Jan.

Hardin, B. O. and Drnevich, V. P. (1920), Shear Modulus and Damping in Soils: I. Measurement and Parameters Effects, II. Design Equations and Curves. Technical Report UKY 27-70-CE 2 and 3, College of Engineering, University of Kentucky, Lexington, July.

Harkrider, D. G., Hales, A. L. and Press, F. (1963), "On Detecting Soft Layers in the Mantle with Rayleigh Waves," Bulletin of the Seismological Society of America, Vol. 53, No. 3, pp. 539-548.

Haskell, N. A. (1953), "The Dispersion of Surface Waves on Multilayered Media," Bulletin of the Seismological Society of America, Vol. 43, No. 1, pp. 17-34, Jan.

Heukelom, W. (1961), "Analysis of Dynamic Deflections of Soils and Pavements, Géotechnique, Vol. 11, No. 3.

Heukelom, W. and Foster, C. R. (1960), "Dynamic Testing of Pavements," Journal of the Soil Mechanics and Foundations Division, ASCE, Vo. 86, No. SM 1, pp. 1-28, January.

Jacobsen, L. S., (1930), "Seady Forced Vibrations as Influenced by Damping," Transactions, ASME, APM - 52 - 15, pp. 169-181.

Jones, R. (1955), "A Vibration Method for Measuring the Thickness of Concrete Road Slabs in-situ," Magazine of Concrete Research, Vol. 7, No. 20, pp. 97-102, July.

Jones, R. (1958), "In-situ Measurement of the Dynamic Properties of Soil by Vibration Methods," Géotechnique, Vol. 8, pp. 1-21, March.

Jones, R. (1962), "Surface Wave Techniques for Measuring the Elastic Properties and Thickness of Roads: Theoretical Development," British Journal of Applied Physics, Vol. 13, pp. 21-29, January.

Jones, R. (1963), "Following Changes in the Properties of Road Bases and Sub-Bases by the Surface-Wave Propagation Method," Civil Engineering, Vol. 58, No. 3. 682 and 683, London.

Jones, R. (1964), "The Use of the Surface Wave Propagation Method for the Testing of Roads," Proceedings of the Second Conference of the Australian Road Research Board, Vol. 2, pp. 692-700.

Jones, R. (1968), "Court historique de l'auscultation des sols et chaussées par ondes superficielles," Bulletin de Liasion des Laboratoires Routiers, Special J, pp. 24-35, Ministère de L'Équipment et du Logement, Paris, July.

Jones, R. and Mayhew H. C. (1965), "Thickness and Quality of Cemented Surfacings and Bases Measured by a Non-Destructive Surface Wave Method," Civil Engineering and Public Works Review, Vol. 60, No. 705 pp. 523-529, London.

Jones, R. and Thrower, E. N. (1965a), "Effect of Interfacial Contact on the Propagation of Flexural Waves Along a Composite Plate," Journal of Sound Vibration, Vol. 2, No. 2, pp. 167-174.

Jones, R. and Thrower, E. N. (1965b), "An Analysis of Waves in a Two-Layer Composite Plate and its Application to Surface Wave Propagation Experiments on Roads," Journal of Sound Vibration, Vol. 2, No. 3, pp. 328-335.

Jones, R., Thrower, E. N. and Gatfield, E. N. (1967), "Surface Wave Method," Proceedings of the Second International Conference on the Structural Design of Asphalt Pavements, pp. 505-519, University of Michigan, Ann Arbor, August.

Jones, R. and Whiffin, A. C. (1960), A Survey of Dynamic Methods of Testing Roads and Runways, Highway Research Board Bulletin, No. 277.

Klomp, A. J. G. and Niesman, T. W. (1967), "Observed and Calculated Strains at Various Depths in Asphalt Pavements," Proceedings of the Second International Conference on the Structural Design of Asphalt Pavements, University of Michigan, Ann Arbor.

Knopoff, L. (1962), "Higher Order Born Approximations for the Inversion of Love Wave Dispersion," Geophysics Journal of the Royal Astronomical Society, Vol. 1, pp. 147-157.

Kuhlemeyer, R. L. (1969), Vertical Vibrations of Footings Embedded in Layered Media, Dissertation submitted in partial satisfaction of the requirements for the degree of Doctor of Philosophy. University of California, Berkeley.

Kuhlemeyer, R. L. and Lysmer, J. (1973), "Finite Element Method Accuracy for Wave Propagation Problems," Journal of the Soil Mechanics and Foundations Division of ASCE, Vol. 99, No. SM 5, pp. 421-427, May.

Kurzeme, M. (1970a), "The Propagation of SH-Waves in Idealized Layered Pavements," Proceedings of the Fifth Conference of the Australian Road Research Board, Vol. 5, Part 4, pp. 138-160, Sydney.

Kurzeme, M. (1970b), "Field Observations of SH-Waves in Layered Pavements," Proceedings of the Fifth Conference of the Australian Road Research Board, Vol. 5, Part 4, pp. 161-177, Sydney.

Kurzeme, M. (1971), "In-situ Investigation Using SH-Waves," Journal of the Soil Mechanics and Foundations Division, ASCE, 97, No. SM 2, pp. 341-356, February.

Laboratoire Central des Ponts et Chaussées (1971), Courbes Theoretiques de Lamb, Transparencies published by Département des Chaussées, Laboratoire Central des Ponts et Chaussées, Ministère de L'Équipment at du Logement, Paris, Nov.

Laboratoire Regional D'Autun (1971), Vibreur Léger, Biplaque Libre, Courbes de Dispersion Theoretiques, Transparencies published by Laboratoire Regional D'Autun, Ministère de L'Équipment et du Logement, Autun, Nov.

Lamb, H. (1904), "On the Propagation of Tremors of the Surface of an Elastic Solid," Philosophical Transactions, Royal Society, Vol. A203, pp. 1-42, London.

Lamb, H. (1916), "On Waves in an Elastic Plate," Proceedings of the Royal Society, Series A, Vol. 93, No. 648, pp. 31-34.

Love, A. E. H. (1926), Some Problems in Geodynamics, Cambridge University Press, London.

Lysmer, J. (1970), "Lumped Mass Method for Rayleigh Waves," Bulletin of the Seismological Society of America, Vol. 60, pp. 80-104.

Lysmer, J. and Drake, L. A. (1972), "A Finite Element Method for Seismology," Ch. 6 of Methods in Computational Physics, Volume II: Seismology, edited by Alder, Fernbach and Bolt, Academic Press, New York.

Lysmer, J. and Kuhlemeyer, R. L. (1969), "Finite Dynamic Model for Infinite Media," Journal of the Engineering Mechanics Division, Vol. 95, No. EM4, pp. 859-877.

Lysmer, J. and Waas, G. (1972), "Shear Waves in Plane Infinite Structures," Journal of the Engineering Mechanics Division of ASCE, Vol. 98, No. EM 1, pp. 85-105.

Maxwell, A. A. and Fry, Z. B. (1967), A Procedure for Determining Elastic Moduli of In-situ Soils by Dynamic Techniques, Miscellaneous Paper No. 4-933, U. S. Army Engineer Waterways Experiment Station, Vicksburg, Mississippi, October.

Maxwell, A. A. and Joseph A. H. (1967), "Vibratory Study of Stabilized Layers of Pavement in Runway at Randolph Air Force Base," Proceedings of the Second International Conference on the Structural Design of Asphalt Pavements, University of Michigan, Ann Arbor, August.

McNiven, H. D., Sackman, J. L. and Shah, A. H. (1965), An Investigation of Elastic Waves with Imaginary and Complex Ware Numbers in Hollow-Rods, Report No. 65-14, Structural Engineering Laboratory, University of California, Berkeley, Dec.

McNiven, H. D. and Shah, A. H. (1966), Extensional Waves in a Semi-Infinite Hollow, Elastic Rod, Report No. 66-5, Structural Engineering Laboratory, University of California, Berkeley, June.

McNiven, H. D., Shah, A. H., and Sackman, J. L. (1965), An Approximate Theory for the Vibrations of Hollow Elastic Rods, Report No. 65-13, Structural Engineering Laboratory, University of California, Berkeley, Nov.

Miller, G. F., and Pursey, H. (1955), "On the Partition of Energy Between Elastic Waves in a Semi-Infinite Solid," Proceedings of the Royal Society, Series A, Vol. 233, pp. 521-541.

Monismith, C. L. (1970), "Some Applications of Theory in the Design of Asphalt Pavements," Proceedings of the Fifth Annual Street and Highway Conference, Reno, Nevada, March 18.

Monismith, C. L., Secor, G. A. and Secor, K. E. (1965), "Temperature Induced Stresses and Deformations in Asphalt Concrete," Proceedings, Association of Asphalt Paving Technologists, pp. 248-285.

Mucci, M. (1968), "Quelques Essais comparatifs du vibreur lourd du Laboratoire Central et due vibreur Goodman," Bulletin de Liaison des Laboratoires Routiers, Special J, pp. 161-169, Ministère de L'Équipment et du Logement, Paris, July.

Nair, K. (1971), "Pavement Evaluation by Wave Propagation Method," Journal of Transportation Engneering Division of ASCE, Vol. 90, NO. TE1, pp. 83-104, February.

Nijboer, L. W. (1955), "Schwingungsmessungen auf Strassen mit verschiendenem Unterbau," Strasse und Autobahn, Vol. 6.

Nijboer, L. W. and Jones, R. (1944), "Investigations into the Dynamic Testing of Roads," Roads and Road Construction, Vol. 5, No. 3, pp. 8-21.

Nijboer, L. W. and Metcalf, C. T. (1962), "Dynamic Testing at the AASHO Road Test," Proceedings of the International Conference on the Structural Design of Asphalt Pavements, University of Michigan, Ann Arbor.

Nijboer, L. W. and Van der Poel, C. (1953), "A Study of Vibration Phenomena in Asphaltic Road Constructions," Proceedings of the Association of Asphalt Paving Technology, Vol. 22, pp. 197-237.

Oliver, J., Press, F. and Ewing, M. (1954) "Two-dimensional model seismology," Geophysics, Vol. 19, pp. 202-219.

Onoe, M., McNiven, H. D. and Mindlin, R. D. (1962), "Dispersion of Axially Symmetric Waves in Elastic Rods," Journal of Applied Mechanics, 29, Trans. ASME Series E, Vol. 84, pp. 729-734.

Osborne, M. F. M. and Hart, S. D. (1945), "Transmission, Reflection and Guiding of an Exponential Pulse by a Steel Plate in Water: I. Theory," Journal of the Accoustical Society of America, Vol. 17, pp. 1-18.

Page, J. (1969), Wave Propagation Tests During the Construction of the Conington Lodge Experiment, RRL Technical Note TN 385, Transport and Road Research Laboratory, Crowthorne, March. Unpublished.

Pagen, C. A. (1963), An Analysis of the Thermorheological Response of Bituminous Concrete," Ph.D. Thesis, Ohio State University, March.

Pagen, C. A. (1965) "Rheological Response of Bituminous Concrete," Highway Research Record, No. 67, Highway Research Board, Washington, D. C., pp. 1-26.

Peutz, M. G. F., van Kempen, H. P. M., and Jones, A. (1968), "Layered Systems under Normal Surface Loads," Highway Research Record No. 228, pp. 34-45, Highway Research Record, Washington, D. C.

Pichumani, R. (1973), Finite Element Analysis of Pavement Structures AFPAV Code (Nonlinear Elastic Analysis), Technical Report No. AFWL-TR-72-186, Air Force Weapons Laboratory, Kirkland Air Force Base, New Mexico, May.

Pickett, G. (1945), "Dynamic Testing of Pavements," Journal of the American Concrete Institute, Vol. 41, pp. 473-489.

Press, F., Harkrider, D. and Seafeldt, C. A. (1961) "A Fast Convenient Program for Computation of Surface Wave Dispersion Curves in Multilayered Media," Bulletin of the Seismological Society of America, Vol. 51, pp. 495-502.

Rao, H. A. B. (1971), Nondestructive Evaluation of Airfield Pavements (Phase I), Technical Report AFWL-TR-71-75, Air Force Weapons Laboratory, Kirkland Air Force Base, December.

Rao, H. A. B. (1973), Results of Non-destructive Tests at Nellis Air Force Base, (W.O. 6.16c), Letter Report II, Eric H. Wang Civil Engineering Research Facility, University of New Mexico, Albuquerque, July.

Rao, H. A. B., and Harnage, D. (1972), "Evaluation of Rigid Pavements by Nondestructive Tests," Highway Research Record No. 407, pp. 76-86, Highway Research Board, Washington, D. C.

Rayleigh, Lord, (Strutt, J. W.) (1885), "On Waves Propagated Along the Plane Surface of an Elastic Solid," Proc. Land. Math. Soc., Vol. 17, pp. 4-11.

Reissner, E. (1936), "Stationaere, Axial-symmetrische durch eine Schuettelnde Masse Erregte Schwingungen eines Homogenen Elastischen Halbraumes," Ingenieur-Archiv., Band VII, S, pp. 381-396.

Richart, F. E., Jr. (1962), "Foundation Vibrations," Transactions, ASCE, Vol. 127, Part I, pp. 863-898.

Richart, F. E., Jr., Hall, J. R., Jr., and Lysmer, J. (1962), Study of the Propagation and Dissipation of 'Elastic' Wave Energy in Granular Soils, Contract DA-22-079-eng-314 for U. S. Army Engineer Waterways Experiment Station, University of Florida.

Richart, F. E., Jr., Hall, J. R., Jr., and Woods, R. D. (1970), Vibrations of Soils and Foundations, Prentice-Hall, Inc., Englewood Cliffs, 1970.

Richter, C. F. (1943), "Mathematical Questions in Seismology," Bulletin of the American Mathematical Society, Vol. 49, pp. 477-493.

Secor, K. E. (1961), Viscoelastic Properties of Asphaltic Paving Mixtures, D. Eng. Thesis, University of California, Berkeley.

Seed, H. B. and Idriss, I. M. (1970), Soil Moduli and Damping Factors for Dynamic Response Analysis, Report No. EERC 70-10, Earthquake Engineering Research Center, University of California, Berkeley, December.

Sezawa, K. (1938),"Anomalous Dispersion of Elastic Surface Waves," Bulletin of the Earthquake Research Institute, Vol. 16, p. 225, Tokyo.

Shipley, S. A., Leistner, H. G., and Jones, R. E. (1967), "Elastic Wave Propagation -- A Comparison Between Finite Element Predictions and Exact Solutions," Proceedings of the International Symposium on

Wave Propagation and Dynamic Properties of Earth Materials, University of New Mexico Press, pp. 509-519, Aug.

Statens Väginstitut (1969), Annual Report of the National Swedish Road Research Institute (Statens Väginstitut) for the Year 1967-68, The National Road Research Institute, Stockholm.

Stokes, G. G. (1849), "On Theories of the Internal Friction of Fluids in Motion, and of the Equilibrium and Motion of Elastic Solids," Transactions of the Cambridge Philosophical Society, Vol. 8, pp. 287-319.

Stoneley, R. (1924), "Elastic Waves at the Surface of Separation of Two Solids," Proceedings of the Royal Society, Series A, Vol. 106, pp. 416-428.

Sung, T. Y. (1953), "Vibrations in Semi-infinite Solids Due to Periodic Surface Loading," American Society for Testing and Materials Special Technical Publication 156, Symposium on Dynamic Testing of Soils, pp. 35-64.

Thomas, P. (1969), Investigation of Flexural Wave Dispersion in a Two-dimensional Layered Road Model, Unpublished notes, Transport and Road Research Laboratory, Crowthorne, England.

Thomson, W. T. (1950), "Transmission of Elastic Waves through a Stratified Solid Medium," Journal of Applied Physics, Vol. 21, No. 2, pp. 89-93, Feb.

Thrower, E. N. (1965), "The Computation of the Dispersion of Elastic Waves in Layered Media," Journal of Sound Vibration, Vol. 2, No. 3, pp. 210-226.

Thrower, E. N. (1972), Personal Communication.

Toksoz, M. N. and Anderson, D. I. (1963), "Generalized Two-dimensional Model Seismology with Application to Anisotropic Earth Models," Journal of Geophysical Research, Vol. 68, No. 4, pp. 1121-1130.

Tolstoy, I. and Usdin, E. (1953), "Dispersive Properties of Stratified Elastic and Liquid Media: A Ray Theory," Geophysics, Vol. 18, No. 4, pp. 844-870, Oct.

Van der Poel, C. (1948), "Dynamic Testing of Pavements and Base Courses," Proceedings of the Second International Conference on Soil Mechanics and Foundation Engineering, V. 4, pp. 157-163, International Society for Soil Mechanics and Foundation Engineering, Rotterdam, June.

Van der Poel, C. (1951), "Dynamic Testing of Road Constructions," Journal of Applied Chemistry, Vol. 1, pp. 281-290.

Van der Poel, C. (1953), "Vibration Research on Road Constructions," Special Technical Publication No. 156: Symposium on Dynamic Testing of Soils, pp. 175-185, American Society for Testing and Materials.

Vidale, R. F. (1964), The Dispersion of Stress Waves in Layered Media Overlying a Half-space of Lesser Accoustic Rigidity. A thesis submitted in partial fulfillment of the requirements for the degree of Doctor of Philosophy, University of Wisconsin.

Waas, G. (1972), Linear Two-dimensional Analysis of Soil Dynamics Problems in Semi-infinite Layered Media, A dissertation submitted in partial satisfaction of the requirements for the degree of Doctor of Philosophy, University of California, Berkeley.

Walker, G. W. (1919), "Surface Reflection of Earthquake Waves," Philosophical Transactions of the Royal Society, Series A, Vol. 218, pp. 373-393.

Wilkinson, J. H. (1965), The Algebraic Eigenvalue Problem, Clarendon Press, Oxford.

Zienkiewicz, O. C. (1971), The Finite Element Methods in Engineering Science, McGraw-Hill, London.